DISSERTATION

der Fakultät für Biologie

der Ludwig-Maximilians-Universität München

Functional Integration of New Neurons into Adult Cortical Circuits

zur Erlangung des Grades

eines Doktors der Naturwissenschaften

vorgelegt von

Mag. Susanne Falkner

München, 21. August 2017

Erstgutachter:	Professor Dr. Mark Hübener
Zweitgutachter:	Professor Dr. Rainer Uhl
Promotionsgesuch eingereicht am:	21. August, 2017
Datum der mündlichen Prüfung:	18. Dezember, 2017

Eidesstattliche Erklärung:

Ich versichere hiermit an Eides statt, dass ich die vorgelegte Dissertation mit dem Titel *Functional Integration of New Neurons into Adult Cortical Circuits* selbständig und ohne unerlaubte Hilfe angefertigt habe.

Erklärung:

Hiermit erkläre ich, dass ich mich nicht anderweitig einer Doktorprüfung ohne Erfolg unterzogen habe. Die Dissertation wurde weder in ihrer jetzigen Form, noch in wesentlichen Teilen einer anderen Prüfungskommission vorgelegt.

München, 21. August 2017

Susanne Falkner

Anfertigungsort

Max-Planck-Institut für Neurobiologie
Abteilung Synapsen - Schaltkreise- Plastizität

und

Helmholtz Zentrum München
Institut für Stammzellforschung

Parentos

Super FlyGuy

Katzi & Spurtifix

Table of Contents

Index of Figures

1 Summary

The capacity of the adult mammalian brain to compensate for neuronal loss is very limited. As a result, acute and chronic neurological diseases almost always cause irreversible damage and impairment of brain function. Emerging therapeutical strategies aim at restoring damaged circuits by substituting lost cells with new neurons or progenitor cells from endogenous or exogenous sources. While new neurons have been shown to survive and send out efferent projections in the adult host brain following transplantation, it is not known whether new neurons in fact receive and integrate the appropriate afferent inputs in order to perform a meaningful function within the damaged target circuit. The correct and precise spatio-temporal integration of thousands of presynaptic inputs from a multitude of cortical and sub-cortical areas is, however, the primary function of excitatory projection neurons in the neocortex during tasks like sensory integration or cognitive processes. Furthermore, no data are available on the development and the integration process of individual new neurons over time, and neither their dendritic arbour morphogenesis, nor the acquisition of function as a result of their progressive integration into the network has been described to date. It is therefore of particular interest to investigate, whether i) adult neocortical circuits retain the capacity to replace lost excitatory neurons with induced or introduced new neurons and ii) new neurons are capable of substituting lost cells by adopting comparable structural and functional properties within the context of their target network.

In this thesis I investigated the progressive structural and functional integration of individual new neurons following the targeted ablation of upper layer projection neurons in the primary visual cortex (V1) of adult mice. In a first step, I established the spatially confined photolytic ablation of specifically targeted layer 2/3 (L2/3) projection neurons in the binocular zone of V1. The photolytic lesion is characterized by its non-invasive nature, a local, minor and transient astroglial response and the progressive apoptotic cell death of targeted neurons over the course of 7 days.

In order to substitute lost L2/3 neurons, I transplanted dissociated embryonic cells labelled with genetically encoded calcium indicators and/ or fluorescent proteins into the lesioned area. Using chronic *in vivo* two-photon imaging through an implanted glass window I followed the morphogenesis, synaptogenesis and functional development of individual transplanted neurons up to 11 months post transplantation (pt). The majority of grafted neurons developed stable layer 2/3 pyramidal cell-like dendritic arbors within 4 weeks. Axonal bouton development preceded dendritic spine formation and both reached stable densities at 4 weeks pt. Elevated turnover rates up to 9 weeks pt however, indicated ongoing refinement of reciprocal synaptic contacts with the host network.

Visual stimulation with moving gratings elicited stimulus-evoked responses and revealed a limited degree of orientation and/ or direction selectivity as early as 5 weeks pt. Grafted neurons subsequently developed selective, stable and persistent tuning properties, indistinguishable from adult L2/3 projection neurons in V1, and this functional maturation correlated well with the refinement of their synaptic connections. New neurons also received stimulus-driven, tuned input onto their dendritic spines, indicating successful integration into host visual processing circuits. Once assimilated into the host network, new neurons remained an integral part of the target circuit for up to 11 months, and thus likely persist for the rest of the animal's life.

It has been reported that apoptosis of deep layer cortical neurons in the mouse forebrain is capable of stimulating the endogenous production of new neurons. In the second part of this thesis I therefore investigated whether photolytic lesion of L2/3 projection neurons in adult V1 also induces the generation of endogenous new neurons. I used a combination of Bromodeoxyuridine (BrdU) labelling, genetic fate mapping of known neuronal and potential parenchymal progenitors expressing fluorescent proteins, as well as chronic *in vivo* two-photon imaging, in order to detect induced new neurons, identify their cellular origin and assess their potential for circuit repair. Despite the successful identification of migrating and/ or proliferating cells within large cortical volumes across time-points, neither neuronal nor resting parenchymal progenitors of the astrocytic lineage gave rise to new neurons following photolytic lesion. Furthermore, a small number of observed lesion-specific BrdU positive new neurons did not overlap with genetically labelled cells in two prominent mouse models of astrocytic and oligodendroglial lineages, respectively. Thus, the puzzling origin of photolytically induced endogenous new neurons remains to be elucidated in subsequent studies.

Taken together, I have shown that the adult mammalian brain i) readily assimilates new neurons into cortical circuits subjected to injury or disease and ii) new neurons are capable of developing area- and cell-type specific structural and functional properties indistinguishable from previously lost cells. This proof of principle study offers encouraging results for cell replacement therapies and substantiates the feasibility of brain circuit restoration.

2 Introduction

2.1 CNS Regeneration - Limitations and Strategies for Repair

The adult mammalian brain is extremely limited in its capacity for self-renewal and regeneration. In contrast to non-mammalian vertebrates, neurons lost due to injury or disease [Gorman 2008] cannot be replaced [Kyritsis 2014, Alunni 2016] and as a result, insults to the central nervous system (CNS) almost always result in irreversible damage and impairment of brain function. Emerging strategies to substitute lost neurons and repair damaged brain circuits include the replacement of lost cells with new neurons or progenitor cells from endogenous [Lindvall 2004, Emsley 2005, Bellenchi 2013, Christie 2013, Bazarek 2014, Sun 2014] (see 2.1.1) or exogenous sources [Lindvall 2000, Lindvall 2004, Emsley 2005] (see 2.1.2; Fig. 1). While the potential regenerative capacity of endogenous progenitors has gained considerable attention throughout the last decade [Bazarek 2014], the first attempts at brain tissue transplantation date back over a century and were conducted in cats [Thompson 1890]. In 1987, the first humans - patients suffering from Parkinson's disease - received striatal transplantations of fetal dopaminergic neurons [Brundin 1986, Piccini 2000, Barker 2013] and since, multiple clinical trials have been conducted in order to assess the safety and efficacy of neuronal grafts in various disease conditions [Piccini 2005, Bang 2016, ClinicalTrial.gov NCT02028104]. However, despite individual reports of improvements or alleviated symptoms in some patients that had received striatal grafts, treatment outcome has been highly variable, and the procedure has never been approved as common medical practice [Piccini 2005, Barker 2013]. Differences in the source of donor cells and their pre-implant processing, the grafting procedure itself and post-graft drug regime may account for some of the reported inconsistencies [Piccini 2005, Barker 2013]. On the other hand, it is simply not clear, whether grafted cells in fact participate in the genuine reconstruction of the damaged circuits. The observed improvements could also be the result of the trophic [Chiba 2003], neuroprotective [Chiba 2003, Aharonowiz 2008], and/ or immunomodulatory effects [Krampera 2006, Aharonowiz 2008] of transplanted cells [Thompson 2015].

Endogenous progenitors on the other hand, have received increasing attention since the discovery of the two neurogenic niches, the subventricular zone (SVZ) lining the wall of the lateral ventricles [Lois 1993, Lois 1994, Alvarez-Buylla 2002] and the dentate gyrus (DG) of the hippocampal formation [Altman 1965, Altman 1969, Kempermann 2004, Ming 2005, Ming 2011], each providing a continuous source of new neurons to the adult mammalian brain. Potential routes of treatment under discussion involve the application of external factors that modify or instruct the proliferation, migration and lineage commitment of endogenous new neurons [Christie 2013], according to the requirements of the disease condition. Similarly, the targeted instruction or reprogramming of potential resting or (re-) activated parenchymal progenitors (see 2.1.1.2) may contribute to

the repair of neuronal circuits [Götz 2015]. Despite their theoretical potential however, the therapeutic exploitation of endogenous new neurons is still highly speculative at present.
Irrespective of their source, in order to truly restore a damaged neuronal circuit new neurons need to physically replace and functionally adopt the properties of previously lost cells (see 2.2; Fig. 2). Concurrently, adult neuronal circuits have to retain the capacity to integrate new cells into the existing neuronal network. Together, both aspects likely involve complex and interdependent processes on a cellular level that to date, have not been investigated in a suitable model system (see 1.1).

2.1.1 Endogenous Sources of New Neurons for Circuit Repair

2.1.1.1 Neurogenic Niches in the Adult Brain

In the adult mammalian brain new neurons are only produced in discreet regions that, in reference to other stem cell harbouring regions throughout the body, are termed neurogenic niches [Schofield 1978, Taupin 2006]. Over the last decades, the SVZ lining the wall of the lateral ventricles [Meisami 1986, Lois 1993, Lois 1994, Alvarez-Buylla 2002] and the sub-granular zone (SGZ) of the DG in the hippocampal formation [Altman 1965, Altman 1969, Kempermann 2004, Ming 2005, Ming 2011] have been studied intensively [Ming 2011]. Both have been found to provide new neurons throughout the adult life of almost all mammalian species investigated so far [Barker 2011], including humans [Eriksson 1998, Curtis 2007, Sanai 2011, Spalding 2013].
The SGZ gives rise to new granule cells that slowly migrate through the granule cell layer, morphologically mature over the course of 7 weeks, eventually extend their dendritic arbour into the molecular layer and project their axons through the hilus to the CA3 region of the hippocampus [Amaral 1989, vanPraag 2002, Kempermann 2004, Zhao 2006]. They receive glutamatergic input from the entorhinal cortex, neuromodulatory input from the ventral tegmental area, raphe nuclei and the septum, as well as GABAergic input from local interneurons [Cooper-Kuhn 2004, Vivar 2012, Deshpande 2013]. Although to date, the physiological function of continued neurogenesis in the adult DG has not been completely elucidated, mature granule cells seem to be involved in context specific memory encoding and retrieval [McHugh 2007, Liu 2012, Basu 2016]. For instance, the specific optogenetic re-activation of granule neurons that were active during the formation of a contextual fear memory is sufficient to induce freezing behaviour in a neutral context [Liu 2012]. In addition, granule neurons are part of the hippocampal tri-synaptic pathway [Yeckel 1990, Amaral 1998, Ribak 2007], passing on inputs from the entorhinal cortex via CA3 neurons onto CA1 pyramidal cells. Together with the perforant path [Nafstad 1967, Hjorth-Simonsen 1972, Doller 1982] and long-range inhibitory inputs from the lateral entorhinal cortex [Germroth 1989, Basu 2016] they comprise a circuit likely awarding saliency to sensory stimuli [Basu 2016]. Since granule

neurons are continuously born and integrated into the hippocampal network, it is speculated that they could even play a role in encoding aspects of temporal information with new memories [Aimone 2006, Aimone 2011].

Neurons born in the adult SVZ on the other hand, mainly comprise of GABAergic interneurons that migrate along the rostral migratory stream [Meisami 1986, Lois 1994] (RMS) to the olfactory bulb (OB), where they radially disperse and give rise to periglomerular cells (PGCs) and granule cells (GCs) in the glomerular and granule cell layer, respectively [Petreanu 2002, Carleton 2003, Ninkovic 2007, Ming 2011]. In humans, newly generated interneurons of the lateral SVZ have been found to continuously integrate into the adjacent striatum [Ernst 2014]. In addition, the dorsal SVZ has been shown to give rise to a small number of glutamatergic juxtaglomerular neurons [Brill 2009], so-called short axon cells [Pinching 1972, Aungst 2003].

Olfactory information reaches the OB via olfactory receptor neurons (ORN) that bind odour molecules in the olfactory epithelium of the nasal cavity [Buck 1991, Bozza 2009, Cho 2009]. ORNs synapse onto mitral/ tufted cells, the main OB output, as well as external tufted cells, short axon cells and PGCs [Mori 1999]. PGCs in turn provide feedforward inhibition to mitral/ tufted and external tufted cells [Aroniadou-Anderjaska 2000, Murphy 2005, Homma 2013], as well as feedback and lateral inhibition driven by mitral [Murphy 2005] and short axon cells [Aungst 2003], respectively. GCs form characteristic dendro-dendritic synapses with basal dendrites of mitral cells in the granule cell layer [Hamilton 2005] and engage in lateral inhibition of neighbouring output cells [Yokoi 1995]. In addition, both, PGCs and GCs receive glutamatergic feedback projections from the olfactory cortex, including the accessory olfactory nucleus [Matsutani 2008, Markopoulos 2012, Deshpande 2013]. Together, they function to increase odour selectivity and/ or discrimination by enhancing odour evoked signal to noise and spiking variability in strongly activated mitral cells [Mori 1999, Aungst 2003, Hamilton 2005, Imam 2012, Najac 2015].

Similar to neurogenesis in the adult DG, the physiological function of continuously generated PGCs and GCs is not completely understood. It is generally thought that the availability of new neurons provides a certain potential for plasticity to the OB circuit [Gheusi 2013, Livneh 2014, Sakamoto 2014]. For instance, genetic ablation and impairment of synaptic integration of new neurons both severely hamper behavioural performance in odour-associated memory tasks [Sakamoto 2014], while selective activation of new neurons facilitates odour based learning and memory [Alonso 2012]. In addition, olfactory discrimination learning and sensory experience increase the survival [Petreanu 2002, Rochefort 2002, Yamaguchi 2005, Alonso 2006], synaptic integration [Alonso 2006, Yoshihara 2015] and long-term odour selectivity [Livneh 2014] of new neurons.

Recently, a third continuous source of new neurons in the adult mammalian brain has been described, the ventro-lateral and/ or ventro-basal region of the 3rd ventricle in the hypothalamus [Markakis 2004, Kokoeva 2005, Lee 2012, Robins 2013, Maggi 2014]. Although the exact cellular origin of these newly generated neurons is still under debate [Lee 2012, Robins 2013], it is becoming

increasingly clear that hypothalamic neurogenesis plays an important role in energy metabolism and weight control [Kokoeva 2005, Lee 2012]. Anecdotal evidence also exists for potential adult neurogenesis in the piriform cortex, despite conflicting reports [Guo 2010, Klempin 2011].

In general, neurogenic niches share a unique cellular architecture that includes extensive vascularization [Mercier 2002, Hama 2011], the presence of neural stem cells [Doetsch 1999, Laywell 2000, Seri 2001, Seki 2007, Lee 2012, Robins 2013], non-neuronal cells including microglia [Battista 2006, Mercier 2002] and a characteristic extracellular matrix (ECM) composition [Fuchs 2004]. Adult neural stem cells are of astroglial origin and termed radial glia [Doetsch 1999, Laywell 2000, Malatesta 2000, Seri 2001, Noctor 2001, Kriegstein 2009] (RG). RGs retain many characteristics of embryonic neuroepithelial cells including an apical-basal polarity [Weigmann 1997, Chenn 1998], their contact with the basal lamina [Mercier 2002, Haubst 2006] and the expression of individual neuroepithelial markers, e.g. the intermediate filament nestin and the transcription factor sex determining region Y-box 2 (SOX2) [Cai 2002, Lagace 2007]. In addition, they exhibit astroglial properties, including the characteristic radial morphology, and express astrocyte specific markers, e.g. the intermediate filament vimentin [Schnitzer 1981, Dupouey 1985], the glutamate-aspartate transporter [Rothstein 1994, Hartfuss 2001] (GLAST) and glial fibrillary acidic protein [Levitt 1980, Abd-el-Basset 1988] (GFAP) [Götz 2005]. Besides self-renewal, RGs give rise to progenitor cells of an intermediate state that exhibit rapid proliferation and expansion of the neurogenic pool, termed transient amplifying or intermediate progenitors [Doetsch 1997, Steiner 2006, Pontious 2008, Ming 2011]. These so-called Type II (DG) and C cells (SVZ) give rise to doublecortin (Dcx) positive neuroblasts [Couillard-Despres 2005] that eventually enter a postmitotic stage, mature and integrate into their respective target circuit. Notably, the progression through each developmental stage is characterized by the expression of a combination of specific markers [Ming 2011].

Methods employed in order to identify newly generated neurons in the adult brain *in vivo* include the systemic administration of thymidine analogues [Bayer 1983, Altman 1965, Eriksson 1998, Kee 2002], retroviral labelling [vanPraag 2002, Carleton 2003] and inducible genetic targeting strategies [Feil 1996, Hunter 2005, Hayashi 2002], amongst others. Thymidine analogues such as ^{3}H-Thymidine [Bayer 1983, Lois 1994, Altman 1965, Altman 1969] (^{3}H-T) or Bromodeoxyuridine [del Rio 1989, Eriksson 1998, Kee 2002] (BrdU) are incorporated during DNA synthesis in the cell cycle S-phase [Takeda 2005] and thus label cells that undergo proliferation. New neurons are identified post mortem by autoradiography (^{3}H-T) and immunohistochemistry (BrdU), respectively. Similar to thymidine analogues, some classes of retrovirus can be used to label proliferating neurons, e.g. members of the gammaretroviral genus such as the murine leukaemia virus [Lewis 1994, vanPraag 2002, Matreyek 2013]. Retroviruses are required to integrate their viral genome into the host cell chromosomes in order to propagate their genetic material [Weiss 1984]. However, gammaviral DNA is only able to integrate once the nuclear envelope is dissolved and host cells progress through mitosis [Roe 1993, Lewis 1994, Matreyek2013]. Retroviral labelling of new neurons with fluorescent

proteins, for instance, has successfully been used to study their morphological development in both, the DG [vanPraag 2002] and SVZ [Carleton 2003]. Finally, it has become possible to target, label or manipulate increasingly selective subpopulations of progenitors and their progeny with inducible genetic constructs [Feil 1996, Feil 1997, Hunter 2005, Hayashi 2002, Mori 2006, Nakamura 2006]. Comprehensive knowledge of gene expression profiles of progenitor cells allowed for the development of so-called driver lines, in which inducible recombinase systems are under the control of progenitor cell- and sub-type specific promotors. The systemic administration of an exogenous ligand activates the recombination of a reporter sequence and, dependent on its genetic composition, enables, terminates or switches the expression of one or more genes of interest [Mori 2006, Nakamura 2006, Faiz2015]. The prevalent recombinase system employs the cre recombinase (cre) fused to the mutated hormone-binding domain of the oestrogen receptor (ERT2), which recombines loxP sites of the reporter gene construct upon binding the oestrogen analogue tamoxifen (TM) [Feil 1996, Feil 1997, Indra 1999, Hayashi 2002]. Nestin-creERT2 driver lines, for instance, have been used to study the contribution of nestin$^+$ stem cells to the generation of new neurons in the adult healthy brain and after injury [Lagace 2007, Li 2010, Faiz 2015].

The discovery of continuous neurogenesis in several discreet regions of the adult mammalian brain has raised hopes that these pools of new neurons might be harnessed for circuit repair after injury or disease [Lindvall 2004, Emsley 2005, Bellenchi 2013, Christie 2013, Sun 2014, Bazarek 2014]. Ideally, external factors could be employed to stimulate the production of new neurons, attract them to respective lesion sites, instruct their differentiation into appropriate neuronal cell types and promote their integration into target circuits. Indeed, infusion of various growth factors, e.g. epidermal growth factor [Craig 1996, Ninomiya 2006, Sun 2010] (EGF), fibroblast growth factor 2 [Kuhn 1997, Sun 2009] (FGF2) and brain-derived neurotrophic factor [Zigova 1998, Im 2010] (BDNF), has been shown to increase progenitor proliferation and/ or neurogenesis in the SVZ and DG, both in the healthy [Craig 1996, Kuhn 1997, Zigova1998] and diseased [Ninomiya 2006, Sun 2009, Sun 2010, Im 2010] brain [Christie 2013]. In addition, nerve growth factor (NGF) specifically promotes the survival, but not the proliferation of new neurons [Frielingsdorf 2007, Zhu 2011], while vascular endothelial growth factor (VEGF) and insulin-like growth factor (IGF) facilitate the migration of SVZ neuroblasts [Wittko 2009, Calvo 2011, Hurtado-Chong 2009].

Endogenous factors have further been implicated in affecting cellular lineage commitment, e.g. promoting a gliogenic over a neuronal cell fate [Doeppner 2011]. Interestingly, increased progenitor cell proliferation has also been observed in the SVZ in response to middle cerebral artery occlusion [Arvidsson 2002] (MCAO) and cortical aspiration lesion [Saha 2013], and in the DG after traumatic brain injury [Dash 2001, Chirumamilla 2002] (TBI). Moreover, vast numbers of SVZ derived Dcx$^+$ neurons infiltrate the penumbra of various cortical and striatal lesion types [Arvidsson 2002, Salman 2004, Li 2010, Saha 2013, Faiz 2015], a process generally regarded as the brains' attempt to repair the damaged tissue [Sun 2014, Bazarek 2014]. It seems however, that areas outside

of the neurogenic niches limit neuronal survival and maturation - although the striatum seems permissive for the maturation of a small fraction of infiltrated Dcx$^+$ cells [Arvidsson 2002, Li 2010], the overwhelming majority of progenitors reaching cortical lesion sites differentiate into astrocytes and oligodendroglial cells [Salman 2004, Buffo 2005, Saha 2013, Faiz 2015]. Successful integration of endogenous new neurons after injury has only been reported in a few isolated studies [Magavi 2000, Nakatomi 2002, Chen 2004, Ohira 2009]. For instance, after an ischemic lesion the pyramidal cell depleted CA1 region of the adult rat hippocampus could in part become repopulated with endogenous progenitors activated by the intraventricular infusion of EGF/ FGF2. New neurons differentiated into CA1 pyramidal cells and seemed to restore at least part of the hippocampal network [Nakatomi 2002]. Another study showed that the adult cortical layer 1 (L1) apparently harbours resting GABAergic progenitors that generate new inhibitory neurons in response to ischemia [Ohira 2009]. Newly generated glutamatergic neurons have also been described in deep cortical layers after induced apoptosis of cortico-thalamic neurons in layer 6 [Magavi 2000] (L6) and cortico-spinal motor neurons in L5 [Chen 2004] of adult mice. New neurons incorporated BrdU, expressed mature neuronal markers, e.g. neuronal nuclear antigen [Mullen 1992] (NeuN), and seemed to form sub-type specific projections to target regions of lost neurons. However, the cellular origin of these new neurons has not been identified to date, despite extensive studies over the last decade [Sohur 2012, Diaz 2013].

2.1.1.2 Parenchymal Progenitors - Astroglial and Oligodendroglial Cells

Besides the neurogenic niches, potential sources of new neurons have also been described in the parenchyma of various regions in the adult mammalian brain, including the neocortex [Palmer 1999], striatum [Reynolds 1992, Palmer 1995], substantia nigra [Lie 2002] and even the spinal cord [Ohori 2006, Barnabé-Heider 2010], amongst others [Kondo 2000, Götz 2015, Ming 2011, Nishiyama 2009]. These collectively termed parenchymal progenitors are characterized by their ability to form neurospheres [Pastrana 2011] out of single cells that can be passaged for multiple rounds *in vitro* and exhibit the potency to differentiate into multiple lineages - thus, displaying the capacity for self-renewal and multipotency [Reynolds 1992, Palmer 1999, Lie 2002, Sirko 2013], the hallmarks of stem cells [De Filippis 2012]. *In vivo*, however, parenchymal progenitors remain largely within their lineage, indicating that the adult brain restricts the stem cell capacity of potential progenitor cells outside of its neurogenic niches [Shihabuddin 2000, Götz 2015]. Indeed, even neuronal progenitors isolated from the SVZ revert to a gliogenic fate when transplanted outside of the niche environment [Seidenfaden 2006]. In contrast, when transplanted into the early postnatal brain, OB, hippocampus or striatum - all regions that have been shown to support neurogenesis [Lois 1993, Lois 1994, Altman 1965, Altman 1969, Ernst 2014] - both, parenchymal and niche derived progenitors are

capable of generating a variety of progeny including astrocytes, oligodendrocytes and neurons [Neumeister 2009, Franklin 1995, Nunes 2003, Aguirre 2004, Windrem 2004, Nishiyama 2009].

In general, neurospheres isolated from the healthy brain are rare, sustain low passage numbers and exhibit limited degrees of multipotency [Sirko 2013, Götz 2015]. The identity of parenchymal progenitors in the healthy brain is not known, but various hypotheses have pointed towards dormant progenitors [Ohira 2009], astrocytes [Götz 2015], NG2 cells [Nishiyama 2009] and pericytes [Nakagomi 2015]. In the diseased brain on the other hand, the peri-lesion environment undergoes marked changes: Protoplasmic astrocytes become re-activated, up-regulate oligodendrocyte transcription factor 2 (Olig2), express intermediate filaments such as glial fibrillary acidic protein (GFAP) and vimentin [Maxwell 1965, Ridet 1997, Pekny 2005, Zamanian 2012, Liu 2014], and start to proliferate [Buffo 2005, Chen 2008]; slow dividing or quiescent NG2 cells re-enter and/ or accelerate their cell cycle [Simon 2011]; resident microglia get activated [Kreutzberg 1996, Kawabori 2015] and in concert with infiltrating immune cells [Jolivel 2015] secrete cytokines and/ or growth factors [Giulian 1988, Kokaia 2012]. In addition, blood and cerebral spinal fluid (CSF) derived factors enter the injury site, e.g. the signalling molecule sonic hedgehog (SHH) [Sirko 2013]. This altered local environment seems to alleviate some of the restrictions the adult brain imposes on its resident parenchymal progenitors. As a result, the neurosphere-forming capacity following various types of insults, including traumatic brain injury (TBI), ischemia and stab wound lesion, is markedly increased [Kondo 2000, Belachew 2003, Buffo 2008, Sirko 2013, Faiz 2015].

Genetic fate mapping studies have identified reactive astrocytes [Buffo 2008, Sirko 2013, Faiz 2015, Götz 2015] and, to a lesser extent, $NG2^{+}$ oligodendrocyte progenitor cells (OPC) [Kondo 2000, Belachew 2003, Ligon 2006, Nishiyama 2009], as the main cellular sources of potential parenchymal progenitors. Reactive astrocytes isolated from GLAST-creERT2 mouse lines, for instance, have been shown to exhibit enhanced capacity for self-renewal and multipotency after stab wound lesions and cerebral ischemia, respectively [Buffo 2008, Sirko 2013]. Moreover, mimicking the lesion induced local enhancement of SHH infiltration *in vitro* was sufficient to induce neurosphere formation also in mature, non-reactive astrocytes [Sirko 2013]. Further, reactive astrocytes could be directly converted into neurons *in vivo*, following the forced expression of the pro-neuronal transcription factor (TF) achaete-scute homolog 1 (Ascl1) in the stroke lesioned cortex [Faiz 2015], and the neuroepithelial TF Sox2 in the striatum [Niu 2013], respectively. Also, inhibiting Olig2 function instructs a neuronal fate in reactive astrocytes *in vivo* after stab wound lesion [Buffo 2005].

While a basic consensus for the role of reactive astrocytes has become apparent over recent years, the contribution and capacity of NG2 cells is still heavily debated [Richardson 2011, Nishiyama 2014, Götz 2015]. Under normal physiological conditions, NG2 cells follow a prolonged cell cycle, proliferate continuously, and, besides self-renewal, give rise to oligodendrocytes [Simon 2011]. During development NG2 cells generate a substantial fraction of

astrocytes [Zhu 2011, Huang 2014] and it seems they retain this capacity in the adult brain under certain conditions [Franklin 1995, Windrem 2004, Zhao 2009]. For instance, OPC transplantation into areas of hypomyelination has been shown to result in the generation of both, remyelinating oligodendrocytes and astrocytes [Franklin 1995, Windrem 2004]. The same bi-potent capacity is displayed in response to acute focal and systemic lesions [Zhao 2009]. In addition isolated NG2 cells *in vitro* can be reverted to a state of multipotency [Kondo 2000, Belachew 2003] and NG2 cells have recently been shown to give rise to new neurons *in vivo*, following the ectopic expression of Sox2 after a cortical stab wound lesion [Heinrich 2014].

Taken together, endogenous new neurons derived from the neurogenic niches, as well as potential progenitors dispersed in the brain parenchyma, could serve as future targets for cellular replacement therapies (Fig. 1). Continuously generated new neurons in neurogenic niches will require appropriate cues for long-range attraction and migration, while parenchymal progenitors already reside in the vicinity of lesioned areas, but require instructive signals to adopt a neurogenic fate. Both subsequently depend on local factors to promote the maturation and integration into damaged circuits.

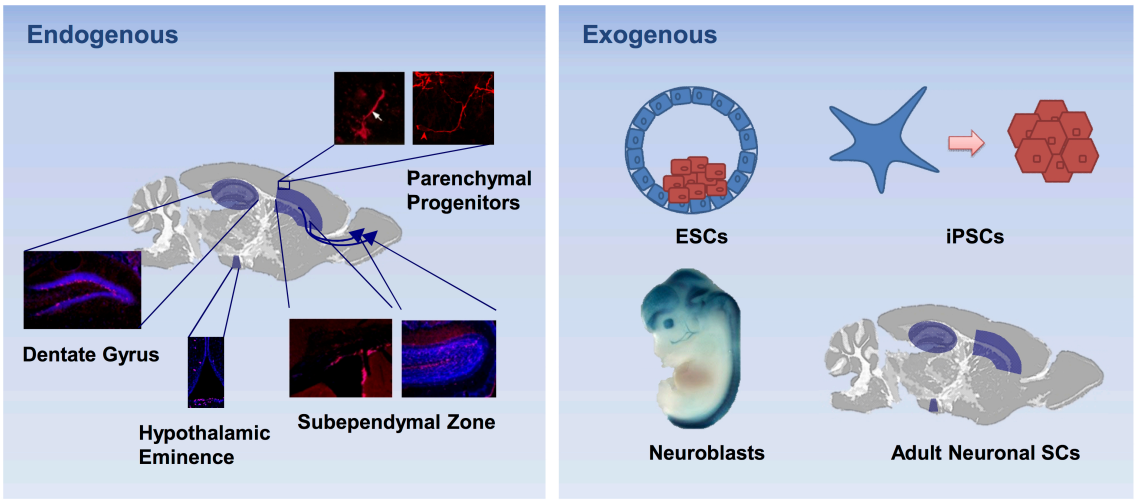

Fig. 1. Potential sources of new neurons for circuit repair. Left, Endogenous sources of new neurons include known neurogenic niches in the adult brain, the dentate gyrus of the hippocampal formation, the subependymal zone lining the lateral ventricles and the medial hypothalamic eminence (modified from Lee et al., 2012). Potential resting or (re-) activated parenchymal progenitors include cells of the astroglial and oligodendroglial lineage (modified from Leavitt et al., 1999 and Heinrich et al., 2014, respectively). Right, Exogenous sources of new neurons suitable for transplantation include embryonic stem cells (ESCs), induced pluripotent stem cells (iPSCs), adult neuronal stem cells and embryonic neuroblasts (modified from Gorski et al., 2002).

2.1.2 Exogenous Sources of New Neurons for Repair

Compared to endogenous sources, the exogenous supply of new neurons offers both, the advantage of the direct, targeted delivery to affected brain areas [Cetin 2006] e.g. via transplantation, as well as the possibility to instruct the required neuronal fate in advance *in vitro* [Kriks 2011, Espuny-Camacho 2013]. An apparent disadvantage constitutes the invasive nature of any cell transplantation and, as a consequence, the concurrent immune reaction [Marion 1990, Okura 1997]. Consequently, dependent on the source of donor cells, recipients might require extensive post transplant immunosuppressive drug regimes in order to avoid graft rejection [Marion 1990, Okura 1997, Piccini 2005, Rosser 2012, Barker 2013]. In the early 1980ies, several successful studies reported the alleviation of motor deficits following the transplantation of rat [Perlow 1979], mouse [Björklund 1982] and human [Brundin 1986] fetal dopaminergic neurons into the striatum of a rat model of Parkinson's disease (PD), respectively, paving the way for subsequent clinical trials.

In 1987, the first PD patients received striatal grafts of fetal ventral mesencephalic dopaminergic neurons [Piccini 2000, Barker 2013]. Since, a multitude of clinical trials has been conducted using various sources of donor cells, including blastocyst derived embryonic stem cells [Vawda 2012], fetal neuronal progenitors [Rosser 2012], mesenchymal stem cells [Barker 2013, Bang 2016], autologous bone marrow mononuclear cells [Bang 2016, ClinicalTrial.gov NCT02028104] and even Schwann cells and oligodendrocytes [Vawda 2012], in order to assess the safety and efficacy of cellular therapy in various CNS disease conditions, including Huntington's disease (HD) [Rosser 2012], spinal cord injury (SCI) [Vawda 2012], stroke [Bang 2016] and traumatic brain injury (TBI) [ClinicalTrial.gov NCT02028104]. Despite these extensive efforts, the procedure has to date not been approved as common medical practice for any disease condition [Piccini 2005, Rosser 2012, Vawda 2012, Barker 2013, Bang 2016]. In general, treatment outcome has been either inconsistent between studies, highly variable between patients, or both [Rosser 2012, Vawda 2012, Barker 2013, Bang 2016]. In addition various studies reported side effects, e.g. the development of allodynia after SCI grafts [Hofstetter 2005] and dyskinesia in a substantial fraction of PD patients that had received fetal nigral transplants [Olanow 2003], respectively. For other conditions the available data is simply not extensive enough to assess potential risks and benefits [Vawda 2012, Lemmens 2013, Bang 2016]. However, some alleviation of symptoms and individual reports of functional improvements have been observed in PD patients that had received striatal grafts [Piccini 2005, Barker 2013], and in HD patients after fetal neuronal grafts [Bachoud-Lévi 2000, Bachoud-Lévi 2009, Rosser 2012].

Taken together, it is still not clear, whether donor cells actively take part in the genuine reconstruction of damaged circuits after transplantation. Also, donor neurons derived from fetal brains have been shown to exert trophic [Chiba 2003], neuroprotective [Chiba 2003, Aharonowiz 2008], and/ or immunomodulatory effects [Krampera 2006, Aharonowiz 2008] on the host tissue. The impact of

these collectively termed by-stander effects varies extensively dependent on host status, e.g. genetic background, general health and age, and could explain both, individual reports of positive treatment outcome, as well as the observed high degree of variability between patients [Thompson 2015].

While cell therapy in PD and HD is aimed at replacing relatively homogenous neuronal populations in comparatively simple, mainly local striatal circuits [Vonsattel 1985, Blandini 2000], the repair of acute injuries that often affect the cerebral cortex, e.g. TBI [Gao 2011] and stroke [Graham 2002], involve the replacement of multiple neuronal cell types and the reconstruction of complex brain-wide circuits. The substitution of cortical pyramidal neurons seems especially challenging, since their primary function - the correct spatio-temporal integration of thousands of presynaptic inputs - requires both, extensive and precise wiring with a multitude of cortical and sub-cortical areas [Yoshimura 2005, Spruston 2008, Brown 2009]. Pre-clinical studies in animal models aim at elucidating the extent to which complex circuits in the cerebral cortex can be restored, which types of donor cells yield the most promising results and to what degree functional deficits can be reverted.

2.1.2.1 Reconstruction of Cortical Circuits in Animal Models of Injury and Disease

Attempts at cortical circuit reconstruction in animal models of injury and disease have employed whole tissue grafts [Soares 1991, Girman 1994, Gaillard 1998, Gaillard 2007], dissociated embryonic neurons [Hernit-Grant 1996, Shin 2000, Fricker-Gates 2002, Southwell 2010, Tang 2014, Davis 2015] and embryonic, as well as induced pluripotent stem cell (ESC; iPSC) derived pyramidal neurons [Ideguchi 2010, Espuny-Camacho 2013, Michelsen 2015], amongst others (Fig. 1). In contrast to slowly progressing neurodegenerative diseases such as PD and HD, acute cortical injuries exhibit a limited time window for intervention [Soares 1991, Lemmens 2013]. Cortical embryonic tissue grafts, for instance, fail to develop host-graft interactions in a rat model of TBI, if transplantation does not occur within 2 weeks after injury [Soares 1991]. Despite a positive effect on glial scar development and extensive reciprocal host-graft innervation however, no improvements of motor deficits could be detected [Soares 1991]. Indeed, grafted neurons exhibit a surprising capacity to re-innervate appropriate target regions [Gaillard 2007, Espuny-Camacho 2013, Michelsen 2015] in an area and layer specific manner [Hernit-Grant 1996, Shin 2000, Fricker-Gates 2002, Ideguchi 2010]. For instance, *in vitro* differentiated, murine ESC derived pyramidal neurons of deep layer identity correctly projected to the dorsal and ventral superior colliculus after transplantation into the neonatal mouse primary visual (V1) and somatosensory cortex (S1), respectively. Grafting of the same neurons into the motor cortex (M1) by contrast, did not result in fibres entering the superior colliculus, but in prominent projections into the descending spinal tract [Ideguchi 2010]. Further, successful axon outgrowth and correct target projections seem to be dependent on matching graft and host

area identity [Ideguchi 2010, Michelsen 2015]. Area identity of projection neurons is defined during early embryonic development when secreted morphogens and signalling molecules induce the graded expression of area specific TFs, dependent on the relative position of each neuron in the cortical primordium [Grove 2003, Greig 2013]. Accordingly, embryonic motor cortex derived neurons fail to generate appropriate target projections after transplantation into the ibotenic acid lesioned V1, and vice versa, despite robust graft survival [Michelsen 2015].

To date, host-derived afferents to grafted neurons have been investigated only occasionally [Girma 1994, Gaillard 1998, Michelsen 2015]. Early studies have shown that individual thalamic projections originating in the lateral geniculate nucleus (LGN) are able to regrow and re-innervate fetal cortical tissue grafts transplanted into the aspiration-lesioned V1 of adult rats [Girman 1994, Gaillard 1998]. Retrograde tracer injections into whole V1 tissue grafts further revealed some correct afferent projections from neighbouring cortical areas. However, cortical afferents exclusively originated in deep layers, mainly layer 6 (L6) [Gaillard 1998], and the density of afferent fibre innervation of two prominent input areas, the LGN and contralateral V1, has been shown to be markedly reduced compared to intact neighbouring tissue [Michelsen 2015]. Thus, in contrast to the successful innervation of appropriate target areas, the formation of afferent connections is impaired and incomplete.

Recent studies have progressed from whole tissue grafts to dissociated embryonic neurons [Hernit-Grant 1996, Shin 2000, Fricker-Gates 2002, Southwell 2010, Tang 2014, Davis 2015] and *in vitro* differentiated ESC/ iPSC derived pyramidal cells [Ideguchi 2010, Espuny-Camacho 2013, Michelsen 2015]. Upon transplantation, these donor neurons have lost their original morphology and all previous synaptic connections. They are subsequently required to re-develop morphologically and re-establish all afferent and efferent connections within the host cortical network, before they are able to adopt a meaningful function within the target circuit. While the morphogenesis of grafted neurons has not been described to date, it has been shown that individual transplanted ESC/ iPSC derived cells are able to acquire a pyramidal cell-like morphology [Ideguchi 2010, Espuny-Camacho 2013], form synaptic connections [Espuny-Camacho 2013, Michelsen 2015] and exhibit some passive electrophysiological properties reminiscent of excitatory neurons [Espuny-Camacho 2013, Michelsen 2015].

However, data on the *in vivo* physiology of transplanted excitatory neurons in the cortex is extremely limited. The current knowledge is comprised of extracellular field potential recordings in whole tissue grafts, as well as basic extracellular recordings in ESC derived neurons, transplanted into the lesioned adult V1, respectively [Gaillard 1998, Michelsen 2015]. Both studies report simple responses to light flashes, but otherwise did not characterise the physiological properties and functional network integration of grafted neurons [Gaillard 1998, Michelsen 2015]. Thus, previously reported LGN projections to grafted neurons [Girman 1994, Gaillard 1998], albeit limited [Michelsen 2015], seem to be able to convey some basic visual information.

Taken together, efferent axonal projections of transplanted neurons exhibit a surprising capacity and accuracy to re-innervate correct target areas. However, given the insufficient information on afferent connectivity and functional integration of pre-synaptic signals, it is still an open question, whether transplanted neurons are capable of receiving and processing multi-area inputs within the host circuitry and eventually, are able to substitute lost neurons.

2.2 The Primary Visual Cortex As a Model to Study Circuit Repair

A prerequisite for the study of the functional integration of new neurons is the possibility to assess the degree to which any adopted function is appropriate for the target circuit. Behaviour is orchestrated by the activity of ensembles of hundreds of neurons across many brain areas, and thus it is difficult to delineate the contribution of an individual cell to the behavioural output. Likewise, it is close to impossible to judge the adequacy of a neuron's function based on the isolated activity pattern of that individual cell. In primary sensory cortical areas however, individual neurons represent key features of the respective modality's sensory space [Dräger 1975, Simons 1979, Rothschild 2010]. In V1 for instance, these features include receptive field properties such as location in visual space, as well as selectivity for orientation/ direction and spatio-temporal dynamics of high contrast transitions [Hubel 1962, Dräger 1975, Niell 2008, Marshel 2011]. Therefore, the exposure to a visual stimulus of defined properties will elicit a characteristic functional response profile in individual successfully integrated new neurons, allowing the assessment of their functional integration at the single cell level.

2.2.1 The Mouse Visual System

Despite poor acuity and low resolution [Prusky 2004], mice rely on vision for innate defence and protective behaviour [Liang 2015] and can be trained to depend on vision in a variety of behavioural tasks [Andermann 2010, Kreile 2012, Pinto 2013, Glickfeld 2013]. In short, visual information detected by photoreceptors is passed through the retinal circuit onto retinal ganglion cells [Dunn 2014] and relayed to the LGN via the optic nerve [Forrester 1967]. At the chiasm, optic nerve fibres from both eyes cross, and up to ~20% of retinal ganglion cell axons diverge [Rebsam2012] and project to the ipsilateral LGN [Reese 1988, Godement 1990, Marcus 1995]. Visual information reaches the 6-layered primary visual cortex via projections from the LGN, which terminate predominantly in layer 4 (L4), and to a lesser extent in L1, layer 2/3 (L2/3) and 6 [Marshel 2011, Piscopo 2013, Constantinople 2013, Cruz-Martin 2014] (Fig. 2A).

The V1 intra-cortical circuit follows a largely hierarchical anatomical organization [Gilbert 1983, Bannister 2005, Xu 2016]. As a general rule, L4 glutamatergic spiny stellate cells synapse onto L2/3 pyramidal neurons [Gilbert 1979, Xu 2016], which in turn connect to large pyramids in layer 5

(L5) [Gilbert 1983, Dantzker 2000, Xu 2016]. L5 neurons subsequently project to layer 6 (L6) pyramidal cells, but also provide excitatory feedback projections to L2/3 [Gilbert 1983, Xu 2016]. Besides intra-cortical feedback to L4, L6 provides excitatory feedback to L5 [Kim 2014] and together, L5 and L6 constitute the main output layers of V1. While L6 pyramidal neurons extensively innervate the LGN [Tömböl 1975, Olsen 2012, Bortone 2014], L5 neurons predominantly project to sub-cortical targets such as the superior colliculus [Solomon 1993], the lateral posterior nucleus of the thalamus [Lund 1975, Roth 2016] and the pons [Albus 1977, Morishima 2011], as well as to other cortical areas e.g. the contralateral V1 [Hübener 1988] and higher visual areas [Lur 2016]. L2/3 pyramidal neurons on the other hand, engage in cortico-cortical connections to higher visual, other sensory and association areas [Gilbert 1975, Olavarria 1982, Olavarria 1989, Wang 2012, Charbonneau 2012], which in turn provide feedback projections to the apical dendritic tufts of V1 pyramidal cells in L1 [Larkum 2013].

Within the binocular zone at the lateral V1 border [Dräger 1975, Dräger 1978], L2/3 neurons also exhibit extensive projections to homotopic locations in the contralateral hemisphere [Cusick 1981, Miller 1984, Rhoades 1984, Olavarria 1984, Hübener 1988]. These interhemispheric cortico-cortical connections, together with input from both eyes via the LGN, render 70 to 90% of neurons in this area binocularly responsive [Diao 1983, Dräger 1978, Lepore 1992, Pietrasanta 2012, Dehmel 2014]. The main part of V1 however, the monocular area, receives predominant input from the contralateral eye only [Dräger 1975, Dräger 1978]. Importantly, V1 exhibits a topographic representation of visual space, the retinotopic map. In short, a certain location in visual space is represented at a defined anatomical position in V1, and the receptive fields (RF) of neighbouring neurons are aligned in visual space [Dräger 1975, Wagor 1980, Schuett 2002, Garrett 2014].

The RFs of individual neurons differ in size and structure [Hubel 1959, Hubel 1962, Wang 2007a, Niell 2008]. Neurons at the medial border generally exhibit larger RFs, whereas RF size is smallest in posterior-lateral V1 [Wang 2007a], representing the central visual field. In addition, based on RF structure, neurons are classified into simple and complex cells [Hubel 1959, Hubel 1962, Niell 2008]. In response to light/ dark stimulation, simple cells exhibit distinctive sub-regions with elongated alternating ON and OFF fields, whereas the RF of complex cells appears homogenous with superimposed ON/ OFF fields. In mouse, increased numbers of simple cells are found in L2/3 and L4, while L5 is predominantly comprised of complex cells [Niell 2008]. Besides RF position, size and structure, individual neurons in V1 also exhibit a preference for the orientation and/ or direction, as well as the spatio-temporal dynamics of high contrast transitions within their RF [Hubel 1962, Dräger 1975, Niell 2008, Marshel 2011].

2.2.2 L2/3 Pyramidal Neurons in V1

L2/3 serves as the first integrative layer for visual information in V1 [Hubel 1962, Niell 2008, Cossell 2015]. Excitatory projection neurons in L2/3 are the main recipients of feedforward excitation

generated by L4 in response to sensory stimuli [Gilbert 1979, Xu 2016], of excitatory and inhibitory intra-cortical feedback [Gilbert 1983, Xu 2016], as well as long-range cortico-cortical [Olavarria 1984, Larkum 2013] and thalamocortical projections [Morgenstern 2016]. They possess the typical morphological characteristics of pyramidal cells [Peters 1970, Miller 1981, Miller 1988, Bannister 2005, Spruston 2008]. In short, a prominent apical dendrite extends towards the pial surface and branches into secondary and tertiary processes. Basal dendrites with infrequent branch points emanate from the base of a rather large, pyramidal shaped cell body and extend sideways, as well as towards L4. Despite this general outline, pyramidal neurons in different layers - and often areas as well as species [Peters 1970, Kasper 1994, Gao 2004, Elston 2014] - differ considerably [Bannister 2005, Spruston 2008] (see Fig. 2C). For instance, L2/3 pyramidal cells exhibit shorter apical dendrites with simpler distal tufts, but a higher number of oblique processes branching from the main apical dendrite compared to L5 neurons [Spruston 2008]. In addition, the normal morphological spectrum of adult mammalian pyramidal cells also includes approximately 5 - 20% of neurons with an atypical orientation across all cortical layers, namely an oblique or even inverted apical dendrite [van der Loos 1965, Miller 1988, Polleux 2000, Mendizabal-Zubiaga 2007]. Despite their deviation from the classical orientation, atypically oriented pyramidal neurons display normal development and maturation [Miller 1988, Parnavela 1983], and do not differ in their physiological properties. For instance, in V1 they exhibit typical receptive field properties of both, simple and complex cells [Parnavelas 1983].

L2/3 pyramidal neurons receive excitatory afferent connections onto dendritic spines, specialized membrane protrusions typically harbouring a fully functional postsynaptic apparatus, and convey their output via axonal boutons containing the presynaptic machinery [Miller 1981b, Spruston 2008, Harris 2012] (see Fig. 2D). Thus, dendritic spines and axonal boutons are generally regarded as reliable structural correlates of synapses [Trachtenberg 2002, Spruston 2008, Harris 2012]. In the adult, synapses are stable but at the same time, allow for sufficient structural plasticity to adapt to a changing environment [Trachtenberg 2002, Holtmaat 2009b], compensate for altered sensory input [Keck 2008, Hofer 2009, Yamahachi 2009, Marik 2010] and adopt new memories [Lai 2012, Hayashi-Takagi 2015, Li 2017]. Accordingly, in V1 dendritic spines and axonal boutons form stable synaptic connections, but exhibit marked changes in both, densities and turnover after e.g. loss of visual input [Keck 2008, Hofer 2009, Yamahachi 2009]. Also, this form of structural plasticity is area and cell type specific [Holtmaat 2009b].

Although V1 L2/3 pyramidal neurons do not constitute a homogenous population [Tasic 2016, Luebke 2017], common molecular programs define their area and subtype specific identity during development [Greig 2013] (Fig. 2B). For instance, activating enhancer binding protein 2γ (AP2γ) specifically promotes the formation of L2/3 neurons in the occipital cortex by regulating neuronal intermediate progenitor expansion during late corticogenesis [Pinto 2009]. Also, some of the key regulators of excitatory upper layer projection neurons continue to be expressed in

the adult. The protein cut like homeobox 1 (Cux1) is not only expressed during neurogenesis of L2/3 neurons, but serves as a marker of L2/3 projection neuron identity [Nieto 2004, Zimmer 2004], including CPNs [Molyneaux 2009], in the adult brain.

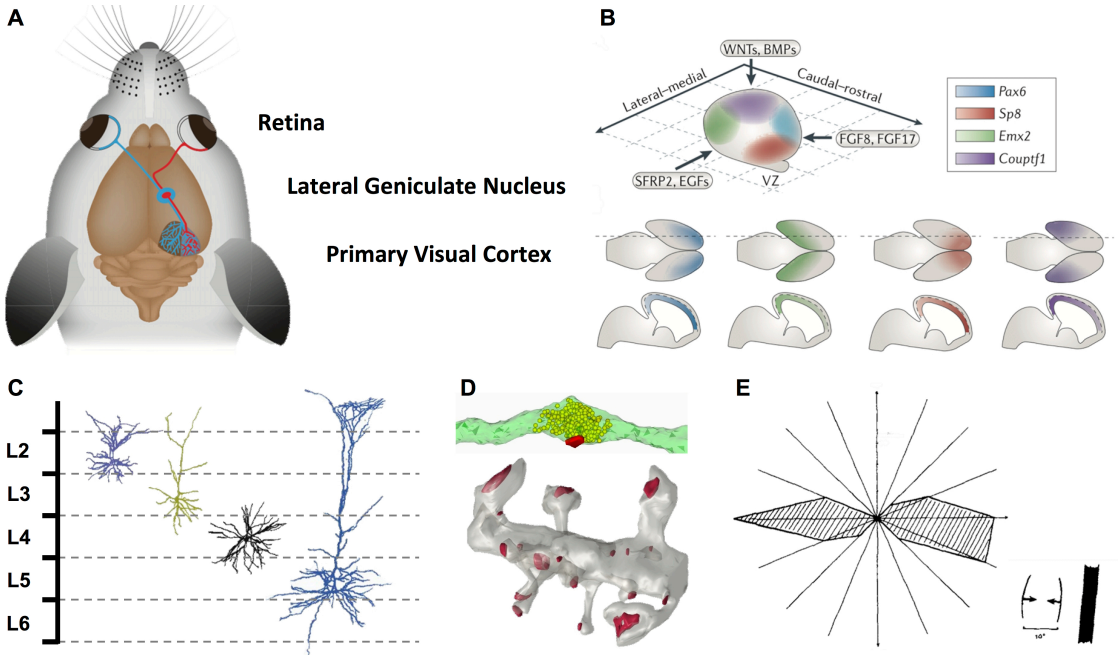

Fig. 2. The mouse visual system – area and layer specific features of excitatory projection neurons in V1. **(A)** Anatomy of the mouse visual system (modified from Levelt and Hübener, 2012). Visual information sensed by the retina is relayed via the lateral geniculate nucleus to the primary visual cortex (V1). **(B)** Spatio-temporally orchestrated molecular programs define area and subtype specific neuronal identity during development (modified from Greig et al., 2013). **(C)** Subtypes of cortical excitatory neurons display layer specific morphology (modified from Bannister et al., 2005). **(D)** Axonal boutons (top) and dendritic spines (bottom) harbour pre- and post-synaptic machineries, respectively (modified from Kristin M. Harris, *SynapseWeb* http://synapseweb.clm.utexas.edu). **(E)** Excitatory projection neurons in V1 exhibit a distinct preference for the orientation and/ or direction of high contrast transitions, e.g. bars moving in different directions. The polar-plot on the left shows a neuron's response (hatched region) to different orientations and directions of a moving bar (modified from Dräger et al., 1975).

As outlined above, individual neurons in V1 encode for key receptive field properties such as position in the visual field, RF size and structure, orientation and/ or direction selectivity, as well as spatio-temporal frequency [Hubel 1962, Dräger 1975, Wagor 1980, Schuett 2002, Wang 2007a, Niell 2008, Marshel 2011, Garrett 2014]. L2/3 neurons are sharply tuned and generally exhibit a strong preference for one orientation and/ or direction over others [Dräger 1975, Niell 2008, Marschel 2011] (Fig. 2E). While a

subset of ganglion cells in the retina already exhibits a strong preference for motion direction [Barlow 1965, Bos 2016] that is passed on the ascending visual pathway [Shi 2017], orientation selectivity is thought to arise at the cortical level.

The mechanism underlying orientation selectivity was first proposed by Hubel and Wiesel following recordings in cat visual cortex [Hubel 1962]. In short, multiple LGN neurons with concentric centre-surround RFs that are aligned along one axis in visual space are thought to provide convergent input onto individual neurons in V1. However, RF structure of LGN neurons differs markedly across species [Chapman 1991, Reid 1995, Ferster 1996, Scholl 2013, Van Hooser 2013]. In mouse, at least some LGN neurons already exhibit an elongated RF and accordingly, a week tuning for orientation and/ or direction [Scholl 2013]. In addition, the dorsal LGN receives strong input from direction selective retinal ganglion cells and in turn, conveys direction selective input directly onto L2/3 neurons [Cruz-Martin 2014, Morgenstern 2016]. Thus, in addition to the proposed mechanisms of de-novo generation of orientation selectivity within L4 or L2/3 of V1 [Hubel 1962, Chapman 1991, Reid 1995, Ferster 1996, Scholl 2013, Van Hooser 2013], intra-cortical processing in these layers also seems to enhance and refine already tuned LGN input. For instance, selectivity is thought to be promoted by shared feed-forward inputs onto preferentially connected L2/3 neurons [Yu 2012, Li 2012, Ko 2013, Morgenstern 2016], and pronounced but unselective lateral inhibition decreases overall responsiveness to weak inputs [Niell 2008, Kerlin 2010, Hofer 2011, Li 2015]. Anatomically, L2/3 neurons with similar orientation and/ or direction preference are randomly distributed across mouse V1 [Ohki 2005, Espinosa 2012] and, on a population level, the tuning preference distributes characteristically across stimulus space [Dräger 1975], while the average selectivity differs from other layers and areas [Niell 2008, Marshel 2011].

Taken together, in many aspects V1 L2/3 pyramidal neurons constitute a homogenous population with distinct structural and functional properties that are experimentally accessible on the level of the individual neuron. Key parameters of visual information are represented in the response profile of individual L2/3 cells and, at the same time, distribute characteristically across the L2/3 population. Thus, L2/3 pyramidal neurons present an ideal target population to investigate the appropriate structural and functional integration of new neurons into previously damaged brain circuits.

2.3 Aim of the Study

A fundamental question in studying the reconstruction of neural circuits damaged due to injury or disease is whether new neurons are in fact capable of appropriately integrating into a target circuit. New neurons are not only required to assume the correct area and cell type specific identity and morphology, but also have to form synaptic connections with all appropriate pre- and post-synaptic areas and eventually, adopt a meaningful function within the pre-existing circuit. These aspects are especially critical in the regeneration of cortical excitatory projection neurons, given their crucial function in the integration of both, local intra- and inter-cortical signals, as well as long-range projections from various input areas throughout the brain [Yoshimura 2005, Spruston 2008, Brown 2009]. Ideally, a fully integrated new neuron becomes structurally and functionally indistinguishable from neurons that have previously been lost.

While numerous studies over the last two decades have focused on the survival and axonal projection pattern of new cortical pyramidal neurons derived from both, endogenous [Buffo 2005, Heinrich 2014, Faiz 2015] and exogenous sources [Fricker-Gates 2002, Gaillard 2007, Ideguchi 2010, Espuny-Camacho 2013, Michelsen 2015] in various physiological and experimental paradigms, host-derived afferent input onto new neurons has been investigated only incidentally [Girman 1994, Gaillard 1998, Michelsen 2015]. Moreover, data on the *in vivo* physiology of newly integrated neurons is extremely scarce and limited to two studies employing *in vivo* extracellular field recordings in whole tissue and ESC derived neuronal grafts following extensive cortical aspiration [Gaillard 1998, Michelsen 2015]. To date, it is not known whether individual cortical pyramidal neurons are capable of acquiring a comprehensive functional spectrum typical for the injured target network. Finally, no data is available on the development and the integration process of individual neurons over time, including their morphological development and the process by which new neurons acquire function as a result of their progressive integration into the network. Taken together, it is of particular interest to study the capacity of new endogenous or exogenous neurons to substitute previously lost excitatory projection neurons in adult neocortical circuits on the level of individual cells across time. Specifically, delineating the individual morphological development, synaptogenesis, as well as the progressive acquisition and maturation of functional properties will help to understand, whether i) individual new neurons are capable of adopting a meaningful function within their cortical target network and ii) adult neocortical circuits retain the capacity to replace lost excitatory projection neurons by assimilating new cells into the pre-existing network.

In this thesis, I investigate the integration of exogenous (transplanted; see 1.1) and endogenous (lesion induced; see 5.3) new neurons into V1 of adult mice previously deprived of cortical L2/3 projection neurons. Targeted ablation of L2/3 neurons is achieved using a

photolytic lesion model [Macklis 1991] that is based on the selective laser photoactivation of the chromophore chlorine e6 (Ce6), the subsequent production of intracellular reactive oxygen species [Sheen 1994, Tsay 2007] and the resulting non-invasive, spatially restricted, apoptotic cell death of Ce6-labelled neurons [Macklis 1991, Madison 1993]. In a first step, the model is adapted to specifically eliminate L2/3 neurons in the binocular zone of V1 (see 5.1).

In order to test the capacity of exogenous new neurons to appropriately integrate and substitute lost L2/3 neurons (see 1.1), embryonic donor cells labelled with genetically encoded calcium indicators (GECIs) [Chen 2013, Thestrup 2014] and/ or fluorescent proteins (GFP, tdT) [Gorski 2002, Nakamura 2006, Madisen 2010] are transplanted into the lesion site. A cranial window implant [Holtmaat 2009a] allows visual access for repeated *in vivo* two-photon imaging [Denk 1990, Stosiek 2003, Helmchen 2005, Andermann 2010] of individual identified transplanted neurons. The overall morphological development, synaptogenesis and pre- and post-synaptic dynamics are investigated starting 3 days post transplantation (dpt), and individual new neurons are followed up to 11 months pt. In order to assess whether transplanted cells develop key receptive field properties typical for L2/3 projection neurons, host mice are repeatedly presented with full field gratings moving in different directions up to 15 weeks pt. The responses of new neurons are recorded as changes in GECI fluorescence relative to baseline [Chen 2013, Thestrup 2014] in somata, axons and dendritic spines.

Photolytic ablation of deep layer neurons in the juvenile mouse forebrain [Magavi 2000] and motor cortex [Chen 2004] has previously been reported to induce a small number of endogenous new neurons, based on the incorporation of the thymidine analogue bromodeoxyuridine (BrdU) and the co-labelling with mature neuronal markers [Magavi 2000, Chen 2004]. In the final part of this thesis, I investigate whether photolytic ablation of L2/3 projection neurons also results in the generation of endogenous new neurons and whether these induced neurons exhibit the potential to substitute lost L2/3 cells (see 5.3). Since the origin of the reported induced new neurons has not been identified to date [Brill 2009, Sohur 2012], mouse lines expressing GFP in neuronal and astroglial [Mori 2006], as well as oligodendroglial [Simon 2012] progenitor populations, respectively, are subjected to photolytic lesion. Combining BrdU treatment with chronic *in vivo* two-photon imaging of a sizable volume of lesioned V1, allows for the identification of both, new neurons generated by proliferating resident progenitor cells, as well as any progenitor derived neurons migrating into the lesion site.

3 Methods

3.1 Mice and Anaesthesia

All animal experiments were carried out in compliance with the institutional guidelines of the Max Planck Society, the Ludwig-Maximilians-Universität and the local government (Regierung von Oberbayern).

Data for this study is derived from a total of 53 adult mice and 14 donor embryos (male and female). Seven C57BL/6J and 2 Thy1.GFP-M mice were used for the characterization of the lesion model. 16 adult host mice (female) received grafts from 14 donor embryos (male and female). For chronic structural in vivo two-photon imaging of transplanted cells we used Emx1-Cre [Gorski 2002] x CAG-CAT-GFP (also called CAG-GFP) [Nakamura 2006] donor cells and Ai9 (Rosa-CAG-LSL-tdTomato reporter mice, Jackson laboratory, JAX Stock #007905) [Madisen 2010] host mice (8 donors, 11 hosts). For functional in vivo two-photon imaging of transplanted cells we used Emx1-Cre [Gorski 2002] x Ai9 donor cells and C57BL/6J host mice (6 donors, 5 hosts). Twenty-six GLAST-creERT2 [Mori 2006] x CAG-GFP and 2 SOX10-cre [Simon 2012] x CAG-GFP mice were used to test the contribution of induced neurogenesis to circuit regeneration after apoptotic photolesion. Four GLAST-creERT2 x CAG-GFP mice underwent chronic two-photon imaging and 12 were subjected to various control treatments (see table Fig. 30A).

Mice were housed in a 12:12 hour light-dark cycle and were a minimum of 8 and a maximum of 14 weeks old at the time they entered the experiment. GLAST-creERT2 x CAG-GFP mice received tamoxifen (TM) treatment (see 3.3) one week prior to their first surgery. For transplantation experiments, host mice were only subjected to surgeries once a plug was confirmed in prospective mothers of donor embryos. Surgeries were performed aseptically under anaesthesia with a mixture of fentanyl (0.05 $mgkg^{-1}$), midazolam (5 $mgkg^{-1}$) and medetomidine (0.5 $mgkg^{-1}$). After surgery, anaesthesia was terminated with atipamezol (2.5 $mgkg^{-1}$), flumazenil (0.5 $mgkg^{-1}$) and naloxone (1.2 $mgkg^{-1}$). Carprofen (5 $mgkg^{-1}$) was administered as analgesic.

3.2 Timed-Pregnant Mice

Prospective mothers of donor embryos were checked for plugs twice a day. The day of plug was defined as E0.5, and male mice were then removed from the cage. Typically, pregnancy could first be detected between E12.5 and E14.5.

3.3 Tamoxifen Treatment

GLAST-creERT2 x CAG-GFP mice were treated with tamoxifen (TM) in order to induce GFP expression. Mice received 3 doses (one every 48 h) of 10 mg TM in corn oil (40 mg/mL) with 5% ethanol via oral gavaging. In short, a stainless steel re-usable feeding needle (20 gauge, smooth ball tip) was placed into the mouth of securely restraint mice. The head was slightly extended backward by directing the needle towards the roof of the mouth. The animal was allowed to swallow the tip and gravity pulled the needle down the oesophagus. TM was administered and the needle was gently removed. Mice were closely monitored for any signs of complication. TM treatment was finished 1 week prior to the first surgery.

3.4 Chlorin e6 Nanobeads Preparation

Chlorin e6 (Ce6) was covalently linked to rhodamine-labelled latex nanobeads [Katz 1984] (RetroBeads) via carbodiimide conjugation, as described previously [Madison 1993]. In short, 1.5 ml of pre-cooled Ce6 solution (0.597 mg/ml in 0.01 M phosphate buffer [PB], pH 7.4) was mixed with 5 mg 1-ethyl-3-(3-dimethylaminopropyl)-carbodiimide (EDC) and incubated at 4 °C for 30 min. 750 µl of activated Ce6 solution was then added to 12.5 µl of red RetroBeads diluted in 100 µl PB. The solution was incubated at room temperature (RT) for 60 min under slow agitation on a rotating shaker, light shielded. The reaction was stopped by adding 335 µl of 0.1 M glycine buffer (pH 8.0), the solution was transferred to an ultracentrifuge tube, and an excess of PB was added. Conjugated Ce6 beads were pelleted by ultracentrifugation (30 min, 100.000 g, 20 °C) and washed at least 3 times with PB. The final pellet was re-suspended in 50 µl PB. Beads were stored in a humid chamber at 4 °C and used within one month.

3.5 Laser Ablation of $Ce6^+$ Cells *In Vitro*

We tested the specificity of laser ablation of Ce6-labelled cells *in vitro.* PC-12 cells were cultured in RPMI 1640 with GlutaMax, 10% horse serum (HS), 5% fetal bovine serum (FBS) and penicillin/ streptomycin (Pen/Strep). At 70 to 80% confluency, cells were subjected to a standard trypsinization protocol and plated at a density of 1 million cells/ 6-well (poly-L-lysine pre-coated). After successful adherence overnight (o/n), the medium was replaced by culture medium containing Ce6 beads (1 µl/ml) and incubated for 24 h. For laser photoactivation, an area of approx. 2 mm diameter was marked at the bottom of each well. Cells were washed with phosphate-buffered saline (PBS) without $Ca2^+Mg2^+$ and laser light (670 nm, Flatbeam Laser) was applied to the marked areas (once per well, 2-3 cm distance, 20 s, 17 J/cm^2).

Control conditions included untreated wells (without Ce6 beads, without laser), wells that received only laser illumination (without Ce6 beads) and areas outside the laser illuminated zone (with Ce6 beads, without laser). Every condition was run in duplicates. Cells were fixed 12 h after laser illumination with 4% paraformaldehyde (PFA) and subjected to TUNEL staining (see 3.12.3). The assay was repeated with every batch of conjugated beads to ensure continuous quality.

3.6 Laser Ablation of $Ce6^+$ Projection Neurons *In Vivo*

In order to specifically and locally ablate a fraction of callosal projection neurons (CPNs) in layer 2/3 of the primary visual cortex (V1), mice were anaesthetized and contralateral V1 was exposed via craniotomy (4 mm diameter, centred 2.5 mm lateral of lambda) as described in 3.9. Borosilicate glass capillaries were pulled and bevelled to exhibit long tapered tips with approximately 15 µm diameter. Ce6 conjugated beads were pressure injected (30 pulses within 5 min, 10 psi, 25-50 ms) into the binocular zone of V1 at 5-6 locations to reach a total volume of 0.5 µl at a depth of 50-500 µm. V1 and the binocular zone were identified using the characteristic blood vessel pattern and intrinsic optical imaging [Schuett 2002, Hofer 2009] (see 3.10). $Ce6^+$ beads were taken up by axon terminals of CPNs and retrogradely transported to their cell somata. Five to 10 days after beads injection a second craniotomy was performed in order to expose ipsilateral V1 containing labelled CPNs. Posterior-lateral V1 was non-invasively subjected to laser-photoactivation of Ce6 with a 670 nm flatbeam laser (beam shaping optics for a collimated parallel beam of 2 mm diameter, working distance 36.7 mm) to induce apoptotic cell death of CPNs (4, 6 and 10 min, 3 and 30 mW; 23 J/cm^2, 344 J/cm^2 and 573 J/cm^2). After the craniotomy, the bone flap was repositioned, fixed with Histoacryl and the skin was sutured.

For experiments involving GLAST-creERT2 x CAG-GFP mice, both craniotomies were performed at the time of the beads injection, and a cranial glass window (see 3.9.) was implanted above the ipsilateral hemisphere. Laser photoactivation was performed through the glass window under light anaesthesia.

3.7 Transplantation of Embryonic Cortical Cells into V1

Embryonic cells for transplantation were fluorescently labelled either genetically in the above mentioned mouse lines (see 3.1) or via *in vitro* viral transduction (see 3.8). Five to seven days after laser-photoactivation, embryonic cells were transplanted into the lesion site. To ensure that transplantations were located within the binocular zone of V1, we performed

intrinsic optical imaging (see 3.10). In a subset of experiments (n=2) host mice received an additional grafting site within V1, but outside of the previously illuminated area.

Embryonic cortical cells were prepared from E18.5 donor embryos using a papain based dissociation system [Huettner 1986]. In short, timed pregnant mice were deeply anaesthetized with isoflurane and killed by cervical dislocation. Embryos were removed from the uterine horns under sterile conditions and immediately sacrificed. Brains were carefully removed and collected in dissociation medium with kynurenic acid and D-AP5 at 4 °C. Cortical hemispheres were separated from the rest of the brain with a scalpel blade, transferred to pre-warmed papain solution (20 U/ml papain, 0.005% DNase in EBSS with 1 mM L-cysteine and 0.5 mM EDTA) and minced to small pieces with long tapered tip glass capillaries. After 45 to 60 min incubation at 37 °C cortex tissue was mechanically dissociated by trituration with flamed, coated Pasteur pipettes. Enzymatic activity was stopped with protease inhibitors (3 mg ovomucoid), and dissociated cells were collected by centrifugation over a one-step density gradient (10 mg/ml ovomucoid, 10 mg/ml BSA). A cell suspension (50 million cells/ml) was prepared in neurobasal medium (NB) supplemented with B27, GlutaMax and Pen/Strep.

Donor cells labelled via *in vitro* viral transduction (see 3.8) were washed at least 5 times with pre-warmed PBS (w/o $Ca2^{+}Mg2^{+}$) in order to remove any remaining viral particles. Gentle trypsinization (0.025%, 10 min at 37 °C) was performed, and a cell suspension (50 million cells/ml) was prepared in neurobasal medium (NB) supplemented with B27, GlutaMax and Pen/Strep.

For transplantation of donor cells, host mice were deeply anaesthetized and the ipsilateral bone flap covering the CPN-ablated V1 was carefully removed. A volume of 0.5 to 1 µl of cell suspension (25.000 - 50.000 cells) was injected with a Hamilton syringe (31 gauge) at a depth of 50-350 µm, and a cranial glass window was implanted (see 3.9).

3.8 *In Vitro* Viral Transduction

In a subset of experiments (n=2), donor cells were labelled via *in vitro* viral transduction using adeno-associated virus (AAV; AAV2/1-hSyn1-flex-mRuby2-P2A-CGaMP6s-WPRE-SV40). In short, neocortical tissue from E14.5 donor embryos was dissociated as described above (see 3.7.) and plated at a density of 300.000 cells/well in poly-L-lysine coated 24-well plates. Cells were plated in DMEM *high glucose* (4.5 g/l) with GlutaMax, Pen/Strep and 10% FBS, allowed to adhere and transduced with AAV (1 µl/well; 10^{7} to 10^{11} transducing units/ml). FBS was gradually removed by replacing half of the medium with DMEM *high glucose* with GlutaMax, Pen/Strep and B27 every two days. Cells were prepared for transplantation after 4 days *in vitro*, corresponding to E18.5 acutely dissociated cells.

3.9 Cranial Window Implant

For chronic structural and functional in vivo imaging experiments a cranial glass window was implanted on top of V1 after cell transplantation. For experiments involving GLAST-creERT2 x CAG-GFP mice, a cranial glass window was implanted 5 to 10 days before laser photoactivation. We followed procedures described previously [Holtmaat 2009a]. In short, mice were deeply anaesthetized and the disinfected skin at the posterior mouse head was removed. The periosteum was locally anaesthetized with 5% lidocaine gel before a craniotomy (4.5 mm diameter) was performed. A coverslip (5 mm diameter, #1 thickness) was loosely placed on the intact dura, resting on the edge of the craniotomy, and sealed to the bone with cyanoacrylate. A small metal bar (5 x 8 mm) with screw holes for head fixation during image acquisition was attached to the skull medial to the window implant. Skin margins, cover-glass and metal bar were embedded in dental acrylic mixed with black pigment.

3.10 Intrinsic Optical Imaging

In a subset of mice (n=16), optical imaging of intrinsic signals [Grinvald 1986] was used to direct $Ce6^{+}$ beads injection and laser photoactivation to the binocular zone of V1. In additional 16 mice, the correct location of cell transplantation was verified at 3 days post transplantation (dpt). In short, anaesthetised mice were presented with square wave drifting gratings (4 orientations, 600 ms stimulus duration; 0.03 cycles deg^{-1}, 2 cycles sec^{-1}) in a 2 x 2 array covering approximately -10° to 70° azimuth, -20° to 40° elevation of the ipsi- or contralateral visual field, respectively. For the identification of V1, visual stimuli were presented to the contralateral eye, while the ipsilateral eye was covered. For the localization of the binocular zone, visual stimuli were presented to the ipsilateral eye, while the contralateral eye was shielded. The cortical surface was evenly illuminated through the cranial window with monochromatic light of 707nm. A cooled, slow scan CCD camera (12 bit) was focused 200-300 µm below the cortical surface, and frames were recorded with 600 ms exposure time. Images of average responses (3 repetitions of 12 stimulus frames per location) were blank-corrected, range-fitted and low-pass-filtered [Schuett 2002]. For visualization, the false color-coded maximum projection of visual responses was mapped on top of the blood vessel image acquired prior to visual stimulation.

3.11 BrdU Treatment

Mice received BrdU treatment in order to label "new-born" cells (cells undergoing S-phase) in the adult mouse before, during and after laser lesion. BrdU was administered via drinking water (1 mg/ml BrdU, 1% glucose) for 2 weeks in various intervals spanning in total 3 weeks prior to 3 weeks post laser lesion. Water bottles were light shielded and BrdU solution was exchanged twice per week.

3.12 Immunocyto- and Immunohistochemistry

3.12.1 Fixation and Perfusion

PC-12 cells were washed with PBS and fixed in freshly diluted 4% PFA in PBS (32% stock solution) for 10 min. Cells were either subjected directly to TUNEL staining or kept in PBS overnight for processing on the following day.
Mice were deeply anaesthetized with fentanyl-based anaesthesia (1.5x dose, see 3.1.) and transcardially perfused using a peristaltic pump. After rinsing with 50 ml cold saline with lidocaine (0,1%) and heparin (1 U/ml), mice were perfused with 200 ml 4% PFA for 20-30 min. Brains were carefully removed from the skull and subjected to short (2 h at RT) or long post-fixation (over night at 4 °C) dependent on the antibodies used during subsequent immuno-labelling. Brains were then transferred to 30% sucrose in PBS and kept at 4 °C until sunken. Brains were subsequently embedded in O.C.T compound, frozen at -70 to -80 °C in isopentane and stored at -80 °C.

3.12.2 Slice Preparation

Coronal serial sections were prepared from frozen brains using a cryostat. After 30 min temperature equilibration in the cryostat chamber at -19 °C, sections were cut at 30 µm (40 µm for BrdU labelling, see 3.12.4.) and either directly mounted on adhesive glass slides (for TUNEL labelling) or collected in PBS in 24-well plates. For analysis of S1 and V1, sections between Bregma 2 to -2 and -2.5 to -4.5 were processed, respectively.

3.12.3 Terminal dUTP Nick End Labelling

PFA-fixed PC-12 cells and brain sections mounted on glass slides were subjected to TUNEL staining using Roche´s In Situ Cell Death Detection Kit. Briefly, cells and sections were permeabilized in 0.1% sodium citrate with 0.1% Triton X-100 (Tx100) for 10 min at 4 °C. After washing in PBS, edges of glass slides and wells were greased with a Pap Pen. Label

solution with fluorescein conjugated dUTPs was mixed with enzyme stock solution (10x terminal deoxynucleotidyl transferase) and samples were incubated for 60 min at 37 °C under light agitation in saturated humidity (waterbath). For positive controls, cells and sections were treated with 2000 U DNase I in 50 mM Tris-HCl with 1 mg/ml BSA, pH 7.5 for 10 min at RT. Label solution (dUTPs) without enzyme was used as negative control. Samples were washed with PBS and counterstained with DAPI (0.01 mg/ml). After a short rinse in dH_2O, samples were de-hydrated and mounted.

3.12.4 Immuno-labelling

Both, glass slide adsorbed and free floating sections were rinsed in PBS to eliminate any excess of O.C.T compound and subsequently treated with 0.1% Tx100 in PBS for 10 min at RT. Samples were washed in PBS and incubated with block solution (3% BSA with 5% goat serum [GS] in PBS) under light agitation for 1 h at 37 °C. Samples were rinsed in PBS and incubated with primary antibodies (see table below) in 1% GS in PBS for 3 h at 37 °C or o/n at 4 °C in saturated humidity. After 10 min in 0.1% Tx100 in PBS samples were washed in PBS and incubated with secondary antibodies (see table below) in 1% GS in PBS for 3 h at 37 °C, light shielded and under saturated humidity.

For immuno-labelling of BrdU, sections (all free-floating) were subsequently fixed in freshly prepared 4% PFA for 10 min. Sodium citrate buffer (10 mM) with 0.05% Tween20 at pH 6 was pre-heated in 2 ml tubes at 95 °C in an orbital shaker with temperature control. Sections were transferred to tubes and incubated at 95 °C for 20 min with intervals of 10 s agitation at 300 rpm every minute. Sections were transferred back to 24-well plates, washed in PBS and incubated with rat anti-BrdU antibodies (1:300) in PBS with 0.5% Tx100 and 10% GS o/n at 4 °C in a humid chamber. Following wash steps in PBS, sections were incubated with secondary goat anti-rat antibodies (1:1000, see table below) in PBS with 1% GS for 3 h at 37 °C, light shielded and under saturated humidity.

Finally, samples were washed and counterstained with DAPI (0.01 mg/ml) in PBS for 10 min. Free-floating sections were transferred to glass slides with fine paint brushes and all samples were rinsed in dH_2O, de-hydrated and mounted.

Primary Antibodies		**Secondary Antibodies**	
Rat monoclonal anti-BrdU	1:300	Alexa Fluor 488, Goat anti-mouse	1:1000
Rabbit polyclonal anti-Dcx	1:2000	Alexa Fluor 594, Goat anti-mouse	1:1000
Rabbit polyclonal anti-GFAP	1:500	Alexa Fluor 594, Goat anti-rabbit	1:1000
Chicken polyclonal anti-GFP	1:500	Alexa Fluor 594, Goat anti-rat	1:1000
Rabbit polyclonal anti-Iba1	1:500	Alexa Fluor 647, Goat anti-mouse	1:1000
Mouse monoclonal anti-NeuN	1:100	Alexa Fluor 647, Goat anti-rat	1:1000
Rabbit polyclonal anti-NG2	1:200	Cy3 conjugated, Goat anti-mouse	1:200
Rabbit polyclonal anti-Olig2	1:500	Cy3 conjugated, Goat anti-rabbit	1:200
Rabbit polyclonal anti-DsRed	1:100	Cy5 conjugated, Goat anti-mouse	1:200
Mouse monoclonal anti-S100β	1:1000	Fluorescein, Goat anti-chicken	1:250

3.12.5 Microscopy

Samples were investigated using an upright Zeiss epifluorescence microscope (Axio Imager M2) equipped with a mercury light source (HXP 120), a high resolution monochrome camera (AxioCam MRm 3) and the following objectives and filter sets: Plan-Neofluar 5x (0.15 NA), Plan-Neofluar 10x (0.3 NA), Plan-Neofluar 20x (0.50 NA), Plan-Neofluar 40x (0.75 NA), Plan-Neofluar 63x, oil immersion (1.25 NA), filter set 68 DAPI, filter set 43 HE Cy3, filter set 65 HE Alexa 488, filter set 64 HE mPlum, filter set 50 Cy5. Images were acquired with AxioVision 4.8.2 using the multichannel and/or mosaic acquisition modules.
For quantitative analysis of BrdU staining, 3D image stacks (566.8 x 566.8 µm, 1.107 px/µm, 1 µm z-steps) were acquired using a Zeiss laser-scanning confocal system (LSM 710) equipped with a 25x water immersion objective (0.8 NA) and the ZEN 2012 acquisition software package.

3.13 Analysis of Immunocyto- and Immunohistochemistry

PC-12 cells and sections labelled with TUNEL were analysed using the Fiji [Schindelin 2012] package of ImageJ. TUNEL$^+$ cells were quantified using the cell counter plugin and normalized to the total number of DAPI$^+$ cell nuclei in the same field of view, expressed in per cent.

Serial sections of SS and V1 were closely examined for the presence of GFP^+ neurons ($NeuN^+$) by screening every section and documenting the slice number as well as the cortical location of each cell. From each brain, example images were acquired.
For the quantification of $NeuN^+BrdU^+$ neurons, confocal z-stacks were examined using ZEN 2012 or Fiji. Serial optical sections were closely investigated for double positive cells using orthogonal views in xz and yz. $NeuN^+BrdU^+$ neurons were identified and counted in three areas (see Figure 26): At the injection site (Inj.), at the lesion site (L) and outside of the lesion site (oL). For each animal, 3 to 6 brain sections were investigated and results are presented as average absolute number of cells per section per area.

3.14 *In Vivo* Two-photon Imaging

In vivo two-photon imaging was carried out on an Olympus FV1000BX61 system equipped with a mode-locked Ti:sapphire laser (Mai Tai DeepSee) through a 25x water immersion objective (1.05 NA). Laser settings and image acquisition were controlled by Fluoview software.

3.14.1 Structural *In Vivo* Two-photon Imaging

For structural *in vivo* imaging mice were anaesthetized with fentanyl based anaesthesia (see 3.1.) and placed on a feedback controlled heating pad. Data were acquired at 910 nm with an average laser power of <30 mW, and the emission signal was directed through a dichroic mirror (split at 570 nm) and red/green bandpass emission filters (570-625 nm and 495-540 nm).
In transplantation experiments a typical imaging session lasted 2-3 h. Host mice were imaged as early as 3 days post transplantation. Individual transplanted cells were identified and followed in short, increasing intervals (2 to 5 days) within the first 4 weeks and weekly thereafter (up to 12 wpt). In two mice we acquired late time points at 9 to 11 months post transplantation. In each imaging session high-resolution tiled volume stacks (510 x 510 µm field of view; 512 x 512 pixel per tile; 0,33 µm/px; 1-3 µm z-steps) were acquired down to a depth of 350 µm from the pial surface for overview and reconstruction of whole cell morphology of transplanted cells. In addition, high-resolution close-up stacks (73 x 73 µm; 0.14 µm/px; 0.5-1 µm z-steps) of typically three individual dendritic and axonal processes, respectively, were acquired at various depths between 50 and 300 µm. For the analysis of synaptic structure density, turnover and survival we included both basal and apical dendritic processes.

A typical imaging session in order to image up to 0.8 mm^3 in GLAST-creERT2 x CAG-GFP mice (see Fig. 31) lasted 2-3 h. Mice were subjected to *in vivo* two-photon imaging directly after laser photoactivation (day 0) and weekly thereafter up to 8 weeks post lesion (wpl). In each imaging session four high-resolution tiled volume stacks (760 x 760 µm field of view; 512 x 512 pixel per tile; 0,49 µm/px; 1 µm z-steps) were acquired down to a depth of 300 µm from the pial surface. Wherever possible, a 5th volume stack (up to 506 x 1520 µm field of view) was acquired (see Fig. 31B). Mice were perfused at 8 wpl and brains subjected to immunohistochemistry (see 3.12.).

3.14.2 *In Vivo* Two-photon Calcium Imaging

For functional *in vivo* imaging experiments donor cells were labelled with the genetically encoded calcium indicators (GECIs) CGaMP6s [Chen 2013] or Twitch2B [Thestrup 2014] (a FRET based sensor). Emx1-Cre x Ai9 donor cells were mixed with AAV encoding a double-floxed inverted open reading frame version of either GECI prior to transplantation (AAV2/1-hSyn1-flex-CGaMP6s-WPRE-SV40; AAV2/1-CAG-flex-Twitch2B-WPRE-SV40). In a subset of experiments (n=2 host mice) donor cells were labelled *in vitro* (AAV2/1-hSyn1-flex-mRuby2-P2A-CGaMP6s-WPRE-SV40, see 3.8.).

Mice were kept on a feedback controlled heating pad and *in vivo* imaging was performed under light anaesthesia. Mice received 0.4x dose for initial anaesthesia and a subsequent 0.2x dose every 90 min. For ipsi- and contralateral visual stimulation, either the left or the right eye was occluded, respectively, and full field moving gratings (square wave, high contrast; 0.04 cyc deg^{-1}, 1.5 cyc s^{-1}; 4 orientations, 8 directions) were presented to the open eye (30 cm distance monitor to eye). The 8 directions were presented in random order, each displayed for 3 seconds, followed by 3 seconds of an isoluminant grey screen. Presentation of 3 x 8 directions was flanked by 10 seconds of grey screen (constituting one stimulus sequence of 3 repeats). Typically, 2-3 stimulus sequences were presented per imaging plane (altogether 6-9 repeats).

Data were acquired either at 940 nm (GCaMP6) or at 860 nm (Twitch2B) with an average laser power of <30 mW; a typical imaging session lasted 2-3 h. Emitted light was directed through a longpass dichroic mirror (split at 570 nm, GCaMP6; 505 nm, Twitch2B) and recorded through emission filters (BA495-540HQ and BA570-625HQ, GCaMP6; ET480/40M and ET535/30M, Twitch2B).

In each imaging session a tiled volume stack (760 x 760 µm field of view; 512 x 512 px per tile; 0.49 µm/px; 3-5 µm z-steps) was acquired up to a depth of 350 µm from the pial surface for an overview of transplanted (tdT^+) neurons. Five to 10 candidate areas with $tdT^+/GECI^+$

neurons were recorded at a frame rate of 2.4 Hz during visual stimulation (73 x 73 µm field of view; 0.28 µm/px).
Host mice were imaged starting at 4 wpt, and individual responsive neurons were repeatedly recorded up to 15 wpt. In a subset of experiments (n=2 mice) we specifically recorded late time points at 11 to 15 wpt.

3.15 Analysis of *In Vivo* Structural Data

Image stacks were processed using the Fiji [Schindelin 2012] package of ImageJ as follows: Fluorescence signals of rhodamine conjugated e6 beads detected with equal intensity through red/green bandpass emission filters were removed by channel subtraction (see Fig. 10). Images were converted to 8 bit and subjected to a small 2D Gaussian filter ($\sigma < 0.6$ px). For display purposes only, maximum intensity z-projections are shown with adjusted brightness/contrast.
Whole cell morphology was reconstructed using Simple Neurite Tracer (http://fiji.sc/Simple_Neurite_Tracer) [Longair 2011]. Briefly, apical and basal dendrites were semi-automatically traced through the high-resolution tiled volume stack. Based on the traced skeleton, a single cell 3D volume model was rendered (see Fig. 9).
In order to determine spine and bouton densities, dynamics and survival, these putative synaptic structures were identified [Holtmaat 2009a] in image stacks at each recorded time point. We included all clearly visible structures in x, y and z. An ID was assigned to each individual identified structure at the time point of its first appearance and registered across time points. Density is reported as structures per µm, and turnover is calculated as fraction of structures (gained + lost) / (total t1 + t2). We calculated the average survival fraction of gained structures dependent on the time point of their first appearance according to the non-parametric Kaplan-Meier estimator [Machin 2006] (using GraphPad PRISM). This method takes into account that there is some uncertainty of the actual survival of synaptic structures present at (and presumably longer than) the last experimental time point. Hazard ratios compare the rate of structure loss between structures that were gained at different time points. Median survival ratios compare the relative median survival of gained structures at different time points (see Fig. 16).
16 dendritic stretches out of 5 mice and 33 axonal stretches out of 6 mice were analysed (average dendritic length: 50.5 ± 12.4 µm; average axonal length: 77.7 ± 25.3 µm). A total of 13251 dendritic spines and 6266 axonal boutons across all time points were identified and registered to 2493 individual dendritic spines and 1600 individual axonal boutons on 0.8 mm total dendritic and 2.6 mm total axonal length.

Pre-processed (see above) high resolution tiled volume stacks of GLAST-creERT2 x CAG-GFP mice were compared across time-points and GFP^+ cells were matched. New, lost and migrating cells were identified based on their respective location to invariable GFP^+ astrocytes (see Fig. 31D). GFP^+ neurons and putative neurons (non-typical astrocyte morphology, see Fig. 31) were identified based on their morphology. Results are presented as average cells per imaged volume (0.7 - 0.8 mm^3).

3.16 Analysis of *In Vivo* Functional Data

Functional imaging data were analysed using Fiji and Matlab. Individual frames were background subtracted using a rolling ball algorithm (>100 px radius), converted to 8 bit and subjected to a small 2D Gaussian filter ($\sigma < 0.8$ px). Stacks were full-frame aligned using linear transformations (StackReg, Thévenaz P., EPFL) and ROIs were selected manually based on the aligned maximum intensity projection across a stimulation sequence. For neuronal somata, ROIs included the cytoplasm and nucleus, for spines, ROIs comprised of the spine head. For axons, two to three individual boutons were identified based on their adjacent position along the axon and the similarity of their response profile (see Fig. 3). The fluorescence signal (F) was calculated as the average fluorescence of all pixels within a given ROI (Twitch2B: $R = av.F_{YFP}/ av.F_{CFP}$). Neuronal activity was measured as the normalized change in fluorescence signal over time: $(F_t\text{-}F0)/F0$ (Twitch: $R_t\text{-}R0/R0$). The baseline (F0, R0) was calculated as the average signal over typically 10 seconds before and after each stimulation sequence (see 3.14.2).

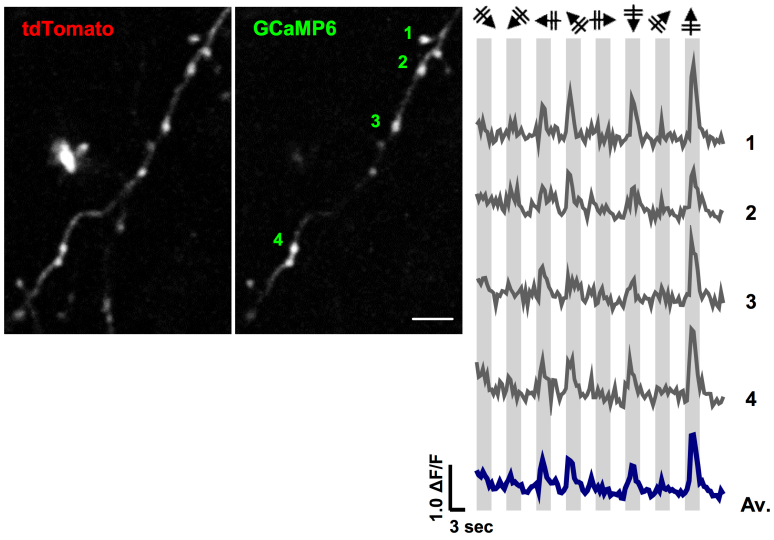

Fig. 3. Individual boutons of the same axon show highly similar responses to visual stimulation. Left, Axon of a transplanted neuron (tdT+) expressing GCaMP6, single optical plane, maximum projection of all frames of one stimulation sequence. Right, individual and average responses (ΔF/F) of 4 boutons (indicated on the left) to visual stimulation with gratings moving in 8 directions (grey bars, direction indicated on top). Note highly similar responses of all boutons. Scale bars: 5 µm.

We classified neurons as visually responsive if the average $\Delta F/F0 > 3\sigma$ (Twitch2B: $\Delta R/R0 > 0.05$ [Thestrup 2014]) for at least one stimulus direction. Tuning properties of each neuron are depicted in complex space using the normalized average peak response for each direction expressed in polar coordinates. In addition, normalized average peak responses are presented with normalized standard errors in 2D column plots.

Orientation and direction tuning selectivity is expressed as the orientation and direction selectivity index (OSI/ DSI), respectively and calculated as follows: $OSI = (R_{pref} - R_{ortho})/ (R_{pref} + R_{ortho})$, $DSI = (R_{pref} - R_{opposite})/ (R_{pref} + R_{opposite})$. R is the average peak response to the preferred direction (R_{pref}), to the mean of the orthogonal directions (R_{ortho}) and the opposing direction ($R_{opposite}$). As ratio based tuning properties do not take into account the distribution of responses across all tested directions, we also calculated single and double Gaussian fits [Mazurek 2014]. Following the assumption that an ideal orientation (or direction) tuned neuron would be perfectly described by a double (or single) Gaussian fit, the goodness of fit (R^2) serves as a measure of tuning quality. In short, curves were fit with non-linear regression using PRISM. Single Gaussian fits were calculated according to $y = a + amp * \exp(-0.5 * ((x-x_{mean})/\sigma)^2)$, with a = offset from x-axis, amp = peak amplitude, x = stimulus directions in degree, x_{mean} = x value at peak amplitude, and the following constraints: $a > 0$, $amp = 1$, $x_{mean} = 180°$, $\sigma \geq 22.5°$. Double Gaussian fits were calculated according to $y = a + amp1 * \exp(-0.5 * ((x-x_{mean1})/\sigma_1)^2) + amp2 * \exp(-0.5 * ((x-x_{mean2})/\sigma_2)^2)$, with a = offset from x-axis, amp1 = peak amplitude, amp2 = amplitude at opposing direction, x = stimulus directions in degree, x_{mean1} = x value at peak amplitude, x_{mean2} = x value at amplitude of opposing direction, and the following constraints: $a > 0$, $amp1 = 1$, $amp2 < amp1$, $\Delta x_{mean1, 2} = 180°$, $\sigma_{1, 2} \geq 22.5°$. R^2 is computed as the normalized sum of least squares.

To further describe the changes in tuning of individual neurons over time, we calculated the difference in preferred orientation at successive imaging time points for all neurons recorded at least twice. With 4 orientations, the individual difference was limited to discrete values of $\Delta 45°$ between 0° and 90°. For the same set of neurons we also compared the reliability of responses over time. In short, we calculated the average correlation coefficients (Pearson correlation) of trial-to-trial responses during visual stimulation to the preferred direction across time-points.

3.17 Statistics

Statistical evaluation was performed using PRISM (Graphpad). *In vitro* quantification of apoptotic cells, as well as spine and bouton data were analysed with one-way ANOVA and Tukey post-tests for multiple comparisons. Survival curves were analysed pairwise using the Gehan-Breslow-Wilcoxon test, and p-value thresholds were adjusted for multiple

comparisons applying a Bonferroni correction. Functional data were subjected to non-parametric tests using Kruskal-Wallis with Dunn's post-tests. In addition, the tuning of individual neurons across time-points, and the average normalized tuning of neurons at 6, 9 and 15 wpt were compared with two-way ANOVA and Tukey post-tests for multiple comparisons.

Results of $BrdU^+NeuN^+$ quantification in SS and V1 were compared using two-way ANOVA. Data from SS and V1 was pooled as no significant difference between areas was found ($p=0.95$, n.s.). The effect of laser photo-lesion was subsequently analysed using one-way ANOVA with Tukey post-tests. Quantification of GFP^+ neurons in controls versus lesioned GLAST-creERT2 x CAG-GFP mice was subjected to non-parametric tests (Kruskal-Wallis with Dunn's post-tests), since the data did not pass D'Agostino and Pearson normality tests. Paired students t-test was applied to compare GFP^+ neurons and non-typical astrocytes at day 0 and 8 wpl in *in vivo* imaging data after laser lesions.

The minimum level of significance was defined as $p<0.05$ and all values are reported ± S.E.M., if not stated otherwise. Levels of significance were defined as: *, $p<0.05$; **, $p<0.01$; ***, $p<0.001$; ****, $p<0.0001$.

4 Materials

4.1 Antibodies

Primary Antibodies

Rat monoclonal anti-BrdU	Abcam	Cambridge, UK
Rabbit polyclonal anti-Doublecortin	Abcam	Cambridge, UK
Rabbit polyclonal anti-GFAP	Dako	Hamburg, GER
Chicken polyclonal anti-GFP IgY	Aves Labs	Oregon, USA
Rabbit polyclonal anti-Iba1	Wako Chemicals	Neuss, GER
Mouse monoclonal anti-NeuN IgG1, clone A60	Millipore	Schwalbach, GER
Rabbit polyclonal anti-NG2 chondroitin sulfate proteoglycan	Millipore	Schwalbach, GER
Rabbit polyclonal anti-Olig2	Millipore	Schwalbach, GER
Rabbit polyclonal anti-DsRed Express	Takara Bio Europe	Saint-Germain, FR
Mouse monoclonal anti-S100beta IgG1	Sigma Aldrich	München, GER

Secondary Antibodies

Alexa Fluor 488, Goat anti-mouse IgG (H+L), highly cross-adsorbed	Life Technologies	Darmstadt, GER
Alexa Fluor, 594, Goat anti-mouse IgG (H+L), highly cross-adsorbed	Life Technologies	Darmstadt, GER
Alexa Fluor, 594, Goat anti-rabbit IgG (H+L), highly cross-adsorbed	Life Technologies	Darmstadt, GER
Alexa Fluor, 594, Goat anti-rat IgG (H+L)	Life Technologies	Darmstadt, GER
Alexa Fluor 647, Goat anti-mouse IgG (H+L), highly cross-adsorbed	Life Technologies	Darmstadt, GER
Alexa Fluor 647, Goat anti-rat IgG (H+L)	Life Technologies	Darmstadt, GER
Cy3 conjugated, Goat anti-mouse IgG (H+L), affinity purified	Dianova	Hamburg, GER
Cy3 conjugated, Goat anti-rabbit IgG (H+L), affinity purified	Dianova	Hamburg, GER
Cy5 conjugated, Goat anti-mouse IgG + IgM (H+L), affinity purified	Dianova	Hamburg, GER
Fluorescein-labeled, Goat anti-chicken IgY (H+L), affinity purified	Aves Labs	Oregon, USA

4.2 Buffers and Solutions

Artificial Cerebrospinal Fluid, ACSF:	119 mM NaCl 26.2 mM NaHCO3 2.5 mM KCl 1.0 mM NaH2PO4 1.3 mM MgCl2 10 mM Glucose
Block Solution, IHC:	3% Bovine Serum Albumin 5% Goat Serum PBS
Citric Acid Buffer, TUNEL:	0.1% Sodium Citrate 0.1% Triton X-100
Glycine Buffer, Beads Coupling:	0.1 M Glycine pH 8.0
Phosphate Buffer, Beads Coupling:	0.01 M Phosphate Buffer pH 7.4
Sodium Citrate Buffer, Antigen Retrieval:	10 mM Sodium Citrate 0.05% Tween20 pH 6.0

HEPES	1M, Gibco	Thermo Fisher Scientific	Braunschweig, GER
PBS	Phosphate buffered saline 10x, Gibco	Thermo Fisher Scientific	Braunschweig, GER

4.3 Cell Lines

Rat Pheochromocytoma cells, PC-12	Cell Line Service	Eppelheim, GER

4.4 Chemicals

D-AP5, Tocris	R&D Systems	Wiesbaden, GER
Kynurenic acid, Tocris	R&D Systems	Wiesbaden, GER
Agarose	Biomol	Hamburg, GER
Black Pigment, Elfenbeinschwarz	Kremer Pigmente	Aichstetten, GER

5-Bromo-2'-deoxyuridine, BrdU	Sigma Aldrich	München, GER
Chlorin e6, Frontier Scientific	LivChem	Frankfurt, GER
Corn oil	Sigma Aldrich	München, GER
DAPI, dilactate	Sigma Aldrich	München, GER
Dental Cement, Paladur	Heraeus Kulzer	Hanau, GER
EDC	MB Biomedical	Eschwege, GER
Ethanol, abs.	Merck	Darmstadt, GER
Fluorescence mounting medium	Dako	Hamburg, GER
Glucose	Sigma Aldrich	München, GER
Glue gel, Pattex Blitz gel	Henkel	Wien, Austria
Glue liquid, Pattex Classic	Henkel	Wien, Austria
Glycine	Sigma Aldrich	München, GER
HCl	Merck	Darmstadt, GER
Histoacryl	Aesculap	Tuttlingen, GER
Iodine Solution	B. Braun Melsungen	Melsungen, GER
Isopentane	Sigma Aldrich	München, GER
Na2HPO4	Merck	Darmstadt, GER
NaH2PO4	Merck	Darmstadt, GER
NaOH	Merck	Darmstadt, GER
Paraformaldehyde, PFA 32%	Science Services	München, GER
Red Retrobeads IX	Lumafluor	Durham NC, USA
Sigmacote SL-2	Sigma Aldrich	München, GER
Sodium citrate C6.H5.Na3.O7	Merck	Darmstadt, GER
Sterican	B. Braun Melsungen	Melsungen, GER
Tamoxifen, TM >99%	Sigma Aldrich	München, GER
O.C.T Compound, Tissue Tec	Sigma Aldrich	München, GER
Tris-HCl	Merck	Darmstadt, GER
Triton X-100	Sigma Aldrich	München, GER
Trypan blue solution, 0.4%	Sigma Aldrich	München, GER
Tween20	Sigma Aldrich	München, GER
Ultrasonic gel	Dahlhausen	Köln, GER

4.5 Drugs

Atipamezol, Antisedan 5 mg/ml	Orion Pharma	Hamburg, GER
Carpofen, Rimadyl 50 mg/ml	Pfizer Animal Health	Madison NJ, USA

Eye lubricant, Oculotect fluid sine 50 mg/ml	Novartis	Melsungen, GER
Fentanyl, 0.1 mg/ 2ml	HEXAL	Holzkirchen, GER
Flumazenil, 0.5 mg/ 5ml	HEXAL	Holzkirchen, GER
Isoflurane, Forane	Baxter	München, GER
Isopto-Max, Eye Ointment	Alcon Pharma	Freiburg, GER
Lidocaine, 5% EMLA	Astra Zeneca	Wedel, GER
Medethomidin, Domitor 1 mg/ml	Orion Pharma	Hamburg, GER
Midazolam, Midazolam-ratiopharm 15 mg/ 3ml	Ratiopharm	Ulm, GER
Naloxon, Naloxon-hameln 0.4 mg/ml	Hameln	Hameln, GER
Saline, Sodium Chloride Solution, 0.9%	B. Braun Melsungen	Melsungen, GER
Stereofundin, VG-5	B. Braun Melsungen	Melsungen, GER
Xylocain gel, 2%	Astra-Zeneca	Wedel, GER

4.6 Glassware

24 well plate insets, chemical resistant	MPI workshop	Martinsried, GER
24 well plates, TPP flat bottom, polystyrene	Sigma Aldrich	München, GER
6 well plates, Biocoat BD, poly-L-Lysine	VWR	Ismaning, GER
Adhesion slides, Superfrost plus	VWR	Ismaning, GER
Borosilicate glass capillaries, 10µL	Karl Hecht	Sonheim, GER
Cell culture flasks, Biocoat BD, poly-D-Lysine	VWR	Ismaning, GER
Coverslip #1	VWR	Ismaning, GER
Cryogenic tubes, Nunc, 1.8 mL	Sigma Aldrich	München, GER
Embedding molds, disposable	Polysciences	Eppelheim, GER
Eppendorf tubes	VWR	Ismaning, GER
Falcon tubes	VWR	Ismaning, GER
Glas capillaries, Borosilicate, ID 0.25 mm, OD 1 mm	Hilgenberg	Malsfeld, GER
Glass cover slip round, 5 mm, #1	Menzel	Braunschweig, GER
Insulin syringes, BD Micro-Fine 0.5 mL	VWR	Ismaning, GER
Millex-GP filter unit, 0.22 µm	Millipore	Schwalbach, GER
Pasteur pipettes, Volac, 150 mm, pre-plugged	Poulten & Graf	Wertheim, GER
Petri dishes, 94 mm	VWR	Ismaning, GER
Serological pipettes, Falcon BD, disposable	VWR	Ismaning, GER

4.7 Instrumentation

Centrifuge tubes, Thinwall ultra clear, 13.5 mL	Beckman Coulter	Krefeld, GER
Cryostat	Leica	Wetzlar, GER
Micro Drill System	Harvard Apparatus	Holliston MA, USA
Dental Drill Bits, Carbide, 1/4 tip	Meisinger	Neuss, GER
Gel imager, ChemiDoc	BioRad	Munich, GER
Heating controler, open loop	MPI workshop	Martinsried, GER
Heating controler, closed loop	MPI workshop	Martinsried, GER
Master 8, Pulse generator	A.M.P.I	Jerusalem, Israel
Microelectrode Beveller	WPI	Berlin, GER
Micromanipulator	Bachofer	Reutlingen, GER
Micromanipulator, MO-10	Narishige	Tokyo, Japan
Optical Power-meter kit PM130D	Thorlabs	Dachau/MU, GER
PM100D digital meter	Thorlabs	Dachau/MU, GER
S130C photodiode sensor	Thorlabs	Dachau/MU, GER
Orbital shaker, ThermoMixer F2.0	Eppendorf	Köln, GER
TooheySpritzer, Pressure System IIe	Science Products	Hofheim, GER
Rotor Ti70.1	Beckman Coulter	Krefeld, GER
Stereotaxic frame	MPI workshop	Martinsried, GER
TFT Monitor, 20"	Dell	Frankfurt, GER
TFT Monitor, 24" W2442PE-BF	Dell	Frankfurt, GER
Ultrazentrifuge	Beckman Coulter	Krefeld, GER
Vertical micro-pipette puller, P-10	Narishige	Tokyo, Japan

4.8 Kits

Papain dissociation system, Worthington	Cell Systems	Troisdorf, GER
In situ cell death detection kit, Fluorescein	Roche	Penzberg, GER

4.9 Media, Supplements and Enzymes

Albumin, bovine serum, lyophilized, >96%	Sigma Aldrich	München, GER
B27, Serum free supplement, 50x	Life Technologies	Darmstadt, GER
dH20, Cell culture grade, Gibco	Thermo Fisher	Braunschweig, GER
DNase I, 2000 U/mg	Roche	Penzberg, GER
Dulbecco's modified eagle medium, DMEM	Life Technologies	Darmstadt, GER

high glucose		
Fetal bovine serum, heat inactivated	Sigma Aldrich	München, GER
Glutamax, 100x	Life Technologies	Darmstadt, GER
Goat serum, Cell culture tested, sterile	Sigma Aldrich	München, GER
Horse serum, heat inactivated, sterile	Sigma Aldrich	München, GER
Minimum essential medium, MEM	Life Technologies	Darmstadt, GER
Neurobasal medium, NBS	Life Technologies	Darmstadt, GER
Penicillin, 100x, 10.000U	Life Technologies	Darmstadt, GER
Recovery cell culture freezing medium	Life Technologies	Darmstadt, GER
RPMI medium, Glutamax, Phenol red	Life Technologies	Darmstadt, GER
Streptomycin, 100x, 10.000U	Life Technologies	Darmstadt, GER
Trypsin-EDTA, 0.25%, phenol red	Life Technologies	Darmstadt, GER

Dissection Medium:	DMEM *high glucose* GlutaMax (10 µL/mL) PenStrep (1000 U/mL) Kynurenate (in dH2O, 0.8 mM) AP5 (in dH2O, 40 µM)
Neuronal culture medium:	NBS 1x B27 GlutaMax (10 µL/mL) PenStrep (1000 U/mL)
PC-12 cell culture medium:	RPMI 1640 GlutaMax (10 µL/mL) 10% Horse Serum 5% FBS/ Calf Serum Pen/Strep (1000 U/mL)

4.10 Microscopes, Laser and Optical Components

Flatbeam Laser, 670 nm, flat-top beam profile, 250mW	Schäfter & Kirchhoff	Hamburg, GER
44TO-0 laser diode source	Schäfter & Kirchhoff	Hamburg, GER
Temperature control & Power supply	Schäfter & Kirchhoff	Hamburg, GER
MMC-VIS/NIR, multimode fibre cable, 300µm	Schäfter & Kirchhoff	Hamburg, GER

diameter, 0.22 NA		
Fibre collimator, 0.4 NA	Schäfter & Kirchhoff	Hamburg, GER
5M-M40, micro-focus-optics, 0.06 NA	Schäfter & Kirchhoff	Hamburg, GER
CCD Cam, 12 bit, ORA 2001	Optical Imaging Inc.	Germantown, USA
Stimulus Generator, VSG Series Three	Cambridge Research Systems	Rochester, UK
Mai Tai DeepSee, Mode-locked Ti:sapphire Laser	Spectra-Physics	Darmstadt, GER
Mouse stage, acrylic, magnetic feet	MPI workshop	Martinsried, GER
XLPLN 25x, water immersion, 1.05 NA	Olympus	Hamburg, GER
LUMPlanFI/IR, 40x, water immersion, 0.80 NA	Olympus	Hamburg, GER
Olympus FV1000BX61 system, 2PLSM	Olympus	Hamburg, GER
Axio Imager M2	Zeiss	Oberkochen, GER
AxioCam MRm3, High resolution, mi range monochrome	Zeiss	Oberkochen, GER
HXP 120	Zeiss	Oberkochen, GER
Plan-Neofluar 10x, 0.3 NA	Zeiss	Oberkochen, GER
Plan-Neofluar 20x, 0.50 NA	Zeiss	Oberkochen, GER
Plan-Apochromat 25x, water immersion, 0.8 NA	Zeiss	Oberkochen, GER
Plan-Neofluar 40x, 0.75 NA	Zeiss	Oberkochen, GER
Plan-Neofluar 5x, 0.15 NA	Zeiss	Oberkochen, GER
Plan-Neofluar 63x, oil immersion, 1.25 NA	Zeiss	Oberkochen, GER
Zeiss LSM 710, Confocal Microscope	Zeiss	Oberkochen, GER
Stereomicroscope	Zeiss	Oberkochen, GER
Surgical microscope, SOM-62	Karl Kaps	Aßlar, GER

Filter set blue/yellow:	Dichroic mirror, 505 nm ET480/40M ET535/30M	Olympus	Hamburg, GER
Filter set red/green:	Dichroic mirror, DM570 Bandpass emission filter, BA495-540HQ Bandpass emission filter, BA570-625HQ	Olympus	Hamburg, GER
Filter set 43 HE Cy3:	EX BP 550/25	Zeiss	Oberkochen, GER

	BS FT 570		
	EM BP 605/70		
Filter set 50 Cy5:	EX BP 640/30	Zeiss	Oberkochen, GER
	BS 660		
	EM BP 690/50		
Filter set 64 HE mPlum:	EX BP 587/25	Zeiss	Oberkochen, GER
	BS 605		
	EM BP 647/70		
Filter set 65 HE Alexa488:	EX BP 475/30	Zeiss	Oberkochen, GER
	BS 495		
	EM BP 550/100		
Filter set 68 DAPI:	EX BP 377/28	Zeiss	Oberkochen, GER
	BS 403		
	EM BP 464/100		

4.11 Mouse Lines

CAG-CAT-GFP	Nakamura et al. 2006
CAG-LSL-tdTomato	Madisen et al. 2010
Emx1-cre	Gorski et al. 2002
GLAST-creERT2 x CAG-GFP	Mori et al. 2006
SOX10-cre	Simon et al. 2012
Thy1.GFP-M	Feng et al. 2000

4.12 Software

Fiji package of ImageJ	NIH	Bethesda MD, USA
ImageJ, Template matching	NIH	Bethesda MD, USA
ImageJ, CLAHE filter	NIH	Bethesda MD, USA
Simple Neurite Tracer	M.H. Longir 2011	Zürich, CH
AxioVision	Zeiss	Oberkochen, GER
Fluoview	Olympus	Hamburg, GER
IDL	Exelis VIS	Gilching, GER
Matlab	MathWorks	Natick MA, USA
GraphPad Prism 6	GraphPad	La Jolla CA, USA
Psychophysics Toolbox240, David H. Brainard	University of	Santa Barbara CA,

	California	USA
ZEN 2012	Zeiss	Oberkochen, GER

4.13 Tools

Surgical Tools:

Bone curette, 140 mm	B. Braun Melsungen	Melsungen, GER
Ethibond excel, 75mm, 6-0, 3/8c 13mm	Johnson & Johnson	Norderstedt, GER
Forceps bent, #7, INOX	B. Braun Melsungen	Melsungen, GER
Forceps blunt, Narrow pattern, 2mm	F.S.T	Heidelberg, GER
Forceps straight, Dumont #5, INOX	B. Braun Melsungen	Melsungen, GER
Forceps straight, Dumont #5, ceramic coat	F.S.T	Heidelberg, GER
Forceps straight, Nr.7 Keramik	F.S.T	Heidelberg, GER
Hemostat Hartman	F.S.T	Heidelberg, GER
Scalpel blades	F.S.T	Heidelberg, GER
Scissors	F.S.T	Heidelberg, GER
Vannas-Tübingen spring scissors, angled, 5mm blades	F.S.T	Heidelberg, GER

Other Tools:

Cotton tips, 15 cm, medical care & serve	Wiros, Wilfried Rosbach GmbH	Willich, GER
Ear tag plier, for small laboratory animals	Hauptner & Herberholz	Solingen, GER
Ear tags, for small laboratory animals	Hauptner & Herberholz	Solingen, GER
Feeding needle, Stainless steel, 20 gauge, 300 mm shaft	F.S.T	Heidelberg, GER
Freezing container, Nalgene Mr. Frosty	Sigma Aldrich	München, GER
Hamilton syringe, 30 gauge	WPI	Berlin, GER
Headbar, custom made metal bar, 2 x 7 mm	MPI workshop	Martinsried, GER
Hemocytometer	Empfenzeder	München, GER
Homeothermic blanket	MPI workshop	Martinsried, GER
Micropipette storage jar, 1.5 mm OD	WPI	Berlin, GER
PAP Pen	Polysciences	Eppelheim, GER
Raser blades	Leica	Wetzlar, GER

Rectal probe, smooth ball tip, for rodents	WPI	Berlin, GER
Sugi	Kettenbach Medical	Eschenburg, GER

4.14 Virus

AAV2/1.CamK2a-cre.WPRE	Vector Core Services, University of Pennsylvania	Philadelphia PA, USA
AAV2/1-hSyn1-flex-CGaMP6s-WPRE-SV40	Vector Core Services, University of Pennsylvania	Philadelphia PA, USA
AAV2/1-hSyn1-flex-mRuby2-P2A-CGaMP6s-WPRE-SV40	Rose et al. 2016	Martinsried, GER
AAV2/1-CAG-flex-Twitch2B-WPRE-SV40	Thestrup et al. 2014	Martinsried, GER

5 Results

In this thesis, I investigated arguably one of the most extreme forms of CNS plasticity, the incorporation of whole new building blocks - in form of new excitatory neurons - into adult neocortical circuits. Specifically, I investigated the structural and functional integration of exogenous (transplanted) or endogenous (lesion induced) new neurons into the primary visual cortex (V1) of adult mice previously deprived of layer 2/3 (L2/3) cortical projection neurons. Besides the survival and morphological development of new neurons, the formation and long-term dynamics of connections to and from the host network were examined. In addition, the capability of new neurons to appropriately respond to visual stimuli, and thus, to perform a meaningful function during the processing of visual information in V1, was investigated.

Parts of this thesis were published as,

Falkner S*, Garde S*, Dimou L, Conzelmann K, Bonhoeffer T, Götz M, Hübener M. *Transplanted embryonic neurons integrate into adult neocortical circuits.* **Nature 2016** vol 539, pp 248-253

5.1 Apoptotic Laser Photolesion

In order to specifically eliminate a fraction of L2/3 projection neurons in V1 of adult mice, I used a photolytic lesion model first published in 1991 [Macklis 1991]. Based on the selective laser photoactivation of heterocyclic aromatic compound chlorine e6 (Ce6) and the subsequent production of intracellular reactive oxygen species (ROS) [Sheen 1994, Tsay 2007], this model reportedly leads to non-invasive, spatially confined, apoptotic cell death in Ce6-labelled cells. In a first step, I adapted the model to V1 and characterized its time course and extent.

5.1.1 Specific and Local Ablation of PC-12 Cells *In Vitro*

I first tested the specificity of laser ablation of Ce6-labelled cells *in vitro*. Ce6 was conjugated to fluorescence latex beads (rhodamine$^+$) as described in 3.4, and PC-12 cells were labelled by incubation in 1 µl/ml Ce6$^+$ beads in culture medium. An area of 2 mm diameter was subsequently illuminated with 670 nm laser light (19 J/cm^2; see Fig 2A). Control conditions included untreated cells (without Ce6$^+$ beads, without laser), cells that received only laser illumination (without Ce6$^+$ beads) and regions outside the laser illuminated zone (with Ce6$^+$ beads, without laser). Apoptosis induction was determined by TUNEL labelling 8 h later.

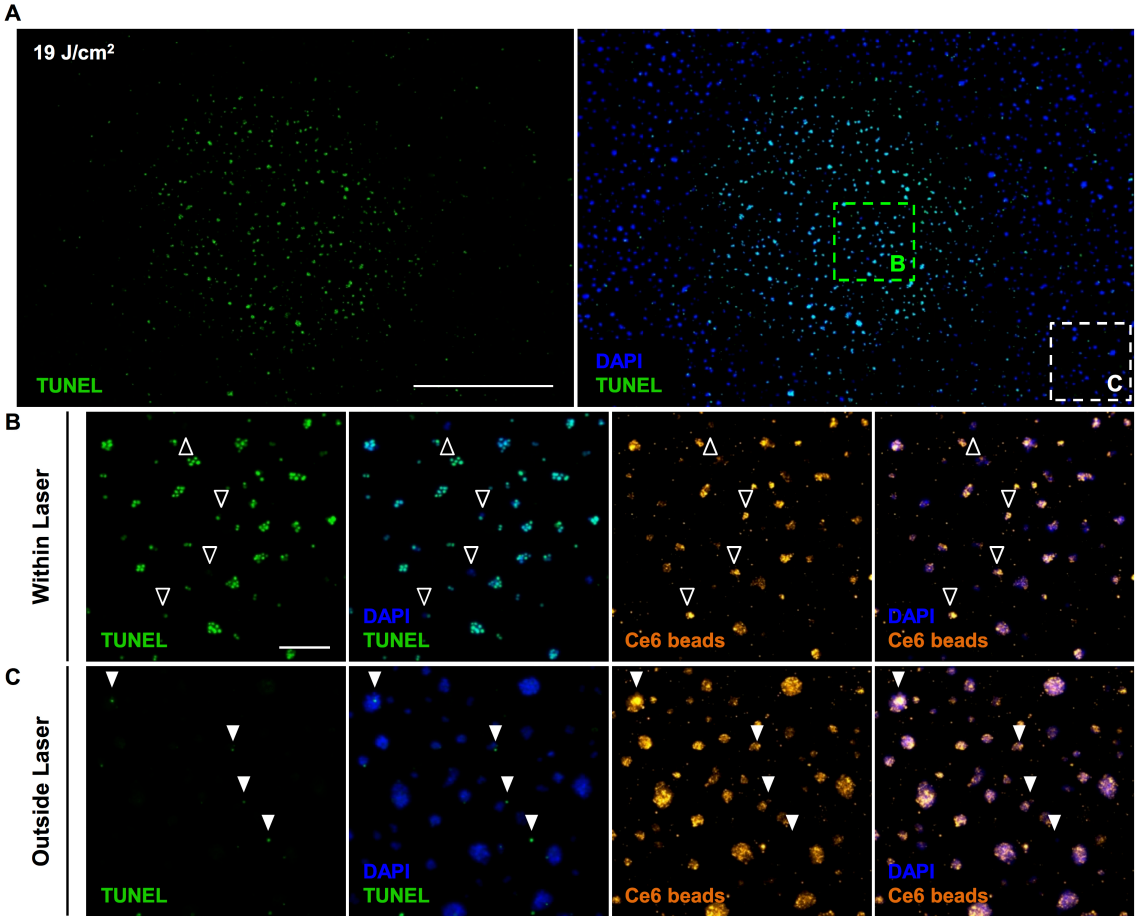

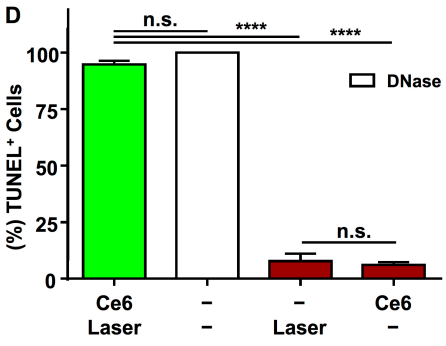

Fig. 4. Specific and local laser ablation of Ce6$^+$ cells *in vitro*. **(A)** Laser photo-activation (670 nm, 29 J/cm^2) induced local apoptotic cell death in Ce6 containing PC12 cells in culture. Wide field fluorescence image, single channel left (TUNEL, green) and multichannel right (TUNEL, green; DAPI, blue). Left, apoptotic cells (TUNEL$^+$, green) are confined to the area of laser illumination (2 mm diameter, centre). Right, cells outside of the laser area (DAPI, blue) are TUNEL$^-$. (B and C) Magnification of insets shown in (A), right panel. **(B)** Exposed cells are TUNEL$^+$ (TUNEL$^-$ Ce6$^+$, open arrowheads), while **(C)** non-exposed Ce6$^+$ cells in the same well are TUNEL$^-$ (TUNEL$^+$ Ce6$^+$, filled arrowheads). Ce6$^-$ cells (cultured without Ce6 coupled beads) are not ablated by laser illumination alone and are TUNEL$^-$ (see D). **(D)** Quantification of TUNEL$^+$ cells cultured with or without Ce6$^+$ beads fixed 8 h after laser illumination, normalized to DAPI$^+$ cells within the same field of view (Ce6$^+$Laser$^+$ 94.9 ±1.41%, n=7; Ce6$^-$Laser$^+$ 7.9 ±3.26%, n=3; Ce6$^+$Laser$^-$ 6.2 ± 1.09%, n=2; DNase treated Ce6$^-$Laser$^-$ 100 ±0.00%, n=3; one-way ANOVA, $p<0.0001$, Tukey post-tests). Scale bars: (A) 1 mm; (B-D) 100 µm.

TUNEL$^+$ cells were confined to areas of laser illumination and comprised a substantial fraction (94.9 ±1.41%, n=7; Fig. 4A, B and D) compared to non-exposed areas in the same well (6.2 ±1.09%, n=2; Fig. 4A, C and D) and laser exposed Ce6$^-$ cells (7.9 ±3.26%, n=3; one-way ANOVA, $p<0.0001$, Tukey post-tests; Fig. 4D). Thus, apoptotic cell death is exclusively and substantially induced in the presence of both, Ce6$^+$ beads and laser illumination, and neither laser exposure alone, nor the presence of intracellular Ce6$^+$ beads leads to cell death on their own. This assay was repeated with every new batch of Ce6-conjugated beads to ensure continuous quality throughout subsequent *in vivo* experiments.

5.1.2 Specific and Local Ablation of L2/3 Contralateral Projection Neurons

Next, I adapted the photolytic lesion model in order to specifically eliminate L2/3 callosal projection neurons (CPNs) in V1 of adult mice. Significant numbers of CPNs in the upper cortical layers are only found at the lateral V1 border [Cusick 1981, Wang 2007b], corresponding to the binocular zone [Hubel 1967, Antonini 1999, Aboitiz 2003], and CPNs project to homotopic locations in the contralateral hemisphere. Since Ce6$^+$ beads are taken up by axon terminals and are retrogradely transported to their cell somata [Katz 1984, Madison 1993], labelling of V1 CPNs was achieved by targeted injections to the contralateral binocular zone (see Fig. 5A). Following transport, an area of 2 mm diameter in posterior lateral V1 was subsequently exposed to 670 nm laser light (see Fig. 6A). Different intensities and exposure times were tested (4 min, 3 mW; 6 and 10 min, 30 mW; corresponding to 23 J/cm^2, 344 J/cm^2 and 573 J/cm^2, respectively) at the same focal position (see 3.6; Fig. 6B-C), with the aim of limiting apoptotic cell death of CPNs to the upper cortical layers. Both, Ce6$^+$ beads injection as well as laser photoactivation were guided by functional maps derived from intrinsic optical imaging during visual stimulation of the respective ipsilateral eye (see 3.10). Control conditions comprised mice that received either Ce6$^+$ beads injection (without laser) or laser photoactivation (without Ce6$^+$ beads). In addition, lesions were also conducted in somatosensory cortex (S1), were CPNs are more evenly distributed [Wang 2007b], and successful photolytic lesion has been demonstrated previously [Hernit-Grant 1996]. Successful apoptosis induction was determined by TUNEL labelling of coronal sections at different time points after laser illumination.

Five to 10 days after Ce6$^+$ beads injection, rhodamine$^+$ clusters of retrogradely transported beads were found predominantly in L2/3 and layer 5 (L5) (see Fig. 5B) consistent with the reported laminar distribution of CPNs [Koester 1992, Mizuno 2007]. Injections in mice with stochastic expression of fluorescent proteins in cortical pyramidal neurons (Thy1.GFP-M [Feng 2000], n=2), revealed that beads form aggregates within the somatic cytoplasm, presumably contained in lysosomes [Sheen 1994] (Fig. 5C).

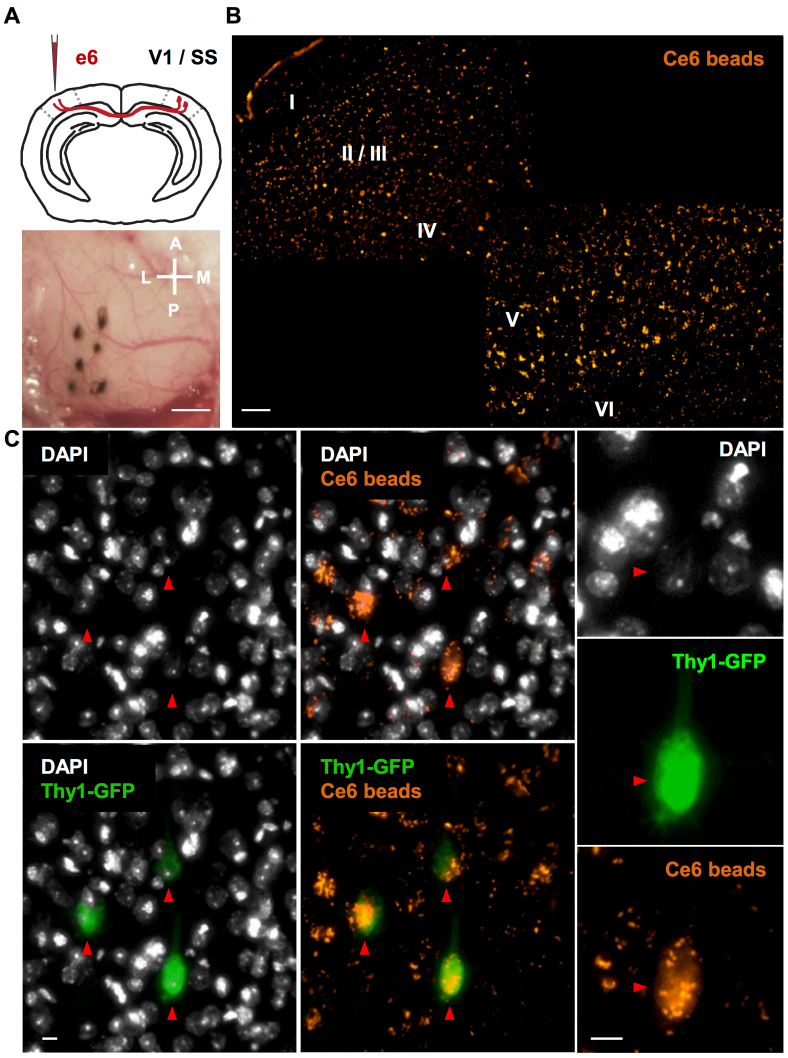

Fig. 5. Ce6 labelling of callosal projection neurons (CPNs) in S1 or V1. (A) Ce6 coupled beads are injected into the contralateral homotopic region of S1 or V1 (binocular region) to label CPNs. Scheme (top) and image of a craniotomy exposing V1 (bottom) displaying 6 injection sites of Ce6$^+$ beads (black, see 3.4). **(B)** Wide field fluorescence image of Ce6$^+$ CPNs 10 days after beads injection (orange, Ce6 coupled rhodamine$^+$ latex beads). Roman numbers denote cortical layers. Labelling is consistent with CPN predominance in layer 2/3 and layer 5 [Koester 1992, Mizuno 2007]. **(C)** Examples of layer 5 CPNs in a Thy1-GFP mouse line (green, red arrowheads) labelled with retrogradely transported Ce6$^+$ beads (orange) located in the cytoplasm (right column). Scale bars: (A) 1 mm; (B) 50 µm; (C) 10 µm.

The presence of intracellular Ce6$^+$ beads alone did not lead to elevated numbers of TUNEL$^+$ cells, nor did laser illumination alone (3.89 ±4.35% and 6.30 ±5.82%; Fig. 6E), while a substantial number of apoptotic cells was detected after combining both, Ce6$^+$ beads and laser illumination, under all conditions tested (Fig. 6B-D). TUNEL labelling across layers varied with the amount of energy delivered to the brain: While 573 J/cm^2 lead to apoptotic cells spanning layers 1 to 5, 23 J/cm^2 only induced cell death in layer 1 (L1) and upper L2/3 (Fig. 6C). A value of 344 J/cm^2 resulted in robust cell loss throughout L2/3, also substantiated by a permanent loss of NeuN$^+$ neurons (Fig. 6B). Consequently, this combination of laser intensity and exposure time was used in all subsequent experiments.

TUNEL labelling at day 0 to 14 after laser photoactivation revealed a fast increase of TUNEL$^+$ cells within hours, and a peak value at 3 days post lesion (dpl) (1 h, 27.93 ±12.39%;

3 dpl 48.22 ±4.65%; 7 dpl 19.68 ±10.40%; 14 dpl 15.75 ±7.34%; ±S.D; Fig. 6D). Note that the investigated time points, especially within the first week, likely contain an overlapping fraction of TUNEL$^+$ cells, since apoptotic cell death progresses over the course of several days [Madison 1993].

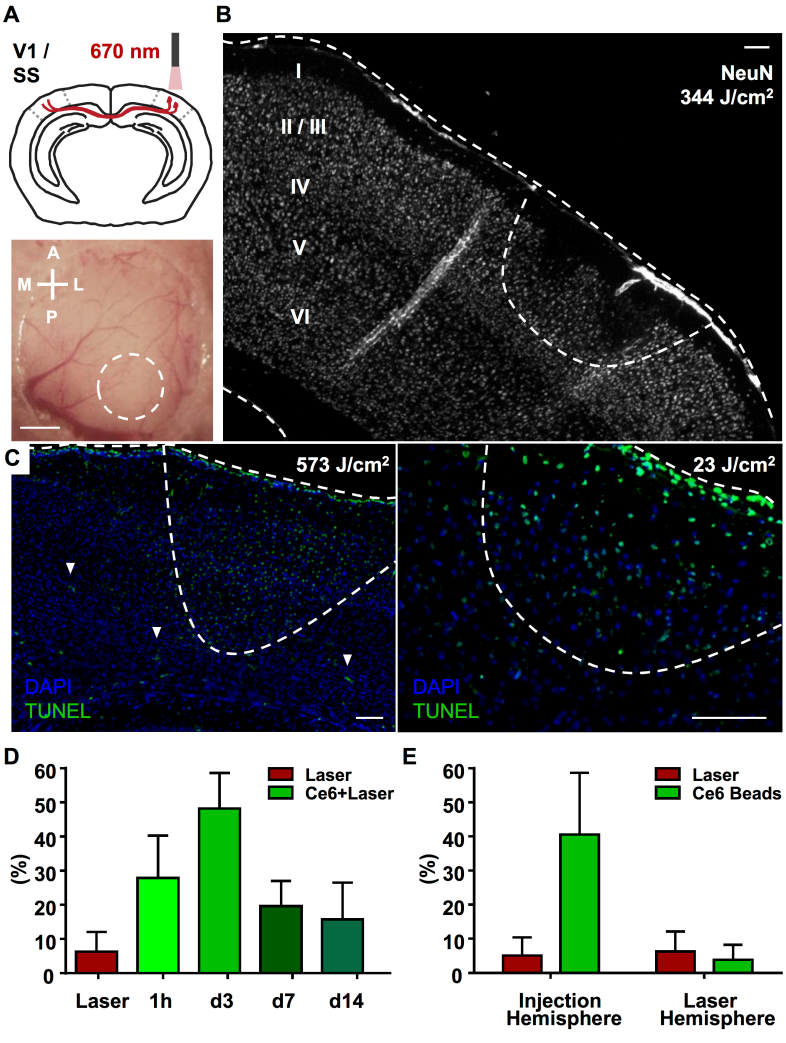

Fig. 6. Specific and local apoptotic photolesion of Ce6$^+$ CPNs *in vivo*. (A) S1 or V1 (binocular region) is exposed to 670 nm laser light (23 J/cm^2, 344 J/cm^2 or 573 J/cm^2). Schematic (top) and image of a craniotomy over V1 (bottom) with the area of laser illumination indicated as dashed circle (white). **(B)** Neuron loss, indicated by decreased NeuN staining (white), 6 weeks after laser illumination (344 J/cm^2) is confined to layer 2/3 in V1 (dashed line, white). **(C)** Apoptotic cell death, indicated by TUNEL labelling (green), across layers depends on the amount of energy delivered to the brain. Left, apoptotic cells in V1 of a GLAST-GFP mouse (see methods; note GFP$^+$ astrocytes, white arrowheads) exposed to 573 J/cm^2 are found in layers 1 to 5 (dashed line, white; 3 days after laser illumination). Right, apoptotic cells in SS exposed to 23 J/cm^2 are confined to layer 1 and upper layer 2/3 (dashed line, white; 3 days after laser illumination). **(D)** Fraction of TUNEL$^+$ cells after laser illumination (0 to 14 dpl, green bars) compared to laser control (laser illumination without prior Ce6 labelling of CPNs, red bar). **(E)** Fraction of TUNEL$^+$ cells in laser control (red bar), same as in (D), and Ce6$^+$ beads control (CPNs labelled with Ce6$^+$ beads, no laser; green bar) in both hemispheres. Both controls show < 7% of apoptotic cells in the laser hemisphere. (D and E) Each bar represents the average (± S.D.) of a minimum of 3 consecutive sections within the lesion site of one mouse (in total n=2 control mice, n=4 lesioned mice across 4 time points). Scale bars: (A) 1 mm; (B and C) 100 µm.

5.1.3 Intact Cytoarchitecture and Minor Inflammatory Response After Lesion

The non-invasive nature of the photolytic lesion causes cell death without compromising the overall cytoarchitecture (Fig. 6C). An additional advantage of the model is its reported lack of reactive gliosis and inflammatory infiltrate [Madison 1993, Sohur2012].

To corroborate these results, I stained for markers of inflammation and qualitatively assessed the reaction of microglia (Iba1$^+$; Fig. 7A), astrocytes (GFAP$^+$; Fig. 7B) and cells of the oligodendrocyte lineage (Olig2$^+$; Fig. 7C) 0 to 14 dpl. Control mice received bilateral craniotomies and subsequent unilateral laser illumination, without prior Ce6$^+$ beads injection. To evaluate the degree of inflammation at each time-point, laser illumination and beads injection hemispheres were compared. Note that puncturing the brain with the injection capillary constitutes a minor stab wound lesion, expected to induce a limited inflammatory reaction [Persson 1976]. Accordingly, for all markers and time points investigated, immunoreactivity was markedly stronger in the beads injection hemisphere (Fig. 7A-C, bottom rows). In the laser illumination hemisphere, only a minor and transient inflammatory reaction was observed (Fig. 7A-C, top rows), characterized by an early (6 h) activation of microglia (Fig. 7A) and a subsequent (3 dpl) upregulation of GFAP in astrocytes (Fig. 7B). Both, Iba1 and GFAP immunoreactivity returned to baseline levels at 7 dpl. Levels of Olig2 immunoreactivity were not substantially altered after photolytic lesion (Fig. 7C, top row), and only a minor increase in the number of Olig2$^+$ cells was observed at 14 dpl. Neither laser illumination alone, nor the surgical procedure of the craniotomy (Fig. 7A-C, bottom rows, w/o Inj.) resulted in a detectable inflammatory response.

5.1.4 Synopsis Part I

In summary, photolytic lesion results in reliable and reproducible, spatially confined apoptotic cell death of Ce6 labelled CPNs in S1 and V1 over the course of 7 days. The lesion is characterized by its non-invasive nature and a minor inflammatory response, leaving the overall cytoarchitecture intact. A combination of focal point and laser intensity allows for the restriction of cell loss to layer 2/3. Therefore, this lesion model is ideally suited to specifically eliminate a spatially restricted fraction of layer 2/3 cortical projection neurons in adult mice.

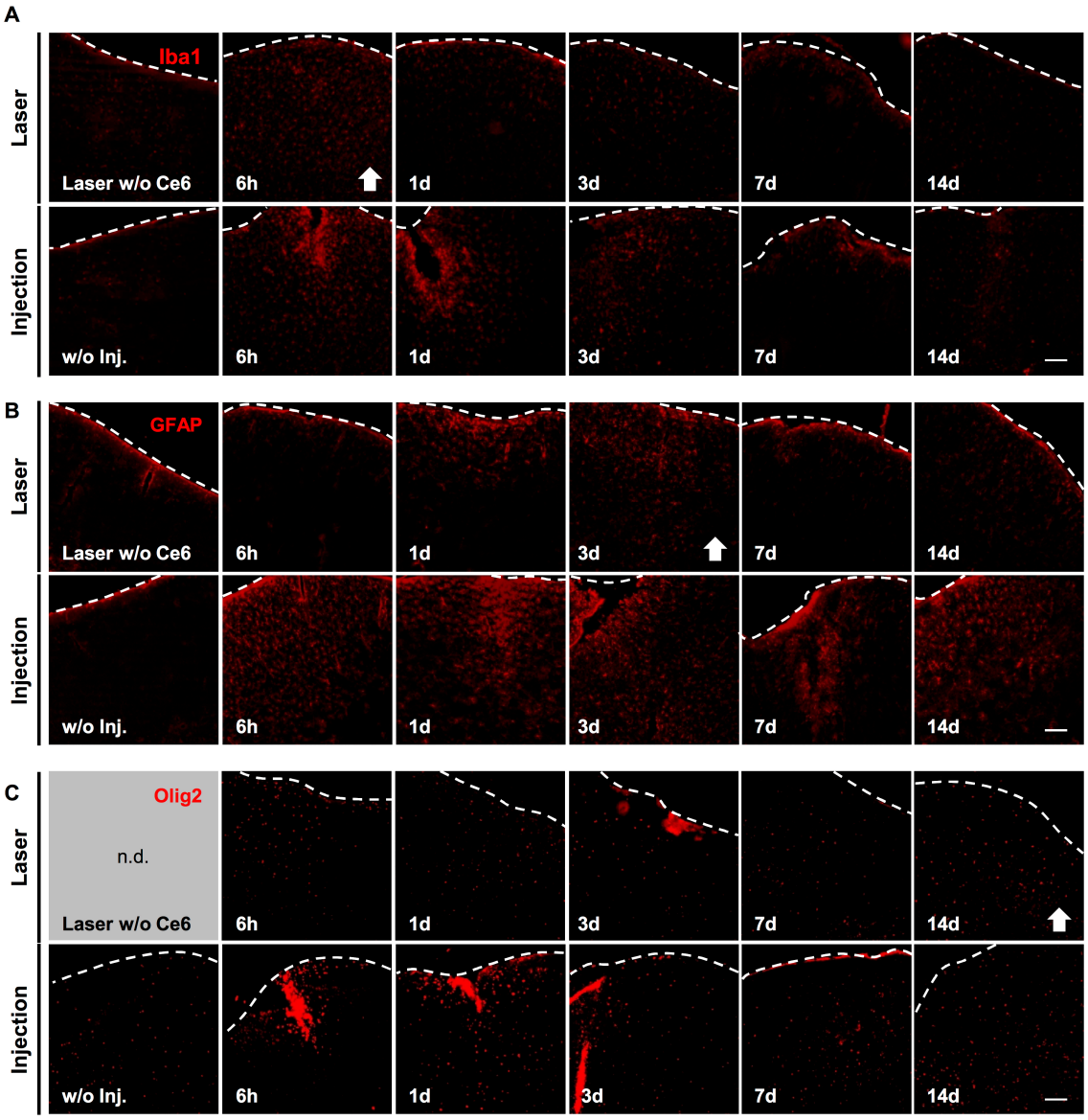

Fig. 7. Intact cytoarchitecture and minor inflammation after apoptotic photolesion *in vivo*. Immunohistochemistry for inflammatory markers after laser illumination (0 to 14 dpl). Top rows, laser hemisphere (Laser). Bottom rows, Ce6^{+} beads injection hemisphere (Injection). Controls (leftmost panels) received laser illumination without prior Ce6 labelling of CPNs (see Fig.6E). **(A)** Transient microglia activation, indicated by increased Iba1 immunoreactivity 6 h after laser illumination (white arrow, top row), followed by **(B)** an increase in GFAP immunoreactivity at day 1 and 3 (reactive astrocytes; white arrow, top row). Iba1 and GFAP return to control levels > day 7. **(C)** Olig2 immunoreactivity is moderately higher at 14 days after laser illumination (white arrow, top row) indicating a minor increase in the number of Olig2^{+} cells. (A-C) Note that the inflammatory response induced by the injection capillary (bottom rows) is more prominent and persistent compared to the inflammation caused by the photolesion. Also, the cytoarchitecture after photolesion remains intact (see also Fig. 6B and C). Scale bars: (A-C) 100 µm.

5.2 Integration of Transplanted Embryonic Neurons in Adult Neocortical Circuits

Next, I investigated the possibility of replacing lost layer 2/3 neurons with exogenous (transplanted) cells. Using chronic *in vivo* two-photon imaging through a cranial glass window [Holtmaat 2009a], I followed the morphological development, structural integration and functional development of transplanted cells.

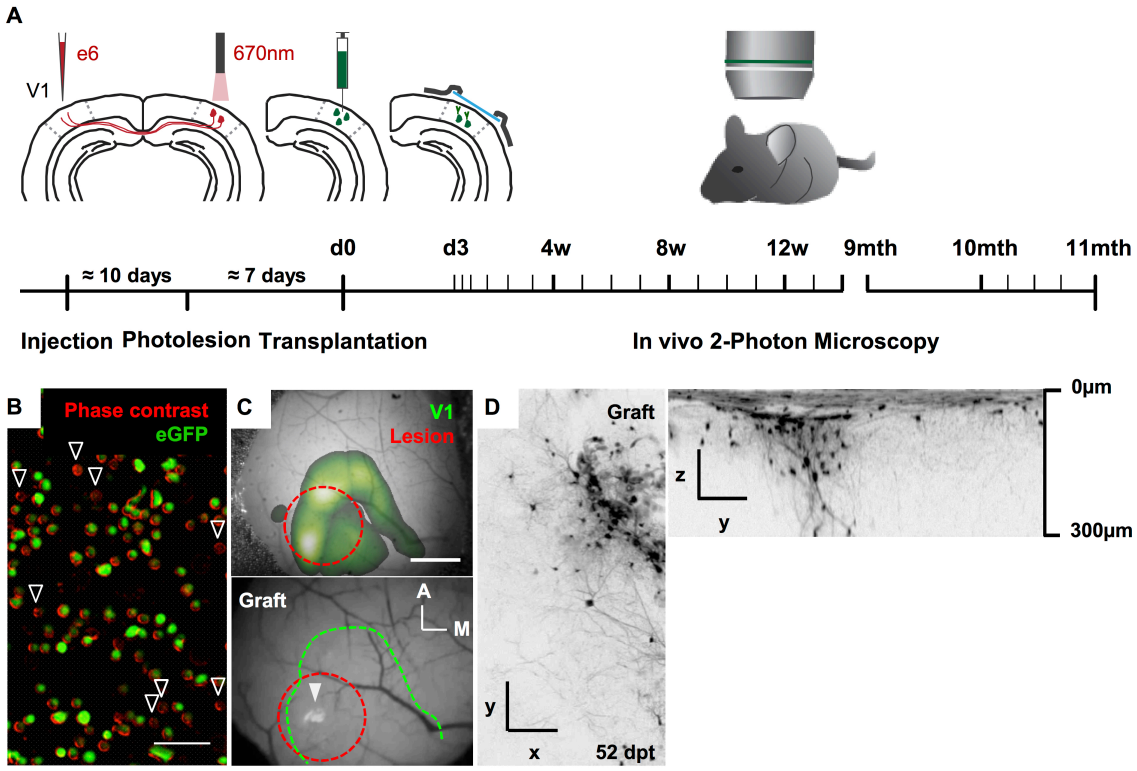

Fig. 8. Transplanted embryonic neurons integrate into the visual cortex of adult mice following local ablation of layer 2/3 CPNs. (A) Experimental procedure and timeline. Seven days after the selective local ablation of layer 2/3 CPNs (red) in V1 (binocular region) via laser photoactivation dissociated embryonic cortical neurons (green) are transplanted into the lesion site. A cranial glass window (blue) is implanted on top of the craniotomy to allow for subsequent chronic *in vivo* imaging up to 11 months. **(B)** Acutely dissociated cortical cells (see Methods) of an Emx1-cre x CAG-GFP mouse. Merge of phase contrast (red, false coloured) and fluorescence image (green). The majority of cells are GFP^+ (GFP^- cells, white arrowheads). **(C)** Top, overlay of visual stimulus evoked intrinsic optical signal (colour coded in green; see Methods) and the blood vessel pattern through a cranial glass window. Red dotted line, area of laser photoactivation. Bottom, wide field fluorescence image through the same cranial window (V1, green dotted line). Grafting site (GFP^+, white arrowhead) in the binocular region of V1. **(D)** *In vivo* two-photon z-stack projection (inverted) of a grafting site 52 dpt, top view and side view. Scale bars: (B) 50 µm; (C and D) 100 µm.

5.2.1 Transplanted Neurons Survive and Adopt L2/3-like Morphology

Donor cells for transplantation were prepared from cortical tissue of E18.5 Emx1-cre x CAG-GFP embryos (see 3.1) using a papain based dissociation system [Huettner 1986] (Fig. 8B; see 3.7). Note that in this mouse line excitatory neurons and a small fraction of glia but no inhibitory neurons are fluorescently labelled [Gorski 2002]. Five to seven days after laser-photoactivation cells were transplanted into the lesion site (see 3.7) and a cranial glass window [Holtmaat 2009a] was implanted on top of the craniotomy (see schematic in Fig. 8A; see 3.9). To verify that transplantations were located within the binocular zone of V1, I performed intrinsic optical imaging (n=16; Fig. 8C; see 3.10) at 3 days post transplantation (dpt), prior to the first *in vivo* two-photon imaging session (see 3.14.1). Individual transplanted neurons were identified and followed at short, increasing intervals (2 to 5 days) within the first 4 weeks and weekly thereafter up to 12 weeks post transplantation (wpt). In two mice I acquired late time-points at 9 to 11 months post transplantation (mth pt). *In vivo* structural imaging was performed under fentanyl based anaesthesia (see 3.1).

Transplanted neurons typically remained within 300-400 µm of the grafting site (Fig. 8D). By 4 wpt the overwhelming majority of cells had acquired layer 2/3 pyramidal cell like morphology [Miller 1981a, Miller 1988], with apical dendrites branching from one prominent dendritic trunk directed towards the pial surface and a number of basal dendrites originating at the soma (Fig. 9B and C). Note that the orientation of new neurons often deviated from the orthogonal, e.g. the main axis was tilted, and the apical dendritic tree extended from the grafting site in oblique angles. In addition, the axons of several example cells could be identified (Fig. 9C, left neuron).

Previously reported cell fusion between transplanted and host neurons [Alvarez-Dolado 2003, Ackman 2006, Brilli 2013] could lead to GFP^+ host neurons being mistaken for differentiated new cells. To control for fusion events, Emx1-Cre driven GFP^+ donor cells were always (11/11 mice in structural *in vivo* imaging experiments) grafted into tdTomato (tdT) reporter mice [Madisen 2010] (Fig. 10; see 3.1). Fusion would lead to Cre mediated expression of both, donor GFP and host tdT in such fused cells. However, GFP^+/tdT^+ cells were completely absent in all mice investigated (n=11; Fig. 10B). In addition (see below), transplanted neurons exhibited an intricate morphological development over time (Fig. 12 and 5.2.3). Together, these findings show that cell fusion did not occur after transplantation of embryonic cortical cells into areas of the photolytic lesion.

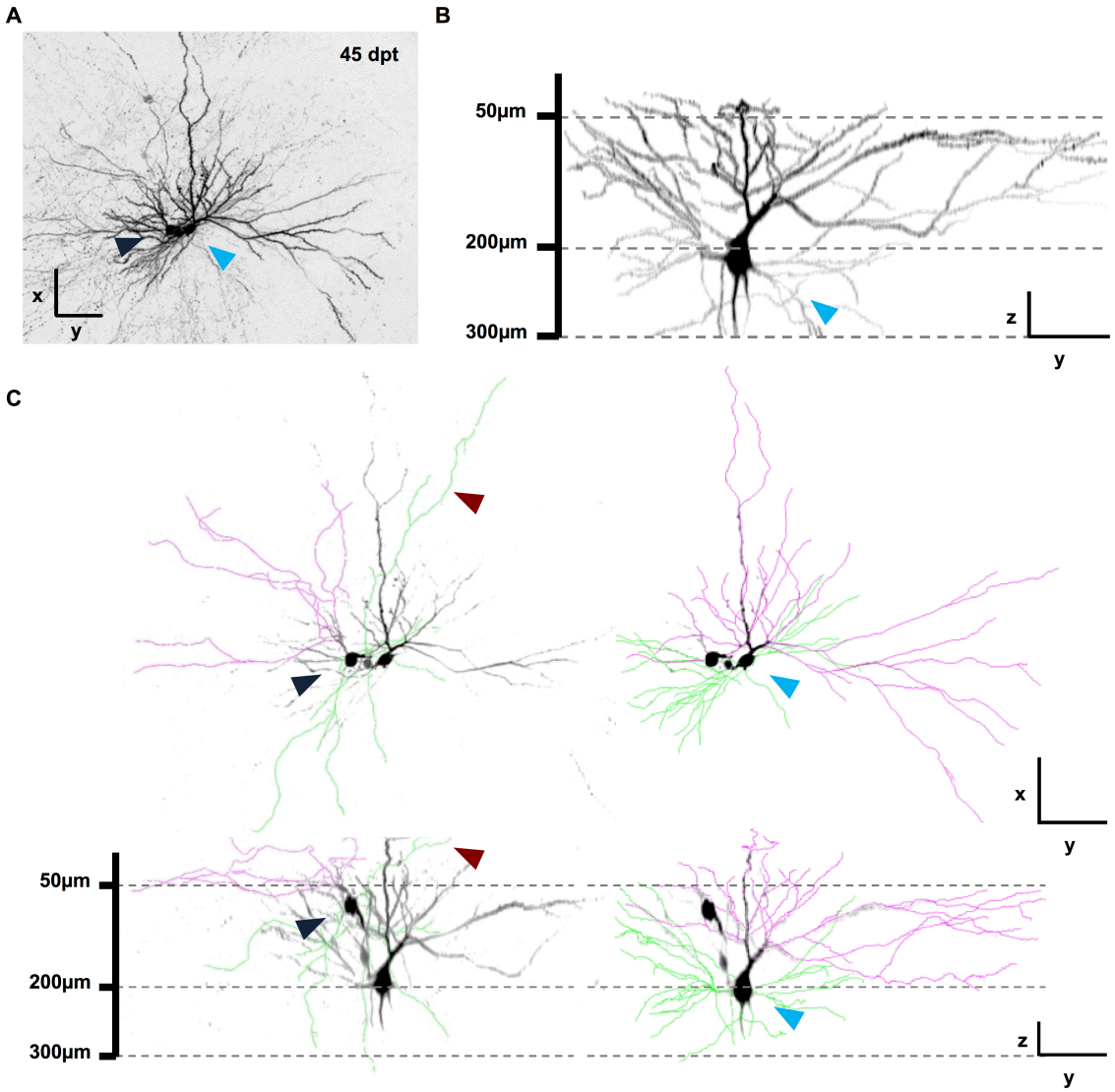

Fig. 9. Transplanted embryonic neurons adopt pyramidal neuron morphology. (A) *In vivo* two-photon z-stack projection (inverted) of transplanted neurons in host V1 at 45 dpt. **(B)** Reconstruction of neuron indicated in (A) (light blue arrowhead), side view. The cell body is located at a depth of 200 µm, apical dendrites extend up to 50 µm below the pial surface, and basal dendrites reach a depth of 300 µm. **(C)** Reconstruction (skeleton traced through *in vivo* z-stack, maximum projection) of example neurons (dark and light blue arrowheads) present in the grafting site depicted in (A) reveals typical layer 2/3 like morphology. Apical dendrites (magenta) branch from one prominent main dendritic trunk and extend to the pial surface. Basal dendrites and axon (green) extend from the cell body. Basal dendrites reach down 300 µm below the pial surface. Axon collateral, red arrowhead. Upper row, top view; lower row, side view. Scale bars: (A-C) 50 µm (x, y and z).

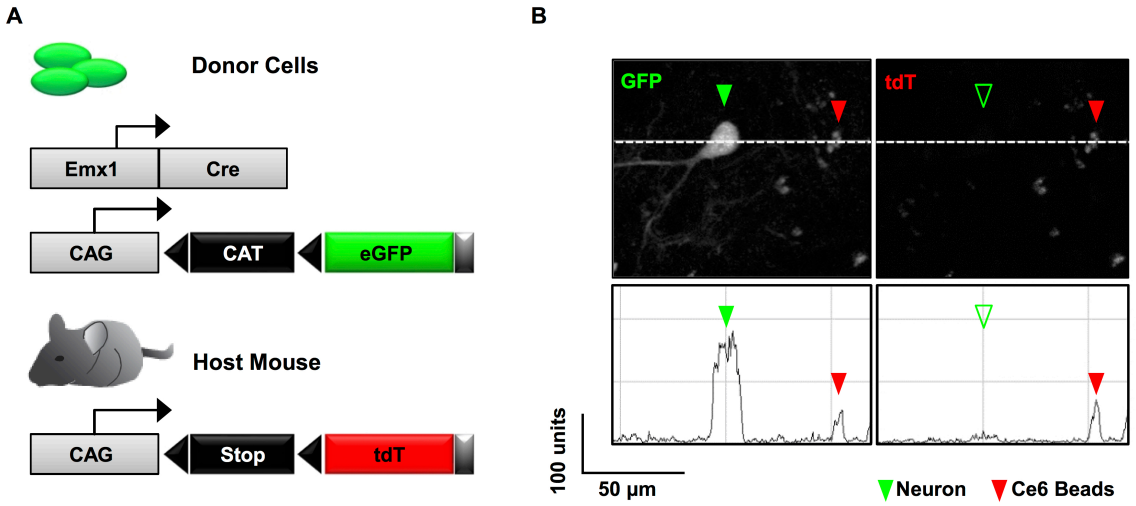

Fig. 10. Control for fusion events. (A) Genetic strategy to control for fusion events. Emx1-Cre driven GFP$^+$ donor cells were always transplanted into tdTomato reporter mice (n=10). **(B)** Absence of tdTomato fluorescence in GFP$^+$ grafted neurons *in vivo*. Line plot (along the white dotted line) across a GFP$^+$ example neuron (green arrowhead) shows that the neuron is tdT negative. Rhodamine$^+$ beads (red arrowheads) are equally detected in both channels. Units, 8 bit grayscale.

5.2.2 Ablation of Host Neurons Is Necessary for the Integration of Transplanted Cells

In a subset of experiments (n=2), host mice received an additional graft within V1, but outside of the area of laser photoactivation (Fig. 11). In contrast to neurons transplanted into the lesion area, only few neurons survived the initial transplantation (< 3 dpt). No morphological maturation was observed over the course of 4 weeks, at which time point neurons within the lesion area exhibited mature layer 2/3 like morphology (27, 28 dpt, Fig. 11; see 5.2.1). Note that despite the absence of mature neurons, cells with glial morphology were present (3, 17 and 27 dpt, Fig. 11A; 13 and 28 dpt, Fig. 11B), indicating successful transplantation. The elimination of host neurons thus seems necessary in order to allow for successful survival and differentiation of grafted neurons.

5.2.3 Early Morphological Development and Long-term Survival of Transplanted Neurons

Within the lesion area transplanted neurons exhibited an intricate morphological development (Fig. 12, A-D): At 3 to 4 dpt neurons extended hundreds of µm of branched neurites with growth cones at their tips (Fig. 12B). Already at this early time point axonal processes could be clearly identified (Fig. 13, B and 5.2.4). As early as 5 to 6 dpt a short,

main apical dendrite featured primary and secondary branch points, outlining the subsequent, more sophisticated structure of the apical dendritic tree (Fig. 12D). Thus, neuronal polarity was unequivocally established by 6 dpt. Until the end of the second week, apical dendrites grew to their full length and formed only few additional secondary or tertiary branches (Fig. 12D).

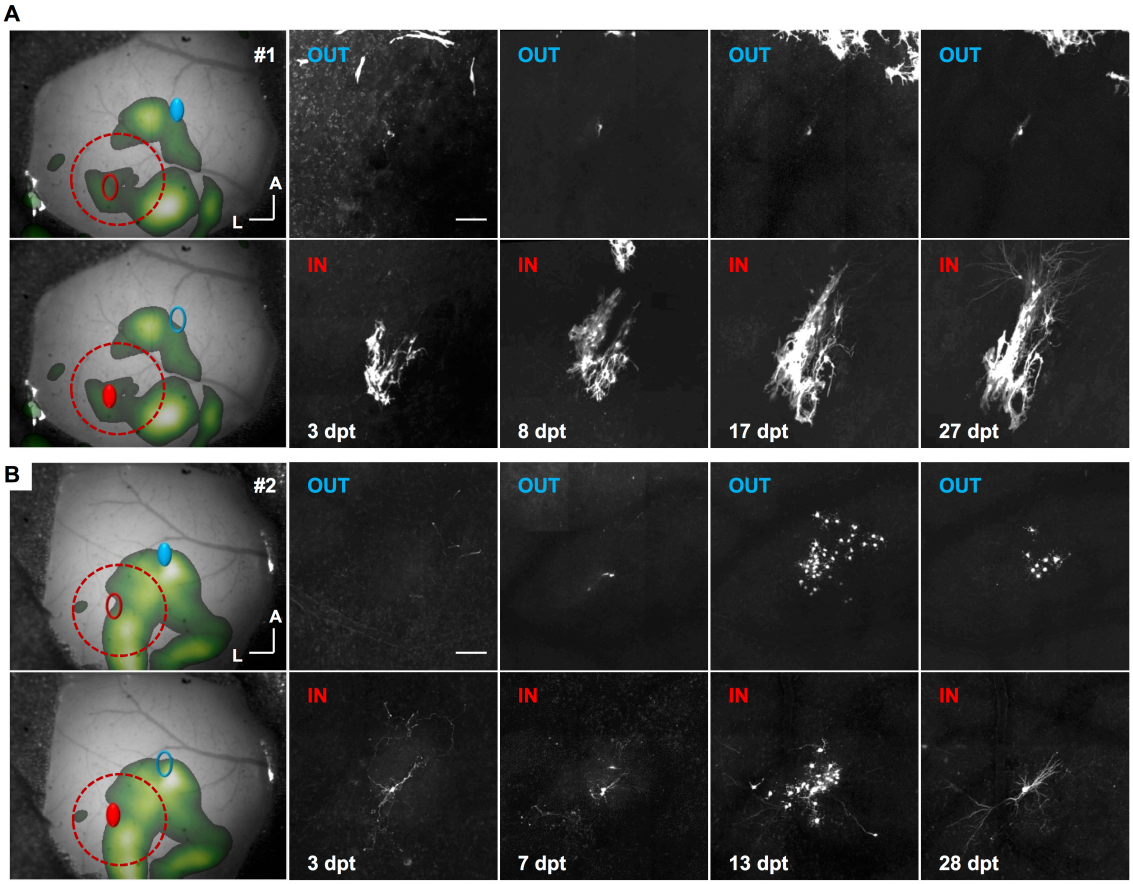

Fig. 11. Cell loss is necessary for the successful integration of transplanted neurons. Grafting inside versus outside of the area of laser photoactivation in two example mice. **(A)** Mouse #1 and **(B)** mouse #2. (A and B) Left, overlay of visual stimulus evoked intrinsic optical signal (colour coded in green) outlining V1 and the blood vessel pattern through a cranial glass window. Two grafting sites are indicated: Filled red dot (bottom), transplantation within the area of laser photoactivation (red dotted circle). Filled blue dot (top), transplantation outside of the area of laser photoactivation. Right, time series (*in* vivo two-photon z-stack projections) of transplantation sites 3 to 28 dpt within (IN, red, bottom row) and outside (OUT, blue, top row) of the laser area. Neurons transplanted within the laser area survive the initial phase of transplantation, develop layer 2/3 morphology and structurally integrate (see also Fig. 12A, Fig. 14 and 15). Few neurons transplanted outside of the laser area do survive the initial transplantation (< 3 dpt) and no morphological maturation was observed. Note the presence of presumptive glia cells albeit the absence of neurons (#1: 3, 17 and 27 dpt and #2: 13 and 28 dpt). Scale bars: (A and B) 100µm.

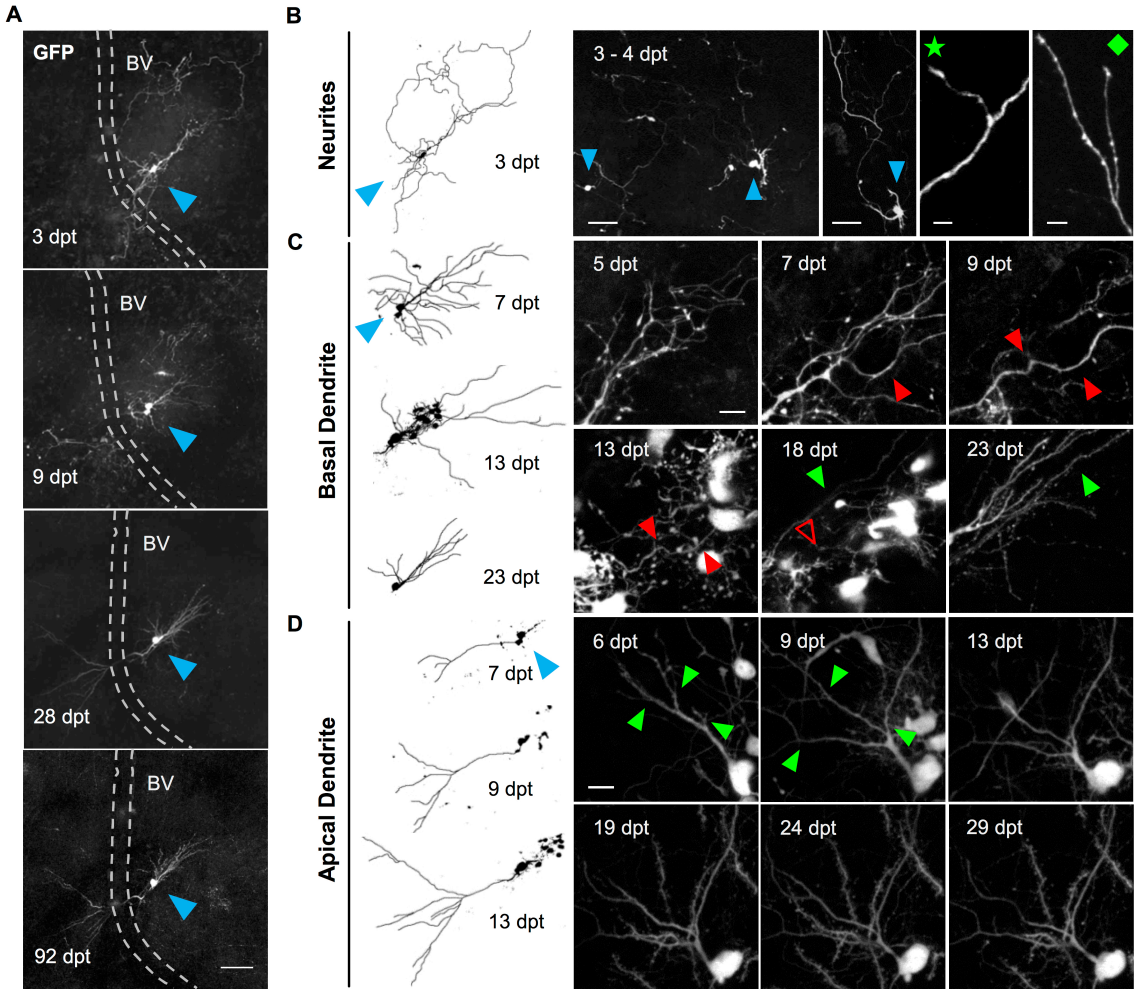

Fig. 12. Development and survival of individual transplanted neurons. **(A)** Development of an individual transplanted neuron (GFP^+) 3 to 92 dpt. Note overall stable morphology between 28 and 92 dpt. BV, blood vessel. **(B)** Left, inverted binary maximum projection of neurites at 3 dpt of neuron depicted in (A). Right, transplanted neurons extending early neurites (blue arrowheads). Star, axonal growth cone; diamond, dendritic growth cone. **(C)** Development of basal dendrites. Left, binary image and right, high magnification of neuron in (A). Pruned process, filled and open red arrowheads; newly formed processes, green arrowheads. **(D)** Development of apical dendrites. Left, binary of neuron in (A). Right, high magnification of another neuron imaged repeatedly from 6 to 29 dpt. Early branch points remain stable (green arrowheads). **(E)** Long-term survival of transplanted neurons. Right, example neuron at 23 dpt that is still present at 304 dpt. Left, inverted binary. Notably, neurons that survive the initial phase of transplantation and extend dendrites by 12 dpt are present until the end of the imaging period (97% after 2 months, 8 mice; 94% after 11 months, 2 mice). (A-D) Blue arrowhead indicates location of the cell body. (A-E) *In vivo* two-photon z-stack projections. Scale bars: (A and B) 50 µm; (B) (star, diamond) 5 µm; (C and D) 10 µm; (E) 20 µm.

In contrast, the initial neurites that would later form the basal dendrites underwent massive rearrangements that lasted until the fourth wpt (Fig. 12C). Structural development of the basal dendrites included pruning as well as *de novo* growth of processes. Note that the maturation of the apical dendritic tree preceded the formation of basal dendrites, similar to the normal embryonic development of pyramidal cells [Lund 1977, Miller 1981b, Marin-Padilla 2014]. Dendritic structural development was completed by 4 wpt, and the dendritic tree remained stable until the end of the imaging period (2 months, n=8 mice; 11 months, n=2 mice). Notably, 97% (n=8 mice) and 94% (n=2 mice) of neurons that survived the initial phase of transplantation and extended dendrites by 12 dpt were present until 2 and 11 months, respectively (Fig. 12E).

5.2.4 Development and Dynamics of Dendritic Spines and Axonal Boutons

The elaborate morphology and stability of dendritic arbors, as well as the long-term survival of transplanted neurons suggests a stable integration also at the synaptic level. As dendritic spines and axonal boutons are regarded as reliable structural correlates of synapses [Knott 2006, Harris 2012], distinct dendrites and axons were selected to follow the formation, development and dynamics of individual synaptic structures within days after transplantation and up to 11 mth pt (Fig. 13-15; see 3.14.1). Synaptic density, turnover, fractional gain and loss, survival fractions, median survival and hazard ratios (relative rate of elimination) were calculated as described in 3.15

Axonal boutons were detected as early as 3 dpt (3-4 dpt time bin, Fig. 13B) and were able to form within a few µm of the growth cone (Fig. 13C). In contrast, dendritic spines were not detected before 6 dpt and usually formed in the second week on pre-grown, arborized dendrites (Fig. 13A). Spine and bouton density increased massively up to 4 wpt, and subsequently reached a plateau (16 dendrites, n=5 mice: 1.38 ±0.17 μm^{-1} at 4 wpt; 33 axons, n=6 mice: 0.23 ±0.016 μm^{-1} at 4 wpt) (Fig. 14C and Fig. 15B). Accordingly, the high initial turnover rates, largely based on a high fractional gain of new structures and an elevated, but less pronounced loss, decreased up to 4 wpt (Fig. 14D and Fig. 15C). Notably, early-formed spines and boutons have a considerably lower survival rate compared to time-points >4 wpt (2493 individual spines, n=5 mice, $p<0.00064$ for 5-6, 7-9, 22-24 dpt; 1600 individual boutons, n=6 mice, $p<0.00018$ for 3-4, 5-6, 22-24 dpt; Gehan-Breslow-Wilcoxon comparison with Bonferroni correction) and >9 mth pt (31 spines, 8 boutons; n=2 mice, $p<0.00064$) (Fig. 14E and Fig. 15D). For instance, newly formed spines at 5-6 dpt exhibited a median survival of only 4 days compared to 28 days for spines formed at 4 to 9 wpt. Similarly, newly formed boutons at 5-6 dpt showed a median survival of 6 days compared to 14 days for boutons formed at 4 to 9 wpt. Concomitant to lower relative survival, early

formed synaptic structures exhibited a higher relative rate of elimination (spines, 2.5 times at 5-6 dpt and 1.5 times at 7-9 dpt; boutons, 8.3 times at 3-4 dpt and 1.84 times at 5-6 dpt; Fig. 16).

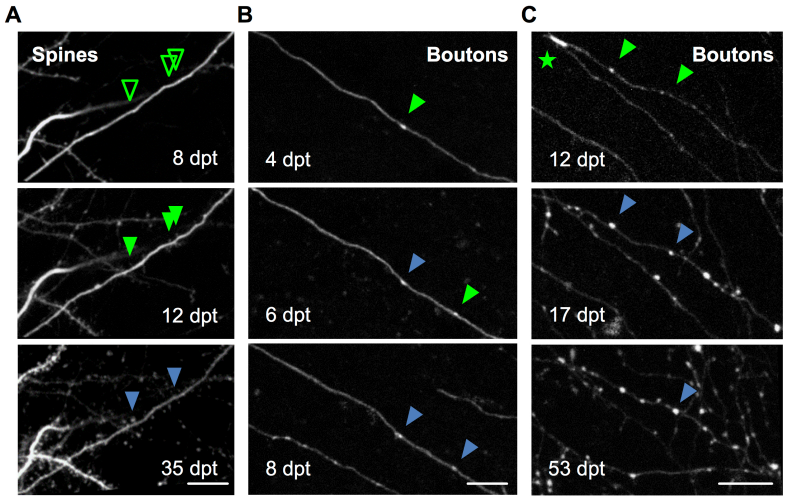

Fig. 13. Transplanted neurons form synaptic structures. **(A)** Dendrites extend and arborize considerably before the first spines form on bare dendrites. Example, bare dendrite at 8 dpt that forms first spines 12 dpt (empty green arrowheads, prospective location of newly formed spines indicated by filled green arrowheads). Two spines remain stable until 35 dpt (blue arrowheads). **(B)** Bouton formation precedes spine formation. Example axon at 4 dpt; arrowheads (green) indicate new boutons that remain stable over subsequent time points (blue arrowheads). **(C)** Boutons are able to form within a few µm of the axonal growth cone (green arrowheads). Individual boutons that have formed in the vicinity of a growth cone are able to survive for days and weeks (blue arrowheads). Scale bars: (A-C) 10 µm.

Between 5 and 8 wpt turnover rates underwent a period of transient increase and only stabilized thereafter (one-way RM-ANOVA 4-10 wpt, $p<0.0001$; Tukey post-tests) at a level of <14% (spines: 0.125 ±0.013; boutons 0.139 ±0.018; both at 10 wpt) (Fig. 14D and Fig. 15C). Notably, spine densities and turnover rates >8 wpt were comparable to the previously reported values for L2/3 pyramidal cells in the visual cortex of young adult and adult mice [Holtmaat 2005, Hofer 2009]. Altogether, at 8-10 wpt transplanted neurons had developed largely stable and persistent pre- and postsynaptic structures that remained constant up to almost a year after transplantation (9-11 mth pt).

Interestingly, spines and boutons that formed at 9 mth pt exhibited a markedly higher median survival (spines, >50 days not reaching 50% loss; boutons, 51 days; Fig. 14E and Fig. 15D) and 50% reduced relative rates of elimination (hazard ratio: spines, 0.51; boutons, 0.44; Fig. 14). Note that host mice were already up to 1.5 years old at that time point and that altered synaptic dynamics could be a result of ageing as previously observed in the normal brain of aged mice [Grillo 2013, Mostany 2013].

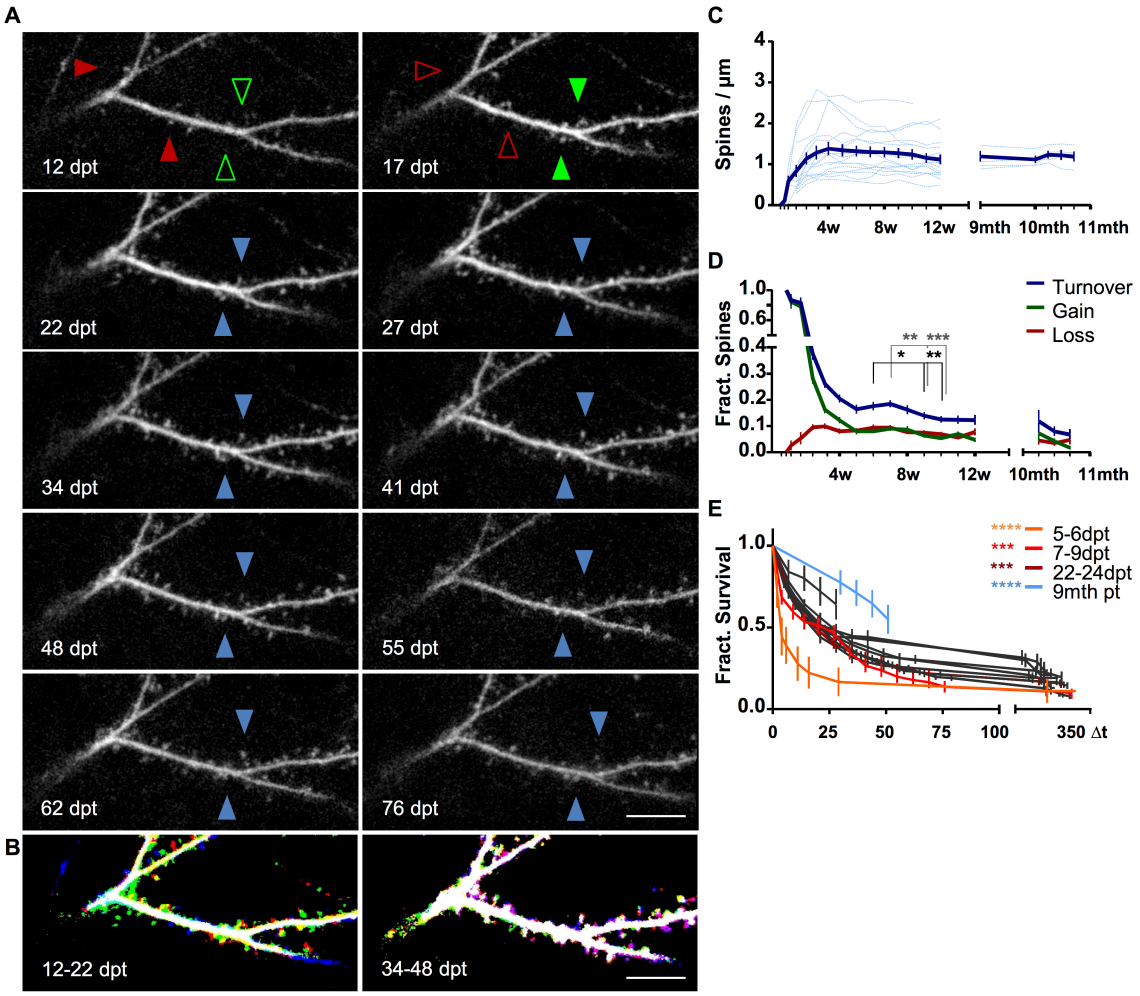

Fig. 14. Initial high turnover and long-term stabilization of dendritic spines *in vivo*. (A) Repeated *in vivo* two-photon imaging of individual dendrites at high magnification (z-stack projections). Examples of lost (red arrowheads), gained (green arrowheads) and stable (blue arrowheads) dendritic spines. **(B)** Early formed spines are dynamic, later formed spines are stable, as demonstrated by overlaying binary, color-coded images of early (left; blue, 12 dpt; red 17 dpt; green 22 dpt) and late (right; blue, 34 dpt; red, 41 dpt; green, 48 dpt) time points. **(C)** Density of dendritic spines (16 cells, n=5 mice) expressed as mean ±S.E.M (dark blue, average; light blue, individual cells). **(D)** Turnover (dark blue; sum of fractional gain, green, and fractional loss, red) of dendritic spines (16 cells, n=5 mice) expressed as mean ±S.E.M; elevated turnover until 8 wpt (one-way repeated measure ANOVA 4-10wpt, $p<0.0001$; Tukey post-tests). **(E)** Survival fraction of newly formed dendritic spines 4 dpt to 11 months post transplantation. Spines formed at early time points (red spectrum) are more prone to be eliminated. Structures formed at 9 months post transplantation (blue) have a higher chance of survival (2493 Spines, n=5 mice; $p<0.00064$, Gehan-Breslow-Wilcoxon comparison with Bonferroni correction for multiple comparison). Grey indicates groups (newly formed structures at binned time points: 3-4, 5-6, 7-9, 12-13, 17-19, 22-24 dpt and weekly bins between 4 to 9 wpt) that are not significantly different. Scale bars: (A) 10 µm.

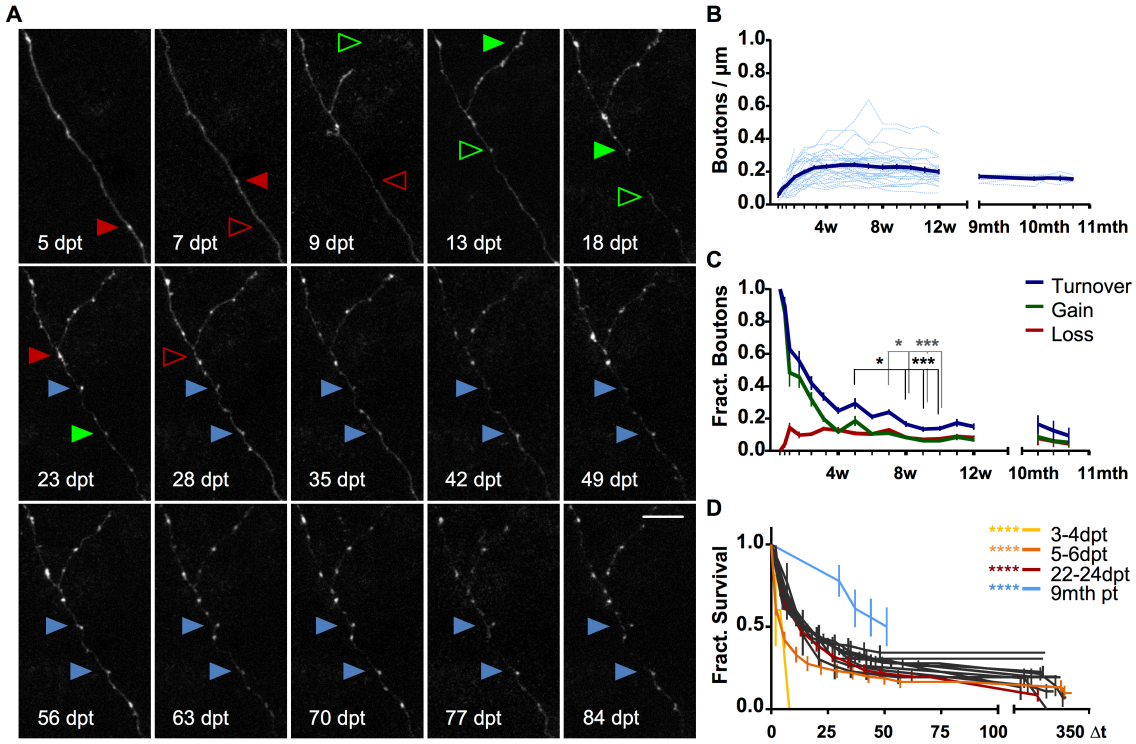

Fig. 15. Initial high turnover and long-term stabilization of axonal boutons *in vivo*. (A) Repeated *in vivo* two-photon imaging of individual axons at high magnification (z-stack projections. Examples of lost (red arrowheads), gained (green arrowheads) and stable (blue arrowheads) axonal boutons. **(B)** Density of axonal boutons (33 processes, n=6 mice), expressed as mean ±S.E.M (dark blue, average; light blue, individual cells). **(C)** Turnover (dark blue; sum of fractional gain, green, and fractional loss, red) of axonal boutons (33 processes, n=6 mice), expressed as mean ±S.E.M; elevated turnover until 8 wpt (one-way repeated measure ANOVA 4-10wpt, $p<0.0001$; Tukey post-tests). **(D)** Survival fraction of newly formed axonal boutons 4 dpt to 11 months post transplantation. Boutons formed at early time points (red spectrum) are more prone to be eliminated. Structures formed at 9 months post transplantation (blue) have a higher chance of survival (1600 boutons, n=6 mice; $p<0.00018$, Gehan-Breslow-Wilcoxon comparison with Bonferroni correction for multiple comparison). Grey indicates groups (newly formed structures at binned time points: 3-4, 5-6, 7-9, 12-13, 17-19, 22-24 dpt and weekly bins between 4 to 9 wpt) that are not significantly different. Scale bars: (A) 10 µm.

5.2.5 Transplanted Neurons Process Visual Information and Adopt Tuning Properties Typical for L2/3 Excitatory Neurons

Next, I investigated whether neurons transplanted into V1 were also able to take part in visual information processing. To this end, embryonic neurons were labelled with a red fluorescent structural marker (tdT) as well as the genetically encoded calcium indicator (GECI) GCaMP6s [Chen 2013] or Twitch2B [Thestrup 2014] (Fig. 17A). Host mice were presented with

full field gratings moving in different directions, and the responses of individual neurons were recorded using *in vivo* two-photon imaging (see 3.14.2).

Donor cells were prepared either from cortical tissue of E18.5 Emx1-Cre x Ai9 [Madisen 2010] (Rosa-CAG-LSL-tdTomato; see 3.1) or E14.5 wild type (wt) embryos using a papain based dissociation system [Huettner 1986] (see 3.7). Five to seven days after laser-photoactivation acutely dissociated Emx1-Cre x Ai9 donor cells were mixed with AAV encoding a double-floxed inverted open reading frame version of either GECI (AAV2/1-hSyn1-flex-CGaMP6s-WPRE-SV40 or AAV2/1-CAG-flex-Twitch2B-WPRE-SV40) and transplanted into the lesion site (schematic in Fig. 17B; see 3.14.2). Alternatively, E14.5 cortical cells were labelled via *in vitro* viral transduction (AAV2/1-hSyn1-flex-mRuby2-P2A-CGaMP6s-WPRE-SV40; see 3.8) and cells were mixed with AAV encoding Cre recombinase (AAV2/1.CamK2a-cre.WPRE) prior to transplantation (see 3.14.2). A cranial glass window [Holtmaat 2009a] was implanted on top of the craniotomy (see 3.9) and intrinsic optical imaging was performed to verify that grafts were located within the binocular zone of V1 (n=5; Fig. 8C; see 3.10).

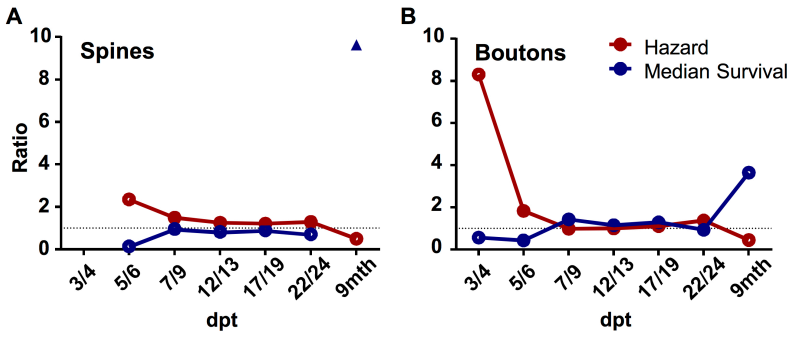

Fig. 16. Survival of newly formed dendritic spines and axonal boutons. Comparison of early-formed spines and boutons with later structures (formed 4 to 9 wpt). Median survival ratios indicate the relative survival. Hazard ratios indicate the relative chance for structures to be lost. **(A)** Early formed dendritic spines (<12 dpt) have a 1.5 to 2.4 times higher chance of being eliminated compared to spines newly formed 4 to 9 wpt. Elevated hazard ratios (>1.2) up to 24 dpt. Spines formed at 9 mths pt have a high chance of survival: While the median survival 4 to 9 wpt is 28 days, more than half of the spines formed at 9 mths pt survive at least for 51 days (blue triangle, arbitrary value as survival is >50%). **(B)** Early formed axonal boutons (<7 dpt) are 2 to 8 times more likely to be eliminated compared to boutons newly formed 4 to 9 wpt. Boutons formed at 9 mths pt, have a 4 times higher chance of survival.

At 4 to 15 wpt full field gratings moving in 8 directions (square wave, high contrast; 0.04 cyc deg^{-1}, 1.5 cyc s^{-1}) were presented to the contralateral eye of lightly anaesthetised mice (see 3.14.2). Individual responsive neurons (tdT^{+}/GECI^{+}) were identified and repeatedly recorded once a week at 4 to 9 wpt and once every two weeks up to 15 wpt (Fig. 17, B and C; see 3.16). Neuronal activity was measured as the average change in GECI

fluorescence relative to baseline during visual stimulation (GCaMP6s: ΔF/F0, Twitch2B: ΔR/R0; see 3.16), and both, somata and individual axons were analysed (Fig. 17, C-G). Neurons were classified as visually responsive if the average ΔF/F0 > 3σ (GCaMP6s) or ΔR/R0 > 0.05 [Thestrup 2014] (Twitch2B) for at least one stimulus direction. In some instances, I was able to record and analyse host input onto grafted neurons on the level of individual dendritic spines (Fig. 17, C-G and Fig. 21).

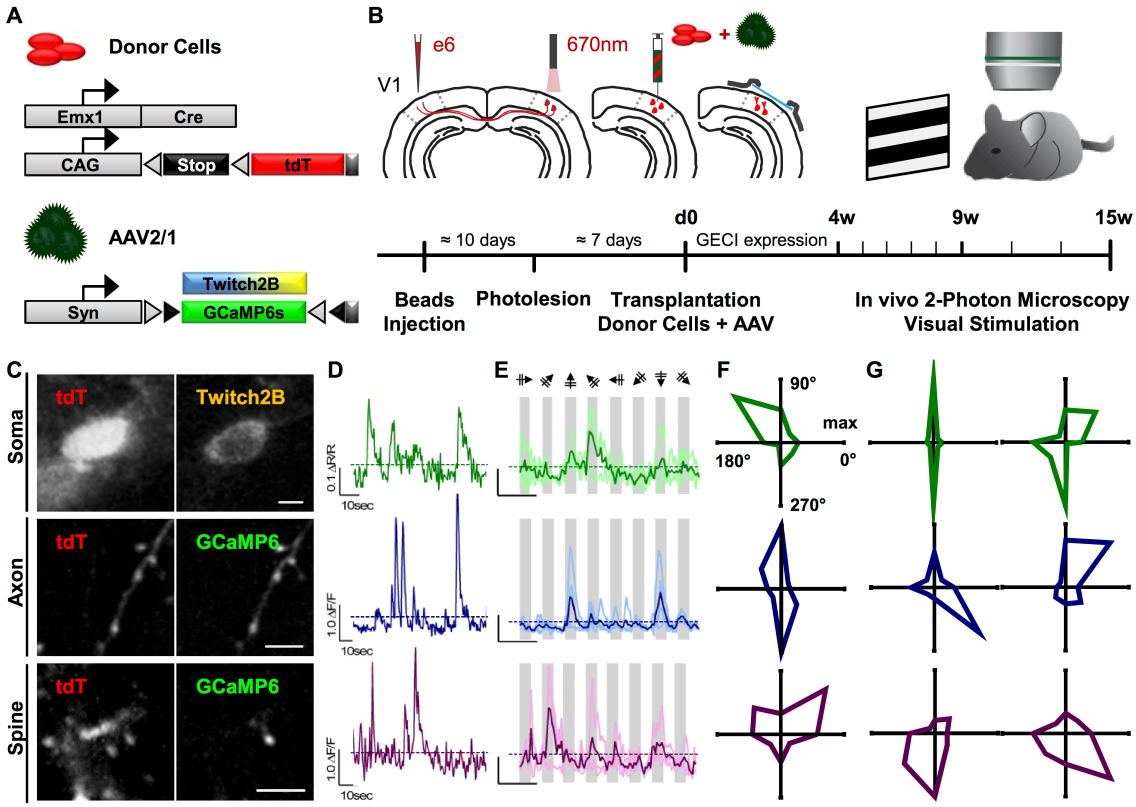

Fig. 17. Transplanted neurons show tuned responses to visual stimuli. (A) Embryonic donor cells were co-labelled with Emx1-Cre driven tdTomato and GECIs (GCaMP6s or Twitch2B, respectively; delivered via AAV). **(B)** Experimental timeline. Following transplantation, chronic two-photon calcium imaging was performed at 4 to 15 wpt. Mice were presented with full field gratings moving in 8 directions. (C-G) Changes in GECI fluorescence was recorded in cell bodies (green traces), axons (blue traces) and dendritic spines (magenta traces) of transplanted neurons. **(C)** Examples of transplanted neurons (tdT^+) also expressing GECIs. Single optical planes, maximum projection of all frames of one stimulation sequence. **(D)** Stimulus evoked changes in fluorescence relative to baseline (dR/R, Twitch2B; dF/F, GCaMP6), example traces. **(E)** Single (thin line) and average responses (thick line) to repeated stimulus presentations, sorted to the respective grating orientation and direction. Grey: stimulus on. **(F)** Normalized average maximum peak response at each direction plotted in polar coordinates for cells depicted in (C). **(G)** Polar plots of further example cells. Transplanted neurons display tuning properties typical for upper layer pyramidal neurons in V1. Scale bars: (C) 5 µm.

Almost all observed neurons with significant changes in fluorescence (ANOVA $p<0.05$; Fig. 17D) exhibited stimulus-evoked responses (27/28 cells, n=5 mice; Fig. 17E) and the majority of visually responsive neurons displayed relatively sharp tuning properties (OSI >0.3 and/or DSI >0.2; see 3.16) typical for excitatory projection neurons in upper L2/3 of adult V1 [Sohya 2007, Neil 2008] (25/27 cells, n=5 mice; Fig. 17, F-G). Notably, almost half of the neurons showed strong orientation and/or direction selectivity with OSI and/or DSI >0.5 (13/27 cells, n=5 mice). Also, input from the host network included stimulus-driven and strongly tuned presynaptic cells, as measured on the level of individual dendritic spines (3/5 spines, n=2 mice, OSI >0.5 and DSI >0.6; Fig. 17, C-G bottom row).

Preferred directions of transplanted neurons across all time points were spread over all directions, with a slight preference for cardinal versus oblique directions (Σ 47 vs. Σ 23 cumulative neurons across all time points; Fig. 18). A similar preference for cardinal directions was previously observed in young and adult mouse V1 [Rochefort 2011, Kreile 2011, Roth 2012].

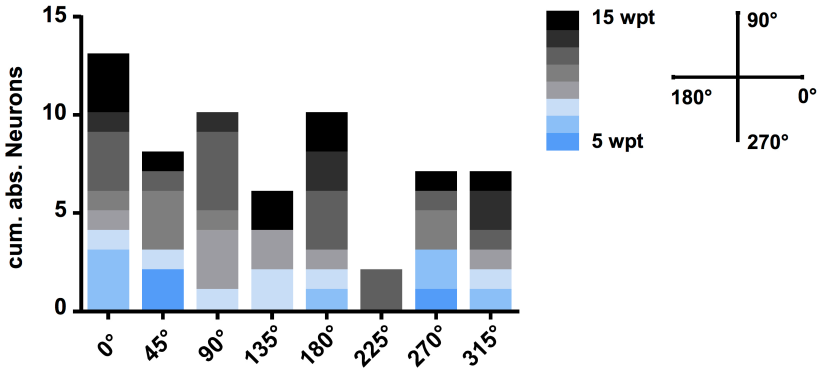

Fig. 18. Direction preference of transplanted neurons covers the full range of presented stimuli. Cumulative absolute number of grafted neurons across imaging time points, sorted according to their respective preferred direction. Transplanted neurons are tuned to all directions, with a slight overrepresentation of cardinal directions.

5.2.6 Transplanted Neurons Show Binocular Responses

At 15 wpt a subset of transplanted neurons responsive to the contralateral eye (5/10 cells, n=3 mice) were also subjected to stimulation of the ipsilateral eye (see 3.16). Consistent with grafting sites in the binocular region of V1 [Dräger 1975] investigated neurons were also responsive to ipsilateral stimulation (Fig. 19). Neurons showed relatively sharp and comparable ipsi- and contralateral tuning properties (ipsilateral: OSI 0.34 ±0.030, DSI 0.25 ±0.070; contralateral: OSI 0.32 ±0.128, DSI 0.32 ±0.074). Note that both, divergent (Fig. 19A) and matching (Fig. 19B) peak preferences were observed.

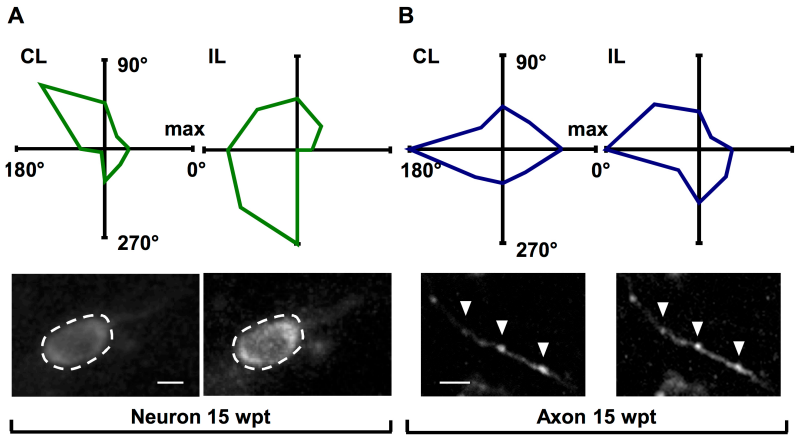

Fig. 19. Transplanted neurons show binocular responses. Individual transplanted neurons respond to ipsi- and contralateral eye stimulation (IL and CL, respectively). Top row, polar plots; bottom row, single planes, maximum projection of all frames of one stimulation sequence. **(A)** Example cell recorded at the soma (dashed line, white) and **(B)** example cell recorded at axonal boutons (white arrowheads). Scale bars: 5 µm.

5.2.7 Functional Development and Long-term Stabilization of Tuning Properties

5.2.7.1 Early Tuning Variability Stabilizes >9 wpt

Transplanted neurons responsive to visual stimulation exhibited some degree of orientation and/or direction preference as early as 5 wpt (Fig. 18, Fig. 20 and Fig. 23A). However, the individual preferred direction and the overall tuning profile of many repeatedly imaged neurons varied markedly over subsequent time points (10/14 cells, n=4 mice; Fig. 20, Fig. 23A and Fig. 24A), indicating ongoing functional development.

Notably, these changes in tuning seemed not to be directed e.g. random, and occurred in neurons with predominant orientation but minor direction selectivity (Fig. 20B), as well as in strongly direction selective neurons (Fig. 20A). Also, a similar variability was recorded at individual spine heads (Fig. 21), again with marked changes in peak preference and tuning profile, indicating that the presynaptic input is variable across time points. Thus, it seems possible that input from the host network undergoes re-arrangement and/or changes in synaptic strength concurrent to the functional development of transplanted neurons.

It is not before 9 wpt that responses of transplanted neurons finally started to stabilize, and from 11 to 15 wpt only very little variability in overall tuning was observed (Fig. 22) compared to <9 wpt (Fig. 23, A vs. B). In order to quantitatively describe the changes in tuning of transplanted neurons over time, the difference in preferred orientation in successive imaging time points was calculated for all neurons recorded without interruption, at least twice (14/27 cells, n=4 mice, 4-5 cells per time point; Kruskal-Wallis test, p=0.0491; see 3.16). The average difference in preferred orientation decreased from high initial values (Δ6-7 wpt, 56.25 ±11.25) to 40% at Δ9-11 wpt (22.5 ±22.5), until finally, no change was observed Δ13-

15 wpt (5 cells, n=2 mice; Fig. 24A). Notably, the stabilisation of tuning closely correlated to the final stabilisation of spine and bouton turnover rates (8-10 wpt; Fig. 14 and Fig. 15; see 5.2.4).

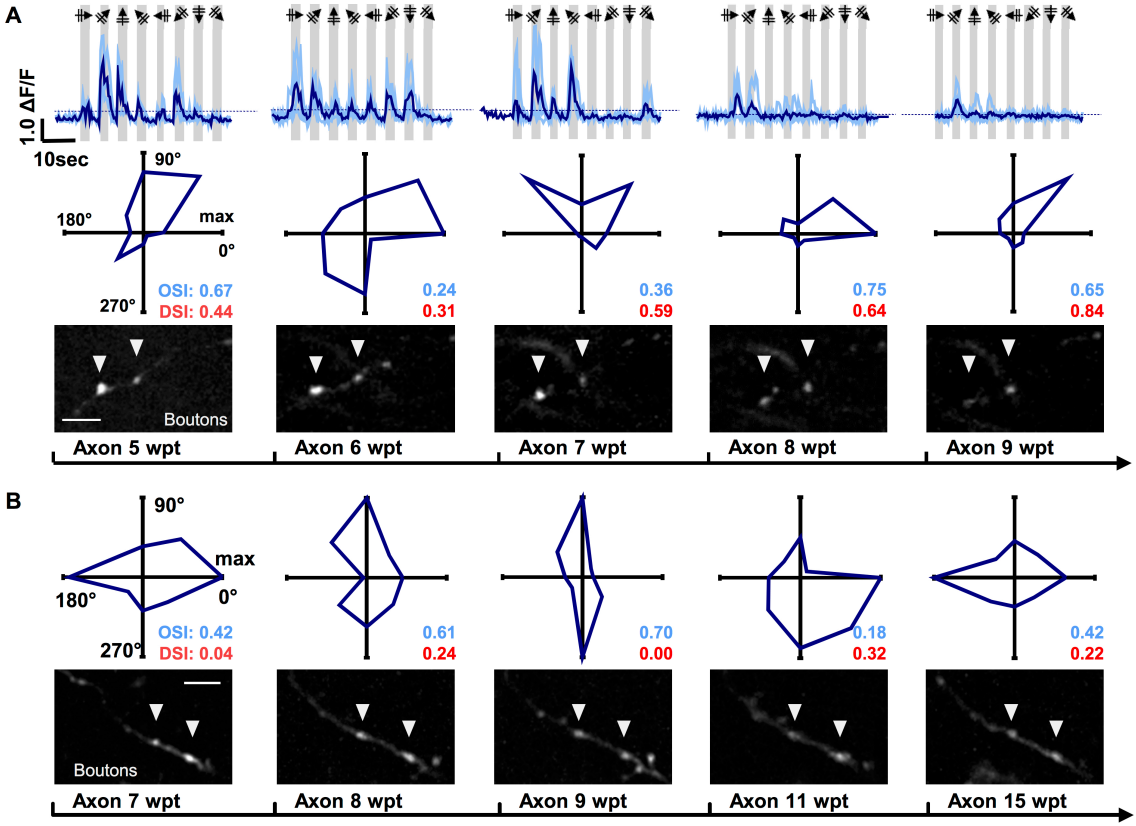

Fig. 20. Tuning properties of transplanted neurons develop over time. (A) Changes in tuning at 5 to 9 wpt, measured from the axon of a direction selective transplanted cell (see 3.16). **(B)** Changes in tuning at 7 to 15 wpt, measured from the axon of an orientation selective cell. Top row in (A), individual (light blue) and average (dark blue) stimulus evoked responses. Grey: stimulus on; Middle row in (A) and top row in (B), polar plots and orientation and direction selectivity indices (OSI/ DSI); (A and B) bottom row, single plane maximum projections of 150 frames during visual stimulation (white arrowheads indicate axonal boutons). Note the marked changes in overall tuning including the preferred direction (peak response, max) across time points. Scale bars: (A and B) 5µm.

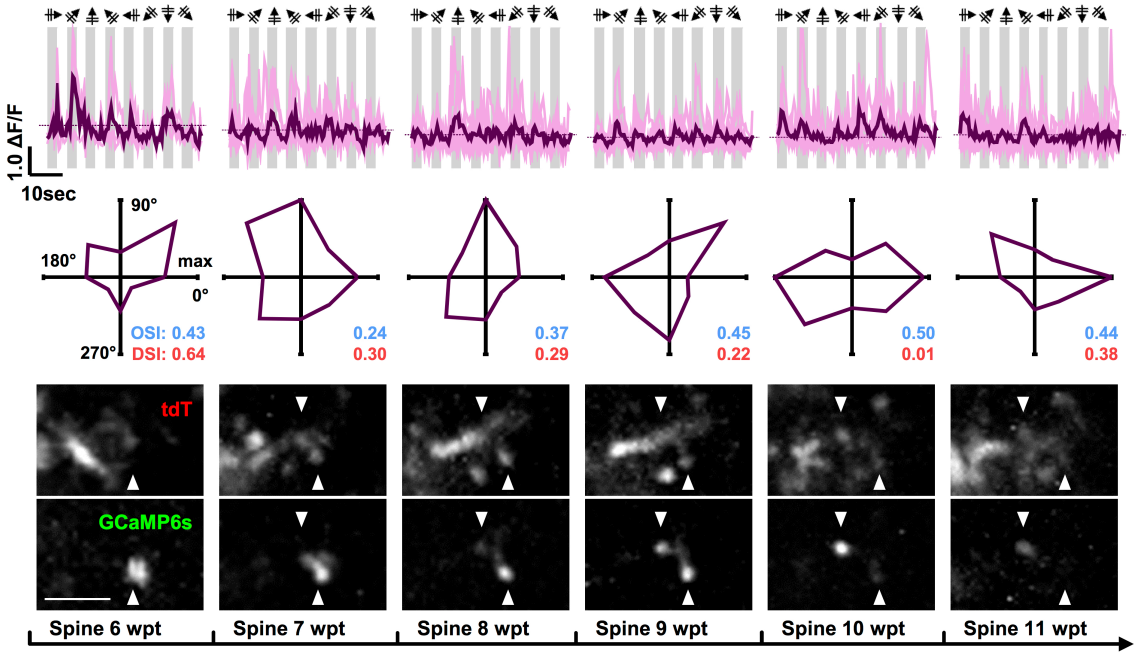

Fig. 21. Transplanted neurons receive stimulus evoked tuned input from host cells. Top row, individual (light magenta) and average (magenta) stimulus evoked responses measured repeatedly from a single spine of a transplanted neuron 6 to 11 wpt. Grey: stimulus on; Middle row, polar plots and orientation and direction selectivity indices (OSI/ DSI); Bottom row, single plane maximum projections of 150 frames during visual stimulation of the red (tdT) and green (GCaMP6s) channel (white arrowheads indicate spine heads of the bifurcated spine). Note the marked changes in overall tuning including the preferred direction (peak response, max) across time points. Scale bars: 5 µm.

5.2.7.2 Selectivity, Sharpness and Reliability of Responses across Time-points

In order to describe the functional development of transplanted neurons more closely, I quantified their average tuning sharpness and selectivity, as well as the overall trial-to-trial reliability of responses between 6 and 15 wpt (see 3.16).

From 6 to 9 wpt, when transplanted neurons exhibited marked changes in individual tuning preference (Fig. 20 and Fig. 24A; see 5.2.7.1), the overall orientation and direction tuning of new neurons sharpened considerably (27 cells, n=5 mice; A). OSI and DSI values increased up to 9 wpt (6 wpt: OSI 0.25 ±0.036, DSI 0.19 ±0.050; 9 wpt: OSI 0.67 ±0.080, DSI 0.61 ±0.134), then decreased slightly and stabilized by 11 wpt at values previously reported for neurons imaged in L2/3 of adult mouse V1 [Marshel 2011] (11 wpt: OSI 0.43 ±0.060, DSI 0.36 ±0.064; 15 wpt: OSI 0.46 ±0.083, DSI 0.32 ±0.063). In addition, a comparison of normalized tuning curves aligned to peak (Fig. 24C) at 6, 9 and 15 wpt (17 cells, n=4 mice; 6-8 cells per time point; two-way ANOVA, p=0.0029, Tukey post-tests) also showed an

overall increase in tuning sharpness, as well as selectivity (6 vs. 9 wpt, p=0.0170), followed by subsequent stabilization (9 vs. 15 wpt, n.s.).

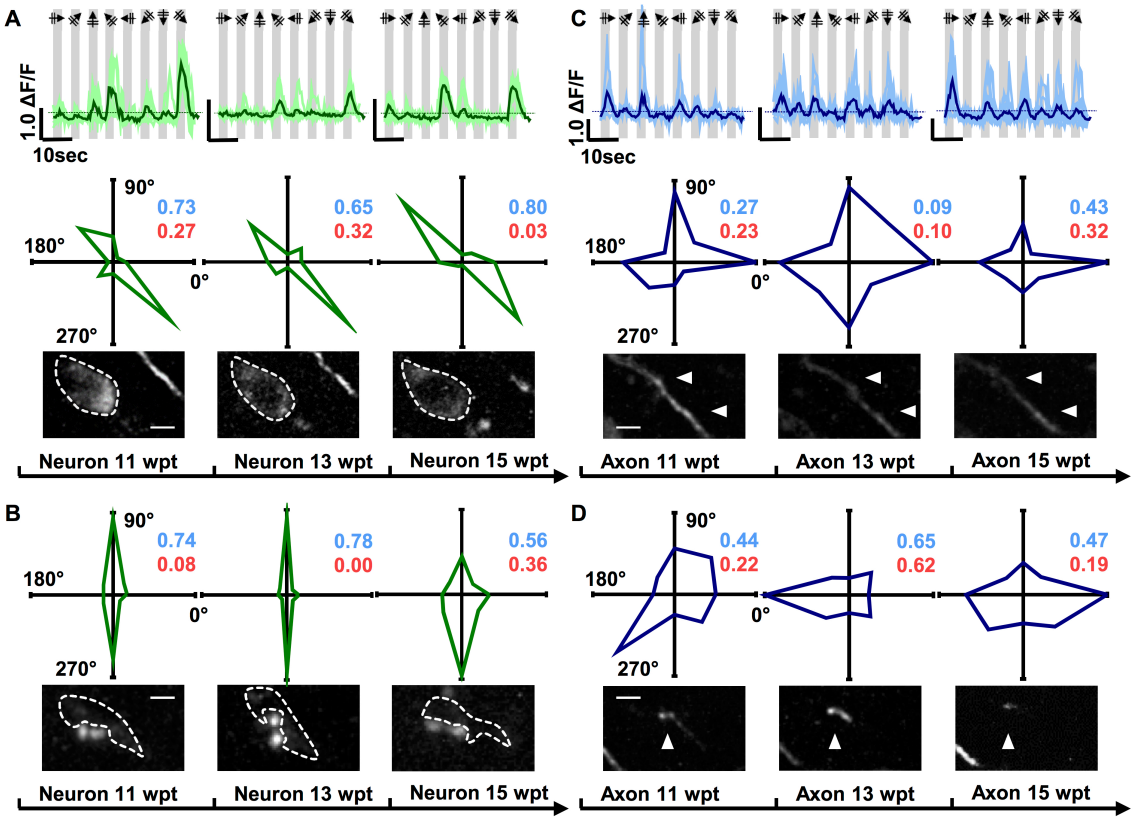

Fig. 22. Tuning properties stabilize at 11 to 15 wpt. Four individual examples of tuning properties measured repeatedly from the soma **(A and B)** and axon **(C and D)** of transplanted neurons at 11, 13 and 15 wpt. (A and C) Top row, individual (light traces) and average (dark trace) stimulus evoked responses to drifting grating in 8 directions (arrows), grey: stimulus on. (A and C) Middle row and (B and D) top row, polar plots and orientation and direction selectivity indices (OSI, blue; DSI, red). (A-D) Bottom row, single plane maximum projections of 150 frames during visual stimulation (white dashed line, soma; arrowheads, axonal boutons). Note the stability of the overall tuning including the preferred direction (peak response, max) and/or orientation (peak response + 180°) across time points. Scale bars: (A-D) 5 µm.

Since OSI and DSI, as ratio based indicators of tuning, do not take into account the distribution of responses across all tested directions, I further calculated single and double Gaussian fits [Mazurek 2014] (Fig. 25) for the same set of cells as shown in Fig. 24B. Following the assumption that an ideal orientation- (Fig. 25A) or direction-tuned neuron (Fig. 25B) would be perfectly described by a double or single Gaussian fit, the goodness of fit (R^2) served as a measure of tuning quality. Both, double and single Gaussian R^2 increased between 6 and 9 wpt (DG: 6 wpt 0.45 ±0.094, 9 wpt 0.79 ±0.064, p=0.0482; SG: 6 wpt 0.29 ±0.067,

9 wpt 0.66 ±0.099, p=0.0482; Kruskal-Wallis test, Dunn's post-tests) and stabilized thereafter (9 vs. 15 wpt, n.s.), further corroborating the above results (Fig. 25E, Fig. 24, A and C).

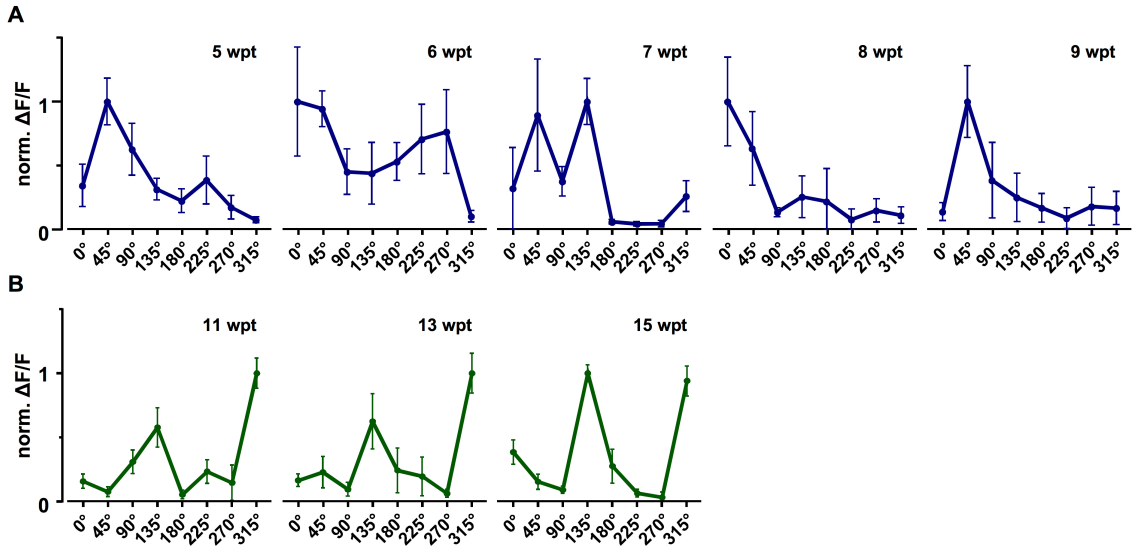

Fig. 23. Early development and late stabilization of tuning. (A) Example cell (same as Fig. 20A) exhibiting changes in overall tuning, displayed as 2D tuning plot (mean ±S.E.M; two-way ANOVA, p=0.0162). ΔF/F normalized to max. average peak amplitude at each time point (5 - 9 wpt). **(B)** Example cell (same as Fig. 22A) displaying invariable tuning (mean ±S.E.M; two-way ANOVA, p=0.6505, n.s.). ΔF/F normalized to max. average peak amplitude at each time point (11 - 15 wpt).

Another measure of tuning quality is the reliability of neuronal responses to the same stimulus direction over multiple repetitions. Therefore, I compared the average trial-to-trial correlation of responses during visual stimulation to the preferred direction across time-points (Fig. 24A, dashed line; same set of neurons for both curves, 14/27 cells, n=4 mice; see 3.16 and 5.2.7.1). Early time-points exhibited poor reliability, with low average correlation coefficients (minimum at 7 wpt, 0.04 ±0.101). Correlations increased over time (Kruskal-Wallis test, p=0.0479) and plateaued at 9 to 15 wpt (9 wpt 0.47 ±0.089, 15 wpt 0.48 ±0.068). Interestingly, this increase in response reliability concurred with the above described decrease in tuning variability at ∆9-11 wpt (Fig. 24A; see 5.2.7.1) and the stabilisation of synaptic turnover rates at 8-10 wpt (Fig. 14 and Fig. 15; see 5.2.4).

In addition, for GCaMP6s cells at 6, 9 and 15 wpt (15 cells, n=3 mice; 5-7 cells per time-point) I calculated the average co-efficient of variation (CoV). As an alternative measure of reliability, CoV reports the trial-to-trial variability of responses (6 wpt 1.07 ±0.111, 9 wpt 0.78 ±0.102, 15 wpt 0.65 ±0.109; see 3.16). Complementary to the reported increase in reliability (Fig. 24A), the average CoV decreased over time (Kruskal-Wallis test, p=0.0379,

Dunn's post-tests; 6 vs. 15 wpt p=0.0489, 9 vs. 15 wpt n.s.). Note that respective changes in both measures, correlation coefficient and CoV, have previously been described during the maturation of the mammalian [Ko 2014] and vertebrate [Xu 2011] visual system.

Together, the observed stabilisation of tuning, the sharpening of orientation and direction tuning, as well as the increase in selectivity and reliability of responses of transplanted neurons strongly indicate a functional maturation over the course of 2-3 months.

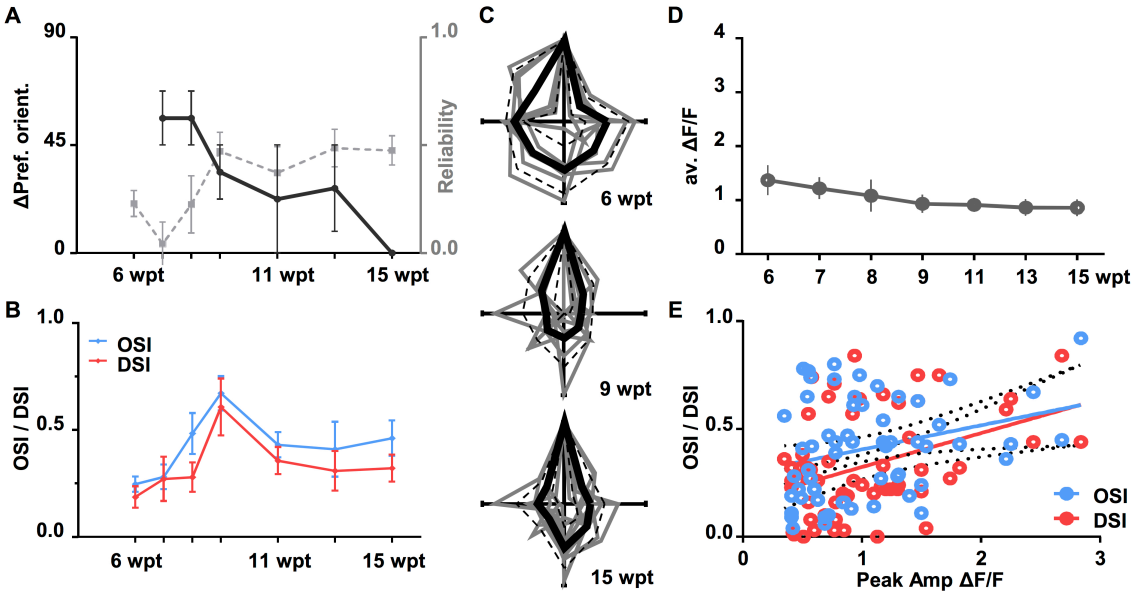

Fig. 24. Tuning of transplanted neurons sharpens over time. (A) Difference in preferred orientation (dark grey; Kruskal-Wallis test, p=0.0491) and reliability (mean trial-to-trial coefficient of correlation, light grey; Kruskal-Wallis test, p=0.0479) of neurons recorded at least at two subsequent time points (one or two weeks interval) from 6 to 15 wpt (mean ±S.E.M; 14 cells, n=4 mice). Note the simultaneous decrease in tuning variability and increase in response reliability to the preferred direction. **(B)** OSI and DSI between 6 and 15 wpt (mean ±S.E.M; 27 cells, n=5 mice). **(C)** Overlay of individual polar plots (grey) and mean ±S.D. (black) at 6, 9 and 15 wpt (preferred direction aligned to 90°, top) shows overall sharpening of tuning (17 cells, n=4 mice; 6-8 cells per time point; two-way ANOVA, p=0.0029). Average peak amplitudes are constant **(D)** across imaging time points (mean ±S.E.M; 25 GCaMP6s cells, n=4 mice; Kruskal-Wallis test, p=0.593, n.s.) and do not correlate with specificity **(E)** OSI (blue), R^2=0.082; DSI (magenta), R^2=0.151; solid lines, linear regression; dashed lines, 95% CI. Reported non-linearity effects of calcium indicators [Nauhaus 2011] would predict higher selectivity indices at lower average peak amplitudes. Note, it is unlikely that the changes in tuning preference and specificity of transplanted neurons reported here are due to non-linearity effects of the calcium indicators, as we see both, marked changes in tuning preference (B) at constant average peak amplitudes (D) across time points, as well as stable tuning at late time points (see Fig. 22).

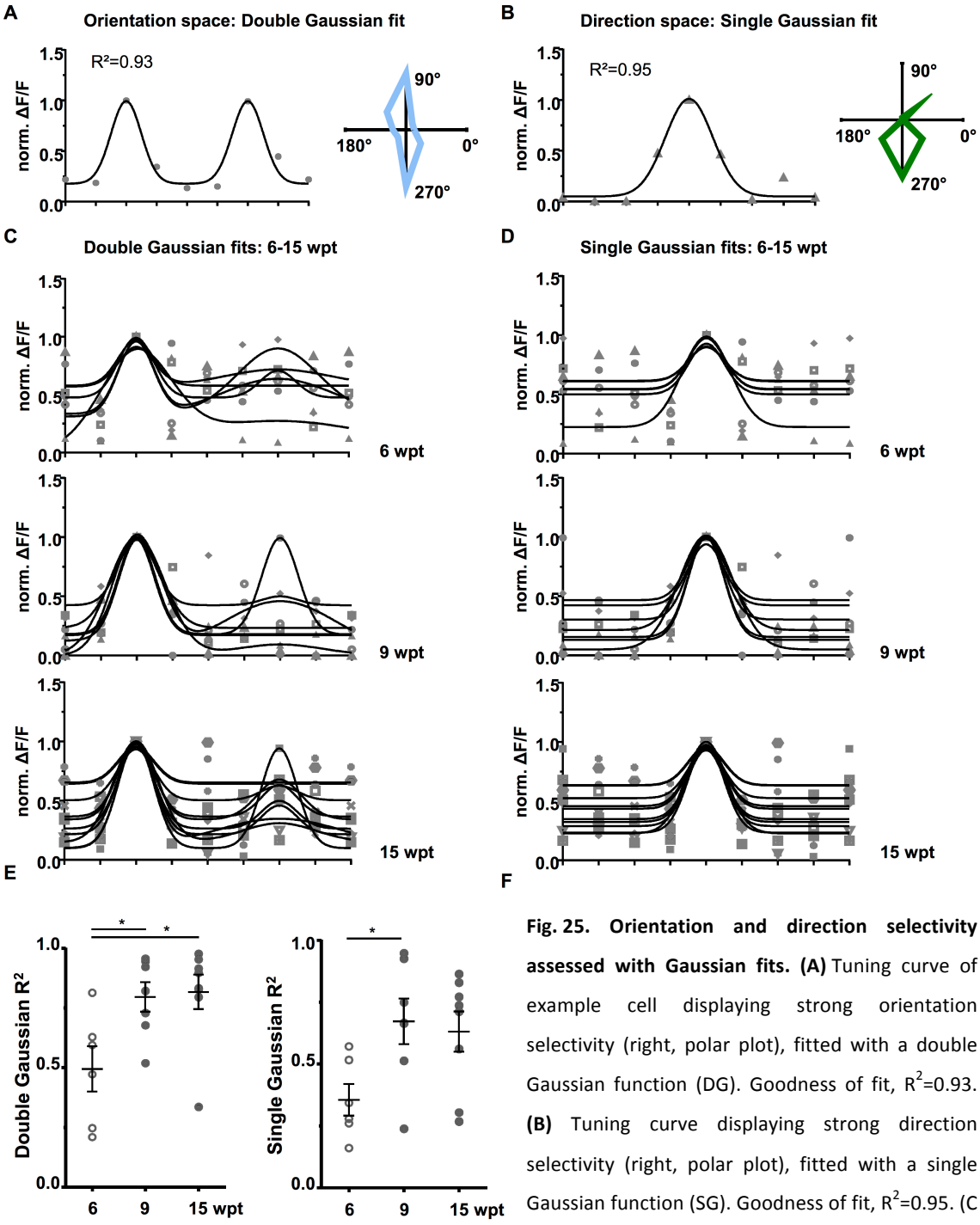

Fig. 25. Orientation and direction selectivity assessed with Gaussian fits. (A) Tuning curve of example cell displaying strong orientation selectivity (right, polar plot), fitted with a double Gaussian function (DG). Goodness of fit, R^2=0.93. **(B)** Tuning curve displaying strong direction selectivity (right, polar plot), fitted with a single Gaussian function (SG). Goodness of fit, R^2=0.95. (C and D) Individual DG fits **(C)** and SG fits **(D)** of 17 cells in total (n=4 mice) at 6, 9 and 15 wpt. (E and F) Average goodness of fit of **(E)** double (DG) and **(F)** single (SG) gauss functions (mean ±S.E.M; 17 cells, n=4 mice; Kruskal-Wallis test, DG p=0.0100 and SG p=0.0382; Dunn's post-tests). Note that the increase in orientation and direction selectivity assessed with Gaussian fits confirms the ratio based increase in selectivity (OSI/ DSI, Fig. 24B).

5.2.7.3 Non-Linearity of Calcium Indicators Is Not a Confounding Factor

GECI fluorescence changes do not scale linearly with increases in neuronal activity, but are subject to threshold and saturation effects [Nauhaus 2011, Chen 2013, Thestrup 2014]. Dependent on the average amplitude, particularly measurements of tuning sharpness and selectivity, as well as response variability (measured as CoV) and, to a lesser extent, reliability (measured as correlation coefficient) are potentially affected by this non-linearity.

In order to address this issue, I compared the average peak amplitude of all responsive GCaMP6s neurons from 6 to 15 wpt (25 cells, n=4 mice, Kruskal-Wallis test, p=0.593, n.s.) and no difference was observed across time-points (Fig. 24D). Also, peak amplitudes did not correlate with orientation and direction selectivity indices (OSI, R^2=0.082; DSI, R^2=0.151; Fig. 24E). Note that non-linearity effects of calcium indicators would have predicted higher selectivity indices at lower average peak amplitudes. Indeed, linear regression even revealed a slightly opposite effect (a minor positive slope). Moreover, transplanted neurons exhibited marked changes in tuning preference (preferred orientation and/or direction) despite constant average peak amplitudes between 6 and 9 wpt (Fig. 20; Fig. 24, A and D), as well as stable overall tuning at late time-points (Fig. 22). Together, since potential non-linearities of the GECIs used had no effect on the tuning preferences, the functional development observed here is not due to confounding effects of the GECIs but rather reflects genuine changes in tuning of transplanted neurons over time.

5.2.8 Synopsis Part II

In summary, embryonic transplanted neurons not only survive in the host adult V1, but also develop mature pyramidal cell-like morphologies with elaborate and clearly distinguishable apical and basal dendritic arbors within 3 to 4 weeks. New neurons quickly form pre- and post-synaptic contacts with the host network that initially are prone to elimination, but stabilize at appropriate levels after a period of heightened plasticity 5 to 8 wpt. Accordingly, transplanted neurons undergo a comparable period of functional development, before assuming stable, selective and persistent tuning properties indistinguishable from endogenous layer 2/3 pyramidal neurons in adult V1. Therefore, adult cortical circuits retain the capability to integrate individual exogenous (transplanted) cells in order to structurally and functionally replace previously lost neurons.

5.3 Integration of Endogenous New Neurons after Apoptotic Photolesion?

The results presented so far demonstrate that the adult mammalian brain is capable of successfully integrating new neurons derived from exogenous sources via transplantation. Another potential way to replace lost neurons is to exploit the brains' own capacity to generate new neurons. In 2000 and 2004 Macklis and colleagues reported that apoptotic degeneration caused the induction of new neurons in deep cortical layers of the juvenile mouse forebrain [Magavi 2000] and motor cortex [Chen 2004]. Here, I investigated whether apoptotic photolesion of layer 2/3 CPNs in S1 and V1 of adult mice also induced the formation of new neurons, and whether these new neurons harbour the potential to replace lost cells. The synthetic thymidine analogue bromodeoxyuridine (BrdU) was used to label newly generated neurons in mouse lines expressing GFP in candidate progenitor populations. This combination allowed for *in vivo* two-photon imaging of potential new neurons (GFP^+) combined with post-hoc verification by immunohistochemistry (IHC) for BrdU and the neuronal marker NeuN.

5.3.1 $NeuN^+BrdU^+$ Neurons in Response to Apoptotic Photolesion in S1 and V1

First, I assessed whether apoptotic photolesion of layer 2/3 CPNs in S1 and/or V1 of adult mice was sufficient to induce the formation of new neurons.

Apoptotic photolesion was performed as described above (see 3.6 and 5.1.2) with minor modifications: Tamoxifen (TM) was administered to GLAST-creERT2 x CAG-GFP mice (see 3.3) in order to induce GFP expression. TM treatment was completed one week prior to the first surgery. Bilateral craniotomies were performed over S1 or V1, and immediately after the $Ce6^+$ beads injection a cranial glass window was implanted on top of prospectively labelled CPNs (Fig. 26A). Subsequent laser photoactivation was performed through the glass window under light anaesthesia. Mice received BrdU via drinking water (see 3.11) starting directly after $Ce6^+$ beads injection (-7 dpl) until 7 dpl (day 0, laser lesion). Mice were sacrificed at 14 dpl or 56 dpl (see 3.12.1 and 3.12.2) and their brains subjected to IHC (see 3.12.4). In order to quantitatively analyse the number and distribution of new ($BrdU^+$) neurons ($NeuN^+$), high-resolution image stacks were acquired with a confocal microscope (see 3.12.5). $NeuN^+BrdU^+$ neurons were identified (Fig. 28C; see 3.13) within (L) and outside (oL) the area of apoptotic photolesion in the lesion hemisphere, as well as within in the $Ce6^+$ beads injection site (Inj.) in the injected hemisphere (Fig. 26D).

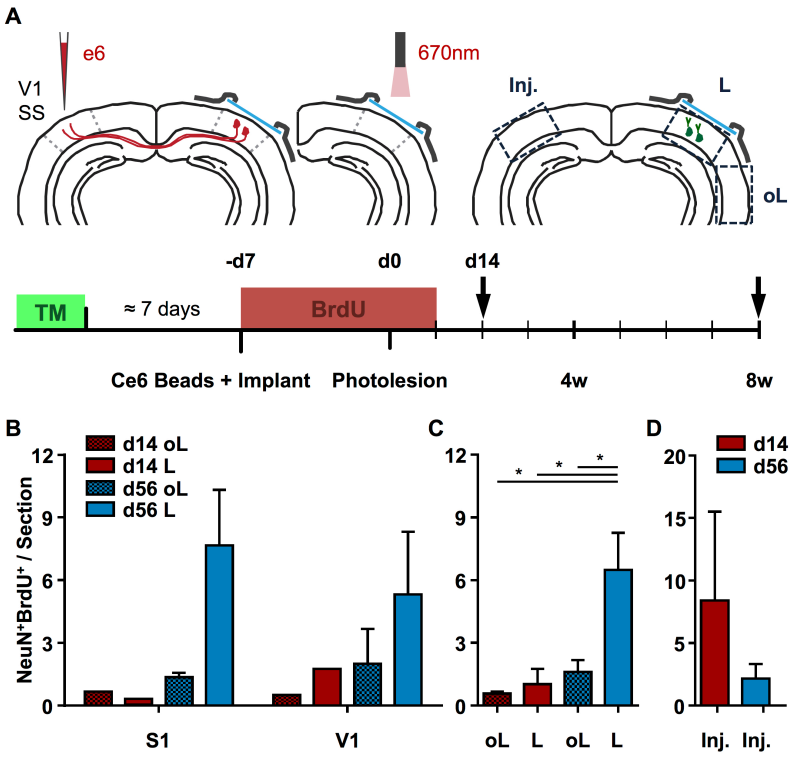

Fig. 26. NeuN$^+$BrdU$^+$ neurons appear specifically in areas undergoing apoptotic photolesion. (A) Experimental procedure and timeline. Ce6 conjugated beads are injected into the homotopic projection area of V1 or S1 CPNs (see Fig. 5). A glass window is implanted on top of V1 or S1, and Ce6$^+$ CPNs are locally ablated in layer 2/3 via exposure to 670 nm laser light (see Fig. 6). Note, here the laser illumination is performed through the previously implanted glass window, and BrdU is administered via drinking water (red box; see 3.11) for 14 days, starting 1 week prior to apoptotic photolesion. Mice are subjected to immunohistochemistry at 14 dpl and 8 wpl (arrows). NeuN$^+$BrdU$^+$ neurons are quantified within the lesion area (L), outside of the lesion area, laser hemisphere (oL) and within the Ce6$^+$ bead injection site, injection hemisphere (Inj.). TM, tamoxifen. (B-D) Average number of NeuN$^+$BrdU$^+$ cells per section 14 dpl (red) and 56 dpl (blue). **(B)** Photolesion to either S1 or V1 yields similar results (two-way ANOVA, p=0.9493, n.s.). Experiments are pooled for statistical analysis in **(C)**. NeuN$^+$BrdU$^+$ neurons are found specifically within the area of laser lesion at 56 dpl, as compared to out of lesion areas in the same hemisphere at 14 and 56 dpl. At 14 dpl, the lesion area does not show increased numbers of NeuN$^+$BrdU$^+$ cells, indicating that BrdU is not incorporated due to repair mechanisms (14 dpl, n=2 mice; 56 dpl, n=5 mice; cells/ section: 14 dpl, oL 0.59 ±0.085, L 1.04 ±0.710; 56 dpl, oL 1.68 ±0.320, L 6.50 ±1.168; one-way ANOVA, p=0.012; Tukey post-tests). **(D)** In the injection hemisphere the number of NeuN$^+$BrdU$^+$ neurons is not different at 14 dpl compared to 56 dpl (cells/ section: 14 dpl, 8.41 ±7.085; 56 dpl, 2.17 ±1.165; two-tailed students t-test, p=0.4758, n.s.). The immediate high number of NeuN$^+$BrdU$^+$ cells and the tendency to decrease with time are consistent with reported DNA repair after injury [Taupin 2007].

Photolesion to either S1 (n=4 mice) or V1 (n=3 mice) yielded a similar distribution of NeuN$^+$BrdU$^+$ neurons across time-points and areas (two-way ANOVA, p=0.9493, n.s.), and results were pooled for further analysis (Fig. 26, B to C). NeuN$^+$BrdU$^+$ neurons were found specifically within the area of the photolytic lesion at 56 dpl, as compared to out of lesion areas in the same hemisphere at 14 and 56 dpl (Fig. 26C). Also, at 14 dpl the lesion area did

not harbour increased numbers of $NeuN^+BrdU^+$ cells, indicating that BrdU was not incorporated due to repair mechanisms by mature neurons damaged (but not killed) by laser photoactivation (14 dpl, n=2 mice; 56 dpl, n=5 mice; cells/ section: 14 dpl, oL 0.59 ±0.085, L 1.04 ±0.710; 56 dpl, oL 1.68 ±0.320, L 6.50 ±1.168; one-way ANOVA, p=0.012; Tukey post-tests).

In contrast, in the injected hemisphere the number of $NeuN^+BrdU^+$ neurons was already elevated at 14 dpl and did not further increase with time (cells/section: 14 dpl, 8.41 ±7.085; 56 dpl, 2.17 ±1.165; two-tailed students t-test, p=0.4758, n.s.), but rather showed a tendency to decrease at 56 dpl (Fig. 26D). Both, the initial high number of BrdU labelled neurons, as well as the drop over time is indicative for DNA repair after injury [Taupin 2007].

In summary, apoptotic photolesion to a subclass of layer 2/3 projection neurons in S1 and V1 seems to induce the formation of new neurons, as previously reported for deep cortical layers in the mouse forebrain [Magavi 2000, Chen 2004].

5.3.2 $NeuN^+BrdU^+$ Neurons Are Not Labelled in the GLAST-creERT2 Driver Line

In order to follow the integration of endogenously generated new neurons and to compare their development and maturation with data obtained from exogenous (transplanted) neurons, $NeuN^+BrdU^+$ cells require an *in vivo* fluorescence label. Since the origin of new cortical neurons induced by apoptotic photolesion has not been identified to date [Brill 2009, Sohur 2012], a mouse line expressing GFP in a broad range of candidate progenitors was used. The GLAST-creERT2 driver line [Mori 2006] labels cells of the astroglial lineage, including radial glia and radial glia-like progenitors, in a tamoxifen (TM) inducible, cre-dependent manner. Cre recombination is induced upon TM binding to the modified human oestrogen receptor ligand binding domain ERT2 and subsequent creERT2 translocation to the nucleus [Feil 1996, Feil 1997, Indra 1999].

The GLAST-creERT2 driver line was crossed to the CAG-GFP reporter [Nakamura 2006] (Fig. 27A; see 3.1) and TM induction was performed as described in 3.3 Intrinsic GFP label was intensified by post-hoc IHC using fluorescein-conjugated (FITC) secondary antibodies to GFP binding primary antibodies (see 3.12.4).

Four weeks after TM induction GFP^+ cells were clearly visible lining the wall of the lateral ventricle (LV) including the subventricular zone (SVZ; Fig. 27B, left). In addition, GFP^+ cells with mature astrocyte morphology were found in the cerebral cortex (Fig. 27B, right) and diencephalon, amongst other regions. Also, immature, doublecortin (Dcx) positive neuronal progenitors migrating in the corpus callosum (Cc) were labelled in GLAST-creERT2 x CAG-GFP mice (Fig. 27C). The fraction of mature $S100ß^+$ cortical astrocytes co-labelled with GFP was determined in order to assess the recombination efficiency. An average of

13.86 ±3.737% of cells (n=9 mice) were found to be S100ß$^{+}$GFP^{+}. Taken together, lesion-induced NeuN^{+}BrdU^{+} neurons would also express GFP in GLAST-creERT2 x CAG-GFP mice, if they were derived from neural stem cells in the SVZ, already migrating neuronal progenitors in the Cc, reactive astrocytes, or resting parenchymal progenitors in the cortex.

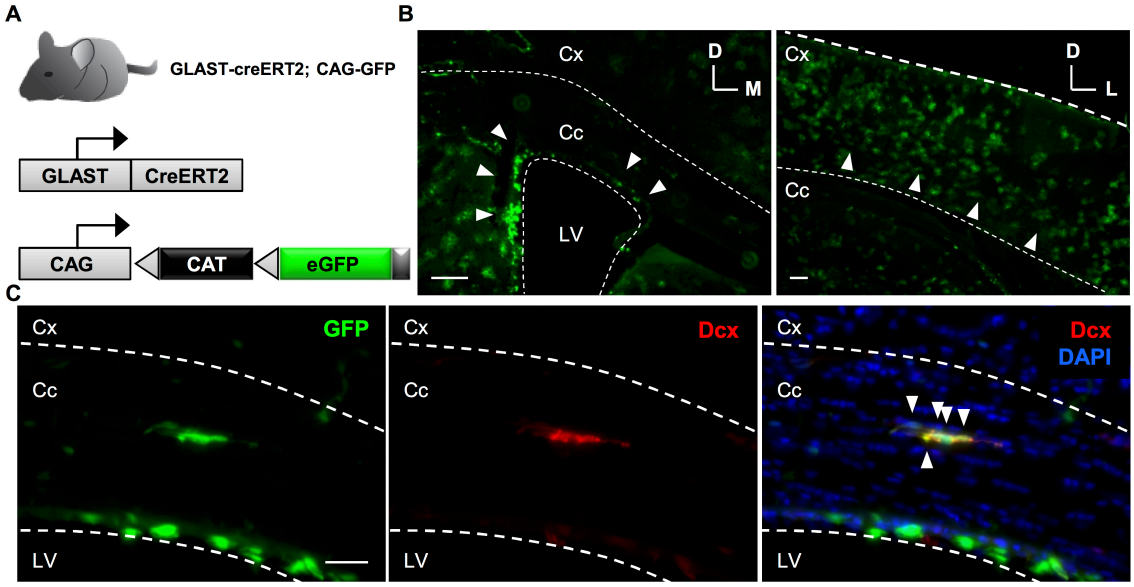

Fig. 27. GLAST-creERT2 labels local progenitors in the subventricular zone, migrating neurons in the corpus callosum and cortical astrocytes. (A) GLAST-creERT2 mice are crossed to a GFP reporter line (CAG-GFP). **(B)** Left, GFP^{+} cells are found in the vicinity of the lateral ventricle (LV), in the subventricular zone (SVZ), white arrowheads. Right, GFP^{+} cortical astrocytes (white arrowheads). **(C)** Doublecortin (Dcx) positive strings of migrating neurons in the corpus callosum (Cc) are GFP^{+}. Scale bars: (B) 100 µm; (C) 30 µm.

Apoptotic photolesion, as well as TM and BrdU administration were performed as described above (Fig. 28A; see 5.3.1) in S1 (n=3) and V1 (n=3). Mice were sacrificed at 8 wpl and subjected to IHC for NeuN, BrdU and GFP (see 3.12). Serial coronal sections of S1 (Bregma 2 to -2) and V1 (Bregma -2.5 to -4.5) were screened for GFP^{+} neurons (NeuN^{+}) that were also BrdU^{+} (see 3.13) Individual sections that contained potential GFP^{+}NeuN^{+}BrdU^{+} cells were subsequently subjected to confocal microscopy (see 3.12.5).

In a total of 6 mice, not a single triple positive neuron was found. While GFP^{+} neurons (NeuN^{+}) with clear neuronal morphology were observed in both, S1 and V1, all of them were negative for BrdU (Fig. 28B). On the other hand, all observed NeuN^{+}BrdU^{+} neurons, also investigated for the quantification presented in Fig. 26 and 5.3.1, were found to be GFP negative (Fig. 28C).

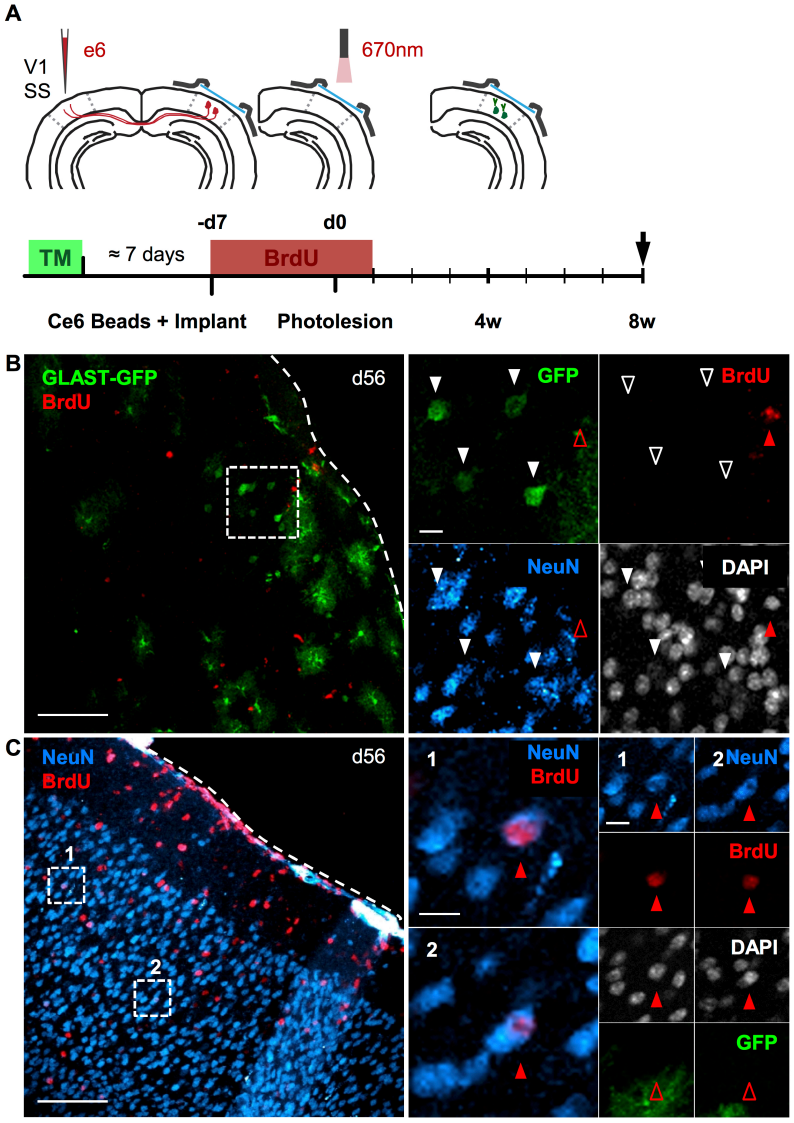

Fig. 28. GFP$^+$BrdU$^-$ and GFP$^-$ BrdU$^+$ neurons after apoptotic photolesion. (A) Experimental procedure and timeline (as in Fig. 26). Mice were subjected to immunohistochemistry at 8 wpl (arrow; see B and C). **(B)** GFP$^+$NeuN$^+$ neurons are BrdU$^-$ (white arrowheads). Left, maximum projection of a confocal z-stack. Right, single optical section, 4 individual channels, of inset left (dashed line, white). Red arrowhead indicates an example cell that is BrdU$^+$ but NeuN$^-$GFP$^-$ in the vicinity. **(C)** NeuN$^+$BrdU$^+$ neurons are GFP$^-$ (red arrowheads). Left, maximum projection of a confocal z-stack. Right, magnification of insets 1 and 2 (dashed line, white) left, indicating 2 NeuN$^+$BrdU$^+$ neurons (maximum projections and single optical sections, 4 individual channels). Scale bars: (B and C) Left, 100 µm; insets, 10 µm.

Assuming that GFP$^+$BrdU$^-$ neurons and NeuN$^+$BrdU$^+$ cells are derived from the same population of progenitors, it is conceivable that BrdU is administered too early relative to the GFP induction by TM treatment. Consequently, I systematically delayed the timing of the standard BrdU protocol by one week (Fig. 29, protocol III. and IV.), to span 0 to 14 dpl (III.) and 7 to 21 dpl (IV.), respectively. Alternatively, GFP$^+$BrdU$^-$ and NeuN$^+$BrdU$^+$ neurons could be derived from different populations of progenitors, and proliferation of GFP$^+$BrdU$^-$ neurons predates standard BrdU treatment. To test for this possibility, BrdU administration was systematically shifted closer to GFP induction (Fig. 29, protocol I. and II.), spanning from the start of the TM treatment to the Ce6$^+$ beads injection (I.), and from the end of TM treatment

to the photolytic lesion (II.), respectively. In a total of 4 mice (n=1 per condition) spanning the time window of -3 wpl to +3 wpl not a single $GFP^+NeuN^+BrdU^+$ neuron was found in serial sections spanning the entire lesion area (a total of 4 to 5 mm in anterior-posterior axis per mouse).

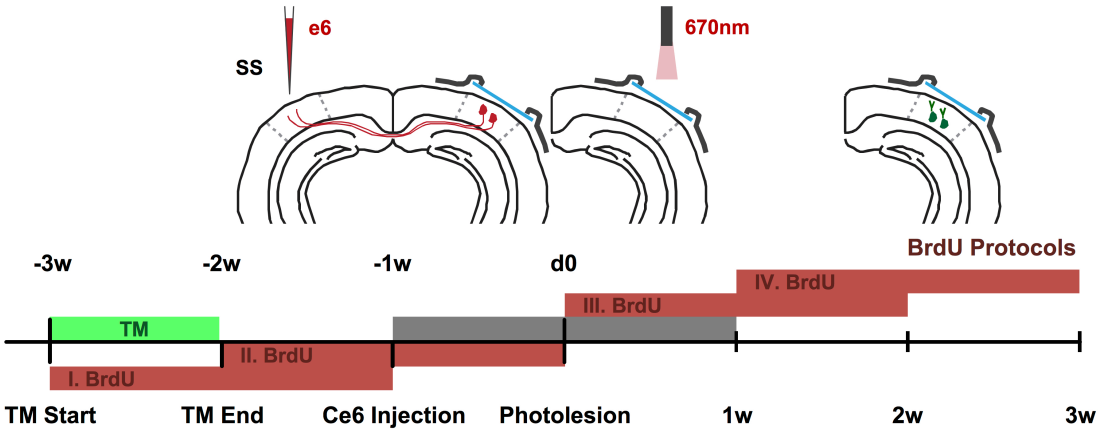

Fig. 29. GFP^+ neurons are not born within a time window spanning 3 weeks prior to 3 weeks post lesion. Alternative BrdU protocols (red boxes) I, II, III and IV (standard protocol, grey box). Each individual protocol spans 14 days of BrdU administration via drinking water (see 3.11). Protocol I. starts simultaneously with tamoxifen-mediated induction (TM, green box) of GFP expression and IV. ends +3 wpl. No GFP^+BrdU^+ neuron ($NeuN^+$) was observed in any regime (n=4 mice, protocol I. to IV; n=10 mice, standard protocol).

Taken together, lesion induced $NeuN^+BrdU^+$ neurons could not be labelled using the GLAST-creERT2 x CAG-GFP mouse line, strongly indicating that this population of new neurons is not derived from an astroglial lineage. However, a population of GFP^+ neurons ($NeuN^+$) that could not be labelled with BrdU -3 to +3 wpl was observed. It might be possible that apoptotic photolesion induces a heterogenic population of new neurons. Note that both, $NeuN^+BrdU^+$ and GFP^+BrdU^- neurons seemed to be equally induced in either S1 or V1, despite V1's considerably greater distance from the SVZ compared to S1.

5.3.3 GFP^+BrdU^- Neurons in Response to Apoptotic Photolesion in S1 and V1

In order to test whether GFP^+BrdU^- neurons were specifically induced in response to apoptotic photolesion, a series of control experiments was conducted (Fig. 30A): Photolesion in sham induced GLAST-creERT2 x CAG-GFP mice (n=2 mice; corn oil without TM, w/o TM); TM induced mice without lesion (n=6 mice; w/o Lesion); laser illumination of CPNs labelled with unconjugated beads (n=2 mice; w/o Ce6); $Ce6^+$ beads injection without laser illumination (n=2 mice; w/o Laser). Mice were sacrificed at 8 wpl (or equivalent) and subjected to IHC for NeuN, GFP and BrdU (see 3.12). Serial coronal sections of S1 and/or

V1 (see 3.12.2) were screened for GFP^+ neurons ($NeuN^+$; see 3.13), results were pooled and compared to mice that had undergone a photolytic lesion (n=10 mice; see 5.3.2).

A

Control	TM	S1/V1	Beads	Ce6	Laser	n
w/o TM	Oil	S1/V1	X	X	X	2
w/o Lesion	TM	S1/V1	–	–	–	6
w/o Ce6	TM	S1/V1	X	–	X	2
w/o Laser	TM	S1/V1	X	X	–	2

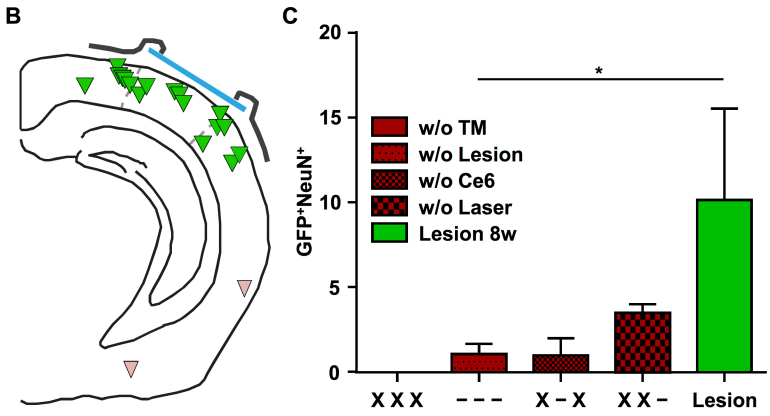

Fig. 30. GFP^+BrdU^- neurons appear specifically in areas undergoing apoptotic photolesion. (A) Table indicating the type of control experiment; X marks the individual procedure applied (latex bead injection, Beads; beads conjugated to Ce6, Ce6; laser illumination, Laser). Mice received either TM induction or sham induction with corn oil and both, S1 and V1 were investigated for each type. Note that n indicates individual mice and areas, except for the control w/o lesion (TM induced mice without beads, Ce6 and laser) were n equals 12 areas out of 6 mice (both, S1 and V1 per mouse). **(B)** Schematic, distribution of GFP^+BrdU^- neurons ($NeuN^+$, green arrowheads) at the lesion site (V1) of one example mouse overlaid on the outline of a reference section. Blue, glass window held in place by dental cement (grey). Some GFP^+BrdU^- neurons were occasionally observed in the perirhinal cortex and amygdala, (light red arrowheads). **(C)** Average number of GFP^+BrdU^- neurons per mouse and area. Increased numbers of GFP^+BrdU^- neurons are detected in areas undergoing photolesion (green bar, S1 and V1 pooled, n=10 mice; 10.15 ±5.346 cells; Kruskal-Wallis test, p=0.0079; Dunn´s post-test) as compared to controls (red bars).

Increased numbers of GFP^+BrdU^- neurons were detected in and adjacent to areas of the photolytic lesion (Fig. 30, B and C) compared to control conditions (mean number of $GFP^+NeuN^+BrdU^-$ cells per mouse and area: Lesion 10.15 ±5.346, w/o TM 0.00 ±0.000, w/o Lesion 1.08 ±0.583, w/o Ce6 1.00 ±1.000, w/o Laser 3.50 ±0.500; Kruskal-Wallis test, p=0.0079; Dunn's post-test). No spontaneous recombination (GFP^+ neurons without TM induction) could be detected even in the presence of the photolytic lesion, and only a small number of neurons was labelled in native mice after TM induction, consistent with previous

reports [Mori 2006]. Both, laser illumination and $Ce6^+$ beads alone (w/o Laser, w/o Ce6) showed similar low levels of GFP^+ neurons, which may reflect the same resident population as in TM induced native mice. Note that occasionally GFP^+ neurons were also observed in the perirhinal cortex and amygdala (Fig. 30B) in both, control and experimental animals, but were not included in the analysis. These results indicate that GFP^+BrdU^- neurons appear predominantly in areas undergoing photolytic lesion.

5.3.4 GFP^+BrdU^- Neurons Are Not Derived from Local Progenitors

Since GFP^+ neurons could not be labelled with BrdU -3 to +3 wpl, it is possible that the photolytic lesion does not induce GFP^+ progenitor cell proliferation, but the migration and/or differentiation of resident progenitors derived from e.g. the local parenchyma [Götz 2015] or the corpus callosum [Agathou 2013]. Using chronic *in vivo* two-photon imaging, I observed the fate of all GFP^+ resident cells in, as well as any labelled cells migrating into, a volume of up to 0.8 mm^3 of V1 after a photolytic lesion in GLAST-creERT2 x CAG-GFP mice. Note that in the GLAST-creERT2 x CAG-GFP mouse line cells of the astroglial lineage, including radial glia-like progenitors in the SVZ, potential progenitors in the parenchyma, as well as mature quiescent astrocytes [Mori 2006] express GFP upon TM induction.

Photolesion, TM treatment and BrdU administration were performed as described in 5.3.1 (Fig. 31A; see 3.3, 3.6 and 3.11). Mice were subjected to *in vivo* two-photon imaging immediately after laser photoactivation (0 dpl) and weekly thereafter up to 8 wpl. In each session a high-resolution tiled volume stack with a field of view of 2.3 to 2.7 mm^2 in total (0.49 µm/pixel) was acquired up to a depth of 300 µm from the pial surface (1 µm z-steps; Fig. 31B and see 3.14.1). Each individual GFP^+ cell was identified at 0 dpl and matched across time-points (>2650 cells, n=4 mice; see 3.15). Based on their morphology, GFP^+ cells were classified as quiescent bushy astrocytes, neurons and putative neurons (cells of undefined morphology). New, lost and migrating cells were identified based on their relative location to invariable GFP^+ bushy astrocytes (Fig. 31D). At 8 wpl mice were sacrificed and subjected to IHC for NeuN, BrdU and GFP (see 3.12).

Overall, GFP^+ cells were extremely stable, with less than 1% average gain and loss of cells (Fig. 31C). Occasionally, labelled cells with undefined morphology (neither typical astrocytic, nor typical neuronal) were observed that seemed to undergo multiple rounds of cell division, cell loss and some migration across time-points (Fig. 31D). This population showed a trend towards increased numbers at 8 wpl compared to 0 dpl (n=4 mice, cells/ mouse, 8 wpl 33.00 ±16.620, 0 dpl 11.50 ±0.646; paired one-tailed t-test, p=0.139, n.s.; Fig. 32B), but none of these cells did develop into clearly identifiable neurons. Moreover, post-hoc IHC revealed that this group of cells did not express the neuronal marker NeuN (Fig. 31E).

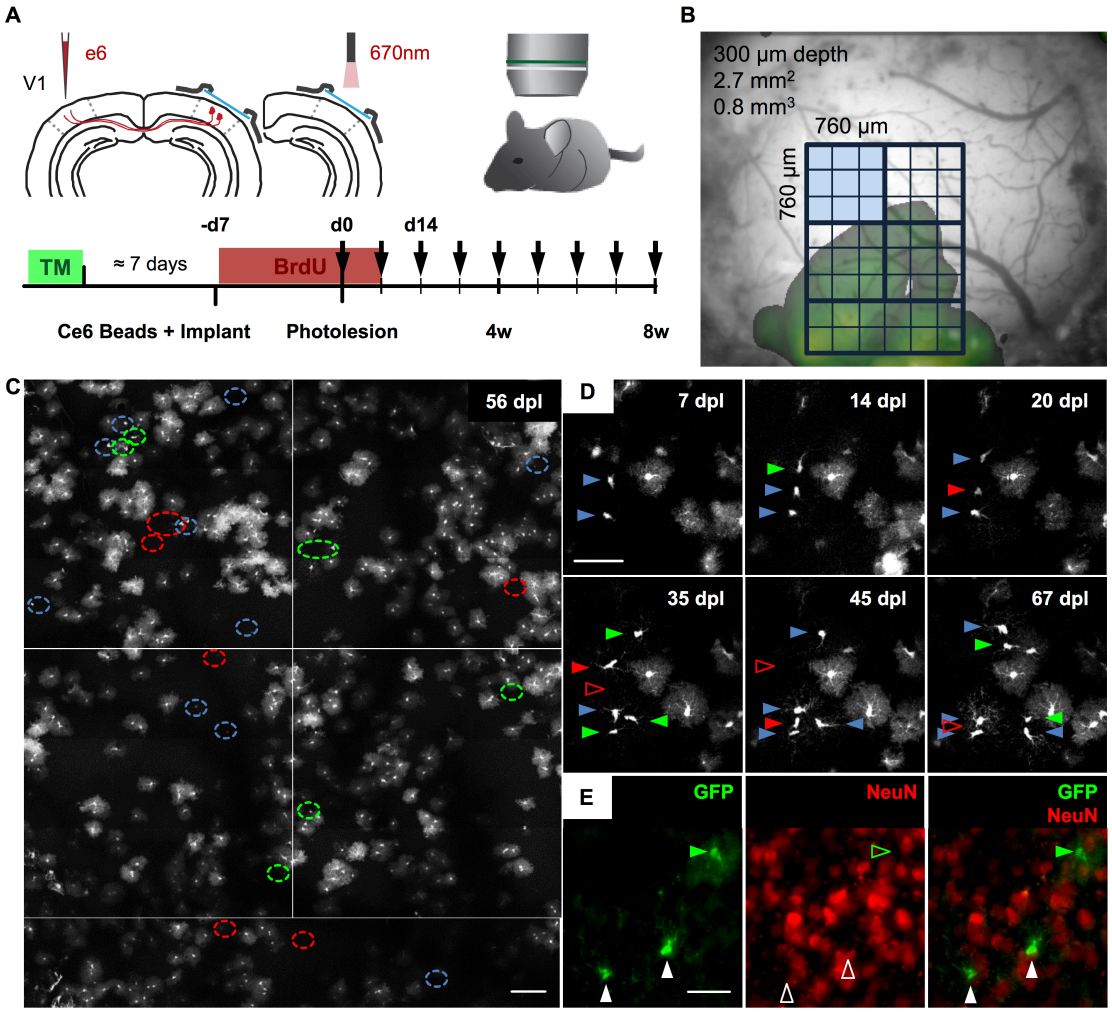

Fig. 31. GFP$^+$BrdU$^-$ neurons are not derived from GLAST$^+$ local or migrating progenitors. (A) Experimental procedure. Mice were subjected to *in vivo* two-photon microscopy at weekly intervals (arrows), starting after laser photoactivation (0 dpl). All individual cells within a volume of 0.7 to 0.8 mm^3 were followed up to 8 wpl. Mice were subsequently subjected to immunohistochemistry (IHC) and co-stained for GFP, NeuN and BrdU. **(B)** Overlay of visual stimulus evoked intrinsic optical signal (colour coded in green; see 3.10) and the blood vessel pattern through a cranial glass window above V1. Blue grid, total maximum area repeatedly imaged with *in vivo* two-photon microscopy, covering V1. Small squares, individual high-resolution z-stacks, recorded in 3x3 tiles (light blue square, 760 µm x 760 µm x 300 µm depth). **(C)** Maximum projection of the total volume imaged *in vivo* at 56 dpl. Dashed circles, location of GFP$^+$ cells without typical astrocyte morphology identified in previous imaging sessions (blue), newly appearing (green) or lost (red). **(D)** Two GFP$^+$ cells (blue arrowheads) without typical astrocyte morphology undergoing multiple rounds of cell division at 7 to 67 dpl. Green arrowheads, new cells; filled and open red arrowheads, cells lost at subsequent time-point. Note the invariability of bushy astrocytes. **(E)** IHC at 8 wpl. GFP$^+$ cells without typical astrocyte morphology (arrowheads, white) are not neurons, do not express NeuN (open white arrowheads) and do not give rise to GFP$^+$BrdU$^-$ neurons. Green arrowhead, bushy astrocyte in the vicinity. Scale bars: (B) 760 µm; (C) 100 µm; (D) 50 µm; (E) 30 µm.

GFP$^+$ neurons exhibited a similar trend of increased numbers at 8 wpl compared to 0 dpl (cells/ mouse, 8 wpl 5.50 ±4.518, 0 dpl 1.50 ±0.646; paired one-tailed t-test, p=0.196, n.s.; Fig. 32B). Surprisingly, however, fully developed new neurons with elaborate dendritic arbors generally appeared within 7 dpl (Fig. 32A), without identifiable progenitors or other parent cells. No morphological development could be observed thereafter and, as before (see 5.3.2), no GFP$^+$ neuron stained positive for BrdU. In addition, the appearance of new neurons was highly variable between animals, ranging from 1 to 29 cells per mouse. Notably, mice that displayed reactive astrocytes after the lesion (Fig. 32A, left), exhibited a higher number of new GFP$^+$ neurons at 7 dpl.

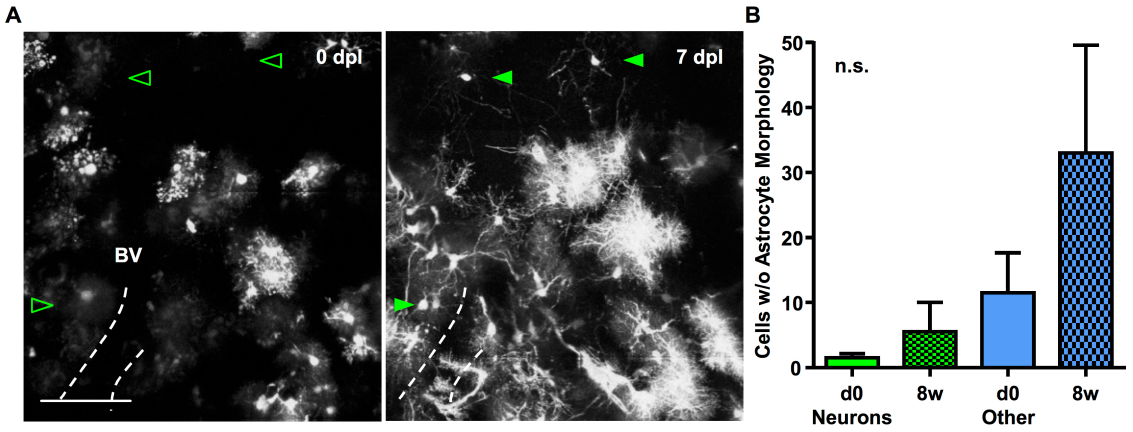

Fig. 32. GFP$^+$BrdU$^-$ neurons appear spontaneously without prior development. (A) *In* vivo two-photon z-stack projections at 0 and 7 dpl. Three example GFP+BrdU$^-$ neurons (green arrowheads) appear within 7 days without identifiable progenitors or other parent cells. **(B)** Quantification of *in vivo* two-photon imaging 0 dpl to 8wpl. Average number of GFP$^+$ cells without typical astrocyte morphology (blue) and neurons (green) at 0 dpl (d0) and 8 wpl (8w). Both populations show a trend towards increased numbers at 8 wpl (n=4 mice, paired t-test; neurons p=0.391, non-neuronal cells p=0.278; n.s.). Scale bar: (A) 100 µm.

Taken together, GFP$^+$ non-neuronal cells could be followed through mitosis and development across all time-points, but never gave rise to a morphologically mature, NeuN$^+$ neuron. GFP$^+$ new neurons, on the other hand, appeared spontaneously without identifiable progenitors and did not exhibit morphological development >7 dpl. Combined with the absence of BrdU labelling, it is very unlikely that new neurons are derived from local or distant progenitors. Thus, GFP$^+$BrdU$^-$ neurons are very unlikely to constitute an additional, induced population of new neurons after photolytic lesion. Their predominant appearance in and adjacent to the lesioned region may reflect spontaneous creERT2 recombinase translocation to the nucleus in the presence of cellular stress, not unlike the heat shock transcription factor 1 (Hsf1) in a physiological stress response [Zou 1998, Hahn 2004, Neudegger 2016] (see 6.3.2).

5.3.5 NeuN$^+$BrdU$^+$ Neurons Are Not Derived from Oligodendrocyte Precursors

Since NeuN$^+$BrdU$^+$ neurons could not be labelled using the GLAST-creERT2 x CAG-GFP mouse line and thus, seem not to be derived from astroglial progenitors, I next tested the possibility that induced new neurons originate from the oligodendroglial lineage. In the CNS the SOX10-creERT2 [Simon 2012] driver line labels glutathione S-transferase Pi (GST-π) and neuron-glia antigen 2 positive (NG2) mature oligodendrocytes and oligodendrocyte progenitor cells (OPCs), respectively, in a TM inducible cre-dependent manner (see 5.3.2). Especially NG2$^+$ OPCs have previously been implicated as potential multipotent progenitors *in vitro* [Belachew 2003] and *in vivo* [Aguirre 2004, Rivers 2008], as well as in the injured brain [Boda 2010, Simon 2011, Heinrich 2014].

The SOX10-creERT2 driver line was crossed to the CAG-GFP reporter [Nakamura 2006] (Fig. 33A; see 3.1). Photolesion, TM induction and BrdU administration were performed as described in 5.3.1 (see also 3.3, 3.6 and 3.11). Mice were sacrificed at 8 wpl and subjected to IHC for GFP, BrdU, NeuN and NG2 (see 3.12). Serial coronal sections were screened for GFP$^+$ neurons (NeuN$^+$; see 3.13) and potential co-labelling with BrdU.

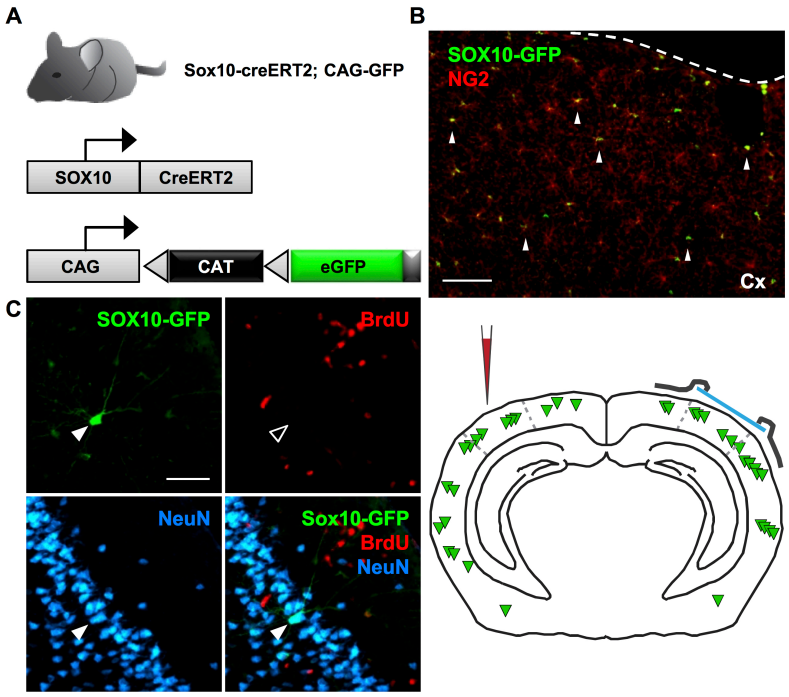

Fig. 33. NeuN$^+$BrdU$^+$ neurons are not derived from oligodendrocyte precursors. **(A)** SOX10-creERT2 driver line was crossed to a GFP reporter mouse (CAG-GFP) in order to label oligodendrocyte precursor cells. **(B)** Immunolabelling of NG2$^+$ cells within the SOX10-creERT2 x CAG-GFP mouse line. **(C)** Left, immunohistochemistry 8 wpl reveals GFP$^+$ neurons (NeuN$^+$, white arrowhead) that are BrdU$^-$ (open white arrowhead). Schematic right, distribution of GFP$^+$BrdU$^-$ neurons (green arrowheads) of one example mouse overlaid on to the outline of a reference coronal section. Blue, glass window held in place by dental cement (grey); Red tip, Ce6$^+$ beads filled injection capillary. Scale bars: (B) 100 µm. (C) 50 µm.

In order to approximate the recombination efficiency, the fraction of GFP labelled $NG2^+$ cells was determined. On average 79.52 ±4.173% of $NG2^+$ cells (n=2 mice) were also GFP^+ (Fig. 33B). In both mice, GFP^+ neurons ($NeuN^+$) were frequently observed (~50 to 100 GFP^+NeuN^+ cells per area per mouse; Fig. 33C), however, not a single GFP^+ neuron was found that co-stained for BrdU. In contrast to GLAST-creERT2 x CAG-GFP mice, labelled neurons were not enriched in and adjacent to the lesion site, but equally dispersed throughout both cortical hemispheres (Fig. 33C, right). GFP^+BrdU^- neurons thus likely represented the previously described fraction of labelled neurons in strongly TM induced SOX10-creERT2 x CAG-GFP mice [Simon 2012].

Taken together, photolytically induced $NeuN^+BrdU^+$ neurons could not be labelled using the SOX10-creERT2 driver line. It is therefore unlikely that this population of new neurons originates from $NG2^+$ OPCs or more mature $SOX10^+$ oligodendrocytes.

5.3.6 Synopsis Part III

In summary, photolytic lesion of a spatially restricted fraction of layer 2/3 projection neurons in both, S1 and V1, seems to induce a similar formation of $NeuN^+BrdU^+$ neurons as previously reported for deep layers of the mouse forebrain. However, neither the GLAST-creERT2 nor the SOX10-creERT2 driver line succeeded in co-labelling these new neurons with GFP, indicating that induced new neurons are not derived from an astroglial or the predominant $NG2^+/SOX10^+$ oligodendroglial lineage. GFP^+ neurons observed in and adjacent to lesion areas are $BrdU^-$ and not derived via differentiation of local resting progenitors - they likely constitute cells of stress induced unspecific GFP expression. Finally, the origin of photolytically induced $NeuN^+BrdU^+$ neurons remains to be elucidated in subsequent studies.

6 Discussion

Of all mammalian tissues, the brain is the most limited in its capacity for self-renewal and regeneration. As a result, brain injuries or disease almost always involve irreversible damage and impairment of brain function, often accompanied by cell loss [Gorman 2008]. Emerging strategies to overcome neuronal loss due to injury or disease include the replacement of lost cells with new neurons or progenitor cells from endogenous [Bazarek 2014] or exogenous sources [Lindvall 2000]. Improvements and/or alleviation of symptoms have been described for instance in humans with Parkinson's disease after transplantation of fetal dopaminergic neurons into the striatum [Piccini 2000, Barker 2013], in epileptic mice after transplantation of inhibitory neurons into the hippocampus [Hunt 2013, Cunningham 2014], and in obese leptin receptor deficient mice after transplantation of wild type hypothalamic neurons into the medial hypothalamus [Czupryn 2011]. While these reports are encouraging, direct evidence for the functional integration of individual new neurons into the respective target circuit *in vivo* remains elusive. Also, it is still under debate, whether behavioural improvements are due to genuine reconstitution of damaged circuits or predominantly due to the trophic [Chiba 2003], neuroprotective [Chiba 2003, Aharonowiz 2008], or immunomodulatory effects [Krampera 2006, Aharonowiz 2008] of transplanted cells [Thompson 2015].

Loss of excitatory neurons in the neocortex seems especially critical since their primary function is the correct spatio-temporal integration of thousands of presynaptic inputs from a multitude of cortical and sub-cortical areas [Yoshimura 2005, Spruston 2008, Brown 2009], a process crucial for sensory information processing, interaction with the environment and ultimately, abstract thinking [Elston 2003]. Notably, while the early postnatal and juvenile cortex exhibits some capacity to compensate for functional deficits, plasticity in the adult is limited. It is therefore of particular interest to investigate, whether i) adult neocortical circuits retain the capacity to replace lost excitatory neurons with induced or introduced new neurons and ii) new neurons are capable of surviving, differentiating and adopting a meaningful function within the context of their target network.

In this thesis I provide direct evidence for the successful structural and functional integration of individual transplanted cells into the adult primary visual cortex locally deprived of layer 2/3 projection neurons by a photolytic lesion. New neurons not only survive but develop mature pyramidal cell-like morphologies, form stable reciprocal synaptic contacts with the host network, and eventually adopt tuning preferences indistinguishable from adult layer 2/3 neurons in response to visual stimuli. Once assimilated into the host network, new neurons remain an integral part of target circuits most likely for the rest of the animal's life.

I found reported lesion-induced endogenous neurons [Magavi 2000, Chen 2004] to be scarce. Also, their origin remains elusive. While small numbers of new neurons were identified based on

their incorporation of the thymidine analogue Bromodeoxyuridine (BrdU), neither astrocytic nor oligodendrocytic lineage tracing was able to substantiate evidence for either origin. Further studies are required to shed light on this elusive pool of endogenous progenitors and to identify their potential to contribute to circuit repair. In any case it seems conceivable that the circuit integration of potential endogenous cells could equal exogenous new neurons in quality, albeit not in quantity.

Taken together, I have shown that new neurons are readily assimilated into adult cortical circuits subjected to injury or disease, at least when a sufficient part of the host network is still intact. This proof of principle study offers encouraging results for cell replacement therapies and substantiates the feasibility of brain circuit restoration.

6.1 Apoptotic Laser Photolesion

In order to assess the quality and extent of transplanted neurons' capacity to restore damaged brain circuits, it was first necessary to establish a reliable, reproducible and well characterized lesion model in a target circuit suited for the investigation of the structural and functional integration of new cells.

Since true circuit restoration requires new neurons to physically replace and adopt the properties of previously lost cells, an ideal lesion model would allow for the targeted ablation of a homogenous population - preferably even a single cell type - within a spatially confined area of reproducible dimensions. If such a lesion is subsequently targeted at a population or cell type that exhibits distinct morphological and/ or functional features, respective features should also become apparent in new cells once they have successfully integrated.

6.1.1 Targeting Layer 2/3 Projection Neurons in V1

One strategy to target neuronal subpopulations for specific and spatially confined ablation was already proposed in the early nineties by Jeffrey Macklis and Roger Madison [Madison 1993]. They took advantage of the photolytic chromophore chlorin e6 (Ce6) coupled to latex based nanospheres [Madison 1990] to target projection neurons in the motor [Madison 1993] (M1) and somatosensory [Hernit-Grant 1996] (S1) cortex. Coupled nanospheres are taken up by axonal processes and retrogradely transported to the cell soma, where the otherwise inert Ce6 can be activated to produce reactive oxygen species (ROS) by exposure to near infrared laser light. The rise of intracellular ROS subsequently causes slow progressive cell death by a process reminiscent of apoptosis [Sheen 1992, Sheen 1994].

In the first part of my thesis I adopted this photolytic lesion paradigm in order to specifically eliminate a spatially restricted population of layer 2/3 (L2/3) pyramidal cells in the primary

visual cortex (V1) of adult mice. L2/3 neurons in V1 possess the typical morphological characteristics of pyramidal cells [Miller 1981a, Miller 1981b] and both, densities and dynamics of pre [Stettler 2006] and post-synaptic [Holtmaat 2005, Hofer 2009] local connections have been well characterized. As a main integration site of visual inputs [Hubel 1962, Dräger 1975, Niell 2008, Marshel 2011], they have also been extensively studied on a functional level. Specifically, key receptive field properties, such as stimulus location in visual space and orientation and/ or direction selectivity to moving bars, are encoded at the level of individual L2/3 pyramidal neurons. Though, from a molecular perspective, L2/3 pyramidal cells do not constitute a homogenous population [Tasic 2016], they do share their common typical morphology and to date, no L2/3 subgroups based on numbers or stability of local synaptic connections have been described. Functionally, individual V1 L2/3 pyramidal cells share a distinct preference for one orientation and/ or direction over others, which renders them orientation and/or direction selective. On a population level this selectivity distributes characteristically across stimulus space [Dräger 1975] and the average degree of selectivity for orientation and/ or direction is distinct from both, other layers and areas [Neill 2008, Marshel 2011]. Also, the anatomical salt and pepper distribution of preferences in rodents [Ohki 2005, Espinosa 2012] renders the sampling of a local neuronal subpopulation representative of V1 L2/3 in general. Thus, V1 L2/3 neurons constitute a suitably distinct population of sufficient homogeneity for specific ablation and subsequent targeted circuit reconstruction.

I targeted the photolytic lesion to the lateral border of V1, the binocular zone [Dräger 1975, Dräger 1978]. This area receives input from both eyes via the lateral geniculate nucleus (LGN) and exhibits extensive cortico-cortical connections between homotopic sites on either hemisphere, rendering >70% of neurons binocularly responsive - dependent on species and demarcation of the binocular zone [Diao 1983, Dräger 1978, Lepore 1992, Pietrasanta 2012, Dehmel 2014]. Callosal projection neurons (CPNs) in L2/3 were targeted for photolytic ablation by injecting Ce6 coupled nanobeads across the anterior-posterior axis of the contralateral binocular zone. Consistent with previous reports [Cusick 1981, Rhoades 1984, Olavarria 1984, Hübener 1988, Fame 2011] retrogradely labelled $Ce6^+$ CPNs were predominantly located in L2/3 and layer 5 (L5). In order to restrict the photolytic ablation to L2/3, I systematically varied laser intensities and exposure times at a fixed subcortical focal point. Exposure to 350 J/cm^2 led to robust TdT-mediated dUTP nick end labelling (TUNEL) of 3' OH chromatin ends [Gavrieli 1992, Nagata 2003], indicating apoptotic cell death, spanning the entire L2/3 without affecting deeper layers.

In addition, targeting cortical L2/3 for circuit reconstruction offers the unique possibility for chronic *in vivo* observation of the complete repair process within the same animal at single cell resolution - an enterprise that so far has not been achieved. To this end, I implanted a chronic glass window [Holtmaat 2009a] on top of the photolytic lesion site and used repeated *in vivo* two-photon laser scanning microscopy to follow individual new neurons during circuit

integration. Chronic window implants have extensively been used in order to study the structure [Holtmaat 2005, Hofer 2009, De Paola 2006, Stettler 2006] and function [Tian 2009, Keller 2012, Margolis 2012, Andermann 2013, Chen 2013, Smith 2015, Rose 2016] of cortical circuits for periods of several days and weeks. Combined with genetic strategies to label exogenous [Gorski 2002, Nakamura 2006, Madisen 2010, Chen 2013, Thestrup 2014] or endogenous [Mori 2006, Simon 2012] new neurons, I was able to identify individual cells directly after photolytic lesion and follow them in regular intervals up to one year (see 3.14.1).

6.1.2 Intact Cytoarchitecture and Minor Inflammatory Response

Besides acute cell death, excessive inflammation mediated by activated microglia [Denes 2010, Hu 2012, Wang 2013, Kim 2016] and glial scar formation [Maxwell 1965, Pekny 2005] by reactive astrocytes are traditionally thought to constitute the main obstacles to circuit regeneration after injury [Rudge 1990, McKeon 1991, McKeon 1999, Morgenstern 2002].

After CNS injury resting microglia are quick to respond [Nimmerjahn 2005, Davalos 2005, Jolivel 2015]. Within hours they change their morphology from a ramified to an amoeboid, activated state and act as phagocytic and cytotoxic cells to clear debris and fight of pathogens [Kreutzberg 1996, Kawabori 2015]. In case of blood-brain barrier (BBB) disruption microglia processes are attracted to damaged vessels and possibly assist in the extravasation of leukocytes [Jolivel 2015]. Microglial derived cytokines, primarily IL-1 [Giulian 1988, Herx 2001, John 2004], and leaking blood proteins like fibrinogen [Schachtrup 2010] lead to activation of quiescent astrocytes.

Characterized by the strong upregulation of intermediate filaments such as glial fibrillary acidic protein (GFAP) and vimentin [Maxwell 1965, Ridet 1997, Pekny 2005, Zamanian 2012, Liu 2014], these reactive astrocytes in turn shield lesioned tissue and non-neuronal, inflammatory infiltrate by proliferation [Miyake 1988], hypertrophy [Maxwell 1965] and the formation of a dense network of secreted extracellular matrix (ECM) components [Rudge 1990, McKeon 1991, McKeon 1999]. Reactive astrocytes thus create a physical barrier to inflammatory and damaged tissue components in order to protect unaffected brain regions [Silver 2004, Sofroniew 2015]. This physical barrier however, is also rich in secreted and membrane bound chondroitin sulphate proteoglycans (CSPGs) that act as strong inhibitors of axonal (re-) growth after injury [Rudge 1990, McKeon 1991, McKeon 1999, Morgenstern 2002]. CSPGs such as NG2 [Dou 1994, Tan 2005], neurocan [Asher 2000, Friedlander 1994], versican [Schmalfeldt 2000], brevican [Yamada 1997] and phosphacan [Milev 1994] are up-regulated by astrocytes and/ or oligodendrocyte progenitor cells (OPCs) after injury and have all been shown to inhibit neurite outgrowth of various neuronal cell types *in vitro.*

In the cortex [Canty 2013] and spinal cord [Kerschensteiner 2005, Farrar 2012], *in vivo* imaging revealed a rapid die back of acutely damaged axons from the lesion site within hours and a continued, more slow degeneration process lasting for several weeks to months. In the presence of CSPGs

severed axons form the characteristic dystrophic end bulbs first described by Ramón y Cajal [Cajal 1928], a form of bulbous, permanently collapsed, entrapped growth cone that continues to exhibit active endocytosis and retrograde vesicular transport [Tom 2004], but fails to regenerate [Bradke 2012, Silver 2014]. Interestingly, in studies where the inhibitory ECM was replaced by a permissive environment e.g. by grafting peripheral nerve tissue into CNS lesion sites, dystrophic axons were capable of resuming active growth even 1 year after insult [Houle 1991, Kwon 2002]. Also, after *in vivo* laser single cell axotomy, which does not result in CSPGs deposition in the first place [Canty 2013], proximal axonal segments exhibited regrowth beyond the lesion site, although they never followed their original path and did not reach their initial target.

Besides the inhibitory effect of the ECM, direct cell-to-cell interactions seem to exert a deleterious effect on the regeneration capability of damaged axons [Horn 2008, Busch 2010]. Both, infiltrating macrophages after spinal cord lesion *in vivo,* and activated isolated resident microglia *in vitro* cause rapid and continuous retraction of injured axons upon contact [Horn 2008]. Interestingly, in the penumbra of spinal cord lesions axons were found to tightly associate with polydendrocytes [Busch 2010] - cells of the oligodendroglial lineage that express high levels of the membrane bound proteoglycan NG2, hence NG2 cells [Nishiyama 2009]. While purified [Dou 1994, Ughrin 2003] and recombinantly expressed [Ughrin 2003, Tan 2005] NG2 has been shown to clearly inhibit neurite outgrowth *in vitro*, the role of NG2 cells during CNS injury is more complex. For instance, isolated adult spinal cord derived NG2 cells form a permissive substrate for neurite growth in co-culture with adult dorsal root ganglion cells [Busch 2010, Filous 2014] (DRGs). And while NG2 cell to axon contact does not protect dystrophic axon bulbs from rapid die back when they encounter activated macrophages, NG2 cells do seem to stabilize the retreating end bulb [Busch 2010, Filous 2014]. Furthermore, NG2 cells possess the capacity to grow through inhibitory CSPG gradients *in vitro* and *in vivo*, a process dependent on the expression of matrix metalloproteinases [Busch 2010, Vadivelu 2015] (MMPs). MMPs dissolve inhibitory CSPGs and create a permissive environment for axon regrowth [Busch 2010, Vadivelu 2015], possibly assisting in the long-term destabilization of the glial scar [Frontczak-Baniewicz 2006]. On the other hand, NG2 cells are discussed in the context of over-stabilization and axon entrapment [Filous 2014, Silver 2014], a process that may involve the formation of synaptic like contacts that persist even after CSPGs have degraded. Taken together, CNS injury leads to a plethora of conflicting inhibitory, stabilizing and growth promoting inflammatory processes, all of which interfere with axon (re-) growth and thus, the brain's own capacity for circuit repair.

One hallmark of the photolytic lesion paradigm I employed in order to eliminate a spatially restricted population of L2/3 pyramidal cells in V1 of adult mice, is the non-invasive, tissue penetrating near infrared laser photo-activation of intracellular Ce6 [Madison 1993]. The

subsequent production of intracellular ROS reportedly causes slow progressive cell death closely reminiscent of apoptosis [Sheen 1992, Sheen 1994]. Apoptotic cell death is characterized by a sequence of morphological changes [Kerr 1972] including cytoskeleton degeneration, membrane blebbing, chromatin condensation and enzymatic chromatin fragmentation [Nagata 2003], eventually leading to the formation of apoptotic bodies [Kerr 1972] that are phagocytosed and degraded by macrophages or microglia [Sierra 2013, Ucker 2009, Napirei 2009]. Following initial laser exposure, I readily found robust, stochastic apoptotic cell death of Ce6 labelled CPNs for up to 2 weeks. TUNEL labelling of 3' OH chromatin ends [Gavrieli 1992, Nagata 2003] was detectable up to several hundreds of µm deep into the cortical tissue, dependent on the amount of laser energy delivered to the brain (see 3.6.). Given the progressive nature of the apoptotic process and the previously reported wide range of survival times after laser photo-activation [Madison 1993, Sheen 1995], the detected fractions of TUNEL$^+$ cells likely constitute an overlapping population of degenerating neurons at different stages. Apparent however, was a rapid apoptosis onset within hours and a peak at 3 days post laser (dpl) with an average maximum of close to 50% TUNEL$^+$ cells. Notably, the individual inert nature of both, incorporated Ce6 beads, as well as near infrared laser light alone [Madison 1993, Sheen 1994], could be confirmed *in vitro* and *in vivo*. Only the combination of intracellular Ce6$^+$ beads with local wide-field laser activation resulted in apoptosis induction. Cortex outside of laser exposure, as well as Ce6$^+$ deep layer neurons within photo-activated areas did not show signs of degeneration, neither programmed nor necrotic.

Importantly, apoptosis constitutes a highly controlled process of intrinsic degeneration, which involves proper shielding of intracellular cytotoxic and immunogenic components from the microenvironment [Kerr 1972, Clarke 1990, Kroemer 2005, Peter 2009]. Apoptotic cells have even been shown to exert a pronounced anti-inflammatory effect on macrophages [Cocco 2001, Ucker 2009], a process that seems to play an important role in the regulation of peripheral immune tolerance and the prevention of autoantibody production [Devitt 2004, Stuart 2005, Casciola-Rosen 1994, Mevorach 1998, Poon 2014]. Therefore, photolytic ablation of Ce6 labelled CPNs in L2/3 of adult mice should elicit no, or only minor inflammatory processes, similar to previous reports [Madison 1993, Sheen 1995, Sohur 2012]. I examined the reaction of microglia, astrocytes and OPCs, which comprise a substantial fraction of NG2 cells [Ligon 2006, Nishiyama 2009], at various time-points after photolytic lesion. Interestingly, within hours after photo-activation microglia in the exposed cortical area displayed an activated phenotype, with marked upregulation of ionized calcium binding adaptor molecule 1 (Iba1) and de-ramified, thickened processes. Microglial activation was followed by a delayed astrocytic response that peaked at 3 dpl. Reactive astrocytes were detected via their characteristic upregulation of glial fibrillary acidic protein (GFAP) and were located predominantly in upper cortical layers of the lesion site. Importantly, activation of microglia and reactive astrocytosis were both transient and subsided within days - already at

7 dpl no aberrant Iba1 or GFAP signals could be detected. Although these results seem inconsistent with earlier reports [Madison 1993, Sheen 1995], the observed inflammatory reaction is still minor, local and comparably brief - and does not result in disruption of the overall cytoarchitecture. The detected cellular differences are easily attributable to the technical advances in staining and microscopy over the last 20 years, and the more detailed analysis of the chronology of inflammatory processes after photolytic lesion presented here. Also, activated microglia and hypertrophic astrocytes have recently been observed in alternative models of neuronal apoptotic cell death, mediated by iCaspase8 and diphtheria toxin fragment A (DTA) expression, respectively [Diaz 2013]. In addition, no change in number or distribution of OPCs was detected at any time-point after photolytic lesion, indicating that NG2 cells were probably not activated and induced to proliferate.

One explanation for the unexpected observation of activated microglia might be the sheer number of local apoptotic cells that needs clearing (< 50%) after photolytic lesion. Iba1$^+$ microglia might still be primed to an overall anti-inflammatory state, but their morphology appears thickened during active phagocytosis [Zhao 2015]. The clearance rate for microglia in the adult mouse hippocampus has previously been described at ≈ 90% under physiological conditions [Sierra 2010]. It is possible that photolytic lesion induced apoptotic cells exceed the phagocytic capacity of resident microglia and require the help of non-professional phagocytic cells, e.g. nearby astrocytes [Parnaik 2000, Cahoy 2008, Iram 2016]. Non-professional phagocytic cells are less specialised and/ or use alternative pathways for exerting phagocytic activity [Cahoy 2008, Iram 2016]. They usually exhibit low efficiency, delayed onset and ingestion of late, more matured apoptotic cells [Parnaik 2000] - offering a possible explanation for the delayed and transient activation of astrocytes at 3 dpl. In addition, apoptotic cells that exceed the clearance capacity of phagocytic cells will eventually progress to a stage termed secondary necrosis [Rovere 1998, Škoberne 2005, Peter 2009]. The membrane integrity of apoptotic cells is lost and intracellular cytotoxic and/ or immunogenic material is released into the extracellular space, potentially eliciting a pro-inflammatory response from local glia cells. The presence of secondary necrosis due to the heavy load of apoptotic cells following laser photo-activation might pose an alternative explanation for the observed transient astrogliosis at 3 dpl.

In many aspects, photolytic lesion more closely resembles the progressive apoptotic and necrotic cell death observed in neurodegenerative disorders and age-related cell loss [Anglade 1997, Shimohama 2000], than the acute focal lesion inflicted by e.g. trauma or stroke.

Taken together, the photolytic lesion paradigm employed here eliminates local, photo-activated L2/3 pyramidal cells in V1 of adult mice over the course of 2 weeks via an apoptotic mechanism. Characterized by only a minor, transient activation of microglia and astrocytes, and a completely intact overall cytoarchitecture, many of the inhibitory inflammatory processes known to interfere with axon regeneration are presumably absent.

Apoptotic photolesion thus offers an ideal environment with minimal inflammatory interference for the potential reconstruction of cortical circuits using transplanted exogenous [Lindvall 2000] (see 6.2) or endogenous [Bazarek 2014] (see 6.3) progenitors.

6.2 Transplanted Embryonic Neurons Integrate into Adult Neocortical Circuits

It has been a longstanding question, whether true circuit reconstruction - that is, the complete substitution of a lost neuron with a structurally and functionally identical new cell that adopts the equivalent position in the CNS network - is at all possible [Lindvall 2000]. In principle, such a neuron should physically replace the lost cell, assume its identity and acquire identical functional properties, e.g. the ability for correspondingly stable, reliable spatio-temporal integration of post-synaptic signals in the same functional context. This degree of reconstitution seems especially difficult for excitatory projection neurons in the cortex given their complex morphology [Miller 1981a, Miller 1988], cell type diversity [Tasic 2016] and brain-wide afferent and efferent connectivity [Marshel 2010, Liu 2013, Oh 2014].

Previous studies have not been designed appropriately to address this specific question. While several subcortical transplantation studies in murine disease models have described alleviation of symptoms and clear behavioural improvements [Piccini 2000, Barker 2013, Hunt 2013, Cunningham 2014, Czupryn 2011], none of these models allowed for the *in vivo* access to the presumably reconstituted brain circuit. This is potentially problematic, since the described behavioural improvements could have also been achieved through passive effects, e.g. spontaneous or unspecific neurotransmitter release, ubiquitous inhibition and arbitrary hormone release, respectively. In addition, it is still under debate to which extent the observed positive effects are attributable to trophic [Chiba 2003], neuroprotective [Chiba 2003, Aharonowiz 2008], or immunomodulatory factors [Krampera 2006, Aharonowiz 2008] secreted by transplanted cells, rather than the genuine reconstitution of the damaged neuronal circuits.

Studies aimed at reconstructing cortical circuits, on the other hand, have predominantly focused on graft survival and the formation of correct efferent projections to appropriate host target areas [Hernit-Grant 1996, Fricker-Gates 2002, Gaillard 2007, Ideguchi 2010, Michelsen 2015]. Data on afferent innervation of grafted neurons, however, are scarce [Gaillard 1998, Michelsen 2015] and compelling evidence for the correct integration of post-synaptic signals into appropriate functional output with respect to the target circuit remains elusive. Likewise, the developmental aspect of integration, including the development of appropriate morphology, synaptic contacts and function, has so far been addressed only partially and only for efferent projections [Michelsen 2015].

In this part of my thesis, I attempted to assess the quality and extent to which individual transplanted embryonic neurons are capable of restoring adult primary visual cortical circuits

after local ablation of L2/3 projection neurons by a photolytic lesion. I used chronic *in vivo* two-photon imaging to follow the structural and functional development, maturation and integration of individual embryonic neurons from 3 days post transplantation (dpt) up to 11 months (mth pt). Within weeks new neurons developed mature pyramidal cell-like morphologies, formed stable and persistent reciprocal synaptic connections with the host network, and responded to visual stimulation in a manner indistinguishable from adult L2/3 neurons. While the morphological development and initial spine and bouton formation resembled processes known from embryonic and early postnatal development [Shoukimas 1978, Cruz-Martin 2010, Marin-Padilla 2014], the emergence of functional properties differed considerably [Rochefort 2011, Hoy 2015]. Initial low selectivity and reliability refined over many weeks until neurons had developed stable, selective and reliable tuning properties. Accompanied by substantial turnover of dendritic spines and axonal boutons, functional development seemed dependent on experience driven refinement of synaptic contacts [Keck 2008, Kreile 2011]. Finally, once integrated into the host network, grafted neurons remained an integral part of the target circuit for the rest of the animal's life.

6.2.1 Transplanted Neurons Develop L2/3 Pyramidal Cell-Like Morphology

Following transplantation, embryonic neurons rapidly developed L2/3 pyramidal cell-like morphologies comparable to adult L2/3 projection neurons [Peters 1970, Miller 1981a, Miller 1988, Bannister 2005, Spruston 2008]. Typically, a single prominent apical dendrite branched into secondary and tertiary processes, while less branched basal dendrites emanated from the cell body. This cell polarity was established as early as 6 dpt, when the rudimentary apical dendrite became apparent, already harbouring the main branch points and outlining the subsequent, mature structure. Here, different modes of growth for apical and basal dendrites became apparent. While the apical dendrite mainly grew in length and reached its mature morphology at the end of the second week post transplantation (wpt), basal dendritic structures underwent extensive pruning and de novo growth of processes. Also, the basal dendritic tree reached its mature morphology not before the end of the third wpt.

The leading apical dendrite and the delayed maturation of the basal dendritic tree observed in transplanted neurons are classical themes described in the development of embryonic cortical pyramidal cells [Shoukimas 1978, Miller 1981b] and during maturation of continuously born neurons in the dentate gyrus [Zhao 2006]. Interestingly, although grafted neurons have to develop in the ectopic environment of an adult cortex, the timing and extent of their morphological maturation seems comparable to early postnatal development of pyramidal cells in *murinae* [Miller 1981b, Marin-Padilla 2014]. This is remarkable given the multiple factors that act together in driving and shaping the dendritic arbour during normal development, including overall

activity [Coleman 1968, Wiesel 1963], afferent innervation [Kossel 1995], neurotrophins [McAllister 1995, McAllister 1997], and guidance molecules [Nedivi 1998, Polleux 2000], to name but a few. Many of these factors are either absent or differentially expressed in the adult.

The observed normal dendritic development of grafted neurons emphasizes the strong component of intrinsic growth programs of cortical neurons. Recent support for the importance of cellular identity in defining dendritic morphology, afferent and efferent connectivity and even physiology comes from studies of ectopic transcription factor (TF) expression in cortical pyramidal neurons [de la Rossa 2013, Rouaux 2013]. Expression of the deep layer TF FEZ family zinc finger 2 (Fezf2) in postmitotic layer 4 (L4) neurons for instance, is sufficient to transform their typical stellate morphology into the phenotype of a classical L5 pyramidal neuron within two weeks. Indeed, the majority of the transplanted embryonic neurons in this thesis expressed the protein cut like homeobox 1 (Cux1) at 4 wpt [Falkner 2016], a typical marker of L2/3 projection neuron identity [Nieto 2004], including CPNs [Molyneaux 2009]. Together with its paralog Cux2, Cux1 has recently been implicated in the regulation of dendritic branching and spine formation selectively in upper layer cortical neurons [Cubelos 2010].

Alternatively, guidance cues and neurotrophins that continue to be expressed in the adult cortex, or that are re-expressed following injury, may help to shape the morphology of the dendritic tree [Wang 1998, Polleux 2000, Han 2007] and axonal arbour [Wizenmann 1993, Ellezam 2001, Knöll 2001] of grafted neurons. Semaphorin 3A (Sema3A) for instance, plays a major role in the oriented growth of apical dendrites towards the marginal zone during development [Polleux 2000], and continues to be expressed in cells of upper L2/3 in the adult mouse cortex [Allen Expression Atlas]. The largely correct ascending orientation of growing apical dendrites of transplanted neurons could well be due to this retained Sema3A expression in the host cortex. Notably, grafted neurons were not exclusively vertically oriented. Some neurons exhibited oblique apical dendrites with varying degrees of deviation from the vertical axis. However, the normal morphological spectrum of adult mammalian L2/3 pyramidal cells also includes approximately 5 - 20% of such "atypically oriented" neurons across all cortical layers [van der Loos 1965, Miller 1988, Polleux 2000, Mendizabal-Zubiaga 2007]. Importantly, the described difference to normal oriented pyramidal cells seems purely morphological. In V1 atypically oriented neurons display similar and concurrent development and maturation [Miller 1988, Parnavelas 1983] and do not differ in their physiological properties, e.g. they exhibit both, typical simple and complex receptive field properties, respectively [Parnavelas 1983]. If there are functional consequences to atypical pyramidal cell morphology, they remain elusive to date [Nieuwenhuys 1994, Mendizabal-Zubiaga 2007]. Therefore, transplanted neurons likely reflect the normal variety of dendritic morphologies present in V1.

Amongst the factors differentially regulated after injury are guidance cues [Wizenmann 1993, Knöll 2001, Wehrle 2005, Han 2007] and neurotrophins [Wang 1998, Oyesiku 1999], some of which have been shown to

exert marked effects on overall neuronal structure and dendritic arbour morphology. Candidate plasticity-regulated gene 15 (cpg15), also known as neuritin-1 (Nrn1), for instance, is strongly expressed in hippocampal pyramidal neurons within the first 2 weeks after apoptosis induction by transient global ischemia (TGI) *in vivo* and within hours after glutamate-induced injury *in vitro* [Han 2007]. Both, soluble and membrane bound cpg15 [Nedivi 1998, Putz 2005] has been implicated in promoting dendritic arbour growth and complexity, an effect restricted to projection neurons [Nedivi 1998, Nedivi 2001]. In line with this, cpg15 depletion after injury hampered neurite re-growth and the formation of new neuronal connections *in vitro* [Han 2007].
Further, increased expression of neurotrophins, including brain derived neurotrophic factor (BDNF), nerve growth factor (NGF), neurotrophin-3 (NT-3) and neurotrophin-4/5 (NT-4/5), and their receptors has been described after traumatic brain injury [Oyesiku 1999] (TBI) and in earlier studies using the photolytic lesion employed in this thesis [Macklis 1993, Wang 1998]. Notably, in a series of elegant experiments, neurotrophins have been implicated as strong modulators of dendritic growth and branching [McAllister 1995, McAllister 1996, McAllister 1997, Horch 1999, Horch 2002, Horch 2004, Cohen-Cory 2010]. They differentially affect apical and basal dendrites [McAllister 1995, McAllister 1997, Horch 1999], exert overlapping and exclusive layer specificity [McAllister 1995, McAllister 1997], act in concert with neuronal activity [McAllister 1996] and exert their effects only over short distances [Horch 2002].
Taken together, donor inherent intrinsic factors, as well as retained and re-expressed embryonic cues of the host neocortex are likely to act in concert to define the correct morphological maturation of grafted embryonic neurons.
The mature L2/3 pyramidal cell-like morphology grafted neurons had developed by 4 wpt subsequently remained stable until the end of the imaging period - a time-point reached by over 94% of investigated neurons and at which host mice were up to 1.2 years old (>450 dpt). Given the average maximum lifespan of C57/BL6 mice is approximately 800 days [Yuan 2009], it is fair to conclude that the majority of grafted neurons remained integrated until the end of the animal's life.

6.2.2 Formation of Dendritic Spines and Axonal Boutons

The observed long-term survival and stable overall morphology of transplanted neurons strongly suggested their successful integration also on a synaptic level. Stable synaptic integration in turn is a prerequisite for both, the correct functional integration of pre-synaptic inputs, as well as the reliable functional transfer to efferent targets [Koleske 2013]. At the same time, stable neuronal networks have to allow for sufficient structural plasticity to adapt to a changing environment [Trachtenberg 2002], adopt new memories [Lai 2012, Hayashi-Takagi 2015, Li 2017] and compensate for altered sensory input [Keck 2008, Hofer 2009, Yamahachi 2009, Marik 2010]. Thus, a perfectly integrated transplanted neuron ideally meets both requirements: Predominantly stable

synaptic connections within the host network, as well as host area and cell type specific rates of structural plasticity [Holtmaat 2009b] - with the first constituting a prerequisite for the latter.
Since dendritic spines and axonal boutons are generally regarded as reliable structural correlates of synapses [Trachtenberg 2002, Harris 2012], I focused on individual dendritic and axonal processes to investigate the formation, stabilization and long-term dynamics of pre- and post-synaptic structures of transplanted neurons. Importantly, by following the *de novo* development of dendritic and axonal processes, I was able to identify the birth date and life cycle of every observed individual synaptic structure formed on a given stretch of neurite, up to 11 mths pt. This way, I could assess the survival and stability of synaptic structures as a function of developmental state of a neuron. Both, dendritic spines and axonal boutons reached stable densities within 4 wpt. Initial high turnover of synaptic structures decreased with densities approaching their plateau, but only stabilized after a subsequent period of transient increase. At 9 wpt transplanted neurons have finally matured on a synaptic level, with stable pre- and post-synaptic connections and constant, low turnover. Notably, spine and bouton densities, as well as turnover rates at late developmental stages (>9 wpt) are consistent with previous reports of L2/3 pyramidal cells in V1 [Holtmaat 2005, Stettler 2006, Hofer 2009].
Interestingly, first axonal boutons clearly pre-dated dendritic spines by a minimum of 3 days, and were detected as early as 3 dpt. The formation of axonal boutons within days of transplantation is remarkable, given the short period of time grafted neurons have had to adapt to the ectopic adult host cortex. Nonetheless, at 3 dpt transplanted neurons have already sent out hundreds of µm of neurites, some of which - in retrospect - could be identified as future axons. Surprisingly, boutons were able to form within a few µm of the axonal growth cone and some of these early structures survived for several subsequent imaging time-points, substantiating the notion that they are indeed part of a true synapse. Accordingly, it has been shown *in vitro* that many pre-synaptic components comprising the future active zone are pre-packaged and transported together, allowing for rapid stabilization and assembly of a fully functional pre-synapse within hours [Ahmari 2000].
It is possible, that the formation of rapid efferent synaptic contacts to host neurons helps to promote the survival and synaptic integration of immature neurons via retrograde synaptic signalling processes. Although such processes have been the subject of extensive studies since the nineties [Thoenen 1995, Fitzsimonds 1998, Tao 2001, Regehr 2009], the molecular mechanisms governing retrogradely induced synaptic development, maturation and plasticity are not well understood. Amongst the retrograde messengers implicated to date are nitric oxide [Garthwaite 2008] (NO), neuropeptides [Simmons 1995, Iremonger 2009], endocannabinoids [Brown 2003] and neurotrophic factors [Magby 2006] - all of which have been shown to be released by the post-synaptic membrane upon depolarization, and all act in turn by modulating pre-synaptic neurotransmitter release probability [Regehr 2009]. Retrograde synaptic modulation however, is

not limited to the pre-synapse directly targeted by retrograde messengers. Long-term potentiation (LTP) induction in dissociated hippocampal neurons, for instance, leads to the spread of potentiation to dendritic post-synaptic sites of the pre-synaptic cell via insertion of additional AMPA receptors [Tao 2000, Zhang 2001]. Accordingly, long-term depression (LTD) induces the spread of depression to the pre-synaptic neuron, possibly by inactivating post-synaptic recpeptors [Fitzsimonds 1997]. *In vivo*, potentiation of retinotectal synapses by local BDNF injection into the tectum has been shown to lead to modified synaptic inputs onto the pre-synaptic retinal ganglion cells (RGCs) and their subsequent enhanced response to light stimulation [Du 2004]. This BDNF mediated retrograde potentiation required the activation of its receptor, tyrosine receptor kinase B (TrkB) and its downstream effectors [Huang 2001] at the pre-synaptic membrane, including a rise in intracellular calcium (Ca^{2+}).

The importance of retrograde signalling for neuronal survival is highlighted in an early *in vivo* study on superior cervical ganglion (SCG) neurons in guinea pigs [Purves 1975]. Chronic ligation or transection of efferent branches not only lead to synaptic depression in SCG neurons upon pre-ganglionic stimulation, but also caused the death of most affected cells within weeks.

Indeed, BDNF/ TrkB seems a promising retrograde messenger system to signal both, trophic support and retrograde synaptic modulation to developing transplanted embryonic neurons through their first efferent synaptic contacts. Both, BDNF and TrkB locate to pre- and post-synaptic structures in cortical and hippocampal neurons [Aoki 2000, Kohara 2001, Magby 2006], with BDNF being predominantly stored in secretory granules [Haubensak 1998, Kohara 2001]. Moderate depolarization of the post-synapse is sufficient to induce Ca^{2+} dependent release of BDNF into the synaptic cleft, independent of spiking activity in the post-synaptic neuron [Magby 2006]. BDNF in turn binds and signals through pre-synaptic TrkB receptors enhancing local neurotransmitter release probabilities [Li 1998, Xu 2000, Magby 2006] and inducing potentiation in the pre-synaptic cell [Du 2004]. Activated BDNF/ TrKB receptor complexes undergo endocytosis [Du 2003] and subsequently exert their long distance effects on gene expression via retrograde signalling to the nucleus [Ginty 2002, Du 2003, Zweifel 2005]. Models under discussion to mediate this long range signalling include the retrograde transportation of the receptor endosome as a scaffold for effector molecule activation [Grimes 1996, Wang 2002, Delcroix 2003, Zweifel 2005], or the direct transportation of such activated effector molecules [Ginty 2002, Zweifel 2005].

Interestingly, donor E18.5 embryonic neurons robustly express TrkB but virtually no BDNF [Timmusk 1994, Allen Expression Atlas]. One could conceive a model where, upon forming first efferent synaptic contacts, grafted neurons undergo retrograde, host-derived synaptic BDNF mediated activation of TrkB, leading to local synaptic stabilization, trophic retrograde support and facilitation of their dendritic post-synaptic development. In addition, Ca^{2+} entry through first synaptic structures likely leads to the stimulation of BDNF synthesis [Ghosh 1994, Shieh 1998,

Deisseroth 2003 via intracellular signalling processes involving the spiking independent activation of cAMP response element-binding protein Deisseroth 1996, Deisseroth 2003 (CREB) in grafted neurons, further promoting neuronal survival and differentiation Ghosh 1994, Horch 2004.

First dendritic spines on the other hand, were observed not before 6 dpt and usually formed only during the second wpt. In contrast to axonal boutons, spines developed on bare, pre-grown and already arborized dendritic processes. It cannot be excluded however, that synaptic structures had not formed on dendritic shafts prior to the observation of first spines. In fact, during embryonic development it has been proposed that dendritic growth cones are stabilized by the initiation of synaptic contacts and that once the growth cone elongates, newly formed synapses progress to sit on the expanding dendritic shaft Vaughn 1974, Miller 1981b, Dailey 1996. Indeed, ultrastructural studies in rat and mouse confirm the presence of synapses predominantly on growth cones and elongating filopodia in the embryonic CNS Vaughn 1974, Fiala 1998, whereas shortly before and after birth, synapses are mainly found on dendritic shafts Cotman 1973, Vaughn 1974, Miller 1981b, Fiala 1998. Notably, dendritic spines are rarely observed before the end of the first postnatal week and thus, similarly to developing transplanted neurons, early postnatal dendritic arbors appear smooth and spineless Cotman 1973, Miller 1981b.

Interestingly, virtually all of these early shaft synapses exhibit symmetric pre- and post-synaptic structures, while synapses with asymmetric junctions appear and increase in number only in the second postnatal week, concurrently with the development of dendritic spines Gray 1959, Miller 1981b, Harris 2012. Although commonly accepted as inhibitory synapses in the adult brain Uchizono 1965, Colonnier 1968, Klemann 2011, many of these early symmetric junctions likely constitute glutamatergic synapses in an early state of development. Accordingly, boutons of pyramidal cell axons have been found to partake exclusively in symmetric synapses in the early postnatal rat visual cortex, before being engaged in asymmetric synapses by the end of the first postnatal week Miller 1981b. Based on the above ultrastructural observations, the following model of dendritic spine maturation during development has been suggested Aghajanian 1967, Cotman 1973, Miller 1981b, Dailey 1996, Fiala 1998 that is also conceivable for developing grafted neurons: An initial shaft synapse with symmetric densities is formed involving either the retraction of early filopodia, or their elongation into nascent dendrites. Subsequently, a rudimentary post-synaptic elevation develops from the shaft, while the synapse gradually undergoes asymmetric pre- and post-synaptic specialization, followed by spine and bouton morphogenesis and functional maturation.

Further support for such a model comes from live cell imaging of post-synaptic density (PSD) dynamics in early postnatal hippocampal neurons in organotypic slices Kennedy 2000, Marrs 2001. Approximately half of the observed newly formed dendritic spines emerged together with their pre-assembled PSD cluster from the shaft, while a further fraction included the transition through a protospine or filopodium. Interestingly, synaptic activity seems sufficient

to induce the formation of dendritic spines during early development. Glutamate uncaging at L2/3 pyramidal cell dendrites in acute slices of neonatal and early postnatal mice lead to the extension of new spines from the local shaft within minutes, followed by stimulus evoked synaptic transmission within half an hour [Kwon 2011]. Considering the rapid timescale of these events, it is possible that pre-assembled shaft synapses respond to the onset of synaptic activity with the morphological maturation into spine synapses.

Among the newly formed, early afferent contacts onto grafted neurons are presumably also GABAergic inputs from the host network. Indeed, during development a sequential establishment of initial GABAergic, followed by glutamatergic synaptic transmission is apparent and occurs in accordance with apical and basal dendritic development, respectively [Tyzio 1999, Khazipov 2001, Hennou 2002, Ben-Ari 2002]. Importantly, within the first postnatal week GABA elicits depolarizing potentials in post-synaptic cells and only starts to exert its inhibitory action in the second week [Ben-Ari 1989, Cherubini 1991, Fukuda 1998, Yamada 2004]. Commonly referred to as "GABA switch", this change from excitatory to inhibitory GABA action is due to the initial elevated intracellular concentration of chloride ions (Cl^-) mediated by the $Na^+K^+2Cl^-$ co-transporter 1 (NKCC1) [Kakazu 1999, Yamada 2004, Achilles 2007] and the delayed Cl^- extrusion due to the late expression of K^+Cl^- co-transporter 2 (KCC2), resulting in a negative shift in the Cl^- reversal potential [Rivera 1999, Ganguly 2001, Ludwig 2011, Valeeva 2013, Leonzino 2016]. Excitatory GABAergic transmission together with first glutamatergic NMDA receptor activation leads to $Ca2^+$ influx, eventually causing the first synchronous activity in the early postnatal network [Ben-Ari 1989, Ben-Ari 2002, Kaila 2014].

Interestingly, GABA mediated activity by itself seems to promote KCC2 expression [Ganguly 2001, Zhang 2001, Ben-Ari 2002]. $GABA_A$ receptor ($GABA_A$-R) activation has been shown to enhance mRNA levels of KCC2, and increased receptor activation and blockage lead to accelerated and delayed GABA switch, respectively [Ganguly 2001]. Also, GABA activity enhances the expression level of BDNF, dependent on $Ca2^+$ influx via voltage-gated $Ca2^+$ channels (VGCC) [Berninger 1995]. BDNF in turn robustly up-regulates KCC2b [Ludwig 2011], the predominant KCC2 isoform in the murine cortex [Uvarov 2007, Uvarov 2009]. Notably, all of these reported effects are differentially regulated with age and limited to the first and second postnatal week, or equivalent days in culture.

Another factor recently implicated in the regulation of KCC2 expression within the same time window is the neuropeptide oxytocin. Besides the transient negative shift in Cl^- reversal potential that protects neurons from excitotoxicity during parturition [Tyzio 2006], oxytocin exerts a permanent effect via its oxytocin receptor similar to $GABA_A$-R activation on both, the timing of the excitatory-to-inhibitory switch and the expression of KCC2 [Leonzino 2016]. Notably, in addition to its function as an ion transporter, KCC2 has recently been linked to the structural

stabilization of dendritic spines [Li 2007] and the clustering of AMPA receptors at glutamatergic synapses [Gauvain 2011, Blaesse 2015].

Immature transplanted neurons likely compare to age matched embryonic neurons in their molecular composition and lack KCC2 expression in the first week post transplantation. One could speculate that early afferent GABAergic contacts from the host network would therefore depolarize grafted neurons and thus, present a source of excitation. The resultant $Ca2^{+}$ influx promotes the gradual expression of KCC2 and the subsequent shift in Cl^{-} reversal potential, eventually leading to the maturation of inhibitory synapses onto new neurons. Also, initial excitatory GABA activity likely helps to ramp up intrinsic BDNF expression [Berninger 1995], further promoting survival [Ghosh 1994], differentiation [Horch 2004] and synaptic maturation [Magby 2006, Ludwig 2011] of grafted neurons. Interestingly, since excitatory GABA activity actively promotes the excitatory-to-inhibitory switch in post-synaptic cells [Ganguly 2001, Zhang 2001, Ben-Ari 2002], the establishment and maturation of host-to-graft inhibition seems to be directed mainly by the host network. In addition, host mediated excitatory GABA action might even set the timing for subsequent dendritic spine morphogenesis and glutamatergic synaptic development of grafted neurons via KCC2's ion transporter independent, structural functions [Li 2007, Gauvain 2011, Blaesse 2015].

Taken together, multiple mechanisms seem to act in concert to mediate the correct pre- and post-synaptic excitatory and inhibitory synaptic integration of transplanted neurons, hinting at a well-orchestrated process that recapitulates many features of the developing neuronal network.

6.2.3 Transplanted Neurons Process Visual Information

As outlined above, the observed stable and persistent reciprocal synaptic connections within the host network are a prerequisite for the correct functional integration of transplanted neurons. I therefore investigated next whether new neurons adopt a meaningful function within their target circuit. Are they truly capable to functionally substitute for lost L2/3 CPNs in the V1 binocular zone? Fluorescent donor neurons were co-labelled with genetically encoded calcium indicators (GECIs) and host mice were stimulated with high contrast gratings moving in eight directions. GECIs report neuronal activity based on $Ca2^{+}$ binding - dependent conformational changes that cause alterations in their fluorescence yield [Kleinfeld 2005, Hendel 2008, Chen 2013, Thestrup 2014]. I repeatedly recorded changes in fluorescence relative to baseline in individual soma, axons and occasionally, dendritic spines at 4 to 15 wpt.

Notably, key receptive field properties, such as stimulus location in visual space and orientation and/ or direction selectivity, are encoded at the level of individual V1 L2/3

pyramidal neurons [Hubel 1962, Dräger 1975, Niell 2008, Marshel 2011]. Therefore, individual L2/3 pyramidal cells exhibit a distinct preference for one direction and/or orientation over others, and this selectivity distributes characteristically across stimulus space on a population level [Dräger 1975]. The average degree of selectivity in turn differs between cortical layers and areas [Neill 2008, Marshel 2011]. In addition, tuning preferences in rodents are anatomically organized in a salt and pepper-like fashion [Ohki 2005, Espinosa 2012], thus the sampling of a local subpopulation sufficiently represents V1 L2/3 pyramidal neurons in general. I specifically ablated L2/3 cells in the binocular zone of V1 [Dräger 1975, Dräger 1978]. This region receives input from both eyes via the LGN and exhibits extensive cortico-cortical connections between homotopic sites on either hemisphere. As a result, >70% of neurons show binocular responses to visual stimulation [Diao 1983, Dräger 1978, Lepore 1992, Pietrasanta 2012, Dehmel 2014].

Importantly, transplanted embryonic neurons were not only visually responsive, but also exhibited characteristic tuning preferences, including cells with strong orientation and/ or direction selectivity as early as 5 wpt. The distribution of preferences across the population of new neurons revealed a modest overrepresentation of cardinal directions, typical for L2/3 pyramidal cells [Kreile 2011, Rochefort 2011]. Likewise, the average orientation and direction selectivity compares to values reported previously for adult V1 L2/3 [Niell 2008, Marshel 2011]. Importantly, repeated stimulation elicited reliable responses in individual cells, and neurons' tuning at late time-points was remarkably stable over time, as is the case in the adult mouse V1 [Mank 2008, Andermann 2013]. Consistent with transplantations into the binocular zone of V1, all cells investigated exhibited binocular responses.

However, tuning properties varied markedly across time-points between 5 and 9 wpt and only stabilized at 11 wpt. Within the same time period, changes in preferred direction between imaging intervals gradually decreased, while both, response selectivity and reliability constantly increased. These results suggest that the functional integration of new neurons into the host network is still ongoing <9 wpt and that functional stability is not reached before 11 wpt. Notably, early tuning was usually broad and non-selective, and responses were highly variable. This differs considerably from the tuning properties of V1 L2/3 cells at eye opening in young mice, the majority of which exhibit sharp tuning and a selectivity for stimulus direction [Rochefort 2011, Hoy 2015]. A potential explanation for this discrepancy lies in the specific way of how neurons attain their tuning during normal development: It has been shown that clonally related neurons share a higher connectivity over non-related neighbours via gap junctions during corticogenesis [Yu 2012]. At eye opening these sister neurons exhibit a higher similarity in their tuning properties [Li 2012] and cells with increased similarity in tuning show a higher probability of excitatory chemical synapses in juvenile V1 L2/3 [Ko 2011]. Accordingly, disruption of early gap junction coupling leads to loss of correlated tuning [Li 2012] in sister neurons due to non-preferential establishment of chemical

synapses [Yu 2012]. At the onset of visual experience, shared feed-forward input onto clonally related neurons thus likely leads to strengthening of feature selectivity and highly selective tuning in the majority of responsive neurons.

On the other hand, neurons' orientation but not direction selectivity evolves after eye opening and steadily increases over several days [Hoy 2015] to weeks [Rochefort 2011]. This process is possibly mediated by visual experience and resembles the gradual maturation of feature selectivity of transplanted neurons. Indeed, prohibiting visual experience in dark reared mice has been shown to delay the characteristic sparsening of neuronal responses at eye opening [Rochefort 2009], to cause increased response variability [Ko 2014] and to diminish the correlation of connectivity and response similarity to natural movies in juvenile mice [Ko 2014]. Restriction of visual experience to one orientation leads to the overrepresentation of the respective orientation in V1 L2/3 pyramidal neurons [Kreile 2011]. In addition, visual impairment due to partial retinal lesions or monocular deprivation is associated with increased turnover of dendritic spines in V1 [Keck 2008, Hofer 2009], likely reflecting the adaptation of the cortical network to alterations in visual input.

It is conceivable that visual experience is a key mechanism in the functional maturation of transplanted neurons. Initially stochastic synaptic connections could be refined in an activity dependent manner, thus gradually shaping the tuning properties of new neurons. Interestingly, the prolonged period of functional development of grafted neurons was paralleled by heightened synaptic turnover, which only subsided once tuning properties became invariant. Also, dynamics and stabilization of dendritic spines and axonal boutons followed the same time course, substantiating the notion that experience driven refinement affects both, pre- and post-synaptic structures. Late synaptic dynamics at 10 to 11 mths pt remained at a continuous low level and the few newly gained structures displayed high stability (see 5.2.4). Thus, major functional changes are unlikely to occur once stable tuning properties have been acquired at 11 to 15 wpt.

Taken together, experience-dependent functional maturation presents an interesting concept that encompasses the possibility of actively shaping the functional properties of new neurons to fit the requirements of a target circuit. In the future, driving neuronal sub-circuits e.g. via manipulation of sensory experience, might even allow for the addition of new neurons to a circuit of choice. While I have shown that new neurons are able to successfully serve as cellular building blocks for circuit reconstruction, further experiments will be required to prove that the integration process is indeed experience-dependent and as a consequence, is susceptible to systematic manipulation.

6.2.4 Appropriate Afferent and Efferent Connectivity

In order for transplanted neurons to develop the specific and selective tuning properties reported above (see 6.2.3), they have to acquire appropriate input from multiple areas involved in the processing of visual information. Visual information detected in the retina is relayed to various layers in V1 via the LGN [Cruz-Martin 2014, Sun 2016, Kondo 2016], processed within layers [Bannister 2005], integrated with signals from the contralateral homotopic hemisphere [Yorke 1975, Blakemore 1983, Pietrasanta 2012] and modulated by other sensory and accessory areas [Iurilli 2012, Bennett 2013, Stehberg 2014].

Using monosynaptic rabies tracing our collaborators determined the brain wide distribution of directly connected input neurons onto transplanted cells [Falkner 2016]. As expected, prominent regions providing input included the dorsal LGN, local L2/3 and L5 neurons, contralateral V1, as well as other sensory areas, motor cortex and multiple associative areas. Surprisingly, there was not only no difference in areas that projected to endogenous V1 L2/3 cells and transplanted neurons, but also a largely comparable density of afferent connections. Importantly, connections from the LGN systematically varied with transplantation sites in V1, revealing a topographic organization of feed-forward inputs onto new neurons. Thus, transplanted neurons seem to take part in the retinotopic organization of the visual system.

In addition, our collaborators traced the efferent projections of grafted new neurons throughout the brain and found largely correct projections to known target areas of upper layer V1. These results confirm various studies that have previously demonstrated the capability of grafted neurons to send efferent projections to correct target regions [Fricker-Gates 2002, Gaillard 2007, Ideguchi 2010, Michelsen 2015], and suggest that transplanted neurons eventually transfer appropriately integrated visual information to correct targets throughout the brain.

6.3 Integration of Endogenous New Neurons after Apoptotic Photolesion?

Besides the striking capacity of transplanted neurons to help in the restoration of damaged brain circuits demonstrated in this thesis (see 6.2), the exogenous supply of new neurons for therapeutic use underlies methodological constraints as well as ethical considerations [Lindvall 2004, Barker 2013, Thompson 2015]. Alternatively, endogenous pools of neuronal progenitors could be activated and instructed to replace neurons lost due to injury or disease [Lindvall 2004, Emsley 2005, Bellenchi 2013, Christie 2013, Sun 2014].

In the adult mammalian brain the generation of new neurons is mostly restricted to its neurogenic niches, the subventricular zone (SVZ) lining the wall of the lateral ventricles [Lois 1993, Lois 1994, Alvarez-Buylla 2002] and the dentate gyrus (DG) of the hippocampal formation [Altman 1965, Altman 1969, Kempermann 2004, Ming 2005, Ming 2011]. Besides, cells with neurogenic

potential *in vitro* have reportedly been isolated from multiple areas of the healthy [Reynolds 1992, Palmer 1995] and diseased brain [Buffo 2008, Sirko 2013, Robel 2013], although technical limitations in respect to progenitor identification [Breunig 2007a] and determination of multipotency [Pastrana 2011] are a cause for on-going controversy. Both, astrocytes and cells of the oligodendroglial lineage are under discussion as potential progenitors that also become (re-) active in response to injury and exhibit neurogenic potential. For instance, it has been reported that isolated reactive astrocytes from the lesioned adult cortex are capable of forming non-adherent, clonally derived agglomerates, so called neurospheres [Buffo 2008, Sirko 2013, Faiz 2015], and exhibit a capacity for multipotency *in vitro* [Buffo 2008, Sirko 2013]. Further, reactive astrocytes could be converted into neurons *in vivo*, following the ectopic expression of the pro-neuronal TF achaete-scute homolog 1 (Ascl1) in the stroke lesioned cortex [Faiz 2015], and the key stem cell TF sex-determining region Y-box 2 (Sox2) in the striatum [Niu 2013], respectively. In both studies however, the number of induced new neurons was extremely low and the overwhelming majority of cells did not progress to express mature neuronal markers, e.g. the neuronal nuclear antigen NeuN [Mullen 1992].

A substantial fraction of postnatal OPCs is comprised of NG2 cells [Ligon 2006, Nishiyama 2009], which constitute another potential source of new neurons. While in the non-injured brain NG2 cells seem restricted to the oligodendrocyte lineage [Simon 2011, Richardson 2011], they convert to a state of multipotency in response to growth factors *in vitro* [Kondo 2000, Belachew 2003]. In addition, NG2 cells have recently been shown to give rise to new neurons *in vivo*, following the ectopic expression of Sox2 after cortical stab wound lesion [Heinrich 2014]. Similar to reprogrammed astrocytes however, the reported numbers of induced new neurons from NG2 progenitors were low, and neuronal maturation was scarce.

Interestingly, multiple invasive cortical [Salman 2004, Saha 2013, Faiz 2015] and striatal [Arvidsson 2002, Li 2010] lesion paradigms elicit a massive multilineage cytogenic response that originates from the SVZ. Increased proliferation has been observed in the SVZ following middle cerebral artery occlusion [Arvidsson 2002] (MCAO) and cortical aspiration lesion [Saha 2013], and vast numbers of SVZ derived doublecortin (Dcx) positive neurons infiltrate the penumbra of various lesion types [Arvidsson 2002, Salman 2004, Li 2010, Saha 2013, Faiz 2015]. While the striatum seems permissive for the maturation of a moderate fraction of infiltrated Dcx^+ cells [Arvidsson 2002, Li 2010] into medium-sized spiny neurons [Arvidsson 2002], the vast majority of progenitors reaching cortical lesion sites differentiate into astrocytes and oligodendroglial cells [Salman 2004, Saha 2013, Faiz 2015]. Although mature SVZ derived $NeuN^+$ neurons occasionally have been observed after cortical lesions [Saha 2013], reported numbers were extremely low.

Notably, low levels of $NeuN^+$ new neurons also have been described after photolytic ablation of cortico-thalamic neurons in layer 6 [Magavi 2000] (L6) and cortico-spinal motor neurons in L5 [Chen 2004] of adult mice. Identified based on the incorporation of the thymidine analogue

BrdU, respective new neurons expressed mature neuronal markers, were detected in deep cortical layers and formed sub-type specific projections to target regions of ablated neurons. However, the cellular origin of these induced new neurons remains elusive to date [Sohur 2012, Diaz 2013].

Thus, while a number of studies have demonstrated that several cellular sources are capable of generating new neurons in various physiological and artificial lesion paradigms, the number of induced new neurons generally is low, and differentiation into mature neurons is extremely scarce.

In this final part of my thesis, I investigated whether the photolytic lesion paradigm employed to specifically eliminate L2/3 CPNs in V1 also induced the generation of endogenous new neurons. Since it is suspected that reported $NeuN^+BrdU^+$ neurons are either derived from the SVZ or local parenchymal progenitors [Magavi 2000, Chen 2004], I combined the photolytic ablation of L2/3 CPNs with genetic fate mapping experiments in suitable mouse models [Mori 2006, Nakamura 2006, Simon 2012]. In addition to revealing the cellular origin of potential, induced new neurons, respective mouse models also allow for the chronic *in vivo* observation of their structural and functional development, and eventually, their integration into the local circuit. In case new neurons originate in the SVZ, the location of V1 in the posterior cortex might prove disadvantageous to the activation of and infiltration by induced neuronal progenitors. Therefore, I performed a second set of experiments in S1.

I detected lesion-induced $NeuN^+BrdU^+$ neurons in both, S1 and V1, albeit at low numbers. Surprisingly, neither astrocytic nor oligodendrocytic lineage tracing could substantiate their cellular origin, as not one induced neuron was co-labelled in either mouse model. On the other hand, photolytic lesion in GLAST-creERT2 x CAG-GFP mice induced GFP^+ morphologically mature neurons that never incorporated BrdU. Although specific to the lesion site, *in vivo* imaging did not detect progressive developmental stages of maturation, excluding the possibility that they differentiated from local quiescent postmitotic progenitors. Interestingly, the lesion specificity of GFP expression in mature, likely non-induced neurons reveals a potential caveat for the use of creERT2 driver lines for lineage tracing in models of injury and disease.

Taken together, further studies will be required to determine the origin and prevalence of the endogenous progenitors that give rise to $NeuN^+BrdU^+$ neurons induced by apoptotic photolesion in the cortex. It seems conceivable, however, that the potential for circuit integration and repair of these induced new neurons equals the demonstrated capacity of exogenous new neurons (see 6.2) in quality and extent.

6.3.1 A Critical View on BrdU as a Marker of New(born) Neurons

In order to investigate the induction and cellular origin of potential new neurons, I ablated L2/3 CPNs in V1 and S1 in GLAST-creERT2 x CAG-GFP and SOX10-creERT2 x CAG-GFP mice. While the GLAST-creERT2 driver line labels cells of the astroglial lineage, including radial glia-like progenitors in the SVZ, potential progenitors in the parenchyma, as well as mature quiescent astrocytes [Mori 2006], SOX10-creERT2 drives GFP expression in mature oligodendrocytes as well as OPCs, including NG2 cells [Simon 2012]. BrdU was supplied continuously via drinking water for a period of one week before and one week after photolytic lesion. Animals were sacrificed and brains subjected to immunohistochemistry (IHC) at 2 and 8 weeks post laser lesion (wpl).

Indeed, at 8 wpl $NeuN^+BrdU^+$ neurons were detected specifically at the site of photolytic lesion in both, S1 and V1, albeit at low numbers. Surprisingly, in both mouse lines, across all areas analysed, not a single $NeuN^+BrdU^+$ neuron was co-labelled with GFP. In addition, consistent (negative) results were obtained after varying the timing of the BrdU supply in respect to GFP induction. Unfortunately, these results render the incorporation of BrdU as the sole indicator of induced mature new neurons, and - given the pitfalls of BrdU labelling that have become apparent over the last decade [Cooper-Kuhn 2002, Taupin 2007, Breunig 2007a, Duque 2011] - should be interpreted with some scrutiny.

As a thymidine analogue BrdU is incorporated into the genome during DNA synthesis in the S phase of the cell cycle [Takeda 2005], thus labelling cells that undergo proliferation. However, outside of the normal cell cycle any form of DNA synthesis will also result in the stochastic incorporation of BrdU, including mechanisms of DNA repair based on base [Zharkov 2008] and nucleotide excision [Dexheimer 2013], respectively. Since a variety of cortical insults, including stroke [Li 2011, Huttner 2014] and oxidative stress due to injury or disease [Fishel 2007, Narciso 2016], have been shown to entail DNA repair, I investigated the possibility that photolytic lesion induced $NeuN^+BrdU^+$ neurons are in fact postmitotic neurons labelled due to cellular repair. However, a comparison of induced new neurons at 2 and 8 wpl revealed that there was no difference in the numbers of $NeuN^+BrdU^+$ cells within the lesion site at 2 wpl and outside of the lesion at both, 2 and 8 wpl. If DNA repair was a confounding factor, significant numbers of mature neurons would have been labelled with BrdU already at early time-points post lesion. In addition, the increase in detected lesion specific $NeuN^+BrdU^+$ neurons over the following weeks suggests that induced new neurons undergo a maturation process until they eventually express NeuN. As expected, the invasive nature of Ce6 beads injection at the homotopic site of the contralateral hemisphere resulted in elevated numbers of $NeuN^+BrdU^+$ neurons already at 2 wpl likely due to repair mechanisms. At 8 wpl these numbers had declined to control levels, consistent with subsequent neuronal death. Thus, photolytic lesion

induced $NeuN^+BrdU^+$ neurons unlikely constitute postmitotic neurons that have incoporated BrdU due to cellular repair.

Another possible route of BrdU incorporation into mature postmitotic neurons is DNA synthesis during a process called abortive cell cycle re-entry [Kuan 2004, Taupin 2007, Breunig 2007a]. Cell cycle re-entry is characterized by the re-expression of S phase cell cycle transition proteins, proliferation markers and the resumption of DNA synthesis. However, cell cycle progression is not completed, and the majority of affected neurons eventually undergo apoptotic cell death [Kuan 2004]. Indeed, postmitotic neurons exhibiting cell cycle re-entry and subsequent apoptosis have been found following hypoxia-ischemia [Kuan 2004], stroke [Hayashi 2000], kainic acid lesions [Verdaguer 2002], as well as in models of Alzheimer's and Parkinson's disease [Yang 2001, Hoglinger 2007]. Interestingly, it has been shown that the re-activation of cell cycle progression is triggered by DNA damage in terminally differentiated cortical neurons *in vitro*. Accordingly, apoptosis induction without affecting the DNA resulted in cell death without prior cell cycle activation [Kruman 2004]. In addition, DNA damage has been linked to cell cycle re-entry and massive apoptosis *in vivo* in the *Harlequin* (Hq) mouse model of progressive oxidative stress-induced neurodegeneration [Klein 2002, Herrup 2004]. In the Hq mouse the level of the flavoprotein apoptosis-inducing factor (Aif) is greatly reduced in cerebellar granule and Purkinje cells, as well as various types of retinal neurons, leading to an imbalance in the ROS scavenging system in affected neurons. As a result, neurons accumulate oxidative DNA damage, subsequently co-express various cell cycle proteins, progressively incorporate BrdU and eventually, undergo apoptotic cell death. Importantly, $BrdU^+$ postmitotic neurons steadily increased in number until Hq mice were 7 months of age [Klein 2002], indicating slow degeneration and long survival times of damaged neurons. In line with this, oxidative DNA damage [Klein 2003], robust cell cycle re-entry [Yang 2001] and substantial DNA synthesis [Yang 2001] also have been described in human post-mortem tissue of Alzheimer's disease (AD) patients. In AD, the near complete DNA replication without subsequent progression to mitosis results in the formation of tetraploid neurons, which accumulate and persist for many months before undergoing neuronal cell death [Yang 2001, Frade 2015].

Photolytic activation of Ce6 labelled CPNs in L2/3 of V1 (see 6.1) induces intracellular ROS formation and subsequent slow progressive cell death via a process reminiscent of apoptosis [Sheen 1992, Sheen 1994]. Given the association of oxidative stress and oxidative DNA damage, abortive cell cycle re-entry and neurodegeneration, it is not unlikely that ROS production due to photolytic lesion triggers similar events. At least a fraction of Ce6 labelled CPNs could re-enter the cell cycle and resume DNA synthesis before eventually progressing to apoptotic cell death. Such neurons would incorporate BrdU, since laser photoactivation takes place mid-way through a 2-week period of BrdU supply. It has been shown that postmitotic neurons with re-activated cell cycle persist in S phase for many months before

their death and clearance from the tissue [Klein 2002, Yang 2001, Frade 2015]. Therefore, $BrdU^+$ CPNs with active cell cycle that do not die with in the characteristic 1 to 2 week period (see 5.3.1) might be able to persist and impede the secure identification of induced new neurons. The comparison of 2 and 8 wpl however, shows a significant increase of $NeuN^+BrdU^+$ neurons over time. If abortive cell-cycle re-entry was responsible for all detected $BrdU^+$ mature neurons, both time-points should have exhibited equal numbers. It is very unlikely that past 2 wpl additional postmitotic neurons acquire BrdU labelling, since BrdU supply was ended 1 week earlier, and BrdU clearance from the organism occurs within hours [Packard 1973, Hayes 2000, Duque 2011]. It cannot be excluded however, that BrdU is released into the local tissue by dying CPNs that have undergone cell cycle re-entry during the first wpl and progress to apoptosis within the second wpl. This way the availability of BrdU in the local tissue could be prolonged past the 2 wpl time-point. Indeed, it has been shown that BrdU derived from labelled donor neurons that do not survive transplantation is released *in vivo* and subsequently transferred to host neurons and glia in the neonatal rat brain [Burns 2006].

Taken together, despite the many pitfalls of BrdU as a sole marker for new neurons, the observed increase of $NeuN^+BrdU^+$ cells between 2 and 8 wpl, specifically at the photolytic lesion site, is still highly indicative of the induction of new neurons, albeit at low numbers. Identifying the progenitor population by lineage tracing could have provided unequivocal evidence. Unfortunately, neither GLAST nor SOX10 driver lines co-label new neurons, indicating that they are not derived from known progenitors of the astroglial and oligodendroglial lineage.

The generation of new neurons after photolytic lesion is thought to be dependent on the apoptotic nature of cell death of targeted pyramidal cells [Magavi 2000, Chen 2004]. In an attempt to independently verify this hypothesis, two different strategies were recently employed in order to genetically induce apoptosis in glutamatergic neurons and investigate the formation of new neurons in the cortex of adult mice [Diaz 2013]. In this study, the targeted expression of the caspase-8 protein and diphtheria toxin, respectively, caused stochastic apoptotic cell death of glutamatergic neurons throughout the brain upon induction. Concurrent BrdU injections for ~3 consecutive weeks lead to the labelling of roughly 25.000 $NeuN^+BrdU^+$ putative new neurons. Importantly, several rounds of analysis with increasing optical resolution revealed not a single truly co-labelled induced new neuron. Instead, seemingly $NeuN^+BrdU^+$ neurons were in fact two closely opposing cells, with the BrdU label likely belonging to a microglial cell [Diaz 2013]. Indeed, loss of extracellular space and tissue shrinkage are known to lead to artificial membrane coagulation, an inherent problem in the preparation of tissue for IHC [Cragg 1980, Karlsson 1965]. In unprecedented detail, the above study underlines the necessity for high-resolution single cell analysis and serial optical sectioning for the correct identification of new neurons labelled with BrdU. Accordingly, in this thesis, $NeuN^+BrdU^+$ neurons induced

by photolytic lesion have been identified using high-resolution confocal microscopy and optical sectioning. However, I did not employ an equal maximum spatial resolution and the multiple rounds of analysis described by Diaz et al [Diaz 2013]. Therefore, it cannot be excluded that at least some identified $NeuN^+BrdU^+$ neurons represent two cells in close apposition. In any case, Diaz et al. have shown that the generation of new neurons in the cortex is not a general process induced by apoptosis of glutamatergic neurons, as had been suggested previously [Magavi 2000, Chen 2004].

6.3.2 A Tale of HSP Complexes, Hormone Receptors and Lesion-Specific GFP^+ Neurons

While none of the observed $NeuN^+BrdU^+$ induced new neurons expressed GFP in lineage tracing experiments (see 5.3.2. and 5.3.5.), multiple GFP^+ cells were found to be co-labelled with NeuN in the GLAST-creERT2 x CAG-GFP mouse [Mori 2006] after photolytic lesion. In this mouse line, GFP expression is induced in cells of the astroglial lineage upon administration of the oestrogen analogue tamoxifen (TM) (see 3.3). TM binds to the mutated hormone-binding domain (HBD) of the oestrogen receptor (ERT2), which is fused to the cre recombinase (cre), enabling the translocation of creERT2 to the nucleus [Indra 1999, Hayashi 2002]. The subsequent recombination between loxP sites in the reporter gene construct [Nakamura 2006] induces GFP expression.

At 8 wpl GFP^+NeuN^+ neurons exhibited mature neuronal morphology and were located in and adjacent to the lesion site. Notably, a number of controls confirmed the lesion specificity of observed GFP^+ neurons. Sham induction of GFP expression with corn oil revealed no TM independent cre activity [Liu 2010] and importantly, no spontaneous recombination of loxP sites even in the presence of the photolytic lesion. Also, TM induction without lesion resulted only in sporadic unspecific GFP^+NeuN^+ neurons of significantly lower number. Indeed, the original study that introduced the GLAST-creERT2 mouse line reported cre expression in a small fraction of cortical neurons, as well as a varying fraction (2-6%) of neurons expressing a reporter gene upon induction that is dependent on the concentration of administered TM [Mori 2006]. Since the number of detected unspecific GFP^+NeuN^+ neurons is well below reported values, recombination in "leaky" cre expressing neurons is not induced by the induction protocol employed here (see 3.3).

Surprisingly, however, GFP^+NeuN^+ neurons consistently failed to incorporate BrdU supplied for 2 weeks at varying intervals spanning 3 weeks prior to 3 weeks post lesion. This result is interesting, as it would suggest that GFP^+BrdU^- new neurons potentially undergo differentiation from a resting, quiescent progenitor [Götz 2015]. Therefore, I employed chronic *in vivo* two-photon imaging to follow the fate of all GFP^+ resident cells in, as well as any

labelled cells migrating into, a volume of up to 0.8 mm^3 of V1 after photolytic lesion. Mice were subjected to imaging immediately after laser photoactivation and weekly thereafter up to 8 wpl. Although occasionally cells without typical astrocyte morphology could be observed that seemed to undergo multiple rounds of cell division and migration across time-points, not a single GFP^+ cell exhibited morphological differentiation into a mature pyramidal neuron. However, fully developed GFP^+ neurons generally appeared within 1 wpl without identifiable progenitor similar to previous reports [Breunig 2007a, Breunig 2007b]. Given the progressive nature of apoptotic photolesion, as well as the observed time period for differentiation of transplanted neurons (see 5.1.2 and 1.1), it is extremely unlikely that a quiescent progenitor would be both, activated and fully mature within such a short period of time.

The lesion specificity of GFP expression in resident, non-induced neurons reported here reveals a potential caveat for the use of creERT2 driver lines in models of injury and disease. In the absence of TM, recombination in cells expressing creERT2 is prohibited by the cytoplasmic retention of cre through its fusion to ERT2 [Indra 1999, Hayashi 2002]. ERT2 constitutes a mutated form of the hormone-binding domain of the oestrogen receptor [Indra 1999], which, like the HBDs of all 5 classes of steroid receptors, is associated with the heat shock protein 90 (Hsp90) heterocomplex [Picard 1988, Mattioni 1994, Picard 1994, Xu 1998, Bouhouche-Chatelier 2001, Pratt 2003]. This interaction serves an important function in the facilitation of hormone binding and steroid receptor activation *in vivo* [Picard 1990, Fliss 2000, Whitesell 2005]. Besides steroid receptors, the multimeric Hsp90 complex is comprised of additional heat shock proteins, molecular chaperones, co-chaperones, nucleotide exchange factors (NEFs), transcription factors and other regulatory proteins, forming a multicomponent molecular machine [Pratt 2003, Hartl 2011, Shiber 2014]. The primary function of this complex is the recognition, stabilization and ATP dependent (re-) folding of proteins exhibiting non-native conformations, as is the case with misfolded or denaturated proteins [Zou 1998, Hartl 2011, Shiber 2014]. If protein (re-) folding fails, Hsp90 complex associated co-factors like CHIP induce the ubiquitylation and subsequent proteolysis via the ubiquitin proteasome system [Connell 2001, Meacham 2001, Marques 2006]. Importantly, it has been demonstrated *in vitro* that denaturated protein is sufficient to cause the release of heat shock transcription factor 1 (Hsf1) from the Hsp90 complex [Zou 1998]. Once released, Hsf1 trimerizes, translocates to the nucleus, binds a characteristic DNA sequence [Neudegger 2016] and induces the transcription of a broad range of proteins to counteract cellular stress [Hahn 2004]. In addition, cellular stress has been shown to lead to the disassembly of the Hsf1 containing Hsp90 complex [Zou 1998], in a process where denaturated proteins compete for interaction with Hsp90 and several of its co-chaperones [Voellmy 2004]. Thus, the Hsp90 heterocomplex presents an effective sensor for cellular stress that disassembles and releases Hsf1, a stress responsive transcription factor, in order to sequester denaturated proteins.

Notably, cellular stress is an integral part of almost any neuronal lesion caused by injury or disease. Traumatic brain injury, stroke, epileptic seizures, excitotoxicity and neurodegenerative diseases all involve an activated or disrupted heat shock response pathway [Bullok 2005, Raghupathi 1995, Marciano 2002, Adachi 2009, Gomez-Pastor 2016]. Since photolytic activation of Ce6 labelled CPNs in L2/3 of V1 (see 6.1) induces intracellular formation of ROS, the majority of activated neurons will experience oxidative protein damage [Dahl 2015] before undergoing subsequent apoptotic cell death [Sheen 1992, Sheen 1994]. Individual surviving neurons will likely exhibit an active heat shock response pathway in order to counteract oxidative stress [Dahl 2015], and, as a result, experience competition between damaged proteins and monomeric Hsf1 for major components of the Hsp90 complex. Accordingly, surviving neurons with "leaky" cre expression will not be able to retain their creERT2 proteins sequestered in the Hsp90 complex. Thus, although the TM concentration employed here may not be able to disengage ERT2 from the Hsp90 complex in GLAST-creERT2 mice in control conditions, the combination with lesion induced oxidative stress may successfully result in nuclear creERT2 translocation and subsequent GFP expression. Given an average pyramidal cell diameter of 15 µm [Miller 1988], a CPN density of 70 to 90% [Diao 1983, Dräger 1978, Lepore 1992, Pietrasanta 2012, Dehmel 2014] of all pyramidal cells and a minimum of 6% unspecific cre$^+$ cortical neurons [Mori 2006], an assumed 0.1% surviving Ce6$^+$ neurons under oxidative stress within the maximum investigated volume of 0.8 mm^3 would result in ~15 GFP$^+$ neurons. This number compares well with the determined average of 10.15 ±5.346 neurons that were found to be GFP$^+$NeuN$^+$ at the lesion site.

The lesion specificity of GFP expression in resident, non-induced neurons reported in this thesis underlines the importance of time-lapse studies and consequently, the observation of morphological development in order to reliably identify new neurons. Particular care should be taken in the interpretation of lineage tracing experiments based on creERT2 driver lines in models of injury or disease.

6.4 Perspectives and Future Directions

Taken together, I have shown that new neurons are readily assimilated into adult cortical circuits subjected to injury or disease. New neurons develop appropriate pyramidal cell-like morphologies, form stable synaptic contacts with the host network, and eventually adopt stable, circuit specific functional properties indistinguishable from adult resident L2/3 neurons. Once integrated, new neurons remain an integral part of target circuits for the rest of the animal's life. Potential lesion induced endogenous new neurons are scarce and seem not to be derived from either astroglial or oligodendroglial lineage, hinting at a hitherto

unknown population of endogenous progenitors. Further studies are required to identify their origin, prevalence and potential to contribute to circuit repair.

This proof of principle study offers encouraging results and a solid starting point for future experiments on brain circuit restoration. The stable synaptic integration of transplanted neurons, for instance, presents an important prerequisite for integrated new neurons to adapt to changes in the environment. Accordingly, new cells should be capable of adopting appropriate levels of host area and cell type specific structural and functional plasticity. Paradigms of sensory deprivation and modality or circuit specific rearing could be well suited to answer these questions. Also, it is worth investigating whether the systematic manipulation of activity could lead to the targeted, sub-circuit specific integration of new neurons.

An open question is the extent to which current attempts at cortical circuit restoration are capable of ameliorating behavioural defects due to injury or disease. While adult V1 is ideally suited to investigate the functional integration of new neurons on a cellular level, the visual system is less appropriate to study subtle differences in behaviour. Cortical areas corresponding to motor planning and execution might be better suited to link circuit restoration with behavioural improvements.

Finally, the comparison of the successful circuit integration presented in this thesis with attempts at circuit repair in models of physiological lesions, including stroke, trauma and neurodegenerative disease, will help to elucidate crucial differences in the process of integration and its limit on a structural, functional and molecular level. Also, it will be important to explore the capabilities of various sources of new neurons currently under consideration for their potential use in cellular therapy. Both will help to design and shape future strategies in brain circuit restoration.

Abbreviations

3' OH	3' hydroxy group
AD	Alzheimer's disease
AIF	apoptosis-inducing factor
AP2γ	activating enhancer binding protein 2γ
ASCL1	Achaete-scute homolog 1
BBB	blood-brain barrier
BDNF	brain-derived neurotrophic factor
BrdU	5-bromo-2'-deoxyuridine
Ca2+	calcium
Cc	corpus callosum
Ce6	chlorine e6
CHIP	carboxyl terminus of Hsc70- interacting protein
Cl-	chloride
CNS	central nervous system
CPG15	candidate plasticity-related gene 15
CPNs	contralateral projection neurons
Cre	cre recombinase
CREB	cAMP response element-binding protein
CSPGs	chondroitin sulphate proteoglycans
Cux1	cut like homeobox 1
Cx	cortex
DAPI	4',6-diamidino-2-phenylindole
Dcx	doublecortin
DG	dentate gyrus
dpl	days post laser
dpt	days post transplantation
DRGs	dorsal root ganglion cells
DTA	diphtheria toxin fragment A
dUTP	2'-deoxyuridine-5'-triphosphate
ECM	extracellular matrix
EGF	epidermal growth factor
ERT2	mutated oestrogen receptor binding domain
Fezf2	FEZ family zinc finger 2
FGF	fibroblast growth factor
FGF2	fibroblast growth factor-2

GABA A-R	GABA A receptor
GC	glomerular cell of the OB
GFAP	glial fibrillary acidic protein
GFP	green fluorescent protein
GST-π	glutathione S-transferase Pi
HBD	hormone-binding domain
HD	Huntington's disease
HSE	heat shock element
Hsf1	heat shock transcription factor 1
Hsp90	heat shock protein 90
Iba1	ionized calcium binding adaptor molecule 1
K^+	potassium
KCC2	K^+C^- co-transporter 2
L1	cortical layer 1
L2/3	cortical layer 2/3
L4	cortical layer 4
L5	cortical layer 5
L6	cortical layer 6
LGN	lateral geniculate nucleus
LTD	long-term depression
LTP	long-term potentiation
LV	lateral ventricle
M1	primary motor cortex
MMPs	matrix metalloproteases
mth pl	months post laser
mth pt	months post transplantation
NEF	nucleotide exchange factor
NeuN	neuronal nuclear antigen
NG2	neuron-glial antigen 2
NGF	nerve growth factor
NKCC1	$Na^+K^+2Cl^-$ co-transporter 1
NO	nitric oxide
Nrn1	neuritin 1
NT-3	neurotrophin-3
NT-4/5	neurotrophin-4/5
OB	olfactory bulb
Olig2	oligodendrocyte transcription factor 2

OPCs	oligodendrocyte progenitor cells
PD	Parkinson's disease
PDGF	platelet-derived growth factor
PFA	paraformaldehyde
PGC	periglomerular cell of the OB
pL	post laser
RG	radial glia
RGCs	retinal ganglion cells
RMS	rostral migratory stream
ROS	reactive oxygen species
S1	somatosensory cortex
SC	stem cell
SCG	superior cervical ganglion
SCI	spinal cord injury
Sema3A	semaphorin 3A
SGZ	sub-granular zone
SOX2	sex determining region Y-box 2
SS	somatosensory cortex
SVZ	subventricular zone
TBI	traumatic brain injury
tdT	tandem dimer Tomato (variant of DsRed)
TdT	terminal deoxynucleotidyl transferase
TF	transcription factor
TGI	transient global ischemia
TM	tamoxifen
TrkB	tyrosine kinase receptor B
TUNEL	TdT-mediated dUTP nick end labelling
V1	primary visual cortex
VGCC	voltage-gated calcium channel
wpl	weeks post laser
wpt	weeks post transplantation
wt	wild type

References

Abd-el-Basset, E. M., V. I. Kalnins, and S. Fedoroff. "Expression of 48-Kilodalton Intermediate Filament-Associated Protein in Differentiating and in Mature Astrocytes in Various Regions of the Central Nervous System." *J Neurosci Res* 21, no. 2-4 (Oct-Dec 1988): 226-37. http://dx.doi.org/10.1002/jnr.490210215.

Aboitiz, F. and J. Montiel. "One Hundred Million Years of Interhemispheric Communication: The History of the Corpus Callosum." *Braz J Med Biol Res* 36, no. 4 (Apr 2003): 409-20. https://www.ncbi.nlm.nih.gov/pubmed/12700818.

Achilles, K., A. Okabe, M. Ikeda, C. Shimizu-Okabe, J. Yamada, A. Fukuda, H. J. Luhmann, and W. Kilb. "Kinetic Properties of Cl Uptake Mediated by Na+-Dependent K+-2cl Cotransport in Immature Rat Neocortical Neurons." *J Neurosci* 27, no. 32 (Aug 08 2007): 8616-27. http://dx.doi.org/10.1523/JNEUROSCI.5041-06.2007.

Ackman, J. B., F. Siddiqi, R. S. Walikonis, and J. J. LoTurco. "Fusion of Microglia with Pyramidal Neurons after Retroviral Infection." *J Neurosci* 26, no. 44 (Nov 01 2006): 11413-22. http://dx.doi.org/10.1523/JNEUROSCI.3340-06.2006.

Adachi, H., M. Katsuno, M. Waza, M. Minamiyama, F. Tanaka, and G. Sobue. "Heat Shock Proteins in Neurodegenerative Diseases: Pathogenic Roles and Therapeutic Implications." *Int J Hyperthermia* 25, no. 8 (Dec 2009): 647-54. http://dx.doi.org/10.3109/02656730903315823.

Agathou, S., R. T. Karadottir, and I. Kazanis. "Niche Derived Oligodendrocyte Progenitors: A Source of Rejuvenation or Complementation for Local Oligodendrogenesis?" *Front Cell Neurosci* 7 (2013): 188. http://dx.doi.org/10.3389/fncel.2013.00188.

Aghajanian, G. K. and F. E. Bloom. "The Formation of Synaptic Junctions in Developing Rat Brain: A Quantitative Electron Microscopic Study." *Brain Res* 6, no. 4 (Dec 1967): 716-27. https://www.ncbi.nlm.nih.gov/pubmed/4169903.

Aguirre, A. and V. Gallo. "Postnatal Neurogenesis and Gliogenesis in the Olfactory Bulb from Ng2-Expressing Progenitors of the Subventricular Zone." *J Neurosci* 24, no. 46 (Nov 17 2004): 10530-41. http://dx.doi.org/10.1523/JNEUROSCI.3572-04.2004.

Aharonowiz, M., O. Einstein, N. Fainstein, H. Lassmann, B. Reubinoff, and T. Ben-Hur. "Neuroprotective Effect of Transplanted Human Embryonic Stem Cell-Derived Neural Precursors in an Animal Model of Multiple Sclerosis." *PLoS One* 3, no. 9 (Sep 05 2008): e3145. http://dx.doi.org/10.1371/journal.pone.0003145.

Ahmari, S. E., J. Buchanan, and S. J. Smith. "Assembly of Presynaptic Active Zones from Cytoplasmic Transport Packets." *Nat Neurosci* 3, no. 5 (May 2000): 445-51. http://dx.doi.org/10.1038/74814.

Aimone, J. B., W. Deng, and F. H. Gage. "Resolving New Memories: A Critical Look at the Dentate Gyrus, Adult Neurogenesis, and Pattern Separation." *Neuron* 70, no. 4 (May 26 2011): 589-96. http://dx.doi.org/10.1016/j.neuron.2011.05.010.

Aimone, J. B., J. Wiles, and F. H. Gage. "Potential Role for Adult Neurogenesis in the Encoding of Time in New Memories." *Nat Neurosci* 9, no. 6 (Jun 2006): 723-7. http://dx.doi.org/10.1038/nn1707.

Albus, K. and F. Donate-Oliver. "Cells of Origin of the Occipito-Pontine Projection in the Cat: Functional Properties and Intracortical Location." *Exp Brain Res* 28, no. 1-2 (May 23 1977): 167-74. https://www.ncbi.nlm.nih.gov/pubmed/881001.

Allen Brain Atlas, Allen Institute. http://mouse.brain-map.org/ (Expression Database).

Alonso, M., G. Lepousez, W. Sebastien, C. Bardy, M. M. Gabellec, N. Torquet, and P. M. Lledo. "Activation of Adult-Born Neurons Facilitates Learning and Memory." *Nat Neurosci* 15, no. 6 (Jun 2012): 897-904. http://dx.doi.org/10.1038/nn.3108.

Alonso, M., C. Viollet, M. M. Gabellec, V. Meas-Yedid, J. C. Olivo-Marin, and P. M. Lledo. "Olfactory Discrimination Learning Increases the Survival of Adult-Born Neurons in the Olfactory Bulb." *J Neurosci* 26, no. 41 (Oct 11 2006): 10508-13. http://dx.doi.org/10.1523/JNEUROSCI.2633-06.2006.

Altman, J. "Autoradiographic and Histological Studies of Postnatal Neurogenesis. Iv. Cell Proliferation and Migration in the Anterior Forebrain, with Special Reference to Persisting Neurogenesis in the Olfactory Bulb." *J Comp Neurol* 137, no. 4 (Dec 1969): 433-57. http://dx.doi.org/10.1002/cne.901370404.

Altman, J. and G. D. Das. "Autoradiographic and Histological Evidence of Postnatal Hippocampal Neurogenesis in Rats." *J Comp Neurol* 124, no. 3 (Jun 1965): 319-35. https://www.ncbi.nlm.nih.gov/pubmed/5861717.

Alunni, A. and L. Bally-Cuif. "A Comparative View of Regenerative Neurogenesis in Vertebrates." *Development* 143, no. 5 (Mar 01 2016): 741-53. http://dx.doi.org/10.1242/dev.122796.

Alvarez-Buylla, A. and J. M. Garcia-Verdugo. "Neurogenesis in Adult Subventricular Zone." *J Neurosci* 22, no. 3 (Feb 01 2002): 629-34. https://www.ncbi.nlm.nih.gov/pubmed/11826091.

Alvarez-Dolado, M., R. Pardal, J. M. Garcia-Verdugo, J. R. Fike, H. O. Lee, K. Pfeffer, C. Lois, S. J. Morrison, and A. Alvarez-Buylla. "Fusion of Bone-Marrow-Derived Cells with Purkinje Neurons, Cardiomyocytes and Hepatocytes." *Nature* 425, no. 6961 (Oct 30 2003): 968-73. http://dx.doi.org/10.1038/nature02069.

Amaral, D. G. and M. P. Witter. "The Three-Dimensional Organization of the Hippocampal Formation: A Review of Anatomical Data." *Neuroscience* 31, no. 3 (1989): 571-91. https://www.ncbi.nlm.nih.gov/pubmed/2687721.

Andermann, M. L., N. B. Gilfoy, G. J. Goldey, R. N. Sachdev, M. Wolfel, D. A. McCormick, R. C. Reid, and M. J. Levene. "Chronic Cellular Imaging of Entire Cortical Columns in Awake Mice Using Microprisms." *Neuron* 80, no. 4 (Nov 20 2013): 900-13. http://dx.doi.org/10.1016/j.neuron.2013.07.052.

Andermann, M. L., A. M. Kerlin, and R. C. Reid. "Chronic Cellular Imaging of Mouse Visual Cortex During Operant Behavior and Passive Viewing." *Front Cell Neurosci* 4 (2010): 3. http://dx.doi.org/10.3389/fncel.2010.00003.

Anglade, P., S. Vyas, E. C. Hirsch, and Y. Agid. "Apoptosis in Dopaminergic Neurons of the Human Substantia Nigra During Normal Aging." *Histol Histopathol* 12, no. 3 (Jul 1997): 603-10. https://www.ncbi.nlm.nih.gov/pubmed/9225140.

Anglade, P., S. Vyas, F. Javoy-Agid, M. T. Herrero, P. P. Michel, J. Marquez, A. Mouatt-Prigent, M. Ruberg, E. C. Hirsch, and Y. Agid. "Apoptosis and Autophagy in Nigral Neurons of Patients with Parkinson's Disease." *Histol Histopathol* 12, no. 1 (Jan 1997): 25-31. https://www.ncbi.nlm.nih.gov/pubmed/9046040.

Antonini, A., M. Fagiolini, and M. P. Stryker. "Anatomical Correlates of Functional Plasticity in Mouse Visual Cortex." *J Neurosci* 19, no. 11 (Jun 01 1999): 4388-406. https://www.ncbi.nlm.nih.gov/pubmed/10341241.

Aoki, C., K. Wu, A. Elste, Gw Len, Sy Lin, G. McAuliffe, and I. B. Black. "Localization of Brain-Derived Neurotrophic Factor and Trkb Receptors to Postsynaptic Densities of Adult Rat Cerebral Cortex." *J*

Neurosci Res 59, no. 3 (Feb 01 2000): 454-63. http://dx.doi.org/10.1002/(SICI)1097-4547(20000201)59:3<454::AID-JNR21>3.0.CO;2-H.

Aroniadou-Anderjaska, V., F. M. Zhou, C. A. Priest, M. Ennis, and M. T. Shipley. "Tonic and Synaptically Evoked Presynaptic Inhibition of Sensory Input to the Rat Olfactory Bulb Via Gaba(B) Heteroreceptors." *J Neurophysiol* 84, no. 3 (Sep 2000): 1194-203. https://www.ncbi.nlm.nih.gov/pubmed/10979995.

Arvidsson, A., T. Collin, D. Kirik, Z. Kokaia, and O. Lindvall. "Neuronal Replacement from Endogenous Precursors in the Adult Brain after Stroke." *Nat Med* 8, no. 9 (Sep 2002): 963-70. http://dx.doi.org/10.1038/nm747.

Asher, R. A., D. A. Morgenstern, P. S. Fidler, K. H. Adcock, A. Oohira, J. E. Braistead, J. M. Levine, R. U. Margolis, J. H. Rogers, and J. W. Fawcett. "Neurocan Is Upregulated in Injured Brain and in Cytokine-Treated Astrocytes." *J Neurosci* 20, no. 7 (Apr 01 2000): 2427-38. https://www.ncbi.nlm.nih.gov/pubmed/10729323.

Aungst, J. L., P. M. Heyward, A. C. Puche, S. V. Karnup, A. Hayar, G. Szabo, and M. T. Shipley. "Centre-Surround Inhibition among Olfactory Bulb Glomeruli." *Nature* 426, no. 6967 (Dec 11 2003): 623-9. http://dx.doi.org/10.1038/nature02185.

Bachoud-Levi, A. C. "Neural Grafts in Huntington's Disease: Viability after 10 Years." *Lancet Neurol* 8, no. 11 (Nov 2009): 979-81. http://dx.doi.org/10.1016/S1474-4422(09)70278-9.

Bachoud-Levi, A. C., P. Remy, J. P. Nguyen, P. Brugieres, J. P. Lefaucheur, C. Bourdet, S. Baudic, V. Gaura, P. Maison, B. Haddad, M. F. Boisse, T. Grandmougin, R. Jeny, P. Bartolomeo, G. Dalla Barba, J. D. Degos, F. Lisovoski, A. M. Ergis, E. Pailhous, P. Cesaro, P. Hantraye, and M. Peschanski. "Motor and Cognitive Improvements in Patients with Huntington's Disease after Neural Transplantation." *Lancet* 356, no. 9246 (Dec 09 2000): 1975-9. https://www.ncbi.nlm.nih.gov/pubmed/11130527.

Bang, O. Y. "Clinical Trials of Adult Stem Cell Therapy in Patients with Ischemic Stroke." *J Clin Neurol* 12, no. 1 (Jan 2016): 14-20. http://dx.doi.org/10.3988/jcn.2016.12.1.14.

Bannister, A. P. "Inter- and Intra-Laminar Connections of Pyramidal Cells in the Neocortex." *Neurosci Res* 53, no. 2 (Oct 2005): 95-103. http://dx.doi.org/10.1016/j.neures.2005.06.019.

Barker, J. M., R. Boonstra, and J. M. Wojtowicz. "From Pattern to Purpose: How Comparative Studies Contribute to Understanding the Function of Adult Neurogenesis." *Eur J Neurosci* 34, no. 6 (Sep 2011): 963-77. http://dx.doi.org/10.1111/j.1460-9568.2011.07823.x.

Barker, R. A., J. Barrett, S. L. Mason, and A. Bjorklund. "Fetal Dopaminergic Transplantation Trials and the Future of Neural Grafting in Parkinson's Disease." *Lancet Neurol* 12, no. 1 (Jan 2013): 84-91. http://dx.doi.org/10.1016/S1474-4422(12)70295-8.

Barlow, H. B. and W. R. Levick. "The Mechanism of Directionally Selective Units in Rabbit's Retina." *J Physiol* 178, no. 3 (Jun 1965): 477-504. https://www.ncbi.nlm.nih.gov/pubmed/5827909.

Barnabe-Heider, F., C. Goritz, H. Sabelstrom, H. Takebayashi, F. W. Pfrieger, K. Meletis, and J. Frisen. "Origin of New Glial Cells in Intact and Injured Adult Spinal Cord." *Cell Stem Cell* 7, no. 4 (Oct 08 2010): 470-82. http://dx.doi.org/10.1016/j.stem.2010.07.014.

Basu, J., J. D. Zaremba, S. K. Cheung, F. L. Hitti, B. V. Zemelman, A. Losonczy, and S. A. Siegelbaum. "Gating of Hippocampal Activity, Plasticity, and Memory by Entorhinal Cortex Long-Range Inhibition." *Science* 351, no. 6269 (Jan 08 2016): aaa5694. http://dx.doi.org/10.1126/science.aaa5694.

Battista, D., C. C. Ferrari, F. H. Gage, and F. J. Pitossi. "Neurogenic Niche Modulation by Activated Microglia: Transforming Growth Factor Beta Increases Neurogenesis in the Adult Dentate Gyrus." *Eur J Neurosci* 23, no. 1 (Jan 2006): 83-93. http://dx.doi.org/10.1111/j.1460-9568.2005.04539.x.

Bayer, S. A. "3h-Thymidine-Radiographic Studies of Neurogenesis in the Rat Olfactory Bulb." *Exp Brain Res* 50, no. 2-3 (1983): 329-40. https://www.ncbi.nlm.nih.gov/pubmed/6641865.

Bazarek, S. and D. A. Peterson. "Prospects for Engineering Neurons from Local Neocortical Cell Populations as Cell-Mediated Therapy for Neurological Disorders." *J Comp Neurol* 522, no. 12 (Aug 15 2014): 2857-76. http://dx.doi.org/10.1002/cne.23618.

Belachew, S., R. Chittajallu, A. A. Aguirre, X. Yuan, M. Kirby, S. Anderson, and V. Gallo. "Postnatal Ng2 Proteoglycan-Expressing Progenitor Cells Are Intrinsically Multipotent and Generate Functional Neurons." *J Cell Biol* 161, no. 1 (Apr 14 2003): 169-86. http://dx.doi.org/10.1083/jcb.200210110.

Bellenchi, G. C., F. Volpicelli, V. Piscopo, C. Perrone-Capano, and U. di Porzio. "Adult Neural Stem Cells: An Endogenous Tool to Repair Brain Injury?" *J Neurochem* 124, no. 2 (Jan 2013): 159-67. http://dx.doi.org/10.1111/jnc.12084.

Ben-Ari, Y. "Excitatory Actions of Gaba During Development: The Nature of the Nurture." *Nat Rev Neurosci* 3, no. 9 (Sep 2002): 728-39. http://dx.doi.org/10.1038/nrn920.

Ben-Ari, Y., E. Cherubini, R. Corradetti, and J. L. Gaiarsa. "Giant Synaptic Potentials in Immature Rat Ca3 Hippocampal Neurones." *J Physiol* 416 (Sep 1989): 303-25. https://www.ncbi.nlm.nih.gov/pubmed/2575165.

Bennett, C., S. Arroyo, and S. Hestrin. "Subthreshold Mechanisms Underlying State-Dependent Modulation of Visual Responses." *Neuron* 80, no. 2 (Oct 16 2013): 350-7. http://dx.doi.org/10.1016/j.neuron.2013.08.007.

Berninger, B., S. Marty, F. Zafra, M. da Penha Berzaghi, H. Thoenen, and D. Lindholm. "Gabaergic Stimulation Switches from Enhancing to Repressing Bdnf Expression in Rat Hippocampal Neurons During Maturation in Vitro." *Development* 121, no. 8 (Aug 1995): 2327-35. https://www.ncbi.nlm.nih.gov/pubmed/7671799.

Bjorklund, A., U. Stenevi, S. B. Dunnett, and F. H. Gage. "Cross-Species Neural Grafting in a Rat Model of Parkinson's Disease." *Nature* 298, no. 5875 (Aug 12 1982): 652-4. https://www.ncbi.nlm.nih.gov/pubmed/7099260.

Blaesse, P. and T. Schmidt. "K-Cl Cotransporter Kcc2--a Moonlighting Protein in Excitatory and Inhibitory Synapse Development and Function." *Pflugers Arch* 467, no. 4 (Apr 2015): 615-24. http://dx.doi.org/10.1007/s00424-014-1547-6.

Blakemore, C., Y. C. Diao, M. L. Pu, Y. K. Wang, and Y. M. Xiao. "Possible Functions of the Interhemispheric Connexions between Visual Cortical Areas in the Cat." *J Physiol* 337 (Apr 1983): 331-49. https://www.ncbi.nlm.nih.gov/pubmed/6875934.

Blandini, F., G. Nappi, C. Tassorelli, and E. Martignoni. "Functional Changes of the Basal Ganglia Circuitry in Parkinson's Disease." *Prog Neurobiol* 62, no. 1 (Sep 2000): 63-88. https://www.ncbi.nlm.nih.gov/pubmed/10821982.

Boda, E. and A. Buffo. "Glial Cells in Non-Germinal Territories: Insights into Their Stem/Progenitor Properties in the Intact and Injured Nervous Tissue." *Arch Ital Biol* 148, no. 2 (Jun 2010): 119-36. https://www.ncbi.nlm.nih.gov/pubmed/20830974.

Bortone, D. S., S. R. Olsen, and M. Scanziani. "Translaminar Inhibitory Cells Recruited by Layer 6 Corticothalamic Neurons Suppress Visual Cortex." *Neuron* 82, no. 2 (Apr 16 2014): 474-85. http://dx.doi.org/10.1016/j.neuron.2014.02.021.

Bos, R., C. Gainer, and M. B. Feller. "Role for Visual Experience in the Development of Direction-Selective Circuits." *Curr Biol* 26, no. 10 (May 23 2016): 1367-75. http://dx.doi.org/10.1016/j.cub.2016.03.073.

Bouhouche-Chatelier, L., A. Chadli, and M. G. Catelli. "The N-Terminal Adenosine Triphosphate Binding Domain of Hsp90 Is Necessary and Sufficient for Interaction with Estrogen Receptor." *Cell Stress Chaperones* 6, no. 4 (Oct 2001): 297-305. https://www.ncbi.nlm.nih.gov/pubmed/11795466.

Bozza, T., A. Vassalli, S. Fuss, J. J. Zhang, B. Weiland, R. Pacifico, P. Feinstein, and P. Mombaerts. "Mapping of Class I and Class Ii Odorant Receptors to Glomerular Domains by Two Distinct Types of Olfactory Sensory Neurons in the Mouse." *Neuron* 61, no. 2 (Jan 29 2009): 220-33. http://dx.doi.org/10.1016/j.neuron.2008.11.010.

Bradke, F., J. W. Fawcett, and M. E. Spira. "Assembly of a New Growth Cone after Axotomy: The Precursor to Axon Regeneration." *Nat Rev Neurosci* 13, no. 3 (Feb 15 2012): 183-93. http://dx.doi.org/10.1038/nrn3176.

Breunig, J. J., J. I. Arellano, J. D. Macklis, and P. Rakic. "Everything That Glitters Isn't Gold: A Critical Review of Postnatal Neural Precursor Analyses." *Cell Stem Cell* 1, no. 6 (Dec 13 2007): 612-27. http://dx.doi.org/10.1016/j.stem.2007.11.008.

Breunig, J. J., J. Silbereis, F. M. Vaccarino, N. Sestan, and P. Rakic. "Notch Regulates Cell Fate and Dendrite Morphology of Newborn Neurons in the Postnatal Dentate Gyrus." *Proc Natl Acad Sci U S A* 104, no. 51 (Dec 18 2007): 20558-63. http://dx.doi.org/10.1073/pnas.0710156104.

Brill, M. S., J. Ninkovic, E. Winpenny, R. D. Hodge, I. Ozen, R. Yang, A. Lepier, S. Gascon, F. Erdelyi, G. Szabo, C. Parras, F. Guillemot, M. Frotscher, B. Berninger, R. F. Hevner, O. Raineteau, and M. Gotz. "Adult Generation of Glutamatergic Olfactory Bulb Interneurons." *Nat Neurosci* 12, no. 12 (Dec 2009): 1524-33. http://dx.doi.org/10.1038/nn.2416.

Brilli, E., E. Reitano, L. Conti, P. Conforti, R. Gulino, G. G. Consalez, E. Cesana, A. Smith, F. Rossi, and E. Cattaneo. "Neural Stem Cells Engrafted in the Adult Brain Fuse with Endogenous Neurons." *Stem Cells Dev* 22, no. 4 (Feb 15 2013): 538-47. http://dx.doi.org/10.1089/scd.2012.0530.

Brown, S. P., S. D. Brenowitz, and W. G. Regehr. "Brief Presynaptic Bursts Evoke Synapse-Specific Retrograde Inhibition Mediated by Endogenous Cannabinoids." *Nat Neurosci* 6, no. 10 (Oct 2003): 1048-57. http://dx.doi.org/10.1038/nn1126.

Brown, S. P. and S. Hestrin. "Intracortical Circuits of Pyramidal Neurons Reflect Their Long-Range Axonal Targets." *Nature* 457, no. 7233 (Feb 26 2009): 1133-6. http://dx.doi.org/10.1038/nature07658.

Brundin, P., O. G. Nilsson, R. E. Strecker, O. Lindvall, B. Astedt, and A. Bjorklund. "Behavioural Effects of Human Fetal Dopamine Neurons Grafted in a Rat Model of Parkinson's Disease." *Exp Brain Res* 65, no. 1 (1986): 235-40. https://www.ncbi.nlm.nih.gov/pubmed/3542544.

Buck, L. and R. Axel. "A Novel Multigene Family May Encode Odorant Receptors: A Molecular Basis for Odor Recognition." *Cell* 65, no. 1 (Apr 05 1991): 175-87. https://www.ncbi.nlm.nih.gov/pubmed/1840504.

Buffo, A., I. Rite, P. Tripathi, A. Lepier, D. Colak, A. P. Horn, T. Mori, and M. Gotz. "Origin and Progeny of Reactive Gliosis: A Source of Multipotent Cells in the Injured Brain." *Proc Natl Acad Sci U S A* 105, no. 9 (Mar 04 2008): 3581-6. http://dx.doi.org/10.1073/pnas.0709002105.

Buffo, A., M. R. Vosko, D. Erturk, G. F. Hamann, M. Jucker, D. Rowitch, and M. Gotz. "Expression Pattern of the Transcription Factor Olig2 in Response to Brain Injuries: Implications for Neuronal Repair." *Proc Natl Acad Sci U S A* 102, no. 50 (Dec 13 2005): 18183-8. http://dx.doi.org/10.1073/pnas.0506535102.

Bullock, Ross and Narendra Nathoo. "Injury and Cell Function." In *Head Injury : Pathophysiology & Management*

, edited by Peter L. Reilly and Ross Bullock, 512 p. London: Hodder Arnold, 2005.

Burns, T. C., X. R. Ortiz-Gonzalez, M. Gutierrez-Perez, C. D. Keene, R. Sharda, Z. L. Demorest, Y. Jiang, M. Nelson-Holte, M. Soriano, Y. Nakagawa, M. R. Luquin, J. M. Garcia-Verdugo, F. Prosper, W. C. Low, and C. M. Verfaillie. "Thymidine Analogs Are Transferred from Prelabeled Donor to Host Cells in the Central Nervous System after Transplantation: A Word of Caution." *Stem Cells* 24, no. 4 (Apr 2006): 1121-7. http://dx.doi.org/10.1634/stemcells.2005-0463.

Busch, S. A., K. P. Horn, F. X. Cuascut, A. L. Hawthorne, L. Bai, R. H. Miller, and J. Silver. "Adult Ng2+ Cells Are Permissive to Neurite Outgrowth and Stabilize Sensory Axons During Macrophage-Induced Axonal Dieback after Spinal Cord Injury." *J Neurosci* 30, no. 1 (Jan 06 2010): 255-65. http://dx.doi.org/10.1523/JNEUROSCI.3705-09.2010.

Cahoy, J. D., B. Emery, A. Kaushal, L. C. Foo, J. L. Zamanian, K. S. Christopherson, Y. Xing, J. L. Lubischer, P. A. Krieg, S. A. Krupenko, W. J. Thompson, and B. A. Barres. "A Transcriptome Database for Astrocytes, Neurons, and Oligodendrocytes: A New Resource for Understanding Brain Development and Function." *J Neurosci* 28, no. 1 (Jan 02 2008): 264-78. http://dx.doi.org/10.1523/JNEUROSCI.4178-07.2008.

Cai, J., Y. Wu, T. Mirua, J. L. Pierce, M. T. Lucero, K. H. Albertine, G. J. Spangrude, and M. S. Rao. "Properties of a Fetal Multipotent Neural Stem Cell (Nep Cell)." *Dev Biol* 251, no. 2 (Nov 15 2002): 221-40. https://www.ncbi.nlm.nih.gov/pubmed/12435354.

Cajal, Santiago Ramon y; DeFelipe, Javier; Jones, Edward G.; May, R. M. *Cajal's Degeneration and Regeneration of the Nervous System*. History of Neuroscience. New York: Oxford University Press, 1991.

Calvo, C. F., R. H. Fontaine, J. Soueid, T. Tammela, T. Makinen, C. Alfaro-Cervello, F. Bonnaud, A. Miguez, L. Benhaim, Y. Xu, M. J. Barallobre, I. Moutkine, J. Lyytikka, T. Tatlisumak, B. Pytowski, B. Zalc, W. Richardson, N. Kessaris, J. M. Garcia-Verdugo, K. Alitalo, A. Eichmann, and J. L. Thomas. "Vascular Endothelial Growth Factor Receptor 3 Directly Regulates Murine Neurogenesis." *Genes Dev* 25, no. 8 (Apr 15 2011): 831-44. http://dx.doi.org/10.1101/gad.615311.

Canty, A. J., L. Huang, J. S. Jackson, G. E. Little, G. Knott, B. Maco, and V. De Paola. "In-Vivo Single Neuron Axotomy Triggers Axon Regeneration to Restore Synaptic Density in Specific Cortical Circuits." *Nat Commun* 4 (2013): 2038. http://dx.doi.org/10.1038/ncomms3038.

Carleton, A., L. T. Petreanu, R. Lansford, A. Alvarez-Buylla, and P. M. Lledo. "Becoming a New Neuron in the Adult Olfactory Bulb." *Nat Neurosci* 6, no. 5 (May 2003): 507-18. http://dx.doi.org/10.1038/nn1048.

Casciola-Rosen, L. A., G. Anhalt, and A. Rosen. "Autoantigens Targeted in Systemic Lupus Erythematosus Are Clustered in Two Populations of Surface Structures on Apoptotic Keratinocytes." *J Exp Med* 179, no. 4 (Apr 01 1994): 1317-30. https://www.ncbi.nlm.nih.gov/pubmed/7511686.

Cetin, A., S. Komai, M. Eliava, P. H. Seeburg, and P. Osten. "Stereotaxic Gene Delivery in the Rodent Brain." *Nat Protoc* 1, no. 6 (2006): 3166-73. http://dx.doi.org/10.1038/nprot.2006.450.

Chapman, B., K. R. Zahs, and M. P. Stryker. "Relation of Cortical Cell Orientation Selectivity to Alignment of Receptive Fields of the Geniculocortical Afferents That Arborize within a Single Orientation Column in Ferret Visual Cortex." *J Neurosci* 11, no. 5 (May 1991): 1347-58. https://www.ncbi.nlm.nih.gov/pubmed/2027051.

Charbonneau, V., M. E. Laramee, V. Boucher, G. Bronchti, and D. Boire. "Cortical and Subcortical Projections to Primary Visual Cortex in Anophthalmic, Enucleated and Sighted Mice." *Eur J Neurosci* 36, no. 7 (Oct 2012): 2949-63. http://dx.doi.org/10.1111/j.1460-9568.2012.08215.x.

Chen, J., S. S. Magavi, and J. D. Macklis. "Neurogenesis of Corticospinal Motor Neurons Extending Spinal Projections in Adult Mice." *Proc Natl Acad Sci U S A* 101, no. 46 (Nov 16 2004): 16357-62. http://dx.doi.org/10.1073/pnas.0406795101.

Chen, T. W., T. J. Wardill, Y. Sun, S. R. Pulver, S. L. Renninger, A. Baohan, E. R. Schreiter, R. A. Kerr, M. B. Orger, V. Jayaraman, L. L. Looger, K. Svoboda, and D. S. Kim. "Ultrasensitive Fluorescent Proteins for Imaging Neuronal Activity." *Nature* 499, no. 7458 (Jul 18 2013): 295-300. http://dx.doi.org/10.1038/nature12354.

Chen, Y., D. K. Miles, T. Hoang, J. Shi, E. Hurlock, S. G. Kernie, and Q. R. Lu. "The Basic Helix-Loop-Helix Transcription Factor Olig2 Is Critical for Reactive Astrocyte Proliferation after Cortical Injury." *J Neurosci* 28, no. 43 (Oct 22 2008): 10983-9. http://dx.doi.org/10.1523/JNEUROSCI.3545-08.2008.

Chenn, A., Y. A. Zhang, B. T. Chang, and S. K. McConnell. "Intrinsic Polarity of Mammalian Neuroepithelial Cells." *Mol Cell Neurosci* 11, no. 4 (Jul 1998): 183-93. http://dx.doi.org/10.1006/mcne.1998.0680.

Cherubini, E., J. L. Gaiarsa, and Y. Ben-Ari. "Gaba: An Excitatory Transmitter in Early Postnatal Life." *Trends Neurosci* 14, no. 12 (Dec 1991): 515-9. https://www.ncbi.nlm.nih.gov/pubmed/1726341.

Chiba, S., Y. Iwasaki, H. Sekino, and N. Suzuki. "Transplantation of Motoneuron-Enriched Neural Cells Derived from Mouse Embryonic Stem Cells Improves Motor Function of Hemiplegic Mice." *Cell Transplant* 12, no. 5 (2003): 457-68. https://www.ncbi.nlm.nih.gov/pubmed/12953919.

Chirumamilla, S., D. Sun, M. R. Bullock, and R. J. Colello. "Traumatic Brain Injury Induced Cell Proliferation in the Adult Mammalian Central Nervous System." *J Neurotrauma* 19, no. 6 (Jun 2002): 693-703. http://dx.doi.org/10.1089/08977150260139084.

Cho, J. H., J. E. Prince, and J. F. Cloutier. "Axon Guidance Events in the Wiring of the Mammalian Olfactory System." *Mol Neurobiol* 39, no. 1 (Feb 2009): 1-9. http://dx.doi.org/10.1007/s12035-008-8047-7.

Christie, K. J., A. Turbic, and A. M. Turnley. "Adult Hippocampal Neurogenesis, Rho Kinase Inhibition and Enhancement of Neuronal Survival." *Neuroscience* 247 (Sep 05 2013): 75-83. http://dx.doi.org/10.1016/j.neuroscience.2013.05.019.

Clarke, P. G. "Developmental Cell Death: Morphological Diversity and Multiple Mechanisms." *Anat Embryol (Berl)* 181, no. 3 (1990): 195-213. https://www.ncbi.nlm.nih.gov/pubmed/2186664.

Cocco, R. E. and D. S. Ucker. "Distinct Modes of Macrophage Recognition for Apoptotic and Necrotic Cells Are Not Specified Exclusively by Phosphatidylserine Exposure." *Mol Biol Cell* 12, no. 4 (Apr 2001): 919-30. https://www.ncbi.nlm.nih.gov/pubmed/11294896.

Cohen-Cory, S., A. H. Kidane, N. J. Shirkey, and S. Marshak. "Brain-Derived Neurotrophic Factor and the Development of Structural Neuronal Connectivity." *Dev Neurobiol* 70, no. 5 (Apr 2010): 271-88. http://dx.doi.org/10.1002/dneu.20774.

Coleman, P. D. and A. H. Riesen. "Evironmental Effects on Cortical Dendritic Fields. I. Rearing in the Dark." *J Anat* 102, no. Pt 3 (Mar 1968): 363-74. https://www.ncbi.nlm.nih.gov/pubmed/5656134.

Colonnier, M. "Synaptic Patterns on Different Cell Types in the Different Laminae of the Cat Visual Cortex. An Electron Microscope Study." *Brain Res* 9, no. 2 (Jul 1968): 268-87. https://www.ncbi.nlm.nih.gov/pubmed/4175993.

Connell, P., C. A. Ballinger, J. Jiang, Y. Wu, L. J. Thompson, J. Hohfeld, and C. Patterson. "The Co-Chaperone Chip Regulates Protein Triage Decisions Mediated by Heat-Shock Proteins." *Nat Cell Biol* 3, no. 1 (Jan 2001): 93-6. http://dx.doi.org/10.1038/35050618.

Constantinople, C. M. and R. M. Bruno. "Deep Cortical Layers Are Activated Directly by Thalamus." *Science* 340, no. 6140 (Jun 28 2013): 1591-4. http://dx.doi.org/10.1126/science.1236425.

Cooper-Kuhn, C. M. and H. G. Kuhn. "Is It All DNA Repair? Methodological Considerations for Detecting Neurogenesis in the Adult Brain." *Brain Res Dev Brain Res* 134, no. 1-2 (Mar 31 2002): 13-21. https://www.ncbi.nlm.nih.gov/pubmed/11947933.

Cooper-Kuhn, C. M., J. Winkler, and H. G. Kuhn. "Decreased Neurogenesis after Cholinergic Forebrain Lesion in the Adult Rat." *J Neurosci Res* 77, no. 2 (Jul 15 2004): 155-65. http://dx.doi.org/10.1002/jnr.20116.

Cossell, L., M. F. Iacaruso, D. R. Muir, R. Houlton, E. N. Sader, H. Ko, S. B. Hofer, and T. D. Mrsic-Flogel. "Functional Organization of Excitatory Synaptic Strength in Primary Visual Cortex." *Nature* 518, no. 7539 (Feb 19 2015): 399-403. http://dx.doi.org/10.1038/nature14182.

Cotman, C. W., D. A. Matthews, D. Taylor, and G. Lynch. "Synaptic Rearrangement in the Dentate Gyrus: Histochemical Evidence of Adjustments after Lesions in Immature and Adult Rats." *Proc Natl Acad Sci U S A* 70, no. 12 (Dec 1973): 3473-7. https://www.ncbi.nlm.nih.gov/pubmed/4519639.

Couillard-Despres, S., B. Winner, S. Schaubeck, R. Aigner, M. Vroemen, N. Weidner, U. Bogdahn, J. Winkler, H. G. Kuhn, and L. Aigner. "Doublecortin Expression Levels in Adult Brain Reflect Neurogenesis." *Eur J Neurosci* 21, no. 1 (Jan 2005): 1-14. http://dx.doi.org/10.1111/j.1460-9568.2004.03813.x.

Cragg, B. "Preservation of Extracellular Space During Fixation of the Brain for Electron Microscopy." *Tissue Cell* 12, no. 1 (1980): 63-72. https://www.ncbi.nlm.nih.gov/pubmed/6987773.

Craig, C. G., V. Tropepe, C. M. Morshead, B. A. Reynolds, S. Weiss, and D. van der Kooy. "In Vivo Growth Factor Expansion of Endogenous Subependymal Neural Precursor Cell Populations in the Adult Mouse Brain." *J Neurosci* 16, no. 8 (Apr 15 1996): 2649-58. https://www.ncbi.nlm.nih.gov/pubmed/8786441.

Cruz-Martin, A., M. Crespo, and C. Portera-Cailliau. "Delayed Stabilization of Dendritic Spines in Fragile X Mice." *J Neurosci* 30, no. 23 (Jun 09 2010): 7793-803. http://dx.doi.org/10.1523/JNEUROSCI.0577-10.2010.

Cruz-Martin, A., R. N. El-Danaf, F. Osakada, B. Sriram, O. S. Dhande, P. L. Nguyen, E. M. Callaway, A. Ghosh, and A. D. Huberman. "A Dedicated Circuit Links Direction-Selective Retinal Ganglion Cells to the Primary Visual Cortex." *Nature* 507, no. 7492 (Mar 20 2014): 358-61. http://dx.doi.org/10.1038/nature12989.

Cubelos, B., A. Sebastian-Serrano, L. Beccari, M. E. Calcagnotto, E. Cisneros, S. Kim, A. Dopazo, M. Alvarez-Dolado, J. M. Redondo, P. Bovolenta, C. A. Walsh, and M. Nieto. "Cux1 and Cux2 Regulate Dendritic Branching, Spine Morphology, and Synapses of the Upper Layer Neurons of the Cortex." *Neuron* 66, no. 4 (May 27 2010): 523-35. http://dx.doi.org/10.1016/j.neuron.2010.04.038.

Cunningham, M., J. H. Cho, A. Leung, G. Savvidis, S. Ahn, M. Moon, P. K. Lee, J. J. Han, N. Azimi, K. S. Kim, V. Y. Bolshakov, and S. Chung. "Hpsc-Derived Maturing Gabaergic Interneurons Ameliorate Seizures and Abnormal Behavior in Epileptic Mice." *Cell Stem Cell* 15, no. 5 (Nov 06 2014): 559-73. http://dx.doi.org/10.1016/j.stem.2014.10.006.

Curtis, M. A., P. S. Eriksson, and R. L. Faull. "Progenitor Cells and Adult Neurogenesis in Neurodegenerative Diseases and Injuries of the Basal Ganglia." *Clin Exp Pharmacol Physiol* 34, no. 5-6 (May-Jun 2007): 528-32. http://dx.doi.org/10.1111/j.1440-1681.2007.04609.x.

Cusick, C. G. and R. D. Lund. "The Distribution of the Callosal Projection to the Occipital Visual Cortex in Rats and Mice." *Brain Res* 214, no. 2 (Jun 15 1981): 239-59. https://www.ncbi.nlm.nih.gov/pubmed/7237170.

Custo Greig, L. F., M. B. Woodworth, M. J. Galazo, H. Padmanabhan, and J. D. Macklis. "Molecular Logic of Neocortical Projection Neuron Specification, Development and Diversity." *Nat Rev Neurosci* 14, no. 11 (Nov 2013): 755-69. http://dx.doi.org/10.1038/nrn3586.

Czupryn, A., Y. D. Zhou, X. Chen, D. McNay, M. P. Anderson, J. S. Flier, and J. D. Macklis. "Transplanted Hypothalamic Neurons Restore Leptin Signaling and Ameliorate Obesity in Db/Db Mice." *Science* 334, no. 6059 (Nov 25 2011): 1133-7. http://dx.doi.org/10.1126/science.1209870.

Dahl, J. U., M. J. Gray, and U. Jakob. "Protein Quality Control under Oxidative Stress Conditions." *J Mol Biol* 427, no. 7 (Apr 10 2015): 1549-63. http://dx.doi.org/10.1016/j.jmb.2015.02.014.

Dailey, M. E. and S. J. Smith. "The Dynamics of Dendritic Structure in Developing Hippocampal Slices." *J Neurosci* 16, no. 9 (May 01 1996): 2983-94. https://www.ncbi.nlm.nih.gov/pubmed/8622128.

Dantzker, J. L. and E. M. Callaway. "Laminar Sources of Synaptic Input to Cortical Inhibitory Interneurons and Pyramidal Neurons." *Nat Neurosci* 3, no. 7 (Jul 2000): 701-7. http://dx.doi.org/10.1038/76656.

Dash, P. K., S. A. Mach, and A. N. Moore. "Enhanced Neurogenesis in the Rodent Hippocampus Following Traumatic Brain Injury." *J Neurosci Res* 63, no. 4 (Feb 15 2001): 313-9. http://dx.doi.org/10.1002/1097-4547(20010215)63:4<313::AID-JNR1025>3.0.CO;2-4.

Davalos, D., J. Grutzendler, G. Yang, J. V. Kim, Y. Zuo, S. Jung, D. R. Littman, M. L. Dustin, and W. B. Gan. "Atp Mediates Rapid Microglial Response to Local Brain Injury in Vivo." *Nat Neurosci* 8, no. 6 (Jun 2005): 752-8. http://dx.doi.org/10.1038/nn1472.

Davis, M. F., D. X. Figueroa Velez, R. P. Guevarra, M. C. Yang, M. Habeeb, M. C. Carathedathu, and S. P. Gandhi. "Inhibitory Neuron Transplantation into Adult Visual Cortex Creates a New Critical Period That Rescues Impaired Vision." *Neuron* 86, no. 4 (May 20 2015): 1055-66. http://dx.doi.org/10.1016/j.neuron.2015.03.062.

De Filippis, L. and E. Binda. "Concise Review: Self-Renewal in the Central Nervous System: Neural Stem Cells from Embryo to Adult." *Stem Cells Transl Med* 1, no. 4 (Apr 2012): 298-308. http://dx.doi.org/10.5966/sctm.2011-0045.

De la Rossa, A., C. Bellone, B. Golding, I. Vitali, J. Moss, N. Toni, C. Luscher, and D. Jabaudon. "In Vivo Reprogramming of Circuit Connectivity in Postmitotic Neocortical Neurons." *Nat Neurosci* 16, no. 2 (Feb 2013): 193-200. http://dx.doi.org/10.1038/nn.3299.

De Paola, V., A. Holtmaat, G. Knott, S. Song, L. Wilbrecht, P. Caroni, and K. Svoboda. "Cell Type-Specific Structural Plasticity of Axonal Branches and Boutons in the Adult Neocortex." *Neuron* 49, no. 6 (Mar 16 2006): 861-75. http://dx.doi.org/10.1016/j.neuron.2006.02.017.

Dehmel, S. and S. Lowel. "Cortico-Cortical Interactions Influence Binocularity of the Primary Visual Cortex of Adult Mice." *PLoS One* 9, no. 8 (2014): e105745. http://dx.doi.org/10.1371/journal.pone.0105745.

Deisseroth, K., H. Bito, and R. W. Tsien. "Signaling from Synapse to Nucleus: Postsynaptic Creb Phosphorylation During Multiple Forms of Hippocampal Synaptic Plasticity." *Neuron* 16, no. 1 (Jan 1996): 89-101. https://www.ncbi.nlm.nih.gov/pubmed/8562094.

Deisseroth, K., P. G. Mermelstein, H. Xia, and R. W. Tsien. "Signaling from Synapse to Nucleus: The Logic Behind the Mechanisms." *Curr Opin Neurobiol* 13, no. 3 (Jun 2003): 354-65. https://www.ncbi.nlm.nih.gov/pubmed/12850221.

del Rio, J. A. and E. Soriano. "Immunocytochemical Detection of 5'-Bromodeoxyuridine Incorporation in the Central Nervous System of the Mouse." *Brain Res Dev Brain Res* 49, no. 2 (Oct 01 1989): 311-7. https://www.ncbi.nlm.nih.gov/pubmed/2805336.

Delcroix, J. D., J. S. Valletta, C. Wu, S. J. Hunt, A. S. Kowal, and W. C. Mobley. "Ngf Signaling in Sensory Neurons: Evidence That Early Endosomes Carry Ngf Retrograde Signals." *Neuron* 39, no. 1 (Jul 03 2003): 69-84. https://www.ncbi.nlm.nih.gov/pubmed/12848933.

Denes, A., P. Thornton, N. J. Rothwell, and S. M. Allan. "Inflammation and Brain Injury: Acute Cerebral Ischaemia, Peripheral and Central Inflammation." *Brain Behav Immun* 24, no. 5 (Jul 2010): 708-23. http://dx.doi.org/10.1016/j.bbi.2009.09.010.

Denk, W., J. H. Strickler, and W. W. Webb. "Two-Photon Laser Scanning Fluorescence Microscopy." *Science* 248, no. 4951 (Apr 06 1990): 73-6. https://www.ncbi.nlm.nih.gov/pubmed/2321027.

Deshpande, A., M. Bergami, A. Ghanem, K. K. Conzelmann, A. Lepier, M. Gotz, and B. Berninger. "Retrograde Monosynaptic Tracing Reveals the Temporal Evolution of Inputs onto New Neurons in the Adult Dentate Gyrus and Olfactory Bulb." *Proc Natl Acad Sci U S A* 110, no. 12 (Mar 19 2013): E1152-61. http://dx.doi.org/10.1073/pnas.1218991110.

Devitt, A., K. G. Parker, C. A. Ogden, C. Oldreive, M. F. Clay, L. A. Melville, C. O. Bellamy, A. Lacy-Hulbert, S. C. Gangloff, S. M. Goyert, and C. D. Gregory. "Persistence of Apoptotic Cells without Autoimmune Disease or Inflammation in Cd14-/- Mice." *J Cell Biol* 167, no. 6 (Dec 20 2004): 1161-70. http://dx.doi.org/10.1083/jcb.200410057.

Dexheimer, Thomas S. "DNA Repair Pathways and Mechanisms." In *DNA Repair of Cancer Stem Cells*, edited by Lesley A. Mathews, Stephanie M. Cabarcas, and Elaine M. Hurt, 19-32. Dordrecht: Springer Netherlands, 2013.

Diao, Y. C., Y. K. Wang, and M. L. Pu. "Binocular Responses of Cortical Cells and the Callosal Projection in the Albino Rat." *Exp Brain Res* 49, no. 3 (1983): 410-8. https://www.ncbi.nlm.nih.gov/pubmed/6641838.

Diaz, F., N. McKeehan, W. Kang, and J. M. Hebert. "Apoptosis of Glutamatergic Neurons Fails to Trigger a Neurogenic Response in the Adult Neocortex." *J Neurosci* 33, no. 15 (Apr 10 2013): 6278-84. http://dx.doi.org/10.1523/JNEUROSCI.5885-12.2013.

Doeppner, T. R., E. Bretschneider, M. Doehring, I. Segura, A. Senturk, A. Acker-Palmer, M. R. Hasan, A. ElAli, D. M. Hermann, and M. Bahr. "Enhancement of Endogenous Neurogenesis in Ephrin-B3 Deficient Mice after Transient Focal Cerebral Ischemia." *Acta Neuropathol* 122, no. 4 (Oct 2011): 429-42. http://dx.doi.org/10.1007/s00401-011-0856-5.

Doetsch, F., I. Caille, D. A. Lim, J. M. Garcia-Verdugo, and A. Alvarez-Buylla. "Subventricular Zone Astrocytes Are Neural Stem Cells in the Adult Mammalian Brain." *Cell* 97, no. 6 (Jun 11 1999): 703-16. https://www.ncbi.nlm.nih.gov/pubmed/10380923.

Doetsch, F., J. M. Garcia-Verdugo, and A. Alvarez-Buylla. "Cellular Composition and Three-Dimensional Organization of the Subventricular Germinal Zone in the Adult Mammalian Brain." *J Neurosci* 17, no. 13 (Jul 01 1997): 5046-61. https://www.ncbi.nlm.nih.gov/pubmed/9185542.

Doller, H. J. and F. F. Weight. "Perforant Pathway Activation of Hippocampal Ca1 Stratum Pyramidale Neurons: Electrophysiological Evidence for a Direct Pathway." *Brain Res* 237, no. 1 (Apr 08 1982): 1-13. https://www.ncbi.nlm.nih.gov/pubmed/7074352.

Dou, C. L. and J. M. Levine. "Inhibition of Neurite Growth by the Ng2 Chondroitin Sulfate Proteoglycan." *J Neurosci* 14, no. 12 (Dec 1994): 7616-28. https://www.ncbi.nlm.nih.gov/pubmed/7996200.

Drager, U. C. "Receptive Fields of Single Cells and Topography in Mouse Visual Cortex." *J Comp Neurol* 160, no. 3 (Apr 01 1975): 269-90. http://dx.doi.org/10.1002/cne.901600302.

Drager, U. C. "Observations on Monocular Deprivation in Mice." *J Neurophysiol* 41, no. 1 (Jan 1978): 28-42. https://www.ncbi.nlm.nih.gov/pubmed/621544.

Du, J., L. Feng, E. Zaitsev, H. S. Je, X. W. Liu, and B. Lu. "Regulation of Trkb Receptor Tyrosine Kinase and Its Internalization by Neuronal Activity and Ca2+ Influx." *J Cell Biol* 163, no. 2 (Oct 27 2003): 385-95. http://dx.doi.org/10.1083/jcb.200305134.

Du, J. L. and M. M. Poo. "Rapid Bdnf-Induced Retrograde Synaptic Modification in a Developing Retinotectal System." *Nature* 429, no. 6994 (Jun 24 2004): 878-83. http://dx.doi.org/10.1038/nature02618.

Dunn, F. A. and R. O. Wong. "Wiring Patterns in the Mouse Retina: Collecting Evidence across the Connectome, Physiology and Light Microscopy." *J Physiol* 592, no. 22 (Nov 15 2014): 4809-23. http://dx.doi.org/10.1113/jphysiol.2014.277228.

Dupouey, P., S. Benjelloun, and D. Gomes. "Immunohistochemical Demonstration of an Organized Cytoarchitecture of the Radial Glia in the Cns of the Embryonic Mouse." *Dev Neurosci* 7, no. 2 (1985): 81-93. https://www.ncbi.nlm.nih.gov/pubmed/3905339.

Duque, A. and P. Rakic. "Different Effects of Bromodeoxyuridine and [3h]Thymidine Incorporation into DNA on Cell Proliferation, Position, and Fate." *J Neurosci* 31, no. 42 (Oct 19 2011): 15205-17. http://dx.doi.org/10.1523/JNEUROSCI.3092-11.2011.

Ellezam, B., I. Selles-Navarro, C. Manitt, T. E. Kennedy, and L. McKerracher. "Expression of Netrin-1 and Its Receptors Dcc and Unc-5h2 after Axotomy and During Regeneration of Adult Rat Retinal Ganglion Cells." *Exp Neurol* 168, no. 1 (Mar 2001): 105-15. http://dx.doi.org/10.1006/exnr.2000.7589.

Elston, G. N. "Cortex, Cognition and the Cell: New Insights into the Pyramidal Neuron and Prefrontal Function." *Cereb Cortex* 13, no. 11 (Nov 2003): 1124-38. https://www.ncbi.nlm.nih.gov/pubmed/14576205.

Elston, G. N. and I. Fujita. "Pyramidal Cell Development: Postnatal Spinogenesis, Dendritic Growth, Axon Growth, and Electrophysiology." *Front Neuroanat* 8 (2014): 78. http://dx.doi.org/10.3389/fnana.2014.00078.

Emsley, J. G., B. D. Mitchell, G. Kempermann, and J. D. Macklis. "Adult Neurogenesis and Repair of the Adult Cns with Neural Progenitors, Precursors, and Stem Cells." *Prog Neurobiol* 75, no. 5 (Apr 2005): 321-41. http://dx.doi.org/10.1016/j.pneurobio.2005.04.002.

Eriksson, P. S., E. Perfilieva, T. Bjork-Eriksson, A. M. Alborn, C. Nordborg, D. A. Peterson, and F. H. Gage. "Neurogenesis in the Adult Human Hippocampus." *Nat Med* 4, no. 11 (Nov 1998): 1313-7. http://dx.doi.org/10.1038/3305.

Ernst, A., K. Alkass, S. Bernard, M. Salehpour, S. Perl, J. Tisdale, G. Possnert, H. Druid, and J. Frisen. "Neurogenesis in the Striatum of the Adult Human Brain." *Cell* 156, no. 5 (Feb 27 2014): 1072-83. http://dx.doi.org/10.1016/j.cell.2014.01.044.

Ernst, M., E. E. Nelson, E. B. McClure, C. S. Monk, S. Munson, N. Eshel, E. Zarahn, E. Leibenluft, A. Zametkin, K. Towbin, J. Blair, D. Charney, and D. S. Pine. "Choice Selection and Reward Anticipation: An Fmri Study." *Neuropsychologia* 42, no. 12 (2004): 1585-97. http://dx.doi.org/10.1016/j.neuropsychologia.2004.05.011.

Espinosa, J. S. and M. P. Stryker. "Development and Plasticity of the Primary Visual Cortex." *Neuron* 75, no. 2 (Jul 26 2012): 230-49. http://dx.doi.org/10.1016/j.neuron.2012.06.009.

Espuny-Camacho, I., K. A. Michelsen, D. Gall, D. Linaro, A. Hasche, J. Bonnefont, C. Bali, D. Orduz, A. Bilheu, A. Herpoel, N. Lambert, N. Gaspard, S. Peron, S. N. Schiffmann, M. Giugliano, A. Gaillard, and P. Vanderhaeghen. "Pyramidal Neurons Derived from Human Pluripotent Stem Cells Integrate Efficiently into Mouse Brain Circuits in Vivo." *Neuron* 77, no. 3 (Feb 06 2013): 440-56. http://dx.doi.org/10.1016/j.neuron.2012.12.011.

Faiz, M., N. Sachewsky, S. Gascon, K. W. Bang, C. M. Morshead, and A. Nagy. "Adult Neural Stem Cells from the Subventricular Zone Give Rise to Reactive Astrocytes in the Cortex after Stroke." *Cell Stem Cell* 17, no. 5 (Nov 05 2015): 624-34. http://dx.doi.org/10.1016/j.stem.2015.08.002.

Falkner, S., S. Grade, L. Dimou, K. K. Conzelmann, T. Bonhoeffer, M. Gotz, and M. Hubener. "Transplanted Embryonic Neurons Integrate into Adult Neocortical Circuits." *Nature* 539, no. 7628 (Nov 10 2016): 248-53. http://dx.doi.org/10.1038/nature20113.

Fame, R. M., J. L. MacDonald, and J. D. Macklis. "Development, Specification, and Diversity of Callosal Projection Neurons." *Trends Neurosci* 34, no. 1 (Jan 2011): 41-50. http://dx.doi.org/10.1016/j.tins.2010.10.002.

Farrar, M. J., I. M. Bernstein, D. H. Schlafer, T. A. Cleland, J. R. Fetcho, and C. B. Schaffer. "Chronic in Vivo Imaging in the Mouse Spinal Cord Using an Implanted Chamber." *Nat Methods* 9, no. 3 (Jan 22 2012): 297-302. http://dx.doi.org/10.1038/nmeth.1856.

Feil, R., J. Brocard, B. Mascrez, M. LeMeur, D. Metzger, and P. Chambon. "Ligand-Activated Site-Specific Recombination in Mice." *Proc Natl Acad Sci U S A* 93, no. 20 (Oct 01 1996): 10887-90. https://www.ncbi.nlm.nih.gov/pubmed/8855277.

Feil, R., J. Wagner, D. Metzger, and P. Chambon. "Regulation of Cre Recombinase Activity by Mutated Estrogen Receptor Ligand-Binding Domains." *Biochem Biophys Res Commun* 237, no. 3 (Aug 28 1997): 752-7. http://dx.doi.org/10.1006/bbrc.1997.7124.

Feng, G., R. H. Mellor, M. Bernstein, C. Keller-Peck, Q. T. Nguyen, M. Wallace, J. M. Nerbonne, J. W. Lichtman, and J. R. Sanes. "Imaging Neuronal Subsets in Transgenic Mice Expressing Multiple Spectral Variants of Gfp." *Neuron* 28, no. 1 (Oct 2000): 41-51. https://www.ncbi.nlm.nih.gov/pubmed/11086982.

Ferster, D., S. Chung, and H. Wheat. "Orientation Selectivity of Thalamic Input to Simple Cells of Cat Visual Cortex." *Nature* 380, no. 6571 (Mar 21 1996): 249-52. http://dx.doi.org/10.1038/380249a0.

Fiala, J. C., M. Feinberg, V. Popov, and K. M. Harris. "Synaptogenesis Via Dendritic Filopodia in Developing Hippocampal Area Ca1." *J Neurosci* 18, no. 21 (Nov 01 1998): 8900-11. https://www.ncbi.nlm.nih.gov/pubmed/9786995.

Filous, A. R., A. Tran, C. J. Howell, S. A. Busch, T. A. Evans, W. B. Stallcup, S. H. Kang, D. E. Bergles, S. I. Lee, J. M. Levine, and J. Silver. "Entrapment Via Synaptic-Like Connections between Ng2 Proteoglycan+ Cells and Dystrophic Axons in the Lesion Plays a Role in Regeneration Failure after Spinal Cord Injury." *J Neurosci* 34, no. 49 (Dec 03 2014): 16369-84. http://dx.doi.org/10.1523/JNEUROSCI.1309-14.2014.

Fishel, M. L., M. R. Vasko, and M. R. Kelley. "DNA Repair in Neurons: So If They Don't Divide What's to Repair?" *Mutat Res* 614, no. 1-2 (Jan 03 2007): 24-36. http://dx.doi.org/10.1016/j.mrfmmm.2006.06.007.

Fitzsimonds, R. M. and M. M. Poo. "Retrograde Signaling in the Development and Modification of Synapses." *Physiol Rev* 78, no. 1 (Jan 1998): 143-70. https://www.ncbi.nlm.nih.gov/pubmed/9457171.

Fitzsimonds, R. M., H. J. Song, and M. M. Poo. "Propagation of Activity-Dependent Synaptic Depression in Simple Neural Networks." *Nature* 388, no. 6641 (Jul 31 1997): 439-48. http://dx.doi.org/10.1038/41267.

Fliss, A. E., S. Benzeno, J. Rao, and A. J. Caplan. "Control of Estrogen Receptor Ligand Binding by Hsp90." *J Steroid Biochem Mol Biol* 72, no. 5 (Apr 2000): 223-30. https://www.ncbi.nlm.nih.gov/pubmed/10822011.

Forrester, J. and A. Peters. "Nerve Fibres in Optic Nerve of Rat." *Nature* 214, no. 5085 (Apr 15 1967): 245-7. https://www.ncbi.nlm.nih.gov/pubmed/4166494.

Frade, J. M. and M. C. Ovejero-Benito. "Neuronal Cell Cycle: The Neuron Itself and Its Circumstances." *Cell Cycle* 14, no. 5 (2015): 712-20. http://dx.doi.org/10.1080/15384101.2015.1004937.

Franklin, R. J., S. A. Bayley, R. Milner, C. Ffrench-Constant, and W. F. Blakemore. "Differentiation of the O-2a Progenitor Cell Line Cg-4 into Oligodendrocytes and Astrocytes Following Transplantation into Glia-Deficient Areas of Cns White Matter." *Glia* 13, no. 1 (Jan 1995): 39-44. http://dx.doi.org/10.1002/glia.440130105.

Fricker-Gates, R. A., J. J. Shin, C. C. Tai, L. A. Catapano, and J. D. Macklis. "Late-Stage Immature Neocortical Neurons Reconstruct Interhemispheric Connections and Form Synaptic Contacts with Increased Efficiency in Adult Mouse Cortex Undergoing Targeted Neurodegeneration." *J Neurosci* 22, no. 10 (May 15 2002): 4045-56. http://dx.doi.org/20026384.

Friedlander, D. R., P. Milev, L. Karthikeyan, R. K. Margolis, R. U. Margolis, and M. Grumet. "The Neuronal Chondroitin Sulfate Proteoglycan Neurocan Binds to the Neural Cell Adhesion Molecules Ng-Cam/L1/Nile and N-Cam, and Inhibits Neuronal Adhesion and Neurite Outgrowth." *J Cell Biol* 125, no. 3 (May 1994): 669-80. https://www.ncbi.nlm.nih.gov/pubmed/7513709.

Frielingsdorf, H., D. R. Simpson, L. J. Thal, and D. P. Pizzo. "Nerve Growth Factor Promotes Survival of New Neurons in the Adult Hippocampus." *Neurobiol Dis* 26, no. 1 (Apr 2007): 47-55. http://dx.doi.org/10.1016/j.nbd.2006.11.015.

Frontczak-Baniewicz, M. and M. Walski. "Glial Scar Instability after Brain Injury." *J Physiol Pharmacol* 57 Suppl 4 (Sep 2006): 97-102. https://www.ncbi.nlm.nih.gov/pubmed/17072035.

Fuchs, E., T. Tumbar, and G. Guasch. "Socializing with the Neighbors: Stem Cells and Their Niche." *Cell* 116, no. 6 (Mar 19 2004): 769-78. https://www.ncbi.nlm.nih.gov/pubmed/15035980.

Fukuda, A., K. Muramatsu, A. Okabe, Y. Shimano, H. Hida, I. Fujimoto, and H. Nishino. "Changes in Intracellular Ca2+ Induced by Gabaa Receptor Activation and Reduction in Cl- Gradient in Neonatal Rat Neocortex." *J Neurophysiol* 79, no. 1 (Jan 1998): 439-46. https://www.ncbi.nlm.nih.gov/pubmed/9425212.

Gaillard, A., L. Prestoz, B. Dumartin, A. Cantereau, F. Morel, M. Roger, and M. Jaber. "Reestablishment of Damaged Adult Motor Pathways by Grafted Embryonic Cortical Neurons." *Nat Neurosci* 10, no. 10 (Oct 2007): 1294-9. http://dx.doi.org/10.1038/nn1970.

Gaillard, F., S. V. Girman, and A. Gaillard. "Afferents to Visually Responsive Grafts of Embryonic Occipital Neocortex Tissue Implanted into V1 (Oc1) Cortical Area of Adult Rats." *Restor Neurol Neurosci* 12, no. 1 (1998): 13-25. https://www.ncbi.nlm.nih.gov/pubmed/12671317.

Ganguly, K., A. F. Schinder, S. T. Wong, and M. Poo. "Gaba Itself Promotes the Developmental Switch of Neuronal Gabaergic Responses from Excitation to Inhibition." *Cell* 105, no. 4 (May 18 2001): 521-32. https://www.ncbi.nlm.nih.gov/pubmed/11371348.

Gao, W. J. and Z. H. Zheng. "Target-Specific Differences in Somatodendritic Morphology of Layer V Pyramidal Neurons in Rat Motor Cortex." *J Comp Neurol* 476, no. 2 (Aug 16 2004): 174-85. http://dx.doi.org/10.1002/cne.20224.

Garrett, M. E., I. Nauhaus, J. H. Marshel, and E. M. Callaway. "Topography and Areal Organization of Mouse Visual Cortex." *J Neurosci* 34, no. 37 (Sep 10 2014): 12587-600. http://dx.doi.org/10.1523/JNEUROSCI.1124-14.2014.

Garthwaite, J. "Concepts of Neural Nitric Oxide-Mediated Transmission." *Eur J Neurosci* 27, no. 11 (Jun 2008): 2783-802. http://dx.doi.org/10.1111/j.1460-9568.2008.06285.x.

Gauvain, G., I. Chamma, Q. Chevy, C. Cabezas, T. Irinopoulou, N. Bodrug, M. Carnaud, S. Levi, and J. C. Poncer. "The Neuronal K-Cl Cotransporter Kcc2 Influences Postsynaptic Ampa Receptor Content and Lateral Diffusion in Dendritic Spines." *Proc Natl Acad Sci U S A* 108, no. 37 (Sep 13 2011): 15474-9. http://dx.doi.org/10.1073/pnas.1107893108.

Gavrieli, Y., Y. Sherman, and S. A. Ben-Sasson. "Identification of Programmed Cell Death in Situ Via Specific Labeling of Nuclear DNA Fragmentation." *J Cell Biol* 119, no. 3 (Nov 1992): 493-501. https://www.ncbi.nlm.nih.gov/pubmed/1400587.

Germroth, P., W. K. Schwerdtfeger, and E. H. Buhl. "Morphology of Identified Entorhinal Neurons Projecting to the Hippocampus. A Light Microscopical Study Combining Retrograde Tracing and Intracellular Injection." *Neuroscience* 30, no. 3 (1989): 683-91. https://www.ncbi.nlm.nih.gov/pubmed/2771045.

Gheusi, G., G. Lepousez, and P. M. Lledo. "Adult-Born Neurons in the Olfactory Bulb: Integration and Functional Consequences." *Curr Top Behav Neurosci* 15 (2013): 49-72. http://dx.doi.org/10.1007/7854_2012_228.

Ghosh, A., J. Carnahan, and M. E. Greenberg. "Requirement for Bdnf in Activity-Dependent Survival of Cortical Neurons." *Science* 263, no. 5153 (Mar 18 1994): 1618-23. https://www.ncbi.nlm.nih.gov/pubmed/7907431.

Gilbert, C. D. and J. P. Kelly. "The Projections of Cells in Different Layers of the Cat's Visual Cortex." *J Comp Neurol* 163, no. 1 (Sep 1975): 81-105. http://dx.doi.org/10.1002/cne.901630106.

Gilbert, C. D. and T. N. Wiesel. "Morphology and Intracortical Projections of Functionally Characterised Neurones in the Cat Visual Cortex." *Nature* 280, no. 5718 (Jul 12 1979): 120-5. https://www.ncbi.nlm.nih.gov/pubmed/552600.

Gilbert, C. D. and T. N. Wiesel. "Clustered Intrinsic Connections in Cat Visual Cortex." *J Neurosci* 3, no. 5 (May 1983): 1116-33. https://www.ncbi.nlm.nih.gov/pubmed/6188819.

Ginty, D. D. and R. A. Segal. "Retrograde Neurotrophin Signaling: Trk-Ing Along the Axon." *Curr Opin Neurobiol* 12, no. 3 (Jun 2002): 268-74. https://www.ncbi.nlm.nih.gov/pubmed/12049932.

Girman, S. V. "Neocortical Grafts Receive Functional Afferents from the Same Neurons of the Thalamus Which Have Innervated the Visual Cortex Replaced by the Graft in Adult Rats." *Neuroscience* 60, no. 4 (Jun 1994): 989-97. https://www.ncbi.nlm.nih.gov/pubmed/7523990.

Giulian, D., D. G. Young, J. Woodward, D. C. Brown, and L. B. Lachman. "Interleukin-1 Is an Astroglial Growth Factor in the Developing Brain." *J Neurosci* 8, no. 2 (Feb 1988): 709-14. https://www.ncbi.nlm.nih.gov/pubmed/3257519.

Glickfeld, L. L., M. H. Histed, and J. H. Maunsell. "Mouse Primary Visual Cortex Is Used to Detect Both Orientation and Contrast Changes." *J Neurosci* 33, no. 50 (Dec 11 2013): 19416-22. http://dx.doi.org/10.1523/JNEUROSCI.3560-13.2013.

Godement, P., J. Salaun, and C. A. Mason. "Retinal Axon Pathfinding in the Optic Chiasm: Divergence of Crossed and Uncrossed Fibers." *Neuron* 5, no. 2 (Aug 1990): 173-86. https://www.ncbi.nlm.nih.gov/pubmed/2383400.

Gomez-Pastor, R., E. T. Burchfiel, D. W. Neef, A. M. Jaeger, E. Cabiscol, S. U. McKinstry, A. Doss, A. Aballay, D. C. Lo, S. S. Akimov, C. A. Ross, C. Eroglu, and D. J. Thiele. "Abnormal Degradation of the Neuronal Stress-Protective Transcription Factor Hsf1 in Huntington's Disease." *Nat Commun* 8 (Feb 13 2017): 14405. http://dx.doi.org/10.1038/ncomms14405.

Gorman, A. M. "Neuronal Cell Death in Neurodegenerative Diseases: Recurring Themes around Protein Handling." *J Cell Mol Med* 12, no. 6A (Dec 2008): 2263-80. http://dx.doi.org/10.1111/j.1582-4934.2008.00402.x.

Gorski, J. A., T. Talley, M. Qiu, L. Puelles, J. L. Rubenstein, and K. R. Jones. "Cortical Excitatory Neurons and Glia, but Not Gabaergic Neurons, Are Produced in the Emx1-Expressing Lineage." *J Neurosci* 22, no. 15 (Aug 01 2002): 6309-14. http://dx.doi.org/20026564.

Gotz, M. and Y. A. Barde. "Radial Glial Cells Defined and Major Intermediates between Embryonic Stem Cells and Cns Neurons." *Neuron* 46, no. 3 (May 05 2005): 369-72. http://dx.doi.org/10.1016/j.neuron.2005.04.012.

Gotz, M., S. Sirko, J. Beckers, and M. Irmler. "Reactive Astrocytes as Neural Stem or Progenitor Cells: In Vivo Lineage, in Vitro Potential, and Genome-Wide Expression Analysis." *Glia* 63, no. 8 (Aug 2015): 1452-68. http://dx.doi.org/10.1002/glia.22850.

Graham, Steven H. and Robert W. Hickey. "Molecular Pathophysiology of Stroke." In *Neuropsychopharmacology*, edited by Kenneth L. Davis, 1317 - 26: Lippincott Williams & Wilkins, 2002, 2002.

Gray, E. G. "Axo-Somatic and Axo-Dendritic Synapses of the Cerebral Cortex: An Electron Microscope Study." *J Anat* 93 (Oct 1959): 420-33. https://www.ncbi.nlm.nih.gov/pubmed/13829103.

Gregory, C. D. and A. Devitt. "The Macrophage and the Apoptotic Cell: An Innate Immune Interaction Viewed Simplistically?" *Immunology* 113, no. 1 (Sep 2004): 1-14. http://dx.doi.org/10.1111/j.1365-2567.2004.01959.x.

Grillo, F. W., S. Song, L. M. Teles-Grilo Ruivo, L. Huang, G. Gao, G. W. Knott, B. Maco, V. Ferretti, D. Thompson, G. E. Little, and V. De Paola. "Increased Axonal Bouton Dynamics in the Aging Mouse Cortex." *Proc Natl Acad Sci U S A* 110, no. 16 (Apr 16 2013): E1514-23. http://dx.doi.org/10.1073/pnas.1218731110.

Grimes, M. L., J. Zhou, E. C. Beattie, E. C. Yuen, D. E. Hall, J. S. Valletta, K. S. Topp, J. H. LaVail, N. W. Bunnett, and W. C. Mobley. "Endocytosis of Activated Trka: Evidence That Nerve Growth Factor Induces Formation of Signaling Endosomes." *J Neurosci* 16, no. 24 (Dec 15 1996): 7950-64. https://www.ncbi.nlm.nih.gov/pubmed/8987823.

Grinvald, A., M. Segal, U. Kuhnt, R. Hildesheim, A. Manker, L. Anglister, and J. A. Freeman. "Real-Time Optical Mapping of Neuronal Activity in Vertebrate Cns in Vitro and in Vivo." *Soc Gen Physiol Ser* 40 (1986): 165-97. https://www.ncbi.nlm.nih.gov/pubmed/2424094.

Grove, E. A. and T. Fukuchi-Shimogori. "Generating the Cerebral Cortical Area Map." *Annu Rev Neurosci* 26 (2003): 355-80. http://dx.doi.org/10.1146/annurev.neuro.26.041002.131137.

Guo, F., Y. Maeda, J. Ma, J. Xu, M. Horiuchi, L. Miers, F. Vaccarino, and D. Pleasure. "Pyramidal Neurons Are Generated from Oligodendroglial Progenitor Cells in Adult Piriform Cortex." *J Neurosci* 30, no. 36 (Sep 08 2010): 12036-49. http://dx.doi.org/10.1523/JNEUROSCI.1360-10.2010.

Hahn, J. S., Z. Hu, D. J. Thiele, and V. R. Iyer. "Genome-Wide Analysis of the Biology of Stress Responses through Heat Shock Transcription Factor." *Mol Cell Biol* 24, no. 12 (Jun 2004): 5249-56. http://dx.doi.org/10.1128/MCB.24.12.5249-5256.2004.

Hama, H., H. Kurokawa, H. Kawano, R. Ando, T. Shimogori, H. Noda, K. Fukami, A. Sakaue-Sawano, and A. Miyawaki. "Scale: A Chemical Approach for Fluorescence Imaging and Reconstruction of Transparent Mouse Brain." *Nat Neurosci* 14, no. 11 (Aug 30 2011): 1481-8. http://dx.doi.org/10.1038/nn.2928.

Hamilton, K. A., T. Heinbockel, M. Ennis, G. Szabo, F. Erdelyi, and A. Hayar. "Properties of External Plexiform Layer Interneurons in Mouse Olfactory Bulb Slices." *Neuroscience* 133, no. 3 (2005): 819-29. http://dx.doi.org/10.1016/j.neuroscience.2005.03.008.

Han, Y., X. Chen, F. Shi, S. Li, J. Huang, M. Xie, L. Hu, J. R. Hoidal, and P. Xu. "Cpg15, a New Factor Upregulated after Ischemic Brain Injury, Contributes to Neuronal Network Re-Establishment after Glutamate-Induced Injury." *J Neurotrauma* 24, no. 4 (Apr 2007): 722-31. http://dx.doi.org/10.1089/neu.2006.0174.

Harris, K. M. and R. J. Weinberg. "Ultrastructure of Synapses in the Mammalian Brain." *Cold Spring Harb Perspect Biol* 4, no. 5 (May 01 2012). http://dx.doi.org/10.1101/cshperspect.a005587.

Hartfuss, E., R. Galli, N. Heins, and M. Gotz. "Characterization of Cns Precursor Subtypes and Radial Glia." *Dev Biol* 229, no. 1 (Jan 01 2001): 15-30. http://dx.doi.org/10.1006/dbio.2000.9962.

Hartl, F. U., A. Bracher, and M. Hayer-Hartl. "Molecular Chaperones in Protein Folding and Proteostasis." *Nature* 475, no. 7356 (Jul 20 2011): 324-32. http://dx.doi.org/10.1038/nature10317.

Haubensak, W., F. Narz, R. Heumann, and V. Lessmann. "Bdnf-Gfp Containing Secretory Granules Are Localized in the Vicinity of Synaptic Junctions of Cultured Cortical Neurons." *J Cell Sci* 111 (Pt 11) (Jun 1998): 1483-93. https://www.ncbi.nlm.nih.gov/pubmed/9580557.

Haubst, N., E. Georges-Labouesse, A. De Arcangelis, U. Mayer, and M. Gotz. "Basement Membrane Attachment Is Dispensable for Radial Glial Cell Fate and for Proliferation, but Affects Positioning of Neuronal Subtypes." *Development* 133, no. 16 (Aug 2006): 3245-54. http://dx.doi.org/10.1242/dev.02486.

Hayashi, S. and A. P. McMahon. "Efficient Recombination in Diverse Tissues by a Tamoxifen-Inducible Form of Cre: A Tool for Temporally Regulated Gene Activation/Inactivation in the Mouse." *Dev Biol* 244, no. 2 (Apr 15 2002): 305-18. http://dx.doi.org/10.1006/dbio.2002.0597.

Hayashi, T., K. Sakai, C. Sasaki, W. R. Zhang, and K. Abe. "Phosphorylation of Retinoblastoma Protein in Rat Brain after Transient Middle Cerebral Artery Occlusion." *Neuropathol Appl Neurobiol* 26, no. 4 (Aug 2000): 390-7. https://www.ncbi.nlm.nih.gov/pubmed/10931373.

Hayashi-Takagi, A., S. Yagishita, M. Nakamura, F. Shirai, Y. I. Wu, A. L. Loshbaugh, B. Kuhlman, K. M. Hahn, and H. Kasai. "Labelling and Optical Erasure of Synaptic Memory Traces in the Motor Cortex." *Nature* 525, no. 7569 (Sep 17 2015): 333-8. http://dx.doi.org/10.1038/nature15257.

Hayes, N. L. and R. S. Nowakowski. "Exploiting the Dynamics of S-Phase Tracers in Developing Brain: Interkinetic Nuclear Migration for Cells Entering Versus Leaving the S-Phase." *Dev Neurosci* 22, no. 1-2 (2000): 44-55. http://dx.doi.org/17426.

Heinrich, C., M. Bergami, S. Gascon, A. Lepier, F. Vigano, L. Dimou, B. Sutor, B. Berninger, and M. Gotz. "Sox2-Mediated Conversion of Ng2 Glia into Induced Neurons in the Injured Adult Cerebral Cortex." *Stem Cell Reports* 3, no. 6 (Dec 09 2014): 1000-14. http://dx.doi.org/10.1016/j.stemcr.2014.10.007.

Helmchen, F. and W. Denk. "Deep Tissue Two-Photon Microscopy." *Nat Methods* 2, no. 12 (Dec 2005): 932-40. http://dx.doi.org/10.1038/nmeth818.

Hendel, T., M. Mank, B. Schnell, O. Griesbeck, A. Borst, and D. F. Reiff. "Fluorescence Changes of Genetic Calcium Indicators and Ogb-1 Correlated with Neural Activity and Calcium in Vivo and in Vitro." *J Neurosci* 28, no. 29 (Jul 16 2008): 7399-411. http://dx.doi.org/10.1523/JNEUROSCI.1038-08.2008.

Hennou, S., I. Khalilov, D. Diabira, Y. Ben-Ari, and H. Gozlan. "Early Sequential Formation of Functional Gaba(a) and Glutamatergic Synapses on Ca1 Interneurons of the Rat Foetal Hippocampus." *Eur J Neurosci* 16, no. 2 (Jul 2002): 197-208. https://www.ncbi.nlm.nih.gov/pubmed/12169102.

Hernit-Grant, C. S. and J. D. Macklis. "Embryonic Neurons Transplanted to Regions of Targeted Photolytic Cell Death in Adult Mouse Somatosensory Cortex Re-Form Specific Callosal Projections." *Exp Neurol* 139, no. 1 (May 1996): 131-42. http://dx.doi.org/10.1006/exnr.1996.0088.

Herrup, K., R. Neve, S. L. Ackerman, and A. Copani. "Divide and Die: Cell Cycle Events as Triggers of Nerve Cell Death." *J Neurosci* 24, no. 42 (Oct 20 2004): 9232-9. http://dx.doi.org/10.1523/JNEUROSCI.3347-04.2004.

Herx, L. M. and V. W. Yong. "Interleukin-1 Beta Is Required for the Early Evolution of Reactive Astrogliosis Following Cns Lesion." *J Neuropathol Exp Neurol* 60, no. 10 (Oct 2001): 961-71. https://www.ncbi.nlm.nih.gov/pubmed/11589427.

Hjorth-Simonsen, A. and B. Jeune. "Origin and Termination of the Hippocampal Perforant Path in the Rat Studied by Silver Impregnation." *J Comp Neurol* 144, no. 2 (Feb 1972): 215-32. http://dx.doi.org/10.1002/cne.901440206.

Hofer, S. B., T. D. Mrsic-Flogel, T. Bonhoeffer, and M. Hubener. "Experience Leaves a Lasting Structural Trace in Cortical Circuits." *Nature* 457, no. 7227 (Jan 15 2009): 313-7. http://dx.doi.org/10.1038/nature07487.

Hofstetter, C. P., N. A. Holmstrom, J. A. Lilja, P. Schweinhardt, J. Hao, C. Spenger, Z. Wiesenfeld-Hallin, S. N. Kurpad, J. Frisen, and L. Olson. "Allodynia Limits the Usefulness of Intraspinal Neural Stem Cell Grafts; Directed Differentiation Improves Outcome." *Nat Neurosci* 8, no. 3 (Mar 2005): 346-53. http://dx.doi.org/10.1038/nn1405.

Hoglinger, G. U., J. J. Breunig, C. Depboylu, C. Rouaux, P. P. Michel, D. Alvarez-Fischer, A. L. Boutillier, J. Degregori, W. H. Oertel, P. Rakic, E. C. Hirsch, and S. Hunot. "The Prb/E2f Cell-Cycle Pathway Mediates Cell Death in Parkinson's Disease." *Proc Natl Acad Sci U S A* 104, no. 9 (Feb 27 2007): 3585-90. http://dx.doi.org/10.1073/pnas.0611671104.

Holtmaat, A., T. Bonhoeffer, D. K. Chow, J. Chuckowree, V. De Paola, S. B. Hofer, M. Hubener, T. Keck, G. Knott, W. C. Lee, R. Mostany, T. D. Mrsic-Flogel, E. Nedivi, C. Portera-Cailliau, K. Svoboda, J. T. Trachtenberg, and L. Wilbrecht. "Long-Term, High-Resolution Imaging in the Mouse Neocortex through a Chronic Cranial Window." *Nat Protoc* 4, no. 8 (2009): 1128-44. http://dx.doi.org/10.1038/nprot.2009.89.

Holtmaat, A. J., J. T. Trachtenberg, L. Wilbrecht, G. M. Shepherd, X. Zhang, G. W. Knott, and K. Svoboda. "Transient and Persistent Dendritic Spines in the Neocortex in Vivo." *Neuron* 45, no. 2 (Jan 20 2005): 279-91. http://dx.doi.org/10.1016/j.neuron.2005.01.003.

Holtmaat, A. and K. Svoboda. "Experience-Dependent Structural Synaptic Plasticity in the Mammalian Brain." *Nat Rev Neurosci* 10, no. 9 (Sep 2009): 647-58. http://dx.doi.org/10.1038/nrn2699.

Homma, R., Y. Kovalchuk, A. Konnerth, L. B. Cohen, and O. Garaschuk. "In Vivo Functional Properties of Juxtaglomerular Neurons in the Mouse Olfactory Bulb." *Front Neural Circuits* 7 (2013): 23. http://dx.doi.org/10.3389/fncir.2013.00023.

Horch, H. W. "Local Effects of Bdnf on Dendritic Growth." *Rev Neurosci* 15, no. 2 (2004): 117-29. https://www.ncbi.nlm.nih.gov/pubmed/15202684.

Horch, H. W. and L. C. Katz. "Bdnf Release from Single Cells Elicits Local Dendritic Growth in Nearby Neurons." *Nat Neurosci* 5, no. 11 (Nov 2002): 1177-84. http://dx.doi.org/10.1038/nn927.

Horch, H. W., A. Kruttgen, S. D. Portbury, and L. C. Katz. "Destabilization of Cortical Dendrites and Spines by Bdnf." *Neuron* 23, no. 2 (Jun 1999): 353-64. https://www.ncbi.nlm.nih.gov/pubmed/10399940.

Horn, K. P., S. A. Busch, A. L. Hawthorne, N. van Rooijen, and J. Silver. "Another Barrier to Regeneration in the Cns: Activated Macrophages Induce Extensive Retraction of Dystrophic Axons through Direct Physical

Interactions." *J Neurosci* 28, no. 38 (Sep 17 2008): 9330-41. http://dx.doi.org/10.1523/JNEUROSCI.2488-08.2008.

Houle, J. D. "Demonstration of the Potential for Chronically Injured Neurons to Regenerate Axons into Intraspinal Peripheral Nerve Grafts." *Exp Neurol* 113, no. 1 (Jul 1991): 1-9. https://www.ncbi.nlm.nih.gov/pubmed/2044676.

Hoy, J. L. and C. M. Niell. "Layer-Specific Refinement of Visual Cortex Function after Eye Opening in the Awake Mouse." *J Neurosci* 35, no. 8 (Feb 25 2015): 3370-83. http://dx.doi.org/10.1523/JNEUROSCI.3174-14.2015.

Hu, X., P. Li, Y. Guo, H. Wang, R. K. Leak, S. Chen, Y. Gao, and J. Chen. "Microglia/Macrophage Polarization Dynamics Reveal Novel Mechanism of Injury Expansion after Focal Cerebral Ischemia." *Stroke* 43, no. 11 (Nov 2012): 3063-70. http://dx.doi.org/10.1161/STROKEAHA.112.659656.

Huang, E. J. and L. F. Reichardt. "Neurotrophins: Roles in Neuronal Development and Function." *Annu Rev Neurosci* 24 (2001): 677-736. http://dx.doi.org/10.1146/annurev.neuro.24.1.677.

Huang, W., N. Zhao, X. Bai, K. Karram, J. Trotter, S. Goebbels, A. Scheller, and F. Kirchhoff. "Novel Ng2-Creert2 Knock-in Mice Demonstrate Heterogeneous Differentiation Potential of Ng2 Glia During Development." *Glia* 62, no. 6 (Jun 2014): 896-913. http://dx.doi.org/10.1002/glia.22648.

Hubel, D. H. and T. N. Wiesel. "Receptive Fields of Single Neurones in the Cat's Striate Cortex." *J Physiol* 148 (Oct 1959): 574-91. https://www.ncbi.nlm.nih.gov/pubmed/14403679.

Hubel, D. H. and T. N. Wiesel. "Receptive Fields, Binocular Interaction and Functional Architecture in the Cat's Visual Cortex." *J Physiol* 160 (Jan 1962): 106-54. https://www.ncbi.nlm.nih.gov/pubmed/14449617.

Hubel, D. H. and T. N. Wiesel. "Cortical and Callosal Connections Concerned with the Vertical Meridian of Visual Fields in the Cat." *J Neurophysiol* 30, no. 6 (Nov 1967): 1561-73. https://www.ncbi.nlm.nih.gov/pubmed/6066454.

Hubener, M. and J. Bolz. "Morphology of Identified Projection Neurons in Layer 5 of Rat Visual Cortex." *Neurosci Lett* 94, no. 1-2 (Nov 22 1988): 76-81. https://www.ncbi.nlm.nih.gov/pubmed/2468117.

Huettner, J. E. and R. W. Baughman. "Primary Culture of Identified Neurons from the Visual Cortex of Postnatal Rats." *J Neurosci* 6, no. 10 (Oct 1986): 3044-60. https://www.ncbi.nlm.nih.gov/pubmed/3760948.

Hunt, R. F., K. M. Girskis, J. L. Rubenstein, A. Alvarez-Buylla, and S. C. Baraban. "Gaba Progenitors Grafted into the Adult Epileptic Brain Control Seizures and Abnormal Behavior." *Nat Neurosci* 16, no. 6 (Jun 2013): 692-7. http://dx.doi.org/10.1038/nn.3392.

Hunter, N. L., R. B. Awatramani, F. W. Farley, and S. M. Dymecki. "Ligand-Activated Flpe for Temporally Regulated Gene Modifications." *Genesis* 41, no. 3 (Mar 2005): 99-109. http://dx.doi.org/10.1002/gene.20101.

Hurtado-Chong, A., M. J. Yusta-Boyo, E. Vergano-Vera, A. Bulfone, F. de Pablo, and C. Vicario-Abejon. "Igf-I Promotes Neuronal Migration and Positioning in the Olfactory Bulb and the Exit of Neuroblasts from the Subventricular Zone." *Eur J Neurosci* 30, no. 5 (Sep 2009): 742-55. http://dx.doi.org/10.1111/j.1460-9568.2009.06870.x.

Huttner, H. B., O. Bergmann, M. Salehpour, A. Racz, J. Tatarishvili, E. Lindgren, T. Csonka, L. Csiba, T. Hortobagyi, G. Mehes, E. Englund, B. W. Solnestam, S. Zdunek, C. Scharenberg, L. Strom, P. Stahl, B. Sigurgeirsson, A. Dahl, S. Schwab, G. Possnert, S. Bernard, Z. Kokaia, O. Lindvall, J. Lundeberg, and J. Frisen. "The Age and Genomic Integrity of Neurons after Cortical Stroke in Humans." *Nat Neurosci* 17, no. 6 (Jun 2014): 801-3. http://dx.doi.org/10.1038/nn.3706.

Ideguchi, M., T. D. Palmer, L. D. Recht, and J. M. Weimann. "Murine Embryonic Stem Cell-Derived Pyramidal Neurons Integrate into the Cerebral Cortex and Appropriately Project Axons to Subcortical Targets." *J Neurosci* 30, no. 3 (Jan 20 2010): 894-904. http://dx.doi.org/10.1523/JNEUROSCI.4318-09.2010.

Im, S. H., J. H. Yu, E. S. Park, J. E. Lee, H. O. Kim, K. I. Park, G. W. Kim, C. I. Park, and S. R. Cho. "Induction of Striatal Neurogenesis Enhances Functional Recovery in an Adult Animal Model of Neonatal Hypoxic-Ischemic Brain Injury." *Neuroscience* 169, no. 1 (Aug 11 2010): 259-68. http://dx.doi.org/10.1016/j.neuroscience.2010.04.038.

Imam, N., T. A. Cleland, R. Manohar, P. A. Merolla, J. V. Arthur, F. Akopyan, and D. S. Modha. "Implementation of Olfactory Bulb Glomerular-Layer Computations in a Digital Neurosynaptic Core." *Front Neurosci* 6 (2012): 83. http://dx.doi.org/10.3389/fnins.2012.00083.

Indra, A. K., X. Warot, J. Brocard, J. M. Bornert, J. H. Xiao, P. Chambon, and D. Metzger. "Temporally-Controlled Site-Specific Mutagenesis in the Basal Layer of the Epidermis: Comparison of the Recombinase Activity of the Tamoxifen-Inducible Cre-Er(T) and Cre-Er(T2) Recombinases." *Nucleic Acids Res* 27, no. 22 (Nov 15 1999): 4324-7. https://www.ncbi.nlm.nih.gov/pubmed/10536138.

Iram, T., Z. Ramirez-Ortiz, M. H. Byrne, U. A. Coleman, N. D. Kingery, T. K. Means, D. Frenkel, and J. El Khoury. "Megf10 Is a Receptor for C1q That Mediates Clearance of Apoptotic Cells by Astrocytes." *J Neurosci* 36, no. 19 (May 11 2016): 5185-92. http://dx.doi.org/10.1523/JNEUROSCI.3850-15.2016.

Iremonger, K. J. and J. S. Bains. "Retrograde Opioid Signaling Regulates Glutamatergic Transmission in the Hypothalamus." *J Neurosci* 29, no. 22 (Jun 03 2009): 7349-58. http://dx.doi.org/10.1523/JNEUROSCI.0381-09.2009.

Iurilli, G., D. Ghezzi, U. Olcese, G. Lassi, C. Nazzaro, R. Tonini, V. Tucci, F. Benfenati, and P. Medini. "Sound-Driven Synaptic Inhibition in Primary Visual Cortex." *Neuron* 73, no. 4 (Feb 23 2012): 814-28. http://dx.doi.org/10.1016/j.neuron.2011.12.026.

John, G. R., L. Chen, M. A. Rivieccio, C. V. Melendez-Vasquez, A. Hartley, and C. F. Brosnan. "Interleukin-1beta Induces a Reactive Astroglial Phenotype Via Deactivation of the Rho Gtpase-Rock Axis." *J Neurosci* 24, no. 11 (Mar 17 2004): 2837-45. http://dx.doi.org/10.1523/JNEUROSCI.4789-03.2004.

Jolivel, V., F. Bicker, F. Biname, R. Ploen, S. Keller, R. Gollan, B. Jurek, J. Birkenstock, L. Poisa-Beiro, J. Bruttger, V. Opitz, S. C. Thal, A. Waisman, T. Bauerle, M. K. Schafer, F. Zipp, and M. H. Schmidt. "Perivascular Microglia Promote Blood Vessel Disintegration in the Ischemic Penumbra." *Acta Neuropathol* 129, no. 2 (Feb 2015): 279-95. http://dx.doi.org/10.1007/s00401-014-1372-1.

Kaila, K., T. J. Price, J. A. Payne, M. Puskarjov, and J. Voipio. "Cation-Chloride Cotransporters in Neuronal Development, Plasticity and Disease." *Nat Rev Neurosci* 15, no. 10 (Oct 2014): 637-54. http://dx.doi.org/10.1038/nrn3819.

Kakazu, Y., N. Akaike, S. Komiyama, and J. Nabekura. "Regulation of Intracellular Chloride by Cotransporters in Developing Lateral Superior Olive Neurons." *J Neurosci* 19, no. 8 (Apr 15 1999): 2843-51. https://www.ncbi.nlm.nih.gov/pubmed/10191302.

Karlsson, U. and R. L. Schultz. "Fixation of the Central Nervous System from Electron Microscopy by Aldehyde Perfusion. I. Preservation with Aldehyde Perfusates Versus Direct Perfusion with Osmium Tetroxide with Special Reference to Membranes and the Extracellular Space." *J Ultrastruct Res* 12 (Feb 1965): 160-86. https://www.ncbi.nlm.nih.gov/pubmed/14289426.

Kasper, E. M., J. Lubke, A. U. Larkman, and C. Blakemore. "Pyramidal Neurons in Layer 5 of the Rat Visual Cortex. Iii. Differential Maturation of Axon Targeting, Dendritic Morphology, and Electrophysiological Properties." *J Comp Neurol* 339, no. 4 (Jan 22 1994): 495-518. http://dx.doi.org/10.1002/cne.903390404.

Katz, L. C., A. Burkhalter, and W. J. Dreyer. "Fluorescent Latex Microspheres as a Retrograde Neuronal Marker for in Vivo and in Vitro Studies of Visual Cortex." *Nature* 310, no. 5977 (Aug 9-15 1984): 498-500. https://www.ncbi.nlm.nih.gov/pubmed/6205278.

Kawabori, M. and M. A. Yenari. "The Role of the Microglia in Acute Cns Injury." *Metab Brain Dis* 30, no. 2 (Apr 2015): 381-92. http://dx.doi.org/10.1007/s11011-014-9531-6.

Keck, T., T. D. Mrsic-Flogel, M. Vaz Afonso, U. T. Eysel, T. Bonhoeffer, and M. Hubener. "Massive Restructuring of Neuronal Circuits During Functional Reorganization of Adult Visual Cortex." *Nat Neurosci* 11, no. 10 (Oct 2008): 1162-7. http://dx.doi.org/10.1038/nn.2181.

Kee, N., S. Sivalingam, R. Boonstra, and J. M. Wojtowicz. "The Utility of Ki-67 and Brdu as Proliferative Markers of Adult Neurogenesis." *J Neurosci Methods* 115, no. 1 (Mar 30 2002): 97-105. https://www.ncbi.nlm.nih.gov/pubmed/11897369.

Keller, G. B., T. Bonhoeffer, and M. Hubener. "Sensorimotor Mismatch Signals in Primary Visual Cortex of the Behaving Mouse." *Neuron* 74, no. 5 (Jun 07 2012): 809-15. http://dx.doi.org/10.1016/j.neuron.2012.03.040.

Kempermann, G., S. Jessberger, B. Steiner, and G. Kronenberg. "Milestones of Neuronal Development in the Adult Hippocampus." *Trends Neurosci* 27, no. 8 (Aug 2004): 447-52. http://dx.doi.org/10.1016/j.tins.2004.05.013.

Kennedy, M. B. "Signal-Processing Machines at the Postsynaptic Density." *Science* 290, no. 5492 (Oct 27 2000): 750-4. https://www.ncbi.nlm.nih.gov/pubmed/11052931.

Kerlin, A. M., M. L. Andermann, V. K. Berezovskii, and R. C. Reid. "Broadly Tuned Response Properties of Diverse Inhibitory Neuron Subtypes in Mouse Visual Cortex." *Neuron* 67, no. 5 (Sep 09 2010): 858-71. http://dx.doi.org/10.1016/j.neuron.2010.08.002.

Kerr, J. F., A. H. Wyllie, and A. R. Currie. "Apoptosis: A Basic Biological Phenomenon with Wide-Ranging Implications in Tissue Kinetics." *Br J Cancer* 26, no. 4 (Aug 1972): 239-57. https://www.ncbi.nlm.nih.gov/pubmed/4561027.

Kerschensteiner, M., M. E. Schwab, J. W. Lichtman, and T. Misgeld. "In Vivo Imaging of Axonal Degeneration and Regeneration in the Injured Spinal Cord." *Nat Med* 11, no. 5 (May 2005): 572-7. http://dx.doi.org/10.1038/nm1229.

Khazipov, R., M. Esclapez, O. Caillard, C. Bernard, I. Khalilov, R. Tyzio, J. Hirsch, V. Dzhala, B. Berger, and Y. Ben-Ari. "Early Development of Neuronal Activity in the Primate Hippocampus in Utero." *J Neurosci* 21, no. 24 (Dec 15 2001): 9770-81. https://www.ncbi.nlm.nih.gov/pubmed/11739585.

Kim, J., C. J. Matney, A. Blankenship, S. Hestrin, and S. P. Brown. "Layer 6 Corticothalamic Neurons Activate a Cortical Output Layer, Layer 5a." *J Neurosci* 34, no. 29 (Jul 16 2014): 9656-64. http://dx.doi.org/10.1523/JNEUROSCI.1325-14.2014.

Kim, J. Y., J. Park, J. Y. Chang, S. H. Kim, and J. E. Lee. "Inflammation after Ischemic Stroke: The Role of Leukocytes and Glial Cells." *Exp Neurobiol* 25, no. 5 (Oct 2016): 241-51. http://dx.doi.org/10.5607/en.2016.25.5.241.

Klein, J. A. and S. L. Ackerman. "Oxidative Stress, Cell Cycle, and Neurodegeneration." *J Clin Invest* 111, no. 6 (Mar 2003): 785-93. http://dx.doi.org/10.1172/JCI18182.

Klein, J. A., C. M. Longo-Guess, M. P. Rossmann, K. L. Seburn, R. E. Hurd, W. N. Frankel, R. T. Bronson, and S. L. Ackerman. "The Harlequin Mouse Mutation Downregulates Apoptosis-Inducing Factor." *Nature* 419, no. 6905 (Sep 26 2002): 367-74. http://dx.doi.org/10.1038/nature01034.

Kleinfeld, D. and O. Griesbeck. "From Art to Engineering? The Rise of in Vivo Mammalian Electrophysiology Via Genetically Targeted Labeling and Nonlinear Imaging." *PLoS Biol* 3, no. 10 (Oct 2005): e355. http://dx.doi.org/10.1371/journal.pbio.0030355.

Klemann, C. J. and E. W. Roubos. "The Gray Area between Synapse Structure and Function-Gray's Synapse Types I and Ii Revisited." *Synapse* 65, no. 11 (Nov 2011): 1222-30. http://dx.doi.org/10.1002/syn.20962.

Klempin, F., G. Kronenberg, G. Cheung, H. Kettenmann, and G. Kempermann. "Properties of Doublecortin-(Dcx)-Expressing Cells in the Piriform Cortex Compared to the Neurogenic Dentate Gyrus of Adult Mice." *PLoS One* 6, no. 10 (2011): e25760. http://dx.doi.org/10.1371/journal.pone.0025760.

Knoll, B., S. Isenmann, E. Kilic, J. Walkenhorst, S. Engel, J. Wehinger, M. Bahr, and U. Drescher. "Graded Expression Patterns of Ephrin-as in the Superior Colliculus after Lesion of the Adult Mouse Optic Nerve." *Mech Dev* 106, no. 1-2 (Aug 2001): 119-27. https://www.ncbi.nlm.nih.gov/pubmed/11472840.

Knott, G. W., A. Holtmaat, L. Wilbrecht, E. Welker, and K. Svoboda. "Spine Growth Precedes Synapse Formation in the Adult Neocortex in Vivo." *Nat Neurosci* 9, no. 9 (Sep 2006): 1117-24. http://dx.doi.org/10.1038/nn1747.

Ko, H., L. Cossell, C. Baragli, J. Antolik, C. Clopath, S. B. Hofer, and T. D. Mrsic-Flogel. "The Emergence of Functional Microcircuits in Visual Cortex." *Nature* 496, no. 7443 (Apr 04 2013): 96-100. http://dx.doi.org/10.1038/nature12015.

Ko, H., S. B. Hofer, B. Pichler, K. A. Buchanan, P. J. Sjostrom, and T. D. Mrsic-Flogel. "Functional Specificity of Local Synaptic Connections in Neocortical Networks." *Nature* 473, no. 7345 (May 05 2011): 87-91. http://dx.doi.org/10.1038/nature09880.

Ko, H., T. D. Mrsic-Flogel, and S. B. Hofer. "Emergence of Feature-Specific Connectivity in Cortical Microcircuits in the Absence of Visual Experience." *J Neurosci* 34, no. 29 (Jul 16 2014): 9812-6. http://dx.doi.org/10.1523/JNEUROSCI.0875-14.2014.

Koester, S. E. and D. D. O'Leary. "Functional Classes of Cortical Projection Neurons Develop Dendritic Distinctions by Class-Specific Sculpting of an Early Common Pattern." *J Neurosci* 12, no. 4 (Apr 1992): 1382-93. https://www.ncbi.nlm.nih.gov/pubmed/1556599.

Kohara, K., A. Kitamura, M. Morishima, and T. Tsumoto. "Activity-Dependent Transfer of Brain-Derived Neurotrophic Factor to Postsynaptic Neurons." *Science* 291, no. 5512 (Mar 23 2001): 2419-23. http://dx.doi.org/10.1126/science.1057415.

Kokaia, Z., G. Martino, M. Schwartz, and O. Lindvall. "Cross-Talk between Neural Stem Cells and Immune Cells: The Key to Better Brain Repair?" *Nat Neurosci* 15, no. 8 (Jul 26 2012): 1078-87. http://dx.doi.org/10.1038/nn.3163.

Kokoeva, M. V., H. Yin, and J. S. Flier. "Neurogenesis in the Hypothalamus of Adult Mice: Potential Role in Energy Balance." *Science* 310, no. 5748 (Oct 28 2005): 679-83. http://dx.doi.org/10.1126/science.1115360.

Koleske, A. J. "Molecular Mechanisms of Dendrite Stability." *Nat Rev Neurosci* 14, no. 8 (Aug 2013): 536-50. http://dx.doi.org/10.1038/nrn3486.

Kondo, S. and K. Ohki. "Laminar Differences in the Orientation Selectivity of Geniculate Afferents in Mouse Primary Visual Cortex." *Nat Neurosci* 19, no. 2 (Feb 2016): 316-9. http://dx.doi.org/10.1038/nn.4215.

Kondo, T. and M. Raff. "Oligodendrocyte Precursor Cells Reprogrammed to Become Multipotential Cns Stem Cells." *Science* 289, no. 5485 (Sep 08 2000): 1754-7. https://www.ncbi.nlm.nih.gov/pubmed/10976069.

Kossel, A., S. Lowel, and J. Bolz. "Relationships between Dendritic Fields and Functional Architecture in Striate Cortex of Normal and Visually Deprived Cats." *J Neurosci* 15, no. 5 Pt 2 (May 1995): 3913-26. https://www.ncbi.nlm.nih.gov/pubmed/7538568.

Krampera, M., A. Pasini, G. Pizzolo, L. Cosmi, S. Romagnani, and F. Annunziato. "Regenerative and Immunomodulatory Potential of Mesenchymal Stem Cells." *Curr Opin Pharmacol* 6, no. 4 (Aug 2006): 435-41. http://dx.doi.org/10.1016/j.coph.2006.02.008.

Kreile, A. K. "Plasticity of Neuronal Response Properties in Mouse Visual Cortex
Assessed with Two-Photon Calcium Imaging." *Dissertation* Ludwigs-Maximilians-Universität München (2012).

Kreile, A. K., T. Bonhoeffer, and M. Hubener. "Altered Visual Experience Induces Instructive Changes of Orientation Preference in Mouse Visual Cortex." *J Neurosci* 31, no. 39 (Sep 28 2011): 13911-20. http://dx.doi.org/10.1523/JNEUROSCI.2143-11.2011.

Kreutzberg, G. W. "Microglia: A Sensor for Pathological Events in the Cns." *Trends Neurosci* 19, no. 8 (Aug 1996): 312-8. https://www.ncbi.nlm.nih.gov/pubmed/8843599.

Kriegstein, A. and A. Alvarez-Buylla. "The Glial Nature of Embryonic and Adult Neural Stem Cells." *Annu Rev Neurosci* 32 (2009): 149-84. http://dx.doi.org/10.1146/annurev.neuro.051508.135600.

Kriks, S., J. W. Shim, J. Piao, Y. M. Ganat, D. R. Wakeman, Z. Xie, L. Carrillo-Reid, G. Auyeung, C. Antonacci, A. Buch, L. Yang, M. F. Beal, D. J. Surmeier, J. H. Kordower, V. Tabar, and L. Studer. "Dopamine Neurons Derived from Human Es Cells Efficiently Engraft in Animal Models of Parkinson's Disease." *Nature* 480, no. 7378 (Nov 06 2011): 547-51. http://dx.doi.org/10.1038/nature10648.

Kroemer, G., W. S. El-Deiry, P. Golstein, M. E. Peter, D. Vaux, P. Vandenabeele, B. Zhivotovsky, M. V. Blagosklonny, W. Malorni, R. A. Knight, M. Piacentini, S. Nagata, G. Melino, and Death Nomenclature Committee on Cell. "Classification of Cell Death: Recommendations of the Nomenclature Committee on Cell Death." *Cell Death Differ* 12 Suppl 2 (Nov 2005): 1463-7. http://dx.doi.org/10.1038/sj.cdd.4401724.

Kruman, II, R. P. Wersto, F. Cardozo-Pelaez, L. Smilenov, S. L. Chan, F. J. Chrest, R. Emokpae, Jr., M. Gorospe, and M. P. Mattson. "Cell Cycle Activation Linked to Neuronal Cell Death Initiated by DNA Damage." *Neuron* 41, no. 4 (Feb 19 2004): 549-61. https://www.ncbi.nlm.nih.gov/pubmed/14980204.

Kuan, C. Y., A. J. Schloemer, A. Lu, K. A. Burns, W. L. Weng, M. T. Williams, K. I. Strauss, C. V. Vorhees, R. A. Flavell, R. J. Davis, F. R. Sharp, and P. Rakic. "Hypoxia-Ischemia Induces DNA Synthesis without Cell Proliferation in Dying Neurons in Adult Rodent Brain." *J Neurosci* 24, no. 47 (Nov 24 2004): 10763-72. http://dx.doi.org/10.1523/JNEUROSCI.3883-04.2004.

Kuhn, H. G., J. Winkler, G. Kempermann, L. J. Thal, and F. H. Gage. "Epidermal Growth Factor and Fibroblast Growth Factor-2 Have Different Effects on Neural Progenitors in the Adult Rat Brain." *J Neurosci* 17, no. 15 (Aug 01 1997): 5820-9. https://www.ncbi.nlm.nih.gov/pubmed/9221780.

Kwon, B. K., J. Liu, C. Messerer, N. R. Kobayashi, J. McGraw, L. Oschipok, and W. Tetzlaff. "Survival and Regeneration of Rubrospinal Neurons 1 Year after Spinal Cord Injury." *Proc Natl Acad Sci U S A* 99, no. 5 (Mar 05 2002): 3246-51. http://dx.doi.org/10.1073/pnas.052308899.

Kwon, H. B. and B. L. Sabatini. "Glutamate Induces De Novo Growth of Functional Spines in Developing Cortex." *Nature* 474, no. 7349 (Jun 02 2011): 100-4. http://dx.doi.org/10.1038/nature09986.

Kyritsis, N., C. Kizil, and M. Brand. "Neuroinflammation and Central Nervous System Regeneration in Vertebrates." *Trends Cell Biol* 24, no. 2 (Feb 2014): 128-35. http://dx.doi.org/10.1016/j.tcb.2013.08.004.

Lagace, D. C., M. C. Whitman, M. A. Noonan, J. L. Ables, N. A. DeCarolis, A. A. Arguello, M. H. Donovan, S. J. Fischer, L. A. Farnbauch, R. D. Beech, R. J. DiLeone, C. A. Greer, C. D. Mandyam, and A. J. Eisch. "Dynamic Contribution of Nestin-Expressing Stem Cells to Adult Neurogenesis." *J Neurosci* 27, no. 46 (Nov 14 2007): 12623-9. http://dx.doi.org/10.1523/JNEUROSCI.3812-07.2007.

Lai, C. S., T. F. Franke, and W. B. Gan. "Opposite Effects of Fear Conditioning and Extinction on Dendritic Spine Remodelling." *Nature* 483, no. 7387 (Feb 19 2012): 87-91. http://dx.doi.org/10.1038/nature10792.

Larkum, M. "A Cellular Mechanism for Cortical Associations: An Organizing Principle for the Cerebral Cortex." *Trends Neurosci* 36, no. 3 (Mar 2013): 141-51. http://dx.doi.org/10.1016/j.tins.2012.11.006.

Laywell, E. D., P. Rakic, V. G. Kukekov, E. C. Holland, and D. A. Steindler. "Identification of a Multipotent Astrocytic Stem Cell in the Immature and Adult Mouse Brain." *Proc Natl Acad Sci U S A* 97, no. 25 (Dec 05 2000): 13883-8. http://dx.doi.org/10.1073/pnas.250471697.

Lee, D. A., J. L. Bedont, T. Pak, H. Wang, J. Song, A. Miranda-Angulo, V. Takiar, V. Charubhumi, F. Balordi, H. Takebayashi, S. Aja, E. Ford, G. Fishell, and S. Blackshaw. "Tanycytes of the Hypothalamic Median Eminence Form a Diet-Responsive Neurogenic Niche." *Nat Neurosci* 15, no. 5 (Mar 25 2012): 700-2. http://dx.doi.org/10.1038/nn.3079.

Lemmens, R. and G. K. Steinberg. "Stem Cell Therapy for Acute Cerebral Injury: What Do We Know and What Will the Future Bring?" *Curr Opin Neurol* 26, no. 6 (Dec 2013): 617-25. http://dx.doi.org/10.1097/WCO.0000000000000023.

Leonzino, M., M. Busnelli, F. Antonucci, C. Verderio, M. Mazzanti, and B. Chini. "The Timing of the Excitatory-to-Inhibitory Gaba Switch Is Regulated by the Oxytocin Receptor Via Kcc2." *Cell Rep* 15, no. 1 (Apr 05 2016): 96-103. http://dx.doi.org/10.1016/j.celrep.2016.03.013.

Lepore, F., A. Samson, M. C. Paradis, M. Ptito, and J. P. Guillemot. "Binocular Interaction and Disparity Coding at the 17-18 Border: Contribution of the Corpus Callosum." *Exp Brain Res* 90, no. 1 (1992): 129-40. https://www.ncbi.nlm.nih.gov/pubmed/1521601.

Levitt, P. and P. Rakic. "Immunoperoxidase Localization of Glial Fibrillary Acidic Protein in Radial Glial Cells and Astrocytes of the Developing Rhesus Monkey Brain." *J Comp Neurol* 193, no. 3 (Oct 01 1980): 815-40. http://dx.doi.org/10.1002/cne.901930316.

Lewis, P. F. and M. Emerman. "Passage through Mitosis Is Required for Oncoretroviruses but Not for the Human Immunodeficiency Virus." *J Virol* 68, no. 1 (Jan 1994): 510-6. https://www.ncbi.nlm.nih.gov/pubmed/8254763.

Li, H., S. Khirug, C. Cai, A. Ludwig, P. Blaesse, J. Kolikova, R. Afzalov, S. K. Coleman, S. Lauri, M. S. Airaksinen, K. Keinanen, L. Khiroug, M. Saarma, K. Kaila, and C. Rivera. "Kcc2 Interacts with the Dendritic Cytoskeleton to Promote Spine Development." *Neuron* 56, no. 6 (Dec 20 2007): 1019-33. http://dx.doi.org/10.1016/j.neuron.2007.10.039.

Li, L., K. M. Harms, P. B. Ventura, D. C. Lagace, A. J. Eisch, and L. A. Cunningham. "Focal Cerebral Ischemia Induces a Multilineage Cytogenic Response from Adult Subventricular Zone That Is Predominantly Gliogenic." *Glia* 58, no. 13 (Oct 2010): 1610-9. http://dx.doi.org/10.1002/glia.21033.

Li, P., X. Hu, Y. Gan, Y. Gao, W. Liang, and J. Chen. "Mechanistic Insight into DNA Damage and Repair in Ischemic Stroke: Exploiting the Base Excision Repair Pathway as a Model of Neuroprotection." *Antioxid Redox Signal* 14, no. 10 (May 15 2011): 1905-18. http://dx.doi.org/10.1089/ars.2010.3451.

Li, W., L. Ma, G. Yang, and W. B. Gan. "Rem Sleep Selectively Prunes and Maintains New Synapses in Development and Learning." *Nat Neurosci* 20, no. 3 (Mar 2017): 427-37. http://dx.doi.org/10.1038/nn.4479.

Li, Y., H. Lu, P. L. Cheng, S. Ge, H. Xu, S. H. Shi, and Y. Dan. "Clonally Related Visual Cortical Neurons Show Similar Stimulus Feature Selectivity." *Nature* 486, no. 7401 (May 02 2012): 118-21. http://dx.doi.org/10.1038/nature11110.

Li, Y. T., B. H. Liu, X. L. Chou, L. I. Zhang, and H. W. Tao. "Strengthening of Direction Selectivity by Broadly Tuned and Spatiotemporally Slightly Offset Inhibition in Mouse Visual Cortex." *Cereb Cortex* 25, no. 9 (Sep 2015): 2466-77. http://dx.doi.org/10.1093/cercor/bhu049.

Li, Y. X., Y. Xu, D. Ju, H. A. Lester, N. Davidson, and E. M. Schuman. "Expression of a Dominant Negative Trkb Receptor, T1, Reveals a Requirement for Presynaptic Signaling in Bdnf-Induced Synaptic Potentiation in Cultured Hippocampal Neurons." *Proc Natl Acad Sci U S A* 95, no. 18 (Sep 01 1998): 10884-9. https://www.ncbi.nlm.nih.gov/pubmed/9724799.

Liang, F., X. R. Xiong, B. Zingg, X. Y. Ji, L. I. Zhang, and H. W. Tao. "Sensory Cortical Control of a Visually Induced Arrest Behavior Via Corticotectal Projections." *Neuron* 86, no. 3 (May 06 2015): 755-67. http://dx.doi.org/10.1016/j.neuron.2015.03.048.

Lie, D. C., G. Dziewczapolski, A. R. Willhoite, B. K. Kaspar, C. W. Shults, and F. H. Gage. "The Adult Substantia Nigra Contains Progenitor Cells with Neurogenic Potential." *J Neurosci* 22, no. 15 (Aug 01 2002): 6639-49. http://dx.doi.org/20026700.

Ligon, K. L., S. Kesari, M. Kitada, T. Sun, H. A. Arnett, J. A. Alberta, D. J. Anderson, C. D. Stiles, and D. H. Rowitch. "Development of Ng2 Neural Progenitor Cells Requires Olig Gene Function." *Proc Natl Acad Sci U S A* 103, no. 20 (May 16 2006): 7853-8. http://dx.doi.org/10.1073/pnas.0511001103.

Lindvall, O. and A. Bjorklund. "First Step Towards Cell Therapy for Huntington's Disease." *Lancet* 356, no. 9246 (Dec 09 2000): 1945-6. http://dx.doi.org/10.1016/S0140-6736(00)03302-X.

Lindvall, O., Z. Kokaia, and A. Martinez-Serrano. "Stem Cell Therapy for Human Neurodegenerative Disorders-How to Make It Work." *Nat Med* 10 Suppl (Jul 2004): S42-50. http://dx.doi.org/10.1038/nm1064.

Liu, X., S. Ramirez, P. T. Pang, C. B. Puryear, A. Govindarajan, K. Deisseroth, and S. Tonegawa. "Optogenetic Stimulation of a Hippocampal Engram Activates Fear Memory Recall." *Nature* 484, no. 7394 (Mar 22 2012): 381-5. http://dx.doi.org/10.1038/nature11028.

Liu, Y. J., M. U. Ehrengruber, M. Negwer, H. J. Shao, A. H. Cetin, and D. C. Lyon. "Tracing Inputs to Inhibitory or Excitatory Neurons of Mouse and Cat Visual Cortex with a Targeted Rabies Virus." *Curr Biol* 23, no. 18 (Sep 23 2013): 1746-55. http://dx.doi.org/10.1016/j.cub.2013.07.033.

Liu, Y., J. Suckale, J. Masjkur, M. G. Magro, A. Steffen, K. Anastassiadis, and M. Solimena. "Tamoxifen-Independent Recombination in the Rip-Creer Mouse." *PLoS One* 5, no. 10 (Oct 22 2010): e13533. http://dx.doi.org/10.1371/journal.pone.0013533.

Liu, Z., Y. Li, Y. Cui, C. Roberts, M. Lu, U. Wilhelmsson, M. Pekny, and M. Chopp. "Beneficial Effects of Gfap/Vimentin Reactive Astrocytes for Axonal Remodeling and Motor Behavioral Recovery in Mice after Stroke." *Glia* 62, no. 12 (Dec 2014): 2022-33. http://dx.doi.org/10.1002/glia.22723.

Livneh, Y., Y. Adam, and A. Mizrahi. "Odor Processing by Adult-Born Neurons." *Neuron* 81, no. 5 (Mar 05 2014): 1097-110. http://dx.doi.org/10.1016/j.neuron.2014.01.007.

Lois, C. and A. Alvarez-Buylla. "Proliferating Subventricular Zone Cells in the Adult Mammalian Forebrain Can Differentiate into Neurons and Glia." *Proc Natl Acad Sci U S A* 90, no. 5 (Mar 01 1993): 2074-7. https://www.ncbi.nlm.nih.gov/pubmed/8446631.

Lois, C. and A. Alvarez-Buylla. "Long-Distance Neuronal Migration in the Adult Mammalian Brain." *Science* 264, no. 5162 (May 20 1994): 1145-8. https://www.ncbi.nlm.nih.gov/pubmed/8178174.

Longair, M. H., D. A. Baker, and J. D. Armstrong. "Simple Neurite Tracer: Open Source Software for Reconstruction, Visualization and Analysis of Neuronal Processes." *Bioinformatics* 27, no. 17 (Sep 01 2011): 2453-4. http://dx.doi.org/10.1093/bioinformatics/btr390.

Ludwig, A., P. Uvarov, S. Soni, J. Thomas-Crusells, M. S. Airaksinen, and C. Rivera. "Early Growth Response 4 Mediates Bdnf Induction of Potassium Chloride Cotransporter 2 Transcription." *J Neurosci* 31, no. 2 (Jan 12 2011): 644-9. http://dx.doi.org/10.1523/JNEUROSCI.2006-10.2011.

Luebke, J. I. "Pyramidal Neurons Are Not Generalizable Building Blocks of Cortical Networks." *Front Neuroanat* 11 (2017): 11. http://dx.doi.org/10.3389/fnana.2017.00011.

Lund, J. S., R. G. Boothe, and R. D. Lund. "Development of Neurons in the Visual Cortex (Area 17) of the Monkey (Macaca Nemestrina): A Golgi Study from Fetal Day 127 to Postnatal Maturity." *J Comp Neurol* 176, no. 2 (Nov 15 1977): 149-88. http://dx.doi.org/10.1002/cne.901760203.

Lund, J. S., R. D. Lund, A. E. Hendrickson, A. H. Bunt, and A. F. Fuchs. "The Origin of Efferent Pathways from the Primary Visual Cortex, Area 17, of the Macaque Monkey as Shown by Retrograde Transport of Horseradish Peroxidase." *J Comp Neurol* 164, no. 3 (Dec 01 1975): 287-303. http://dx.doi.org/10.1002/cne.901640303.

Lur, G., M. A. Vinck, L. Tang, J. A. Cardin, and M. J. Higley. "Projection-Specific Visual Feature Encoding by Layer 5 Cortical Subnetworks." *Cell Rep* 14, no. 11 (Mar 22 2016): 2538-45. http://dx.doi.org/10.1016/j.celrep.2016.02.050.

Machin, David, Yin Bun Cheung, Mahesh K. B. Parmar, and Mahesh K. B. Parmar. *Survival Analysis : A Practical Approach*. 2nd ed. Chichester, West Sussex, England ; Hoboken, NJ: John Wiley & Sons, 2006.

Macklis, J. D. "Transplanted Neocortical Neurons Migrate Selectively into Regions of Neuronal Degeneration Produced by Chromophore-Targeted Laser Photolysis." *J Neurosci* 13, no. 9 (Sep 1993): 3848-63. https://www.ncbi.nlm.nih.gov/pubmed/8366349.

Macklis, J. D. and R. D. Madison. "Neuroblastoma Grafts Are Noninvasively Removed within Mouse Neocortex by Selective Laser Activation of Intracellular Photolytic Chromophore." *J Neurosci* 11, no. 7 (Jul 1991): 2055-62. https://www.ncbi.nlm.nih.gov/pubmed/2066774.

Madisen, L., T. A. Zwingman, S. M. Sunkin, S. W. Oh, H. A. Zariwala, H. Gu, L. L. Ng, R. D. Palmiter, M. J. Hawrylycz, A. R. Jones, E. S. Lein, and H. Zeng. "A Robust and High-Throughput Cre Reporting and Characterization System for the Whole Mouse Brain." *Nat Neurosci* 13, no. 1 (Jan 2010): 133-40. http://dx.doi.org/10.1038/nn.2467.

Madison, R. D. and J. D. Macklis. "Noninvasively Induced Degeneration of Neocortical Pyramidal Neurons in Vivo: Selective Targeting by Laser Activation of Retrogradely Transported Photolytic Chromophore." *Exp Neurol* 121, no. 2 (Jun 1993): 153-9. http://dx.doi.org/10.1006/exnr.1993.1082.

Magavi, S. S., B. R. Leavitt, and J. D. Macklis. "Induction of Neurogenesis in the Neocortex of Adult Mice." *Nature* 405, no. 6789 (Jun 22 2000): 951-5. http://dx.doi.org/10.1038/35016083.

Magby, J. P., C. Bi, Z. Y. Chen, F. S. Lee, and M. R. Plummer. "Single-Cell Characterization of Retrograde Signaling by Brain-Derived Neurotrophic Factor." *J Neurosci* 26, no. 52 (Dec 27 2006): 13531-6. http://dx.doi.org/10.1523/JNEUROSCI.4576-06.2006.

Maggi, R., J. Zasso, and L. Conti. "Neurodevelopmental Origin and Adult Neurogenesis of the Neuroendocrine Hypothalamus." *Front Cell Neurosci* 8 (2014): 440. http://dx.doi.org/10.3389/fncel.2014.00440.

Mank, M., A. F. Santos, S. Direnberger, T. D. Mrsic-Flogel, S. B. Hofer, V. Stein, T. Hendel, D. F. Reiff, C. Levelt, A. Borst, T. Bonhoeffer, M. Hubener, and O. Griesbeck. "A Genetically Encoded Calcium Indicator for Chronic in Vivo Two-Photon Imaging." *Nat Methods* 5, no. 9 (Sep 2008): 805-11. http://dx.doi.org/10.1038/nmeth.1243.

Marciano, P. G., J. H. Eberwine, R. Ragupathi, K. E. Saatman, D. F. Meaney, and T. K. McIntosh. "Expression Profiling Following Traumatic Brain Injury: A Review." *Neurochem Res* 27, no. 10 (Oct 2002): 1147-55. https://www.ncbi.nlm.nih.gov/pubmed/12462413.

Marcus, R. C., R. Blazeski, P. Godement, and C. A. Mason. "Retinal Axon Divergence in the Optic Chiasm: Uncrossed Axons Diverge from Crossed Axons within a Midline Glial Specialization." *J Neurosci* 15, no. 5 Pt 2 (May 1995): 3716-29. https://www.ncbi.nlm.nih.gov/pubmed/7751940.

Margolis, D. J., H. Lutcke, K. Schulz, F. Haiss, B. Weber, S. Kugler, M. T. Hasan, and F. Helmchen. "Reorganization of Cortical Population Activity Imaged Throughout Long-Term Sensory Deprivation." *Nat Neurosci* 15, no. 11 (Nov 2012): 1539-46. http://dx.doi.org/10.1038/nn.3240.

Marik, S. A., H. Yamahachi, J. N. McManus, G. Szabo, and C. D. Gilbert. "Axonal Dynamics of Excitatory and Inhibitory Neurons in Somatosensory Cortex." *PLoS Biol* 8, no. 6 (Jun 15 2010): e1000395. http://dx.doi.org/10.1371/journal.pbio.1000395.

Marin-Padilla, M. "The Mammalian Neocortex New Pyramidal Neuron: A New Conception." *Front Neuroanat* 7 (Jan 06 2014): 51. http://dx.doi.org/10.3389/fnana.2013.00051.

Marion, D. W., I. F. Pollack, and R. D. Lund. "Patterns of Immune Rejection of Mouse Neocortex Transplanted into Neonatal Rat Brain, and Effects of Host Immunosuppression." *Brain Res* 519, no. 1-2 (Jun 11 1990): 133-43. https://www.ncbi.nlm.nih.gov/pubmed/2397402.

Markakis, E. A., T. D. Palmer, L. Randolph-Moore, P. Rakic, and F. H. Gage. "Novel Neuronal Phenotypes from Neural Progenitor Cells." *J Neurosci* 24, no. 12 (Mar 24 2004): 2886-97. http://dx.doi.org/10.1523/JNEUROSCI.4161-03.2004.

Markopoulos, F., D. Rokni, D. H. Gire, and V. N. Murthy. "Functional Properties of Cortical Feedback Projections to the Olfactory Bulb." *Neuron* 76, no. 6 (Dec 20 2012): 1175-88. http://dx.doi.org/10.1016/j.neuron.2012.10.028.

Marques, C., W. Guo, P. Pereira, A. Taylor, C. Patterson, P. C. Evans, and F. Shang. "The Triage of Damaged Proteins: Degradation by the Ubiquitin-Proteasome Pathway or Repair by Molecular Chaperones." *FASEB J* 20, no. 6 (Apr 2006): 741-3. http://dx.doi.org/10.1096/fj.05-5080fje.

Marrs, G. S., S. H. Green, and M. E. Dailey. "Rapid Formation and Remodeling of Postsynaptic Densities in Developing Dendrites." *Nat Neurosci* 4, no. 10 (Oct 2001): 1006-13. http://dx.doi.org/10.1038/nn717.

Marshel, J. H., M. E. Garrett, I. Nauhaus, and E. M. Callaway. "Functional Specialization of Seven Mouse Visual Cortical Areas." *Neuron* 72, no. 6 (Dec 22 2011): 1040-54. http://dx.doi.org/10.1016/j.neuron.2011.12.004.

Marshel, J. H., T. Mori, K. J. Nielsen, and E. M. Callaway. "Targeting Single Neuronal Networks for Gene Expression and Cell Labeling in Vivo." *Neuron* 67, no. 4 (Aug 26 2010): 562-74. http://dx.doi.org/10.1016/j.neuron.2010.08.001.

Matreyek, K. A. and A. Engelman. "Viral and Cellular Requirements for the Nuclear Entry of Retroviral Preintegration Nucleoprotein Complexes." *Viruses* 5, no. 10 (Oct 07 2013): 2483-511. http://dx.doi.org/10.3390/v5102483.

Matsutani, S. and N. Yamamoto. "Centrifugal Innervation of the Mammalian Olfactory Bulb." *Anat Sci Int* 83, no. 4 (Dec 2008): 218-27. http://dx.doi.org/10.1111/j.1447-073X.2007.00223.x.

Mattioni, T., J. F. Louvion, and D. Picard. "Regulation of Protein Activities by Fusion to Steroid Binding Domains." *Methods Cell Biol* 43 Pt A (1994): 335-52. https://www.ncbi.nlm.nih.gov/pubmed/7823870.

Maxwell, D. S. and L. Kruger. "The Fine Structure of Astrocytes in the Cerebral Cortex and Their Response to Focal Injury Produced by Heavy Ionizing Particles." *J Cell Biol* 25, no. 2 (May 01 1965): 141-57. https://www.ncbi.nlm.nih.gov/pubmed/19866658.

Mazurek, M., M. Kager, and S. D. Van Hooser. "Robust Quantification of Orientation Selectivity and Direction Selectivity." *Front Neural Circuits* 8 (2014): 92. http://dx.doi.org/10.3389/fncir.2014.00092.

McAllister, A. K., L. C. Katz, and D. C. Lo. "Neurotrophin Regulation of Cortical Dendritic Growth Requires Activity." *Neuron* 17, no. 6 (Dec 1996): 1057-64. https://www.ncbi.nlm.nih.gov/pubmed/8982155.

McAllister, A. K., L. C. Katz, and D. C. Lo. "Opposing Roles for Endogenous Bdnf and Nt-3 in Regulating Cortical Dendritic Growth." *Neuron* 18, no. 5 (May 1997): 767-78. https://www.ncbi.nlm.nih.gov/pubmed/9182801.

McAllister, A. K., D. C. Lo, and L. C. Katz. "Neurotrophins Regulate Dendritic Growth in Developing Visual Cortex." *Neuron* 15, no. 4 (Oct 1995): 791-803. https://www.ncbi.nlm.nih.gov/pubmed/7576629.

McHugh, T. J., M. W. Jones, J. J. Quinn, N. Balthasar, R. Coppari, J. K. Elmquist, B. B. Lowell, M. S. Fanselow, M. A. Wilson, and S. Tonegawa. "Dentate Gyrus Nmda Receptors Mediate Rapid Pattern Separation in the Hippocampal Network." *Science* 317, no. 5834 (Jul 06 2007): 94-9. http://dx.doi.org/10.1126/science.1140263.

McKeon, R. J., M. J. Jurynec, and C. R. Buck. "The Chondroitin Sulfate Proteoglycans Neurocan and Phosphacan Are Expressed by Reactive Astrocytes in the Chronic Cns Glial Scar." *J Neurosci* 19, no. 24 (Dec 15 1999): 10778-88. https://www.ncbi.nlm.nih.gov/pubmed/10594061.

McKeon, R. J., R. C. Schreiber, J. S. Rudge, and J. Silver. "Reduction of Neurite Outgrowth in a Model of Glial Scarring Following Cns Injury Is Correlated with the Expression of Inhibitory Molecules on Reactive Astrocytes." *J Neurosci* 11, no. 11 (Nov 1991): 3398-411. https://www.ncbi.nlm.nih.gov/pubmed/1719160.

Meacham, G. C., C. Patterson, W. Zhang, J. M. Younger, and D. M. Cyr. "The Hsc70 Co-Chaperone Chip Targets Immature Cftr for Proteasomal Degradation." *Nat Cell Biol* 3, no. 1 (Jan 2001): 100-5. http://dx.doi.org/10.1038/35050509.

Meisami, E. and S. Hamedi. "Relative Contribution of Brain and Peripheral Connections to Postnatal Growth and Cell Accretion in the Rat Olfactory Bulb." *Brain Res* 394, no. 2 (Oct 1986): 282-6. https://www.ncbi.nlm.nih.gov/pubmed/3768730.

Mendizabal-Zubiaga, J. L., C. Reblet, and J. L. Bueno-Lopez. "The Underside of the Cerebral Cortex: Layer V/Vi Spiny Inverted Neurons." *J Anat* 211, no. 2 (Aug 2007): 223-36. http://dx.doi.org/10.1111/j.1469-7580.2007.00779.x.

Mercier, F., J. T. Kitasako, and G. I. Hatton. "Anatomy of the Brain Neurogenic Zones Revisited: Fractones and the Fibroblast/Macrophage Network." *J Comp Neurol* 451, no. 2 (Sep 16 2002): 170-88. http://dx.doi.org/10.1002/cne.10342.

Mevorach, D., J. L. Zhou, X. Song, and K. B. Elkon. "Systemic Exposure to Irradiated Apoptotic Cells Induces Autoantibody Production." *J Exp Med* 188, no. 2 (Jul 20 1998): 387-92. https://www.ncbi.nlm.nih.gov/pubmed/9670050.

Michelsen, K. A., S. Acosta-Verdugo, M. Benoit-Marand, I. Espuny-Camacho, N. Gaspard, B. Saha, A. Gaillard, and P. Vanderhaeghen. "Area-Specific Reestablishment of Damaged Circuits in the Adult Cerebral Cortex by Cortical Neurons Derived from Mouse Embryonic Stem Cells." *Neuron* 85, no. 5 (Mar 04 2015): 982-97. http://dx.doi.org/10.1016/j.neuron.2015.02.001.

Milev, P., D. R. Friedlander, T. Sakurai, L. Karthikeyan, M. Flad, R. K. Margolis, M. Grumet, and R. U. Margolis. "Interactions of the Chondroitin Sulfate Proteoglycan Phosphacan, the Extracellular Domain of a Receptor-Type Protein Tyrosine Phosphatase, with Neurons, Glia, and Neural Cell Adhesion Molecules." *J Cell Biol* 127, no. 6 Pt 1 (Dec 1994): 1703-15. https://www.ncbi.nlm.nih.gov/pubmed/7528221.

Miller, M. "Maturation of Rat Visual Cortex. I. A Quantitative Study of Golgi-Impregnated Pyramidal Neurons." *J Neurocytol* 10, no. 5 (Oct 1981): 859-78. https://www.ncbi.nlm.nih.gov/pubmed/6171624.

Miller, M. and A. Peters. "Maturation of Rat Visual Cortex. Ii. A Combined Golgi-Electron Microscope Study of Pyramidal Neurons." *J Comp Neurol* 203, no. 4 (Dec 20 1981): 555-73. http://dx.doi.org/10.1002/cne.902030402.

Miller, M. W. "Maturation of Rat Visual Cortex: Iv. The Generation, Migration, Morphogenesis, and Connectivity of Atypically Oriented Pyramidal Neurons." *J Comp Neurol* 274, no. 3 (Aug 15 1988): 387-405. http://dx.doi.org/10.1002/cne.902740308.

Miller, M. W. and B. A. Vogt. "Heterotopic and Homotopic Callosal Connections in Rat Visual Cortex." *Brain Res* 297, no. 1 (Apr 09 1984): 75-89. https://www.ncbi.nlm.nih.gov/pubmed/6722538.

Ming, G. L. and H. Song. "Adult Neurogenesis in the Mammalian Central Nervous System." *Annu Rev Neurosci* 28 (2005): 223-50. http://dx.doi.org/10.1146/annurev.neuro.28.051804.101459.

Ming, G. L. and H. Song. "Adult Neurogenesis in the Mammalian Brain: Significant Answers and Significant Questions." *Neuron* 70, no. 4 (May 26 2011): 687-702. http://dx.doi.org/10.1016/j.neuron.2011.05.001.

Miyake, T., T. Hattori, M. Fukuda, T. Kitamura, and S. Fujita. "Quantitative Studies on Proliferative Changes of Reactive Astrocytes in Mouse Cerebral Cortex." *Brain Res* 451, no. 1-2 (Jun 07 1988): 133-8. https://www.ncbi.nlm.nih.gov/pubmed/3251580.

Mizuno, H., T. Hirano, and Y. Tagawa. "Evidence for Activity-Dependent Cortical Wiring: Formation of Interhemispheric Connections in Neonatal Mouse Visual Cortex Requires Projection Neuron Activity." *J Neurosci* 27, no. 25 (Jun 20 2007): 6760-70. http://dx.doi.org/10.1523/JNEUROSCI.1215-07.2007.

Molyneaux, B. J., P. Arlotta, R. M. Fame, J. L. MacDonald, K. L. MacQuarrie, and J. D. Macklis. "Novel Subtype-Specific Genes Identify Distinct Subpopulations of Callosal Projection Neurons." *J Neurosci* 29, no. 39 (Sep 30 2009): 12343-54. http://dx.doi.org/10.1523/JNEUROSCI.6108-08.2009.

Morgenstern, D. A., R. A. Asher, and J. W. Fawcett. "Chondroitin Sulphate Proteoglycans in the Cns Injury Response." *Prog Brain Res* 137 (2002): 313-32. https://www.ncbi.nlm.nih.gov/pubmed/12440375.

Morgenstern, N. A., J. Bourg, and L. Petreanu. "Multilaminar Networks of Cortical Neurons Integrate Common Inputs from Sensory Thalamus." *Nat Neurosci* 19, no. 8 (Aug 2016): 1034-40. http://dx.doi.org/10.1038/nn.4339.

Mori, K., H. Nagao, and Y. Yoshihara. "The Olfactory Bulb: Coding and Processing of Odor Molecule Information." *Science* 286, no. 5440 (Oct 22 1999): 711-5. https://www.ncbi.nlm.nih.gov/pubmed/10531048.

Mori, T., K. Tanaka, A. Buffo, W. Wurst, R. Kuhn, and M. Gotz. "Inducible Gene Deletion in Astroglia and Radial Glia--a Valuable Tool for Functional and Lineage Analysis." *Glia* 54, no. 1 (Jul 2006): 21-34. http://dx.doi.org/10.1002/glia.20350.

Morishima, M., K. Morita, Y. Kubota, and Y. Kawaguchi. "Highly Differentiated Projection-Specific Cortical Subnetworks." *J Neurosci* 31, no. 28 (Jul 13 2011): 10380-91. http://dx.doi.org/10.1523/JNEUROSCI.0772-11.2011.

Mostany, R., J. E. Anstey, K. L. Crump, B. Maco, G. Knott, and C. Portera-Cailliau. "Altered Synaptic Dynamics During Normal Brain Aging." *J Neurosci* 33, no. 9 (Feb 27 2013): 4094-104. http://dx.doi.org/10.1523/JNEUROSCI.4825-12.2013.

Mullen, R. J., C. R. Buck, and A. M. Smith. "Neun, a Neuronal Specific Nuclear Protein in Vertebrates." *Development* 116, no. 1 (Sep 1992): 201-11. https://www.ncbi.nlm.nih.gov/pubmed/1483388.

Murphy, G. J., D. P. Darcy, and J. S. Isaacson. "Intraglomerular Inhibition: Signaling Mechanisms of an Olfactory Microcircuit." *Nat Neurosci* 8, no. 3 (Mar 2005): 354-64. http://dx.doi.org/10.1038/nn1403.

Nafstad, P. H. "An Electron Microscope Study on the Termination of the Perforant Path Fibres in the Hippocampus and the Fascia Dentata." *Z Zellforsch Mikrosk Anat* 76, no. 4 (1967): 532-42. https://www.ncbi.nlm.nih.gov/pubmed/5585500.

Nagata, S., H. Nagase, K. Kawane, N. Mukae, and H. Fukuyama. "Degradation of Chromosomal DNA During Apoptosis." *Cell Death Differ* 10, no. 1 (Jan 2003): 108-16. http://dx.doi.org/10.1038/sj.cdd.4401161.

Najac, M., A. Sanz Diez, A. Kumar, N. Benito, S. Charpak, and D. De Saint Jan. "Intraglomerular Lateral Inhibition Promotes Spike Timing Variability in Principal Neurons of the Olfactory Bulb." *J Neurosci* 35, no. 10 (Mar 11 2015): 4319-31. http://dx.doi.org/10.1523/JNEUROSCI.2181-14.2015.

Nakagomi, T., S. Kubo, A. Nakano-Doi, R. Sakuma, S. Lu, A. Narita, M. Kawahara, A. Taguchi, and T. Matsuyama. "Brain Vascular Pericytes Following Ischemia Have Multipotential Stem Cell Activity to Differentiate into Neural and Vascular Lineage Cells." *Stem Cells* 33, no. 6 (Jun 2015): 1962-74. http://dx.doi.org/10.1002/stem.1977.

Nakamura, T., M. C. Colbert, and J. Robbins. "Neural Crest Cells Retain Multipotential Characteristics in the Developing Valves and Label the Cardiac Conduction System." *Circ Res* 98, no. 12 (Jun 23 2006): 1547-54. http://dx.doi.org/10.1161/01.RES.0000227505.19472.69.

Nakatomi, H., T. Kuriu, S. Okabe, S. Yamamoto, O. Hatano, N. Kawahara, A. Tamura, T. Kirino, and M. Nakafuku. "Regeneration of Hippocampal Pyramidal Neurons after Ischemic Brain Injury by Recruitment of Endogenous Neural Progenitors." *Cell* 110, no. 4 (Aug 23 2002): 429-41. https://www.ncbi.nlm.nih.gov/pubmed/12202033.

Napirei, Markus and Hans Georg Mannherz. "Molecules Involved in Recognition and Clearance of Apoptotic/Necrotic Cellsand Cell Debris." In *Phagocytosis of Dying Cells: From Molecular Mechanisms to Human Diseases*, edited by Dmitri V. Krysko and Peter Vandenabeele, 103-45. Dordrecht: Springer Netherlands, 2009.

Narciso, L., E. Parlanti, M. Racaniello, V. Simonelli, A. Cardinale, D. Merlo, and E. Dogliotti. "The Response to Oxidative DNA Damage in Neurons: Mechanisms and Disease." *Neural Plast* 2016 (2016): 3619274. http://dx.doi.org/10.1155/2016/3619274.

Nauhaus, I., K. J. Nielsen, and E. M. Callaway. "Nonlinearity of Two-Photon Ca2+ Imaging Yields Distorted Measurements of Tuning for V1 Neuronal Populations." *J Neurophysiol* 107, no. 3 (Feb 2012): 923-36. http://dx.doi.org/10.1152/jn.00725.2011.

Nedivi, E., A. Javaherian, I. Cantallops, and H. T. Cline. "Developmental Regulation of Cpg15 Expression in Xenopus." *J Comp Neurol* 435, no. 4 (Jul 09 2001): 464-73. https://www.ncbi.nlm.nih.gov/pubmed/11406826.

Nedivi, E., G. Y. Wu, and H. T. Cline. "Promotion of Dendritic Growth by Cpg15, an Activity-Induced Signaling Molecule." *Science* 281, no. 5384 (Sep 18 1998): 1863-6. https://www.ncbi.nlm.nih.gov/pubmed/9743502.

Neudegger, T., J. Verghese, M. Hayer-Hartl, F. U. Hartl, and A. Bracher. "Structure of Human Heat-Shock Transcription Factor 1 in Complex with DNA." *Nat Struct Mol Biol* 23, no. 2 (Feb 2016): 140-6. http://dx.doi.org/10.1038/nsmb.3149.

Neumeister, B., A. Grabosch, O. Basak, R. Kemler, and V. Taylor. "Neural Progenitors of the Postnatal and Adult Mouse Forebrain Retain the Ability to Self-Replicate, Form Neurospheres, and Undergo Multipotent Differentiation in Vivo." *Stem Cells* 27, no. 3 (Mar 2009): 714-23. http://dx.doi.org/10.1634/stemcells.2008-0985.

Niell, C. M. and M. P. Stryker. "Highly Selective Receptive Fields in Mouse Visual Cortex." *J Neurosci* 28, no. 30 (Jul 23 2008): 7520-36. http://dx.doi.org/10.1523/JNEUROSCI.0623-08.2008.

Nieto, M., E. S. Monuki, H. Tang, J. Imitola, N. Haubst, S. J. Khoury, J. Cunningham, M. Gotz, and C. A. Walsh. "Expression of Cux-1 and Cux-2 in the Subventricular Zone and Upper Layers Ii-Iv of the Cerebral Cortex." *J Comp Neurol* 479, no. 2 (Nov 08 2004): 168-80. http://dx.doi.org/10.1002/cne.20322.

Nieuwenhuys, R. "The Neocortex. An Overview of Its Evolutionary Development, Structural Organization and Synaptology." *Anat Embryol (Berl)* 190, no. 4 (Oct 1994): 307-37. https://www.ncbi.nlm.nih.gov/pubmed/7840420.

Nimmerjahn, A., F. Kirchhoff, and F. Helmchen. "Resting Microglial Cells Are Highly Dynamic Surveillants of Brain Parenchyma in Vivo." *Science* 308, no. 5726 (May 27 2005): 1314-8. http://dx.doi.org/10.1126/science.1110647.

Ninkovic, J., T. Mori, and M. Gotz. "Distinct Modes of Neuron Addition in Adult Mouse Neurogenesis." *J Neurosci* 27, no. 40 (Oct 03 2007): 10906-11. http://dx.doi.org/10.1523/JNEUROSCI.2572-07.2007.

Ninomiya, M., T. Yamashita, N. Araki, H. Okano, and K. Sawamoto. "Enhanced Neurogenesis in the Ischemic Striatum Following Egf-Induced Expansion of Transit-Amplifying Cells in the Subventricular Zone." *Neurosci Lett* 403, no. 1-2 (Jul 31 2006): 63-7. http://dx.doi.org/10.1016/j.neulet.2006.04.039.

Nishiyama, A., M. Komitova, R. Suzuki, and X. Zhu. "Polydendrocytes (Ng2 Cells): Multifunctional Cells with Lineage Plasticity." *Nat Rev Neurosci* 10, no. 1 (Jan 2009): 9-22. http://dx.doi.org/10.1038/nrn2495.

Nishiyama, A., R. Suzuki, and X. Zhu. "Ng2 Cells (Polydendrocytes) in Brain Physiology and Repair." *Front Neurosci* 8 (2014): 133. http://dx.doi.org/10.3389/fnins.2014.00133.

Niu, W., T. Zang, Y. Zou, S. Fang, D. K. Smith, R. Bachoo, and C. L. Zhang. "In Vivo Reprogramming of Astrocytes to Neuroblasts in the Adult Brain." *Nat Cell Biol* 15, no. 10 (Oct 2013): 1164-75. http://dx.doi.org/10.1038/ncb2843.

Noctor, S. C., A. C. Flint, T. A. Weissman, R. S. Dammerman, and A. R. Kriegstein. "Neurons Derived from Radial Glial Cells Establish Radial Units in Neocortex." *Nature* 409, no. 6821 (Feb 08 2001): 714-20. http://dx.doi.org/10.1038/35055553.

Nunes, M. C., N. S. Roy, H. M. Keyoung, R. R. Goodman, G. McKhann, 2nd, L. Jiang, J. Kang, M. Nedergaard, and S. A. Goldman. "Identification and Isolation of Multipotential Neural Progenitor Cells from the Subcortical White Matter of the Adult Human Brain." *Nat Med* 9, no. 4 (Apr 2003): 439-47. http://dx.doi.org/10.1038/nm837.

Oh, S. W., J. A. Harris, L. Ng, B. Winslow, N. Cain, S. Mihalas, Q. Wang, C. Lau, L. Kuan, A. M. Henry, M. T. Mortrud, B. Ouellette, T. N. Nguyen, S. A. Sorensen, C. R. Slaughterbeck, W. Wakeman, Y. Li, D. Feng, A. Ho, E. Nicholas, K. E. Hirokawa, P. Bohn, K. M. Joines, H. Peng, M. J. Hawrylycz, J. W. Phillips, J. G. Hohmann, P. Wohnoutka, C. R. Gerfen, C. Koch, A. Bernard, C. Dang, A. R. Jones, and H. Zeng. "A Mesoscale Connectome of the Mouse Brain." *Nature* 508, no. 7495 (Apr 10 2014): 207-14. http://dx.doi.org/10.1038/nature13186.

Ohira, K., T. Furuta, H. Hioki, K. C. Nakamura, E. Kuramoto, Y. Tanaka, N. Funatsu, K. Shimizu, T. Oishi, M. Hayashi, T. Miyakawa, T. Kaneko, and S. Nakamura. "Ischemia-Induced Neurogenesis of Neocortical Layer 1 Progenitor Cells." *Nat Neurosci* 13, no. 2 (Feb 2010): 173-9. http://dx.doi.org/10.1038/nn.2473.

Ohki, K., S. Chung, Y. H. Ch'ng, P. Kara, and R. C. Reid. "Functional Imaging with Cellular Resolution Reveals Precise Micro-Architecture in Visual Cortex." *Nature* 433, no. 7026 (Feb 10 2005): 597-603. http://dx.doi.org/10.1038/nature03274.

Ohori, Y., S. Yamamoto, M. Nagao, M. Sugimori, N. Yamamoto, K. Nakamura, and M. Nakafuku. "Growth Factor Treatment and Genetic Manipulation Stimulate Neurogenesis and Oligodendrogenesis by Endogenous Neural Progenitors in the Injured Adult Spinal Cord." *J Neurosci* 26, no. 46 (Nov 15 2006): 11948-60. http://dx.doi.org/10.1523/JNEUROSCI.3127-06.2006.

Okura, Y., R. Tanaka, K. Ono, S. Yoshida, N. Tanuma, and Y. Matsumoto. "Immunohistochemical Analysis on the Rejection of Xenogeneic Brain Grafts." *Restor Neurol Neurosci* 11, no. 4 (Jan 01 1997): 177-87. http://dx.doi.org/10.3233/RNN-1997-11401.

Olanow, C. W., C. G. Goetz, J. H. Kordower, A. J. Stoessl, V. Sossi, M. F. Brin, K. M. Shannon, G. M. Nauert, D. P. Perl, J. Godbold, and T. B. Freeman. "A Double-Blind Controlled Trial of Bilateral Fetal Nigral Transplantation in Parkinson's Disease." *Ann Neurol* 54, no. 3 (Sep 2003): 403-14. http://dx.doi.org/10.1002/ana.10720.

Olavarria, J., L. R. Mignano, and R. C. Van Sluyters. "Pattern of Extrastriate Visual Areas Connecting Reciprocally with Striate Cortex in the Mouse." *Exp Neurol* 78, no. 3 (Dec 1982): 775-9. https://www.ncbi.nlm.nih.gov/pubmed/7173380.

Olavarria, J. and V. M. Montero. "Organization of Visual Cortex in the Mouse Revealed by Correlating Callosal and Striate-Extrastriate Connections." *Vis Neurosci* 3, no. 1 (Jul 1989): 59-69. https://www.ncbi.nlm.nih.gov/pubmed/2487092.

Olavarria, J. and R. C. van Sluyters. "Callosal Connections of the Posterior Neocortex in Normal-Eyed, Congenitally Anophthalmic, and Neonatally Enucleated Mice." *J Comp Neurol* 230, no. 2 (Dec 01 1984): 249-68. http://dx.doi.org/10.1002/cne.902300209.

Olsen, S. R., D. S. Bortone, H. Adesnik, and M. Scanziani. "Gain Control by Layer Six in Cortical Circuits of Vision." *Nature* 483, no. 7387 (Feb 22 2012): 47-52. http://dx.doi.org/10.1038/nature10835.

Oyesiku, N. M., C. O. Evans, S. Houston, R. S. Darrell, J. S. Smith, Z. L. Fulop, C. E. Dixon, and D. G. Stein. "Regional Changes in the Expression of Neurotrophic Factors and Their Receptors Following Acute Traumatic Brain Injury in the Adult Rat Brain." *Brain Res* 833, no. 2 (Jul 03 1999): 161-72. https://www.ncbi.nlm.nih.gov/pubmed/10375691.

Packard, D. S., Jr., R. A. Menzies, and R. G. Skalko. "Incorportaiton of Thymidine and Its Analogue, Bromodeoxyuridine, into Embryos and Maternal Tissues of the Mouse." *Differentiation* 1, no. 6 (Dec 1973): 397-404. https://www.ncbi.nlm.nih.gov/pubmed/4802502.

Palmer, T. D., E. A. Markakis, A. R. Willhoite, F. Safar, and F. H. Gage. "Fibroblast Growth Factor-2 Activates a Latent Neurogenic Program in Neural Stem Cells from Diverse Regions of the Adult Cns." *J Neurosci* 19, no. 19 (Oct 01 1999): 8487-97. https://www.ncbi.nlm.nih.gov/pubmed/10493749.

Palmer, T. D., J. Ray, and F. H. Gage. "Fgf-2-Responsive Neuronal Progenitors Reside in Proliferative and Quiescent Regions of the Adult Rodent Brain." *Mol Cell Neurosci* 6, no. 5 (Oct 1995): 474-86. http://dx.doi.org/10.1006/mcne.1995.1035.

Parnaik, R., M. C. Raff, and J. Scholes. "Differences between the Clearance of Apoptotic Cells by Professional and Non-Professional Phagocytes." *Curr Biol* 10, no. 14 (Jul 13 2000): 857-60. https://www.ncbi.nlm.nih.gov/pubmed/10899007.

Parnavelas, J. G., R. A. Burne, and C. S. Lin. "Distribution and Morphology of Functionally Identified Neurons in the Visual Cortex of the Rat." *Brain Res* 261, no. 1 (Feb 14 1983): 21-9. https://www.ncbi.nlm.nih.gov/pubmed/6301626.

Pastrana, E., V. Silva-Vargas, and F. Doetsch. "Eyes Wide Open: A Critical Review of Sphere-Formation as an Assay for Stem Cells." *Cell Stem Cell* 8, no. 5 (May 06 2011): 486-98. http://dx.doi.org/10.1016/j.stem.2011.04.007.

Pekny, M. and M. Nilsson. "Astrocyte Activation and Reactive Gliosis." *Glia* 50, no. 4 (Jun 2005): 427-34. http://dx.doi.org/10.1002/glia.20207.

Perlow, M. J., W. J. Freed, B. J. Hoffer, A. Seiger, L. Olson, and R. J. Wyatt. "Brain Grafts Reduce Motor Abnormalities Produced by Destruction of Nigrostriatal Dopamine System." *Science* 204, no. 4393 (May 11 1979): 643-7. https://www.ncbi.nlm.nih.gov/pubmed/571147.

Persson, L. "Cellular Reactions to Small Cerebral Stab Wounds in the Rat Frontal Lobe. An Ultrastructural Study." *Virchows Arch B Cell Pathol* 22, no. 1 (Oct 18 1976): 21-37. https://www.ncbi.nlm.nih.gov/pubmed/827093.

Peter, Christoph, Sebastian Wesselborg, and Lauber Kirsten. "Role of Attraction and Danger Signals in the Uptake of Apoptotic and Necrotic Cells and Its Immunological Outcome." In *Phagocytosis of Dying Cells: From Molecular Mechanisms to Human Diseases*, edited by Dmitri V. Krysko and Peter Vandenabeele, 63-101. Dordrecht: Springer Netherlands, 2009.

Peters, A. and I. R. Kaiserman-Abramof. "The Small Pyramidal Neuron of the Rat Cerebral Cortex. The Perikaryon, Dendrites and Spines." *Am J Anat* 127, no. 4 (Apr 1970): 321-55. http://dx.doi.org/10.1002/aja.1001270402.

Petreanu, L. and A. Alvarez-Buylla. "Maturation and Death of Adult-Born Olfactory Bulb Granule Neurons: Role of Olfaction." *J Neurosci* 22, no. 14 (Jul 15 2002): 6106-13. http://dx.doi.org/20026588.

Picard, D. "Regulation of Protein Function through Expression of Chimaeric Proteins." *Curr Opin Biotechnol* 5, no. 5 (Oct 1994): 511-5. https://www.ncbi.nlm.nih.gov/pubmed/7765465.

Picard, D., B. Khursheed, M. J. Garabedian, M. G. Fortin, S. Lindquist, and K. R. Yamamoto. "Reduced Levels of Hsp90 Compromise Steroid Receptor Action in Vivo." *Nature* 348, no. 6297 (Nov 08 1990): 166-8. http://dx.doi.org/10.1038/348166a0.

Picard, D., S. J. Salser, and K. R. Yamamoto. "A Movable and Regulable Inactivation Function within the Steroid Binding Domain of the Glucocorticoid Receptor." *Cell* 54, no. 7 (Sep 23 1988): 1073-80. https://www.ncbi.nlm.nih.gov/pubmed/2843290.

Piccini, P., O. Lindvall, A. Bjorklund, P. Brundin, P. Hagell, R. Ceravolo, W. Oertel, N. Quinn, M. Samuel, S. Rehncrona, H. Widner, and D. J. Brooks. "Delayed Recovery of Movement-Related Cortical Function in

Parkinson's Disease after Striatal Dopaminergic Grafts." *Ann Neurol* 48, no. 5 (Nov 2000): 689-95. https://www.ncbi.nlm.nih.gov/pubmed/11079531.

Piccini, P., N. Pavese, P. Hagell, J. Reimer, A. Bjorklund, W. H. Oertel, N. P. Quinn, D. J. Brooks, and O. Lindvall. "Factors Affecting the Clinical Outcome after Neural Transplantation in Parkinson's Disease." *Brain* 128, no. Pt 12 (Dec 2005): 2977-86. http://dx.doi.org/10.1093/brain/awh649.

Pietrasanta, M., L. Restani, and M. Caleo. "The Corpus Callosum and the Visual Cortex: Plasticity Is a Game for Two." *Neural Plast* 2012 (2012): 838672. http://dx.doi.org/10.1155/2012/838672.

Pinching, A. J. and T. P. Powell. "Experimental Studies on the Axons Intrinsic to the Glomerular Layer of the Olfactory Bulb." *J Cell Sci* 10, no. 3 (May 1972): 637-55. https://www.ncbi.nlm.nih.gov/pubmed/5038409.

Pinto, L., D. Drechsel, M. T. Schmid, J. Ninkovic, M. Irmler, M. S. Brill, L. Restani, L. Gianfranceschi, C. Cerri, S. N. Weber, V. Tarabykin, K. Baer, F. Guillemot, J. Beckers, N. Zecevic, C. Dehay, M. Caleo, H. Schorle, and M. Gotz. "Ap2gamma Regulates Basal Progenitor Fate in a Region- and Layer-Specific Manner in the Developing Cortex." *Nat Neurosci* 12, no. 10 (Oct 2009): 1229-37. http://dx.doi.org/10.1038/nn.2399.

Pinto, L., M. J. Goard, D. Estandian, M. Xu, A. C. Kwan, S. H. Lee, T. C. Harrison, G. Feng, and Y. Dan. "Fast Modulation of Visual Perception by Basal Forebrain Cholinergic Neurons." *Nat Neurosci* 16, no. 12 (Dec 2013): 1857-63. http://dx.doi.org/10.1038/nn.3552.

Piscopo, D. M., R. N. El-Danaf, A. D. Huberman, and C. M. Niell. "Diverse Visual Features Encoded in Mouse Lateral Geniculate Nucleus." *J Neurosci* 33, no. 11 (Mar 13 2013): 4642-56. http://dx.doi.org/10.1523/JNEUROSCI.5187-12.2013.

Polleux, F., T. Morrow, and A. Ghosh. "Semaphorin 3a Is a Chemoattractant for Cortical Apical Dendrites." *Nature* 404, no. 6778 (Apr 06 2000): 567-73. http://dx.doi.org/10.1038/35007001.

Pontious, A., T. Kowalczyk, C. Englund, and R. F. Hevner. "Role of Intermediate Progenitor Cells in Cerebral Cortex Development." *Dev Neurosci* 30, no. 1-3 (2008): 24-32. http://dx.doi.org/10.1159/000109848.

Poon, I. K., C. D. Lucas, A. G. Rossi, and K. S. Ravichandran. "Apoptotic Cell Clearance: Basic Biology and Therapeutic Potential." *Nat Rev Immunol* 14, no. 3 (Mar 2014): 166-80. http://dx.doi.org/10.1038/nri3607.

Pratt, W. B. and D. O. Toft. "Regulation of Signaling Protein Function and Trafficking by the Hsp90/Hsp70-Based Chaperone Machinery." *Exp Biol Med (Maywood)* 228, no. 2 (Feb 2003): 111-33. https://www.ncbi.nlm.nih.gov/pubmed/12563018.

Prusky, G. T. and R. M. Douglas. "Characterization of Mouse Cortical Spatial Vision." *Vision Res* 44, no. 28 (Dec 2004): 3411-8. http://dx.doi.org/10.1016/j.visres.2004.09.001.

Purves, D. "Functional and Structural Changes in Mammalian Sympathetic Neurones Following Interruption of Their Axons." *J Physiol* 252, no. 2 (Nov 1975): 429-63. https://www.ncbi.nlm.nih.gov/pubmed/1206535.

Putz, U., C. Harwell, and E. Nedivi. "Soluble Cpg15 Expressed During Early Development Rescues Cortical Progenitors from Apoptosis." *Nat Neurosci* 8, no. 3 (Mar 2005): 322-31. http://dx.doi.org/10.1038/nn1407.

Raghupathi, R., T. K. McIntosh, and D. H. Smith. "Cellular Responses to Experimental Brain Injury." *Brain Pathol* 5, no. 4 (Oct 1995): 437-42. https://www.ncbi.nlm.nih.gov/pubmed/8974626.

Rebsam, A., P. Bhansali, and C. A. Mason. "Eye-Specific Projections of Retinogeniculate Axons Are Altered in Albino Mice." *J Neurosci* 32, no. 14 (Apr 04 2012): 4821-6. http://dx.doi.org/10.1523/JNEUROSCI.5050-11.2012.

Reese, B. E. "'Hidden Lamination' in the Dorsal Lateral Geniculate Nucleus: The Functional Organization of This Thalamic Region in the Rat." *Brain Res* 472, no. 2 (Apr-Jun 1988): 119-37. https://www.ncbi.nlm.nih.gov/pubmed/3289687.

Regehr, W. G., M. R. Carey, and A. R. Best. "Activity-Dependent Regulation of Synapses by Retrograde Messengers." *Neuron* 63, no. 2 (Jul 30 2009): 154-70. http://dx.doi.org/10.1016/j.neuron.2009.06.021.

Reid, R. C. and J. M. Alonso. "Specificity of Monosynaptic Connections from Thalamus to Visual Cortex." *Nature* 378, no. 6554 (Nov 16 1995): 281-4. http://dx.doi.org/10.1038/378281a0.

Reilly, Peter L. and Ross Bullock. *Head Injury : Pathophysiology & Management*. 2nd ed. London: Hodder Arnold, 2005.

Reynolds, B. A. and S. Weiss. "Generation of Neurons and Astrocytes from Isolated Cells of the Adult Mammalian Central Nervous System." *Science* 255, no. 5052 (Mar 27 1992): 1707-10. https://www.ncbi.nlm.nih.gov/pubmed/1553558.

Rhoades, R. W., R. D. Mooney, and S. E. Fish. "A Comparison of Visual Callosal Organization in Normal, Bilaterally Enucleated and Congenitally Anophthalmic Mice." *Exp Brain Res* 56, no. 1 (1984): 92-105. https://www.ncbi.nlm.nih.gov/pubmed/6468571.

Ribak, C. E. and L. A. Shapiro. "Ultrastructure and Synaptic Connectivity of Cell Types in the Adult Rat Dentate Gyrus." *Prog Brain Res* 163 (2007): 155-66. http://dx.doi.org/10.1016/S0079-6123(07)63009-X.

Richardson, W. D., K. M. Young, R. B. Tripathi, and I. McKenzie. "Ng2-Glia as Multipotent Neural Stem Cells: Fact or Fantasy?" *Neuron* 70, no. 4 (May 26 2011): 661-73. http://dx.doi.org/10.1016/j.neuron.2011.05.013.

Ridet, J. L., S. K. Malhotra, A. Privat, and F. H. Gage. "Reactive Astrocytes: Cellular and Molecular Cues to Biological Function." *Trends Neurosci* 20, no. 12 (Dec 1997): 570-7. https://www.ncbi.nlm.nih.gov/pubmed/9416670.

Rivera, C., J. Voipio, J. A. Payne, E. Ruusuvuori, H. Lahtinen, K. Lamsa, U. Pirvola, M. Saarma, and K. Kaila. "The K+/Cl- Co-Transporter Kcc2 Renders Gaba Hyperpolarizing During Neuronal Maturation." *Nature* 397, no. 6716 (Jan 21 1999): 251-5. http://dx.doi.org/10.1038/16697.

Rivers, L. E., K. M. Young, M. Rizzi, F. Jamen, K. Psachoulia, A. Wade, N. Kessaris, and W. D. Richardson. "Pdgfra/Ng2 Glia Generate Myelinating Oligodendrocytes and Piriform Projection Neurons in Adult Mice." *Nat Neurosci* 11, no. 12 (Dec 2008): 1392-401. http://dx.doi.org/10.1038/nn.2220.

Robel, S., B. Berninger, and M. Gotz. "The Stem Cell Potential of Glia: Lessons from Reactive Gliosis." *Nat Rev Neurosci* 12, no. 2 (Feb 2011): 88-104. http://dx.doi.org/10.1038/nrn2978.

Robins, S. C., I. Stewart, D. E. McNay, V. Taylor, C. Giachino, M. Goetz, J. Ninkovic, N. Briancon, E. Maratos-Flier, J. S. Flier, M. V. Kokoeva, and M. Placzek. "Alpha-Tanycytes of the Adult Hypothalamic Third Ventricle Include Distinct Populations of Fgf-Responsive Neural Progenitors." *Nat Commun* 4 (2013): 2049. http://dx.doi.org/10.1038/ncomms3049.

Rochefort, C., G. Gheusi, J. D. Vincent, and P. M. Lledo. "Enriched Odor Exposure Increases the Number of Newborn Neurons in the Adult Olfactory Bulb and Improves Odor Memory." *J Neurosci* 22, no. 7 (Apr 01 2002): 2679-89. http://dx.doi.org/20026260.

Rochefort, N. L., O. Garaschuk, R. I. Milos, M. Narushima, N. Marandi, B. Pichler, Y. Kovalchuk, and A. Konnerth. "Sparsification of Neuronal Activity in the Visual Cortex at Eye-Opening." *Proc Natl Acad Sci U S A* 106, no. 35 (Sep 01 2009): 15049-54. http://dx.doi.org/10.1073/pnas.0907660106.

Rochefort, N. L., M. Narushima, C. Grienberger, N. Marandi, D. N. Hill, and A. Konnerth. "Development of Direction Selectivity in Mouse Cortical Neurons." *Neuron* 71, no. 3 (Aug 11 2011): 425-32. http://dx.doi.org/10.1016/j.neuron.2011.06.013.

Roe, T., T. C. Reynolds, G. Yu, and P. O. Brown. "Integration of Murine Leukemia Virus DNA Depends on Mitosis." *EMBO J* 12, no. 5 (May 1993): 2099-108. https://www.ncbi.nlm.nih.gov/pubmed/8491198.

Rose, T., J. Jaepel, M. Hubener, and T. Bonhoeffer. "Cell-Specific Restoration of Stimulus Preference after Monocular Deprivation in the Visual Cortex." *Science* 352, no. 6291 (Jun 10 2016): 1319-22. http://dx.doi.org/10.1126/science.aad3358.

Rosser, A. E. and A. C. Bachoud-Levi. "Clinical Trials of Neural Transplantation in Huntington's Disease." *Prog Brain Res* 200 (2012): 345-71. http://dx.doi.org/10.1016/B978-0-444-59575-1.00016-8.

Roth, M. M., J. C. Dahmen, D. R. Muir, F. Imhof, F. J. Martini, and S. B. Hofer. "Thalamic Nuclei Convey Diverse Contextual Information to Layer 1 of Visual Cortex." *Nat Neurosci* 19, no. 2 (Feb 2016): 299-307. http://dx.doi.org/10.1038/nn.4197.

Roth, M. M., F. Helmchen, and B. M. Kampa. "Distinct Functional Properties of Primary and Posteromedial Visual Area of Mouse Neocortex." *J Neurosci* 32, no. 28 (Jul 11 2012): 9716-26. http://dx.doi.org/10.1523/JNEUROSCI.0110-12.2012.

Rothschild, G., I. Nelken, and A. Mizrahi. "Functional Organization and Population Dynamics in the Mouse Primary Auditory Cortex." *Nat Neurosci* 13, no. 3 (Mar 2010): 353-60. http://dx.doi.org/10.1038/nn.2484.

Rothstein, J. D., L. Martin, A. I. Levey, M. Dykes-Hoberg, L. Jin, D. Wu, N. Nash, and R. W. Kuncl. "Localization of Neuronal and Glial Glutamate Transporters." *Neuron* 13, no. 3 (Sep 1994): 713-25. https://www.ncbi.nlm.nih.gov/pubmed/7917301.

Rouaux, C. and P. Arlotta. "Direct Lineage Reprogramming of Post-Mitotic Callosal Neurons into Corticofugal Neurons in Vivo." *Nat Cell Biol* 15, no. 2 (Feb 2013): 214-21. http://dx.doi.org/10.1038/ncb2660.

Rovere, P., C. Vallinoto, A. Bondanza, M. C. Crosti, M. Rescigno, P. Ricciardi-Castagnoli, C. Rugarli, and A. A. Manfredi. "Bystander Apoptosis Triggers Dendritic Cell Maturation and Antigen-Presenting Function." *J Immunol* 161, no. 9 (Nov 01 1998): 4467-71. https://www.ncbi.nlm.nih.gov/pubmed/9794367.

Rudge, J. S. and J. Silver. "Inhibition of Neurite Outgrowth on Astroglial Scars in Vitro." *J Neurosci* 10, no. 11 (Nov 1990): 3594-603. https://www.ncbi.nlm.nih.gov/pubmed/2230948.

Saha, B., S. Peron, K. Murray, M. Jaber, and A. Gaillard. "Cortical Lesion Stimulates Adult Subventricular Zone Neural Progenitor Cell Proliferation and Migration to the Site of Injury." *Stem Cell Res* 11, no. 3 (Nov 2013): 965-77. http://dx.doi.org/10.1016/j.scr.2013.06.006.

Sakamoto, M., N. Ieki, G. Miyoshi, D. Mochimaru, H. Miyachi, T. Imura, M. Yamaguchi, G. Fishell, K. Mori, R. Kageyama, and I. Imayoshi. "Continuous Postnatal Neurogenesis Contributes to Formation of the Olfactory Bulb Neural Circuits and Flexible Olfactory Associative Learning." *J Neurosci* 34, no. 17 (Apr 23 2014): 5788-99. http://dx.doi.org/10.1523/JNEUROSCI.0674-14.2014.

Salman, H., P. Ghosh, and S. G. Kernie. "Subventricular Zone Neural Stem Cells Remodel the Brain Following Traumatic Injury in Adult Mice." *J Neurotrauma* 21, no. 3 (Mar 2004): 283-92. http://dx.doi.org/10.1089/089771504322972077.

Sanai, N., T. Nguyen, R. A. Ihrie, Z. Mirzadeh, H. H. Tsai, M. Wong, N. Gupta, M. S. Berger, E. Huang, J. M. Garcia-Verdugo, D. H. Rowitch, and A. Alvarez-Buylla. "Corridors of Migrating Neurons in the Human Brain and Their Decline During Infancy." *Nature* 478, no. 7369 (Sep 28 2011): 382-6. http://dx.doi.org/10.1038/nature10487.

Schachtrup, C., J. K. Ryu, M. J. Helmrick, E. Vagena, D. K. Galanakis, J. L. Degen, R. U. Margolis, and K. Akassoglou. "Fibrinogen Triggers Astrocyte Scar Formation by Promoting the Availability of Active Tgf-Beta after Vascular Damage." *J Neurosci* 30, no. 17 (Apr 28 2010): 5843-54. http://dx.doi.org/10.1523/JNEUROSCI.0137-10.2010.

Schindelin, J., I. Arganda-Carreras, E. Frise, V. Kaynig, M. Longair, T. Pietzsch, S. Preibisch, C. Rueden, S. Saalfeld, B. Schmid, J. Y. Tinevez, D. J. White, V. Hartenstein, K. Eliceiri, P. Tomancak, and A. Cardona. "Fiji: An Open-Source Platform for Biological-Image Analysis." *Nat Methods* 9, no. 7 (Jun 28 2012): 676-82. http://dx.doi.org/10.1038/nmeth.2019.

Schmalfeldt, M., C. E. Bandtlow, M. T. Dours-Zimmermann, K. H. Winterhalter, and D. R. Zimmermann. "Brain Derived Versican V2 Is a Potent Inhibitor of Axonal Growth." *J Cell Sci* 113 (Pt 5) (Mar 2000): 807-16. https://www.ncbi.nlm.nih.gov/pubmed/10671370.

Schnitzer, J., W. W. Franke, and M. Schachner. "Immunocytochemical Demonstration of Vimentin in Astrocytes and Ependymal Cells of Developing and Adult Mouse Nervous System." *J Cell Biol* 90, no. 2 (Aug 1981): 435-47. https://www.ncbi.nlm.nih.gov/pubmed/7026573.

Schofield, R. "The Relationship between the Spleen Colony-Forming Cell and the Haemopoietic Stem Cell." *Blood Cells* 4, no. 1-2 (1978): 7-25. https://www.ncbi.nlm.nih.gov/pubmed/747780.

Scholl, B., A. Y. Tan, J. Corey, and N. J. Priebe. "Emergence of Orientation Selectivity in the Mammalian Visual Pathway." *J Neurosci* 33, no. 26 (Jun 26 2013): 10616-24. http://dx.doi.org/10.1523/JNEUROSCI.0404-13.2013.

Schuett, S., T. Bonhoeffer, and M. Hubener. "Mapping Retinotopic Structure in Mouse Visual Cortex with Optical Imaging." *J Neurosci* 22, no. 15 (Aug 01 2002): 6549-59. http://dx.doi.org/20026635.

Seidenfaden, R., A. Desoeuvre, A. Bosio, I. Virard, and H. Cremer. "Glial Conversion of Svz-Derived Committed Neuronal Precursors after Ectopic Grafting into the Adult Brain." *Mol Cell Neurosci* 32, no. 1-2 (May-Jun 2006): 187-98. http://dx.doi.org/10.1016/j.mcn.2006.04.003.

Seki, T., T. Namba, H. Mochizuki, and M. Onodera. "Clustering, Migration, and Neurite Formation of Neural Precursor Cells in the Adult Rat Hippocampus." *J Comp Neurol* 502, no. 2 (May 10 2007): 275-90. http://dx.doi.org/10.1002/cne.21301.

Seri, B., J. M. Garcia-Verdugo, B. S. McEwen, and A. Alvarez-Buylla. "Astrocytes Give Rise to New Neurons in the Adult Mammalian Hippocampus." *J Neurosci* 21, no. 18 (Sep 15 2001): 7153-60. https://www.ncbi.nlm.nih.gov/pubmed/11549726.

Sheen, V. L., E. B. Dreyer, and J. D. Macklis. "Calcium-Mediated Neuronal Degeneration Following Singlet Oxygen Production." *Neuroreport* 3, no. 8 (Aug 1992): 705-8. https://www.ncbi.nlm.nih.gov/pubmed/1520860.

Sheen, V. L. and J. D. Macklis. "Apoptotic Mechanisms in Targeted Neuronal Cell Death by Chromophore-Activated Photolysis." *Exp Neurol* 130, no. 1 (Nov 1994): 67-81. http://dx.doi.org/10.1006/exnr.1994.1186.

Sheen, V. L. and J. D. Macklis. "Targeted Neocortical Cell Death in Adult Mice Guides Migration and Differentiation of Transplanted Embryonic Neurons." *J Neurosci* 15, no. 12 (Dec 1995): 8378-92. https://www.ncbi.nlm.nih.gov/pubmed/8613770.

Shi, X., J. Barchini, H. A. Ledesma, D. Koren, Y. Jin, X. Liu, W. Wei, and J. Cang. "Retinal Origin of Direction Selectivity in the Superior Colliculus." *Nat Neurosci* 20, no. 4 (Apr 2017): 550-58. http://dx.doi.org/10.1038/nn.4498.

Shiber, A. and T. Ravid. "Chaperoning Proteins for Destruction: Diverse Roles of Hsp70 Chaperones and Their Co-Chaperones in Targeting Misfolded Proteins to the Proteasome." *Biomolecules* 4, no. 3 (Jul 17 2014): 704-24. http://dx.doi.org/10.3390/biom4030704.

Shieh, P. B., S. C. Hu, K. Bobb, T. Timmusk, and A. Ghosh. "Identification of a Signaling Pathway Involved in Calcium Regulation of Bdnf Expression." *Neuron* 20, no. 4 (Apr 1998): 727-40. https://www.ncbi.nlm.nih.gov/pubmed/9581764.

Shihabuddin, L. S., P. J. Horner, J. Ray, and F. H. Gage. "Adult Spinal Cord Stem Cells Generate Neurons after Transplantation in the Adult Dentate Gyrus." *J Neurosci* 20, no. 23 (Dec 01 2000): 8727-35. https://www.ncbi.nlm.nih.gov/pubmed/11102479.

Shimohama, S. "Apoptosis in Alzheimer's Disease--an Update." *Apoptosis* 5, no. 1 (Feb 2000): 9-16. https://www.ncbi.nlm.nih.gov/pubmed/11227497.

Shin, J. J., R. A. Fricker-Gates, F. A. Perez, B. R. Leavitt, D. Zurakowski, and J. D. Macklis. "Transplanted Neuroblasts Differentiate Appropriately into Projection Neurons with Correct Neurotransmitter and Receptor Phenotype in Neocortex Undergoing Targeted Projection Neuron Degeneration." *J Neurosci* 20, no. 19 (Oct 01 2000): 7404-16. https://www.ncbi.nlm.nih.gov/pubmed/11007899.

Shoukimas, G. M. and J. W. Hinds. "The Development of the Cerebral Cortex in the Embryonic Mouse: An Electron Microscopic Serial Section Analysis." *J Comp Neurol* 179, no. 4 (Jun 15 1978): 795-830. http://dx.doi.org/10.1002/cne.901790407.

Sierra, A., O. Abiega, A. Shahraz, and H. Neumann. "Janus-Faced Microglia: Beneficial and Detrimental Consequences of Microglial Phagocytosis." *Front Cell Neurosci* 7 (2013): 6. http://dx.doi.org/10.3389/fncel.2013.00006.

Sierra, A., J. M. Encinas, J. J. Deudero, J. H. Chancey, G. Enikolopov, L. S. Overstreet-Wadiche, S. E. Tsirka, and M. Maletic-Savatic. "Microglia Shape Adult Hippocampal Neurogenesis through Apoptosis-Coupled Phagocytosis." *Cell Stem Cell* 7, no. 4 (Oct 08 2010): 483-95. http://dx.doi.org/10.1016/j.stem.2010.08.014.

Silver, D. J. and J. Silver. "Contributions of Chondroitin Sulfate Proteoglycans to Neurodevelopment, Injury, and Cancer." *Curr Opin Neurobiol* 27 (Aug 2014): 171-8. http://dx.doi.org/10.1016/j.conb.2014.03.016.

Silver, J. and J. H. Miller. "Regeneration Beyond the Glial Scar." *Nat Rev Neurosci* 5, no. 2 (Feb 2004): 146-56. http://dx.doi.org/10.1038/nrn1326.

Simmons, M. L., G. W. Terman, S. M. Gibbs, and C. Chavkin. "L-Type Calcium Channels Mediate Dynorphin Neuropeptide Release from Dendrites but Not Axons of Hippocampal Granule Cells." *Neuron* 14, no. 6 (Jun 1995): 1265-72. https://www.ncbi.nlm.nih.gov/pubmed/7605635.

Simon, C., M. Gotz, and L. Dimou. "Progenitors in the Adult Cerebral Cortex: Cell Cycle Properties and Regulation by Physiological Stimuli and Injury." *Glia* 59, no. 6 (Jun 2011): 869-81. http://dx.doi.org/10.1002/glia.21156.

Simon, C., H. Lickert, M. Gotz, and L. Dimou. "Sox10-Icreert2 : A Mouse Line to Inducibly Trace the Neural Crest and Oligodendrocyte Lineage." *Genesis* 50, no. 6 (Jun 2012): 506-15. http://dx.doi.org/10.1002/dvg.22003.

Simons, D. J. and T. A. Woolsey. "Functional Organization in Mouse Barrel Cortex." *Brain Res* 165, no. 2 (Apr 13 1979): 327-32. https://www.ncbi.nlm.nih.gov/pubmed/421142.

Sirko, S., G. Behrendt, P. A. Johansson, P. Tripathi, M. Costa, S. Bek, C. Heinrich, S. Tiedt, D. Colak, M. Dichgans, I. R. Fischer, N. Plesnila, M. Staufenbiel, C. Haass, M. Snapyan, A. Saghatelyan, L. H. Tsai, A. Fischer, K. Grobe, L. Dimou, and M. Gotz. "Reactive Glia in the Injured Brain Acquire Stem Cell Properties in Response to Sonic Hedgehog. [Corrected]." *Cell Stem Cell* 12, no. 4 (Apr 04 2013): 426-39. http://dx.doi.org/10.1016/j.stem.2013.01.019.

Škoberne, M., A.-S. Beignon, M. Larsson, and N. Bhardwaj. "Apoptotic Cells at the Crossroads of Tolerance and Immunity." In *Role of Apoptosis in Infection*, edited by Diane E. Griffin, 259-92. Berlin, Heidelberg: Springer Berlin Heidelberg, 2005.

Smith, G. B., A. Sederberg, Y. M. Elyada, S. D. Van Hooser, M. Kaschube, and D. Fitzpatrick. "The Development of Cortical Circuits for Motion Discrimination." *Nat Neurosci* 18, no. 2 (Feb 2015): 252-61. http://dx.doi.org/10.1038/nn.3921.

Soares, H. and T. K. McIntosh. "Fetal Cortical Transplants in Adult Rats Subjected to Experimental Brain Injury." *J Neural Transplant Plast* 2, no. 3-4 (1991): 207-20. http://dx.doi.org/10.1155/NP.1991.207.

Sofroniew, M. V. "Astrocyte Barriers to Neurotoxic Inflammation." *Nat Rev Neurosci* 16, no. 5 (May 2015): 249-63. http://dx.doi.org/10.1038/nrn3898.

Sohur, U. S., P. Arlotta, and J. D. Macklis. "Developmental Controls Are Re-Expressed During Induction of Neurogenesis in the Neocortex of Young Adult Mice." *Front Neurosci* 6 (2012): 12. http://dx.doi.org/10.3389/fnins.2012.00012.

Sohya, K., K. Kameyama, Y. Yanagawa, K. Obata, and T. Tsumoto. "Gabaergic Neurons Are Less Selective to Stimulus Orientation Than Excitatory Neurons in Layer Ii/Iii of Visual Cortex, as Revealed by in Vivo Functional Ca2+ Imaging in Transgenic Mice." *J Neurosci* 27, no. 8 (Feb 21 2007): 2145-9. http://dx.doi.org/10.1523/JNEUROSCI.4641-06.2007.

Solomon, J. S. and J. M. Nerbonne. "Hyperpolarization-Activated Currents in Isolated Superior Colliculus-Projecting Neurons from Rat Visual Cortex." *J Physiol* 462 (Mar 1993): 393-420. https://www.ncbi.nlm.nih.gov/pubmed/8331588.

Southwell, D. G., R. C. Froemke, A. Alvarez-Buylla, M. P. Stryker, and S. P. Gandhi. "Cortical Plasticity Induced by Inhibitory Neuron Transplantation." *Science* 327, no. 5969 (Feb 26 2010): 1145-8. http://dx.doi.org/10.1126/science.1183962.

Spalding, K. L., O. Bergmann, K. Alkass, S. Bernard, M. Salehpour, H. B. Huttner, E. Bostrom, I. Westerlund, C. Vial, B. A. Buchholz, G. Possnert, D. C. Mash, H. Druid, and J. Frisen. "Dynamics of Hippocampal Neurogenesis in Adult Humans." *Cell* 153, no. 6 (Jun 06 2013): 1219-27. http://dx.doi.org/10.1016/j.cell.2013.05.002.

Spruston, N. "Pyramidal Neurons: Dendritic Structure and Synaptic Integration." *Nat Rev Neurosci* 9, no. 3 (Mar 2008): 206-21. http://dx.doi.org/10.1038/nrn2286.

Stehberg, J., P. T. Dang, and R. D. Frostig. "Unimodal Primary Sensory Cortices Are Directly Connected by Long-Range Horizontal Projections in the Rat Sensory Cortex." *Front Neuroanat* 8 (2014): 93. http://dx.doi.org/10.3389/fnana.2014.00093.

Steiner, B., F. Klempin, L. Wang, M. Kott, H. Kettenmann, and G. Kempermann. "Type-2 Cells as Link between Glial and Neuronal Lineage in Adult Hippocampal Neurogenesis." *Glia* 54, no. 8 (Dec 2006): 805-14. http://dx.doi.org/10.1002/glia.20407.

Stettler, D. D., H. Yamahachi, W. Li, W. Denk, and C. D. Gilbert. "Axons and Synaptic Boutons Are Highly Dynamic in Adult Visual Cortex." *Neuron* 49, no. 6 (Mar 16 2006): 877-87. http://dx.doi.org/10.1016/j.neuron.2006.02.018.

Stosiek, C., O. Garaschuk, K. Holthoff, and A. Konnerth. "In Vivo Two-Photon Calcium Imaging of Neuronal Networks." *Proc Natl Acad Sci U S A* 100, no. 12 (Jun 10 2003): 7319-24. http://dx.doi.org/10.1073/pnas.1232232100.

Stuart, L. M., K. Takahashi, L. Shi, J. Savill, and R. A. Ezekowitz. "Mannose-Binding Lectin-Deficient Mice Display Defective Apoptotic Cell Clearance but No Autoimmune Phenotype." *J Immunol* 174, no. 6 (Mar 15 2005): 3220-6. https://www.ncbi.nlm.nih.gov/pubmed/15749852.

Sun, C., C. Liang, Y. Ren, Y. Zhen, Z. He, H. Wang, H. Tan, X. Pan, and Z. Wu. "Advanced Glycation End Products Depress Function of Endothelial Progenitor Cells Via P38 and Erk 1/2 Mitogen-Activated Protein Kinase Pathways." *Basic Res Cardiol* 104, no. 1 (Jan 2009): 42-9. http://dx.doi.org/10.1007/s00395-008-0738-8.

Sun, D. "The Potential of Endogenous Neurogenesis for Brain Repair and Regeneration Following Traumatic Brain Injury." *Neural Regen Res* 9, no. 7 (Apr 01 2014): 688-92. http://dx.doi.org/10.4103/1673-5374.131567.

Sun, D., M. R. Bullock, N. Altememi, Z. Zhou, S. Hagood, A. Rolfe, M. J. McGinn, R. Hamm, and R. J. Colello. "The Effect of Epidermal Growth Factor in the Injured Brain after Trauma in Rats." *J Neurotrauma* 27, no. 5 (May 2010): 923-38. http://dx.doi.org/10.1089/neu.2009.1209.

Sun, W., Z. Tan, B. D. Mensh, and N. Ji. "Thalamus Provides Layer 4 of Primary Visual Cortex with Orientation- and Direction-Tuned Inputs." *Nat Neurosci* 19, no. 2 (Feb 2016): 308-15. http://dx.doi.org/10.1038/nn.4196.

Takeda, D. Y. and A. Dutta. "DNA Replication and Progression through S Phase." *Oncogene* 24, no. 17 (Apr 18 2005): 2827-43. http://dx.doi.org/10.1038/sj.onc.1208616.

Tan, A. M., W. Zhang, and J. M. Levine. "Ng2: A Component of the Glial Scar That Inhibits Axon Growth." *J Anat* 207, no. 6 (Dec 2005): 717-25. http://dx.doi.org/10.1111/j.1469-7580.2005.00452.x.

Tang, Y., M. P. Stryker, A. Alvarez-Buylla, and J. S. Espinosa. "Cortical Plasticity Induced by Transplantation of Embryonic Somatostatin or Parvalbumin Interneurons." *Proc Natl Acad Sci U S A* 111, no. 51 (Dec 23 2014): 18339-44. http://dx.doi.org/10.1073/pnas.1421844112.

Tao, H. W. and M. Poo. "Retrograde Signaling at Central Synapses." *Proc Natl Acad Sci U S A* 98, no. 20 (Sep 25 2001): 11009-15. http://dx.doi.org/10.1073/pnas.191351698.

Tao, H., L. I. Zhang, G. Bi, and M. Poo. "Selective Presynaptic Propagation of Long-Term Potentiation in Defined Neural Networks." *J Neurosci* 20, no. 9 (May 01 2000): 3233-43. https://www.ncbi.nlm.nih.gov/pubmed/10777788.

Tasic, B., V. Menon, T. N. Nguyen, T. K. Kim, T. Jarsky, Z. Yao, B. Levi, L. T. Gray, S. A. Sorensen, T. Dolbeare, D. Bertagnolli, J. Goldy, N. Shapovalova, S. Parry, C. Lee, K. Smith, A. Bernard, L. Madisen, S. M. Sunkin, M. Hawrylycz, C. Koch, and H. Zeng. "Adult Mouse Cortical Cell Taxonomy Revealed by Single Cell Transcriptomics." *Nat Neurosci* 19, no. 2 (Feb 2016): 335-46. http://dx.doi.org/10.1038/nn.4216.

Taupin, P. "Adult Neural Stem Cells, Neurogenic Niches, and Cellular Therapy." *Stem Cell Rev* 2, no. 3 (2006): 213-9. http://dx.doi.org/10.1007/s12015-006-0049-0.

Taupin, P. "Brdu Immunohistochemistry for Studying Adult Neurogenesis: Paradigms, Pitfalls, Limitations, and Validation." *Brain Res Rev* 53, no. 1 (Jan 2007): 198-214. http://dx.doi.org/10.1016/j.brainresrev.2006.08.002.

Thestrup, T., J. Litzlbauer, I. Bartholomaus, M. Mues, L. Russo, H. Dana, Y. Kovalchuk, Y. Liang, G. Kalamakis, Y. Laukat, S. Becker, G. Witte, A. Geiger, T. Allen, L. C. Rome, T. W. Chen, D. S. Kim, O. Garaschuk, C.

Griesinger, and O. Griesbeck. "Optimized Ratiometric Calcium Sensors for Functional in Vivo Imaging of Neurons and T Lymphocytes." *Nat Methods* 11, no. 2 (Feb 2014): 175-82. http://dx.doi.org/10.1038/nmeth.2773.

Thoenen, H. "Neurotrophins and Neuronal Plasticity." *Science* 270, no. 5236 (Oct 27 1995): 593-8. https://www.ncbi.nlm.nih.gov/pubmed/7570017.

Thompson, L. H. and A. Bjorklund. "Reconstruction of Brain Circuitry by Neural Transplants Generated from Pluripotent Stem Cells." *Neurobiol Dis* 79 (Jul 2015): 28-40. http://dx.doi.org/10.1016/j.nbd.2015.04.003.

Thompson, W. G. "Successful Brain Grafting." *N. Y. Med J.* 51 (1890): 701–02.

Tian, L., S. A. Hires, T. Mao, D. Huber, M. E. Chiappe, S. H. Chalasani, L. Petreanu, J. Akerboom, S. A. McKinney, E. R. Schreiter, C. I. Bargmann, V. Jayaraman, K. Svoboda, and L. L. Looger. "Imaging Neural Activity in Worms, Flies and Mice with Improved Gcamp Calcium Indicators." *Nat Methods* 6, no. 12 (Dec 2009): 875-81. http://dx.doi.org/10.1038/nmeth.1398.

Timmusk, T., N. Belluardo, H. Persson, and M. Metsis. "Developmental Regulation of Brain-Derived Neurotrophic Factor Messenger Rnas Transcribed from Different Promoters in the Rat Brain." *Neuroscience* 60, no. 2 (May 1994): 287-91. https://www.ncbi.nlm.nih.gov/pubmed/8072683.

Tom, V. J., M. P. Steinmetz, J. H. Miller, C. M. Doller, and J. Silver. "Studies on the Development and Behavior of the Dystrophic Growth Cone, the Hallmark of Regeneration Failure, in an in Vitro Model of the Glial Scar and after Spinal Cord Injury." *J Neurosci* 24, no. 29 (Jul 21 2004): 6531-9. http://dx.doi.org/10.1523/JNEUROSCI.0994-04.2004.

Tombol, T., F. Hajdu, and G. Somogyi. "Identification of the Golgi Picture of the Layer Vi Cortic-Geniculate Projection Neurons." *Exp Brain Res* 24, no. 1 (Nov 28 1975): 107-10. https://www.ncbi.nlm.nih.gov/pubmed/1204697.

Trachtenberg, J. T., B. E. Chen, G. W. Knott, G. Feng, J. R. Sanes, E. Welker, and K. Svoboda. "Long-Term in Vivo Imaging of Experience-Dependent Synaptic Plasticity in Adult Cortex." *Nature* 420, no. 6917 (Dec 19-26 2002): 788-94. http://dx.doi.org/10.1038/nature01273.

Tsay, J. M., M. Trzoss, L. Shi, X. Kong, M. Selke, M. E. Jung, and S. Weiss. "Singlet Oxygen Production by Peptide-Coated Quantum Dot-Photosensitizer Conjugates." *J Am Chem Soc* 129, no. 21 (May 30 2007): 6865-71. http://dx.doi.org/10.1021/ja070713i.

Tyzio, R., R. Cossart, I. Khalilov, M. Minlebaev, C. A. Hubner, A. Represa, Y. Ben-Ari, and R. Khazipov. "Maternal Oxytocin Triggers a Transient Inhibitory Switch in Gaba Signaling in the Fetal Brain During Delivery." *Science* 314, no. 5806 (Dec 15 2006): 1788-92. http://dx.doi.org/10.1126/science.1133212.

Tyzio, R., A. Represa, I. Jorquera, Y. Ben-Ari, H. Gozlan, and L. Aniksztejn. "The Establishment of Gabaergic and Glutamatergic Synapses on Ca1 Pyramidal Neurons Is Sequential and Correlates with the Development of the Apical Dendrite." *J Neurosci* 19, no. 23 (Dec 01 1999): 10372-82. https://www.ncbi.nlm.nih.gov/pubmed/10575034.

Uchizono, K. "Characteristics of Excitatory and Inhibitory Synapses in the Central Nervous System of the Cat." *Nature* 207, no. 997 (Aug 07 1965): 642-3. https://www.ncbi.nlm.nih.gov/pubmed/5883646.

Ucker, David S. "Innate Apoptotic Immunity: A Potent Immunosuppressive Response Repertoire Elicited by Specific Apoptotic Cell Recognition." In *Phagocytosis of Dying Cells: From Molecular Mechanisms to Human Diseases*, edited by Dmitri V. Krysko and Peter Vandenabeele, 163-87. Dordrecht: Springer Netherlands, 2009.

Ughrin, Y. M., Z. J. Chen, and J. M. Levine. "Multiple Regions of the Ng2 Proteoglycan Inhibit Neurite Growth and Induce Growth Cone Collapse." *J Neurosci* 23, no. 1 (Jan 01 2003): 175-86. https://www.ncbi.nlm.nih.gov/pubmed/12514214.

Uvarov, P., A. Ludwig, M. Markkanen, P. Pruunsild, K. Kaila, E. Delpire, T. Timmusk, C. Rivera, and M. S. Airaksinen. "A Novel N-Terminal Isoform of the Neuron-Specific K-Cl Cotransporter Kcc2." *J Biol Chem* 282, no. 42 (Oct 19 2007): 30570-6. http://dx.doi.org/10.1074/jbc.M705095200.

Uvarov, P., A. Ludwig, M. Markkanen, S. Soni, C. A. Hubner, C. Rivera, and M. S. Airaksinen. "Coexpression and Heteromerization of Two Neuronal K-Cl Cotransporter Isoforms in Neonatal Brain." *J Biol Chem* 284, no. 20 (May 15 2009): 13696-704. http://dx.doi.org/10.1074/jbc.M807366200.

Vadivelu, S., T. J. Stewart, Y. Qu, K. Horn, S. Liu, Q. Li, J. Silver, and J. W. McDonald. "Ng2+ Progenitors Derived from Embryonic Stem Cells Penetrate Glial Scar and Promote Axonal Outgrowth into White Matter after Spinal Cord Injury." *Stem Cells Transl Med* 4, no. 4 (Apr 2015): 401-11. http://dx.doi.org/10.5966/sctm.2014-0107.

Valeeva, G., F. Valiullina, and R. Khazipov. "Excitatory Actions of Gaba in the Intact Neonatal Rodent Hippocampus in Vitro." *Front Cell Neurosci* 7 (2013): 20. http://dx.doi.org/10.3389/fncel.2013.00020.

van der Loos, H. "The Improperly Oriented Pyramidal Cell in the Cerebral Cortex and Its Possible Bearing on Problems of Neuronal Growth and Cell Orientation. ." *Bull Johns Hopkins Hos* 117 (1965): 228-50.

Van Hooser, S. D., A. Roy, H. J. Rhodes, J. H. Culp, and D. Fitzpatrick. "Transformation of Receptive Field Properties from Lateral Geniculate Nucleus to Superficial V1 in the Tree Shrew." *J Neurosci* 33, no. 28 (Jul 10 2013): 11494-505. http://dx.doi.org/10.1523/JNEUROSCI.1464-13.2013.

van Praag, H., A. F. Schinder, B. R. Christie, N. Toni, T. D. Palmer, and F. H. Gage. "Functional Neurogenesis in the Adult Hippocampus." *Nature* 415, no. 6875 (Feb 28 2002): 1030-4. http://dx.doi.org/10.1038/4151030a.

Vaughn, J. E., C. K. Henrikson, and J. A. Grieshaber. "A Quantitative Study of Synapses on Motor Neuron Dendritic Growth Cones in Developing Mouse Spinal Cord." *J Cell Biol* 60, no. 3 (Mar 1974): 664-72. https://www.ncbi.nlm.nih.gov/pubmed/4824291.

Vawda, R., J. Wilcox, and M. Fehlings. "Current Stem Cell Treatments for Spinal Cord Injury." *Indian J Orthop* 46, no. 1 (Jan 2012): 10-8. http://dx.doi.org/10.4103/0019-5413.91629.

Verdaguer, E., E. Garcia-Jorda, A. M. Canudas, E. Dominguez, A. Jimenez, D. Pubill, E. Escubedo, J. C. Pallas, and A. Camins. "Kainic Acid-Induced Apoptosis in Cerebellar Granule Neurons: An Attempt at Cell Cycle Re-Entry." *Neuroreport* 13, no. 4 (Mar 25 2002): 413-6. https://www.ncbi.nlm.nih.gov/pubmed/11930151.

Vivar, C., M. C. Potter, J. Choi, J. Y. Lee, T. P. Stringer, E. M. Callaway, F. H. Gage, H. Suh, and H. van Praag. "Monosynaptic Inputs to New Neurons in the Dentate Gyrus." *Nat Commun* 3 (2012): 1107. http://dx.doi.org/10.1038/ncomms2101.

Voellmy, R. "On Mechanisms That Control Heat Shock Transcription Factor Activity in Metazoan Cells." *Cell Stress Chaperones* 9, no. 2 (Summer 2004): 122-33. https://www.ncbi.nlm.nih.gov/pubmed/15497499.

Vonsattel, J. P., R. H. Myers, T. J. Stevens, R. J. Ferrante, E. D. Bird, and E. P. Richardson, Jr. "Neuropathological Classification of Huntington's Disease." *J Neuropathol Exp Neurol* 44, no. 6 (Nov 1985): 559-77. https://www.ncbi.nlm.nih.gov/pubmed/2932539.

Wagor, E., N. J. Mangini, and A. L. Pearlman. "Retinotopic Organization of Striate and Extrastriate Visual Cortex in the Mouse." *J Comp Neurol* 193, no. 1 (Sep 01 1980): 187-202. http://dx.doi.org/10.1002/cne.901930113.

Wang, G., J. Zhang, X. Hu, L. Zhang, L. Mao, X. Jiang, A. K. Liou, R. K. Leak, Y. Gao, and J. Chen. "Microglia/Macrophage Polarization Dynamics in White Matter after Traumatic Brain Injury." *J Cereb Blood Flow Metab* 33, no. 12 (Dec 2013): 1864-74. http://dx.doi.org/10.1038/jcbfm.2013.146.

Wang, Q. and A. Burkhalter. "Area Map of Mouse Visual Cortex." *J Comp Neurol* 502, no. 3 (May 20 2007): 339-57. http://dx.doi.org/10.1002/cne.21286.

Wang, Q., E. Gao, and A. Burkhalter. "In Vivo Transcranial Imaging of Connections in Mouse Visual Cortex." *J Neurosci Methods* 159, no. 2 (Jan 30 2007): 268-76. http://dx.doi.org/10.1016/j.jneumeth.2006.07.024.

Wang, Q., O. Sporns, and A. Burkhalter. "Network Analysis of Corticocortical Connections Reveals Ventral and Dorsal Processing Streams in Mouse Visual Cortex." *J Neurosci* 32, no. 13 (Mar 28 2012): 4386-99. http://dx.doi.org/10.1523/JNEUROSCI.6063-11.2012.

Wang, Y., S. Pennock, X. Chen, and Z. Wang. "Internalization of Inactive Egf Receptor into Endosomes and the Subsequent Activation of Endosome-Associated Egf Receptors. Epidermal Growth Factor." *Sci STKE* 2002, no. 161 (Dec 03 2002): pl17. http://dx.doi.org/10.1126/stke.2002.161.pl17.

Wang, Y., V. L. Sheen, and J. D. Macklis. "Cortical Interneurons Upregulate Neurotrophins in Vivo in Response to Targeted Apoptotic Degeneration of Neighboring Pyramidal Neurons." *Exp Neurol* 154, no. 2 (Dec 1998): 389-402. http://dx.doi.org/10.1006/exnr.1998.6965.

Wehrle, R., E. Camand, A. Chedotal, C. Sotelo, and I. Dusart. "Expression of Netrin-1, Slit-1 and Slit-3 but Not of Slit-2 after Cerebellar and Spinal Cord Lesions." *Eur J Neurosci* 22, no. 9 (Nov 2005): 2134-44. http://dx.doi.org/10.1111/j.1460-9568.2005.04419.x.

Weigmann, A., D. Corbeil, A. Hellwig, and W. B. Huttner. "Prominin, a Novel Microvilli-Specific Polytopic Membrane Protein of the Apical Surface of Epithelial Cells, Is Targeted to Plasmalemmal Protrusions of Non-Epithelial Cells." *Proc Natl Acad Sci U S A* 94, no. 23 (Nov 11 1997): 12425-30. https://www.ncbi.nlm.nih.gov/pubmed/9356465.

Weiss, R. A. "Human Retroviruses in Health and Disease." *Princess Takamatsu Symp* 15 (1984): 3-12. https://www.ncbi.nlm.nih.gov/pubmed/6100647.

Whitesell, L. and S. L. Lindquist. "Hsp90 and the Chaperoning of Cancer." *Nat Rev Cancer* 5, no. 10 (Oct 2005): 761-72. http://dx.doi.org/10.1038/nrc1716.

Wiesel, T. N. and D. H. Hubel. "Single-Cell Responses in Striate Cortex of Kittens Deprived of Vision in One Eye." *J Neurophysiol* 26 (Nov 1963): 1003-17. https://www.ncbi.nlm.nih.gov/pubmed/14084161.

Windrem, M. S., M. C. Nunes, W. K. Rashbaum, T. H. Schwartz, R. A. Goodman, G. McKhann, 2nd, N. S. Roy, and S. A. Goldman. "Fetal and Adult Human Oligodendrocyte Progenitor Cell Isolates Myelinate the Congenitally Dysmyelinated Brain." *Nat Med* 10, no. 1 (Jan 2004): 93-7. http://dx.doi.org/10.1038/nm974.

Wittko, I. M., A. Schanzer, A. Kuzmichev, F. T. Schneider, M. Shibuya, S. Raab, and K. H. Plate. "Vegfr-1 Regulates Adult Olfactory Bulb Neurogenesis and Migration of Neural Progenitors in the Rostral Migratory Stream in Vivo." *J Neurosci* 29, no. 27 (Jul 08 2009): 8704-14. http://dx.doi.org/10.1523/JNEUROSCI.5527-08.2009.

Wizenmann, A., E. Thies, S. Klostermann, F. Bonhoeffer, and M. Bahr. "Appearance of Target-Specific Guidance Information for Regenerating Axons after Cns Lesions." *Neuron* 11, no. 5 (Nov 1993): 975-83. https://www.ncbi.nlm.nih.gov/pubmed/8240818.

Xu, B., W. Gottschalk, A. Chow, R. I. Wilson, E. Schnell, K. Zang, D. Wang, R. A. Nicoll, B. Lu, and L. F. Reichardt. "The Role of Brain-Derived Neurotrophic Factor Receptors in the Mature Hippocampus: Modulation of Long-Term Potentiation through a Presynaptic Mechanism Involving Trkb." *J Neurosci* 20, no. 18 (Sep 15 2000): 6888-97. https://www.ncbi.nlm.nih.gov/pubmed/10995833.

Xu, H., A. S. Khakhalin, A. V. Nurmikko, and C. D. Aizenman. "Visual Experience-Dependent Maturation of Correlated Neuronal Activity Patterns in a Developing Visual System." *J Neurosci* 31, no. 22 (Jun 01 2011): 8025-36. http://dx.doi.org/10.1523/JNEUROSCI.5802-10.2011.

Xu, M., K. D. Dittmar, G. Giannoukos, W. B. Pratt, and S. S. Simons, Jr. "Binding of Hsp90 to the Glucocorticoid Receptor Requires a Specific 7-Amino Acid Sequence at the Amino Terminus of the Hormone-Binding Domain." *J Biol Chem* 273, no. 22 (May 29 1998): 13918-24. https://www.ncbi.nlm.nih.gov/pubmed/9593740.

Xu, X., N. D. Olivas, T. Ikrar, T. Peng, T. C. Holmes, Q. Nie, and Y. Shi. "Primary Visual Cortex Shows Laminar-Specific and Balanced Circuit Organization of Excitatory and Inhibitory Synaptic Connectivity." *J Physiol* 594, no. 7 (Apr 01 2016): 1891-910. http://dx.doi.org/10.1113/JP271891.

Yamada, H., B. Fredette, K. Shitara, K. Hagihara, R. Miura, B. Ranscht, W. B. Stallcup, and Y. Yamaguchi. "The Brain Chondroitin Sulfate Proteoglycan Brevican Associates with Astrocytes Ensheathing Cerebellar Glomeruli and Inhibits Neurite Outgrowth from Granule Neurons." *J Neurosci* 17, no. 20 (Oct 15 1997): 7784-95. https://www.ncbi.nlm.nih.gov/pubmed/9315899.

Yamada, J., A. Okabe, H. Toyoda, W. Kilb, H. J. Luhmann, and A. Fukuda. "Cl- Uptake Promoting Depolarizing Gaba Actions in Immature Rat Neocortical Neurones Is Mediated by Nkcc1." *J Physiol* 557, no. Pt 3 (Jun 15 2004): 829-41. http://dx.doi.org/10.1113/jphysiol.2004.062471.

Yamaguchi, M. and K. Mori. "Critical Period for Sensory Experience-Dependent Survival of Newly Generated Granule Cells in the Adult Mouse Olfactory Bulb." *Proc Natl Acad Sci U S A* 102, no. 27 (Jul 05 2005): 9697-702. http://dx.doi.org/10.1073/pnas.0406082102.

Yamahachi, H., S. A. Marik, J. N. McManus, W. Denk, and C. D. Gilbert. "Rapid Axonal Sprouting and Pruning Accompany Functional Reorganization in Primary Visual Cortex." *Neuron* 64, no. 5 (Dec 10 2009): 719-29. http://dx.doi.org/10.1016/j.neuron.2009.11.026.

Yang, Y., D. S. Geldmacher, and K. Herrup. "DNA Replication Precedes Neuronal Cell Death in Alzheimer's Disease." *J Neurosci* 21, no. 8 (Apr 15 2001): 2661-8. https://www.ncbi.nlm.nih.gov/pubmed/11306619.

Yeckel, M. F. and T. W. Berger. "Feedforward Excitation of the Hippocampus by Afferents from the Entorhinal Cortex: Redefinition of the Role of the Trisynaptic Pathway." *Proc Natl Acad Sci U S A* 87, no. 15 (Aug 1990): 5832-6. https://www.ncbi.nlm.nih.gov/pubmed/2377621.

Yokoi, M., K. Mori, and S. Nakanishi. "Refinement of Odor Molecule Tuning by Dendrodendritic Synaptic Inhibition in the Olfactory Bulb." *Proc Natl Acad Sci U S A* 92, no. 8 (Apr 11 1995): 3371-5. https://www.ncbi.nlm.nih.gov/pubmed/7724568.

Yorke, C. H., Jr. and V. S. Caviness, Jr. "Interhemispheric Neocortical Connections of the Corpus Callosum in the Normal Mouse: A Study Based on Anterograde and Retrograde Methods." *J Comp Neurol* 164, no. 2 (Nov 15 1975): 233-45. http://dx.doi.org/10.1002/cne.901640206.

Yoshihara, S., H. Takahashi, and A. Tsuboi. "Molecular Mechanisms Regulating the Dendritic Development of Newborn Olfactory Bulb Interneurons in a Sensory Experience-Dependent Manner." *Front Neurosci* 9 (2015): 514. http://dx.doi.org/10.3389/fnins.2015.00514.

Yoshimura, Y., J. L. Dantzker, and E. M. Callaway. "Excitatory Cortical Neurons Form Fine-Scale Functional Networks." *Nature* 433, no. 7028 (Feb 24 2005): 868-73. http://dx.doi.org/10.1038/nature03252.

Yu, Y. C., S. He, S. Chen, Y. Fu, K. N. Brown, X. H. Yao, J. Ma, K. P. Gao, G. E. Sosinsky, K. Huang, and S. H. Shi. "Preferential Electrical Coupling Regulates Neocortical Lineage-Dependent Microcircuit Assembly." *Nature* 486, no. 7401 (May 02 2012): 113-7. http://dx.doi.org/10.1038/nature10958.

Yuan, R., S. W. Tsaih, S. B. Petkova, C. Marin de Evsikova, S. Xing, M. A. Marion, M. A. Bogue, K. D. Mills, L. L. Peters, C. J. Bult, C. J. Rosen, J. P. Sundberg, D. E. Harrison, G. A. Churchill, and B. Paigen. "Aging in Inbred Strains of Mice: Study Design and Interim Report on Median Lifespans and Circulating Igf1 Levels." *Aging Cell* 8, no. 3 (Jun 2009): 277-87. http://dx.doi.org/10.1111/j.1474-9726.2009.00478.x.

Zamanian, J. L., L. Xu, L. C. Foo, N. Nouri, L. Zhou, R. G. Giffard, and B. A. Barres. "Genomic Analysis of Reactive Astrogliosis." *J Neurosci* 32, no. 18 (May 02 2012): 6391-410. http://dx.doi.org/10.1523/JNEUROSCI.6221-11.2012.

Zhang, L. I. and M. M. Poo. "Electrical Activity and Development of Neural Circuits." *Nat Neurosci* 4 Suppl (Nov 2001): 1207-14. http://dx.doi.org/10.1038/nn753.

Zhao, C., E. M. Teng, R. G. Summers, Jr., G. L. Ming, and F. H. Gage. "Distinct Morphological Stages of Dentate Granule Neuron Maturation in the Adult Mouse Hippocampus." *J Neurosci* 26, no. 1 (Jan 04 2006): 3-11. http://dx.doi.org/10.1523/JNEUROSCI.3648-05.2006.

Zhao, J. W., R. Raha-Chowdhury, J. W. Fawcett, and C. Watts. "Astrocytes and Oligodendrocytes Can Be Generated from Ng2+ Progenitors after Acute Brain Injury: Intracellular Localization of Oligodendrocyte Transcription Factor 2 Is Associated with Their Fate Choice." *Eur J Neurosci* 29, no. 9 (May 2009): 1853-69. http://dx.doi.org/10.1111/j.1460-9568.2009.06736.x.

Zhao, L., M. K. Zabel, X. Wang, W. Ma, P. Shah, R. N. Fariss, H. Qian, C. N. Parkhurst, W. B. Gan, and W. T. Wong. "Microglial Phagocytosis of Living Photoreceptors Contributes to Inherited Retinal Degeneration." *EMBO Mol Med* 7, no. 9 (Sep 2015): 1179-97. http://dx.doi.org/10.15252/emmm.201505298.

Zharkov, D. O. "Base Excision DNA Repair." *Cell Mol Life Sci* 65, no. 10 (May 2008): 1544-65. http://dx.doi.org/10.1007/s00018-008-7543-2.

Zhu, W., S. Cheng, G. Xu, M. Ma, Z. Zhou, D. Liu, and X. Liu. "Intranasal Nerve Growth Factor Enhances Striatal Neurogenesis in Adult Rats with Focal Cerebral Ischemia." *Drug Deliv* 18, no. 5 (Jul 2011): 338-43. http://dx.doi.org/10.3109/10717544.2011.557785.

Zigova, T., V. Pencea, S. J. Wiegand, and M. B. Luskin. "Intraventricular Administration of Bdnf Increases the Number of Newly Generated Neurons in the Adult Olfactory Bulb." *Mol Cell Neurosci* 11, no. 4 (Jul 1998): 234-45. http://dx.doi.org/10.1006/mcne.1998.0684.

Zimmer, C., M. C. Tiveron, R. Bodmer, and H. Cremer. "Dynamics of Cux2 Expression Suggests That an Early Pool of Svz Precursors Is Fated to Become Upper Cortical Layer Neurons." *Cereb Cortex* 14, no. 12 (Dec 2004): 1408-20. http://dx.doi.org/10.1093/cercor/bhh102.

Zou, J., Y. Guo, T. Guettouche, D. F. Smith, and R. Voellmy. "Repression of Heat Shock Transcription Factor Hsf1 Activation by Hsp90 (Hsp90 Complex) That Forms a Stress-Sensitive Complex with Hsf1." *Cell* 94, no. 4 (Aug 21 1998): 471-80. https://www.ncbi.nlm.nih.gov/pubmed/9727490.

Zweifel, L. S., R. Kuruvilla, and D. D. Ginty. "Functions and Mechanisms of Retrograde Neurotrophin Signalling." *Nat Rev Neurosci* 6, no. 8 (Aug 2005): 615-25. http://dx.doi.org/10.1038/nrn1727.